



Universiteit
Leiden
The Netherlands

Neandertals in the forests : a palaeomagnetic study of the Eemian interglacial stage deposits from north-western and central Europe
Sier, M.J.

Citation

Sier, M. J. (2014, January 21). *Neandertals in the forests : a palaeomagnetic study of the Eemian interglacial stage deposits from north-western and central Europe*. Retrieved from <https://hdl.handle.net/1887/22207>

Version: Corrected Publisher's Version

License: [Licence agreement concerning inclusion of doctoral thesis in the Institutional Repository of the University of Leiden](#)

Downloaded from: <https://hdl.handle.net/1887/22207>

Note: To cite this publication please use the final published version (if applicable).

Cover Page



Universiteit Leiden



The handle <http://hdl.handle.net/1887/22207> holds various files of this Leiden University dissertation

Author: Sier, Mark J.

Title: Neandertals in the forests : a palaeomagnetic study of the Eemian interglacial stage deposits from north-western and central Europe

Issue Date: 2013-11-13



NEANDERTALS

IN THE FORESTS

A PALAEO-MAGNETIC STUDY OF THE EEMIAN
INTERGLACIAL STAGE DEPOSITS
FROM NORTH WESTERN AND CENTRAL EUROPE

MARK J. SIER

NEANDERTALS IN THE FORESTS

A PALAEOMAGNETIC STUDY
OF THE EEMIAN INTERGLACIAL STAGE DEPOSITS
FROM NORTH-WESTERN AND CENTRAL EUROPE

PROEFSCHRIFT
TER VERKRIJGING VAN
DE GRAAD VAN DOCTOR AAN DE UNIVERSITEIT LEIDEN,
OP GEZAG VAN RECTOR MAGNIFICUS PROF. MR. C.J.J.M. STOLKER,
VOLGENS BESLUIT VAN HET COLLEGE VOOR PROMOTIES
TE VERDEDIGEN OP 13 NOVEMBER 2013
KLOKKE 16:15 UUR

DOOR
MARK JAN SIER
GEBOREN TE AMSTELVEEN, NEDERLAND
IN 1972

Promotiecommissie:

Promotor: Prof. dr. J.W.M. Roebroeks

Co-promotoren: Dr. M.J. Dekkers (Utrecht University), Dr. J.M. Parés (Cenieh, Burgos, Spain)

Overige leden: Prof. dr. C.G. Langereis (Utrecht University), Prof. dr. C.C. Bakels, Prof. dr. M. Van Kolfschoten, Prof. dr. ir. J van der Plicht, Dr. M.H. Field, Dr. W.E. Westerhof (Geological Survey of the Netherlands – TNO)

De totstandkoming van dit proefschrift werd financieel mogelijk gemaakt door de Nederlandse Organisatie voor Wetenschappelijk Onderzoek (NWO); Spinozaprijs Prof. dr. J.W.M. Roebroeks.

Cover image: illustration by Kennis&Kennis © and photo of palaeomagnetic samples at Neumark Nord 2.

Photo taken by author.

Cover design by Joanne Porck (geodesigns.arch@gmail.com)

Layout by exitweb

For my family and especially for Maria

CONTENTS

Bibliography	10
Chapter 1	
Introduction.....	13
Chapter 2	
Direct terrestrial–marine correlation demonstrates surprisingly late onset of the last interglacial in central Europe.....	29
Chapter 3	
Magnetic property analysis as palaeoenvironmental proxy: a case study of the Last Interglacial Middle Palaeolithic site at Neumark-Nord 2 (Germany).....	81
Chapter 4	
The Blake Event recorded near the Eemian Type locality: revised timing of the onset of the Eemian in north-western Europe.....	113
Chapter 5	
The Blake Event recorded at the Eemian archaeological site of Caours, France.....	173
Chapter 6	
Conclusions.....	209
Summary	226
Samenvatting	228
Acknowledgements	230
Curriculum Vitae	234

BIBLIOGRAPHY

This thesis

Chapter 2

Sier, M. J., Roebroeks, W., Bakels, C. C., Dekkers, M. J., Brühl, E., De Loecker, D., Gaudzinski-Windheuser, S., Hesse, N., Jagich, A., Kindler, L., Kuijper, W. J., Laurat, T., Mücher, H. J., Penkman, K. E. H., Richter, D., and van Hinsbergen, D. J. J. (2011). Direct terrestrial–marine correlation demonstrates surprisingly late onset of the last interglacial in central Europe. *Quaternary Research* 75, 213-218.

Chapter 3

Sier, M. J., and Dekkers, M. J. (2013). Magnetic property analysis as palaeoenvironmental proxy: a case study of the Last Interglacial Middle Palaeolithic site at Neumark-Nord 2 (Germany) In “Multidisciplinary Studies of the Middle Palaeolithic Record from Neumark-Nord (Germany)” (S. Gaudzinski-Windheuser, and W. Roebroeks, Eds.), Saxony-Anhalt, Germany.

Chapter 4

Sier, M. J., Peeters, J., Dekkers, M. J., Parés, J. M., Chang, L., Busschers, F. S., Wallinga, J., Frans P.M. Bunnik and Roebroeks, W. (in prep). The Blake Event recorded near the Eemian Type locality – revised timing of the onset of the Eemian in north-western Europe.

Chapter 5

Sier, M. J., Parés, J. M., Antoine, P., Loch, J. L., Dekkers, M. J., and Roebroeks, W. (submitted in revised form). Palaeomagnetic results of the Eemian archaeological site of Caours, France. *Quaternary International*.

Not in this thesis

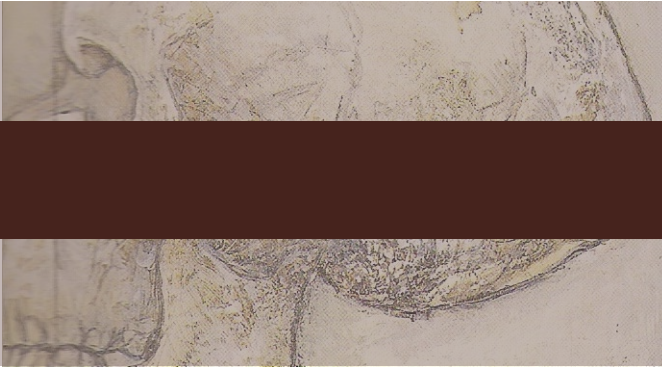
Dupont-Nivet, G., Sier, M., Campisano, C. J., Arrowsmith, R., DiMaggio, E., Reed, K., Lockwood, C. A., Franke, C., and Hüsing, S. (2008). Magnetostratigraphy of the eastern Hadar Basin (Ledi-Gerau research area, Ethiopia) and implications for hominin paleoenvironments. In "The Geology of Early Humans in the Horn of Africa." (J. Quade, and J. G. Wynn, Eds.), pp. 67-85.

Joordens, J. C. A., Vonhof, H. B., Feibel, C. S., Lourens, L. J., van der Lubbe, H. J. L., Dupont-Nivet, G., Sier, M. J., Davies, G. R., and Kroon, D. (2011). An astronomically-tuned climate framework for hominins in the Turkana Basin. *Earth and Planetary Science Letters* 307, 1-8.

Roebroeks, W., Sier, M. J., Nielsen, T. K., De Loecker, D., Parés, J. M., Arps, C. E. S., and Múcher, H. J. (2012). Use of red ochre by early Neandertals. *Proceedings of the National Academy of Sciences* 109, 1889-1894.

Joordens, J. C. A., Dupont-Nivet, G., Feibel, C. S., Spoor, F., Sier, M. J., Lubbe, J. H. J. L. v. d., Nielsen, T. K., Knul, M., Davies, G. R., and Vonhof, H. B. (in press). Improved age control on early Homo fossils from the upper Burgi Member at Koobi Fora, Kenya. *Journal of Human Evolution*.

Pias Peleteiro, J. M., Aldrey-Vázquez, J. M., Martínón-Torres, M., and Sier, M. J. (in press). El torvisco (*Daphne gnidium* L.): un timbó ancestral europeo. *Revista de Neurología*.



CHAPTER 1

INTRODUCTION



CHAPTER 1

INTRODUCTION

Modern humans are distributed all over the globe, occupying a wide variety of habitats. However, we can infer from the fossil record that earlier hominins had more limited geographic distributions. Starting from one or more core areas in Africa, hominins slowly expanded (as well as contracted) their geographical ranges over the last two to three million years to their present day distribution. Changes in geographic ranges are mostly attributed to climate change, environmental variation and technological innovations that provide new ways of exploiting or competing for resources (e.g. Dennell, 2003; Potts, 2012; Roebroeks, 2001). Thus, understanding the nature and variation of dispersals within a geographic range together with the corresponding climatic and environmental variations may provide us with data to study changes in the behaviour or biology of hominins that allowed them to colonize or adapt to a specific geographical region (e.g. Dennell and Roebroeks, 2005; Joordens et al., 2011; Roebroeks and Kolfshoten, 1994; Speleers, 2000).

Of all fossil hominin species, *Homo neanderthalensis* is not only the first to be discovered but it is also the most numerous in terms of fossil specimens and in studied archaeological sites. This, together with the long European research history, makes *Homo neanderthalensis* the best known hominin species after *Homo sapiens*. However, many details of the geographic range of the Neandertal lineage and especially modifications of this range through time are still poorly understood. Especially, a better knowledge of the migration of *Homo neanderthalensis* towards, and occupation of, middle and higher latitudes after glacial periods would be instrumental for our understanding of their limitations in terms of the biological and cultural capacities of this species (e.g. Potts, 2012; Roebroeks, 2001). In this respect, one of the key periods in Europe to assess the Neandertal ecological niche is the Eemian stage, also known as the Last Interglacial or

Marine Isotope Stage (MIS) 5e, the last and best documented interglacial stage in which Neandertals were present in Europe.

During the end of the 19th and the beginning of the 20th century, warm and temperate interglacial periods were considered ideal for the survival of hominins, because of their high faunal diversity and their climatically favourable conditions. It was even hypothesized that hominins did not need living structures or other forms of protection against the elements for survival (Obermaier, 1912). However, in the mid 1980's alternative interpretations arose. Steered by the ecological studies of hunter-gatherers of Kelly (1983), Gamble (1986) stated that interglacial Europe may have formed a hostile environment for hominins. That line of argument was based on the rationale that despite the biomass being higher during an interglacial period in comparison to a glacial period, most biomass is stored in primary biomass. Primary biomass consists of leave and stems of plants which are mostly inedible for hominins. Given the rarity of traces of full-interglacial occupation, Gamble (1986, 1987) concluded that, in contrast to the modern human hunter-gatherers of the Holocene, hominins in Last interglacial Europe lacked the social structures, specialized knowledge and skills that would have enabled them to survive in this type of ecosystem (Gamble, 1986; Gamble, 1987). The lack of well dated Eemian stage sites in north-western Europe with good indications of Neandertal presence was central in Gamble's theory. In terms of site distribution, this observation remains true for the British Isles. However, for the rest of north-western Europe it was refuted in 1992, when Roebroeks and colleagues (1992) proved, by analyzing in detail the chronological, archaeological and palaeoecological record available for this region and period, that not only there were archaeological sites in north-western Europe during glacial periods but also in fully interglacial deciduous forest conditions, long before the Upper Palaeolithic.

The debate about Neandertal ecological tolerances, particularly in north-western Europe, is however still ongoing, with the real limits of their distribution, in both time and space being an important issue. To investigate this distribution, it is essential to have reliable dates of the sites of interest, which place these occurrences in a precise chronological framework and thus facilitate consistent inter-site comparisons of the time and conditions of the occupation. The studies presented in this thesis aim to contribute to the debate by developing more precise correlations between the chronology and the environmental conditions of certain north-western European sites with documented *Homo neanderthalensis* presence. The studies use one of the main tools to build reliable geochronological frameworks for the study of early human evolution, but one which

has seen only very limited application in the Neandertal time range. This tool concerns the identification of certain palaeomagnetic reversals and excursions. The first are well documented full reversals, the latter are short-duration anomalies or events of the Earth's magnetic field (e.g. Laj and Channell, 2007; Merrill and McFadden, 1994). The behaviour of the earth's magnetic field is recorded in the sediments while they are being formed. Thus, from a sedimentary sequence a geomagnetic record can be retrieved and scrutinized for its veracity (post-depositional diagenetic processes may alter the record). As will be explained below in detail, the identification of a specific palaeomagnetic event, the so-called Blake Event, is an important new aid in the study of the Neandertal occupation of north-western Europe. The Blake Event, a palaeomagnetic excursion which occurs during our period of interest, has been correlated to MIS 5e (e.g. Channell et al., 2012; Thouveny et al., 2004) and can be used as a tool for environmental, marine and terrestrial sedimentary correlations.

However, in order to make meaningful inter-site comparisons of thin time slices it is necessary to clarify the relationship among the different "interglacial terminologies". The Eemian stage, Last Interglacial and MIS 5e are concepts which are often used as virtual synonyms in the archaeological literature, but with each having its own definition; the Eemian stage was defined on the basis of sediments in a terrestrial record while MIS 5e was defined on basis of the study of fossils from marine sediments. The term "Last Interglacial" has no clear definition and is being used indiscriminately, to both indicate Eemian stage as well as MIS 5e sediments. Also the correlation of the marine and terrestrial records is less straightforward than previously thought (Sánchez-Goñi et al., 1999; Shackleton et al., 2003), with significant consequences for our views of past climate changes, as will be explained in this thesis.

Summarizing, the main goal of this thesis is to provide a better geochronological control of the Last Interglacial or Eemian stage in north-western Europe and to add to the palaeoenvironmental dataset of this period. North-western Europe is of particular interest, as it is the region where the Eemian stage was defined, and as it is under the strong influence of glaciations which, in turn, had a profound effect on the range of hominin occupations.

Background on terminology

It is important to stress the differences between the several terms used to describe our period of study. Often, the terms Eemian stage, Last Interglacial and MIS 5e are used indiscriminately in the literature. It is true that there is a large chronological overlap between the time periods these three terms refer to but all three have different definitions. The boundaries need not be synchronous and may even be diachronous from one region to another.

Harting was the first to use the term Eemian as a stratigraphic unit, back in 1874 (Harting, 1874). During his investigations of the sediments near Amsterdam and Amersfoort, he noticed a consistent occurrence of sands and clays containing abundant diatom and mollusc fossils. Among the fossil molluscs, there were Mediterranean and Lusitanian species which do not occur in the present-day Netherlands. Unable to correlate the stratigraphic unit with the known ones, Harting introduced a new stratigraphic unit, the Eemian (after the Dutch river Eem). With the development of Eemian pollen research from the late 1920's onwards, it became possible to identify the non-mollusc pollen-bearing levels of the Eemian. This also improved correlations of sequences over large parts over Europe and enabled studies of the Eemian vegetation development (for a recent overview see Bosch et al., 2000). The first pollen research of the Eemian stage in Denmark and northwest Germany indicated a temperate flora with woodland dominated phases (Jessen and Milthers, 1928). In the middle of the last century, Zagwijn (1961) restudied the Amersfoort section of Harting and expanded on the work of Van der Vlerk and Florschütz (1950; 1953). They had defined the Eemian stage, similar to Jessen and Milthers before them (1928), on the basis of the vegetation succession as reconstructed from the pollen record. The lower boundary of the Eemian stage was placed where tree taxa exceed 50% of the total terrestrial pollen sum and the upper boundary where the pollen signal falls below the 50%, stratigraphically in between the open vegetation of the Saalian and Weichselian glaciations (Zagwijn, 1961). For a long time, the Amersfoort section served as the stratotype locality of the Eemian stage. As a result of discussions about the delimitation and identification of the Eemian stage, the Geological Survey of the Netherlands was asked during the 1995 INQUA (International Union for Quaternary Research) Congress to re-investigate the type area (van Kolfschoten and Gibbard, 2000). Some results of the TNO (Dutch Geological Survey) Eemian stage project were published in a special volume of the Netherlands Journal of Geosciences (volume 79, 2/3, 2000). The

stratotype locality was re-evaluated (Cleveringa et al., 2000) and a parastratotype was selected in borehole 'Amsterdam-Terminal' (Cleveringa et al., 2000; de Gans et al., 2000; van Kolfschoten and Gibbard, 2000; van Leeuwen et al., 2000). Moreover, the Amsterdam-Terminal borehole publication provided the basis for a proposal to assign the official base of the Late Pleistocene; this still awaits formal approval of the international commission on stratigraphy (Gibbard, 2003; Gibbard et al., 2008). A problem for this boundary, as this thesis will show, is its diachroneity, as moving south of the Netherlands the proposed boundary increases in age.

The duration of the Eemian stage in north-western Europe has been constrained to approximately 11,000 years by varve counting and extrapolation of sedimentation rates at the German site of Bispingen (Müller, 1974), confirmed by studies of other localities north of the Alps (Turner, 2002). Various estimates exist for the duration of the Eemian stage in southern Europe, from around 15,500 years (Tzedakis et al., 2003) to ~16,000 years (Shackleton et al., 2003) and to 16,400 years (Sánchez-Goñi et al., 1999). The difference in age duration estimates for the north and the south of Europe already suggests diachroneity of the upper or lower boundary (or both) of the Eemian stage. In order to distinguish between the Eemian stage in northern and southern Europe, we use the term Eemian stage *sensu stricto* for Eemian stage in northern Europe.

It needs to be emphasized that the definition of Last Interglacial is not a straightforward one. An interglacial is defined as a period of warmer climate, much like the present day climate or warmer, which separates two glacial periods. Or as Fairbanks (1972: 293) puts it, "A certain formation is said to be "interglacial" if it is characterized by an assemblage of sediments, soil, fauna or flora that are characteristic of climatic conditions generally as warm as or warmer than today". The problem is that these boundaries are inherently diachronous (Fairbridge, 1972) e.g. due to migration of flora and fauna. Recognizing an interglacial in the geological record is difficult, and setting boundaries is even more complicated (Kukla et al., 2002). In practice, pollen stratigraphy is used for defining an interglacial in terrestrial sediments and oxygen-isotope ratios are employed to establish MIS boundaries in marine sediments. These boundaries between land and sea may not correspond in time and correlating over large geographical areas can only be done with a global chronological marker that is not restricted to either the terrestrial record or the marine record. Palaeomagnetic reversals and excursions, if present and identifiable in the studied time period, are excellent global chronological markers.

The development of the MIS record represented a major advancement in Quaternary stratigraphy (e.g. Shackleton, 1967; Shackleton, 1987). In the MIS record, changes in the oxygen isotope ratios of benthic foraminifera indicate changes in global ice volume and by inference, warm and cold periods can be identified over time. The precise boundaries between periods with high and low sea levels are to some extent arbitrary, for the “last interglacial” (or MIS 5e) drawn halfway on the curve between the minimum and maximum oxygen isotope values of MIS 5d/5e (upper boundary) and MIS 5e/6 (lower). Just as the boundaries of the Eemian stage, these boundaries are arbitrary but more likely to be global as they reflect changes in global ice volume. MIS 5e has been correlated to the Eemian stage by means of amino acid racemization of shells from the distinctive sediments by Miller and Mangerud (1985), but the precise relation of the boundaries remained unclear until the work of Sánchez-Goñi and colleagues (Sánchez-Goñi et al., 1999). They analyzed a marine core taken from offshore Iberia and used pollen, washed in from terrestrial settings, to correlate the southern Europe Eemian stage with the MIS record from the same core. They concluded that the lower boundary of the Eemian stage is around 5000 to 6000 years younger with respect to the lower boundary of MIS 5e (Sánchez-Goñi et al., 1999; Shackleton et al., 2003). This method, however, cannot work for terrestrial records as no direct MIS record is registered in terrestrial sediments.

Fortunately, there is a global stratigraphic marker around the period of our interest, the palaeomagnetic Blake Event. The Blake Event was first discovered in 1969 in marine cores taken near the Blake Outer Ridge, western subtropical North Atlantic (Smith and Foster, 1969) and, in recent years, it has served as a marker event for MIS 5e (e.g. Laj and Channell, 2007; Langereis et al., 1997; Lourens, 2004). Short polarity intervals like the Blake Event are global and can be recorded both in marine and terrestrial records. Even though the chronostratigraphic relation between MIS 5e and the Blake Event is quite well established, no terrestrial records are known that contain both an Eemian stage pollen signal and the palaeomagnetic Blake Event.

Key Research Questions and outline of thesis

As mentioned in the introduction, the overall goal of this thesis is contribute to a better geochronological control of, and add to, the palaeoenvironmental dataset of the Eemian stage in north-western Europe. This study is performed in order to contribute to our understanding of the distribution limits of Neandertals in north-western Europe and thus, their ecological tolerance. The following key research questions were put forward.

1. To identify, by means of detailed palaeomagnetic studies, the chronostratigraphic marker known as the Blake Event in Eemian stage sites such as Neumark-Nord 2 (Germany), Caours (France) and Rutten Gemaalweg (The Netherlands) of north-western Europe (see figure 1).

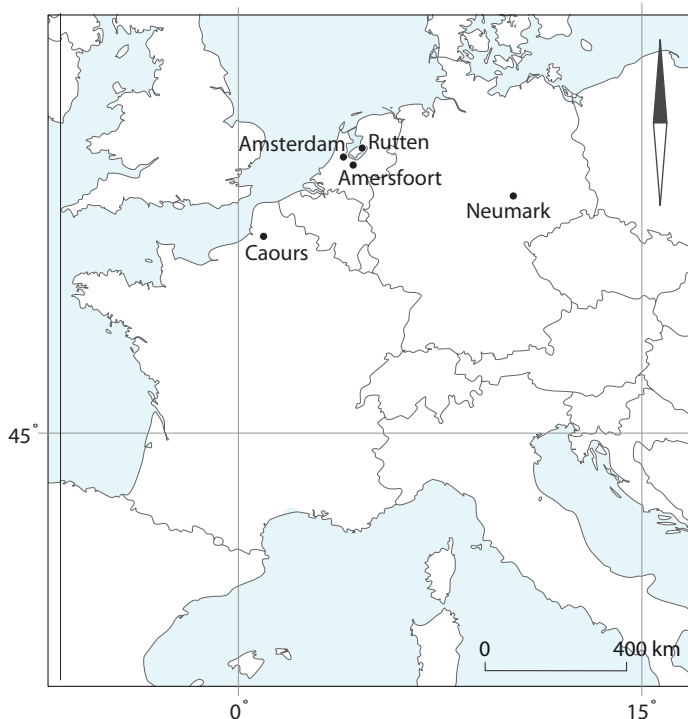


Figure 1.

Location map with the sites of Caours (France), Rutten (The Netherlands) and Neumark-Nord 2 (Germany) and the Eemian stage type-localities of Amsterdam and Amersfoort.

2. To get a better age control of the Blake Event by collecting new palaeomagnetic, environmental magnetic and palaeoenvironmental data and by reviewing published datasets.
3. To establish the relationship between the Blake Event and the environmental developments within the Eemian stage.
4. To evaluate the consequences of the newly dated Eemian stage sites and their palaeoenvironment for our understanding of hominin behaviour in north-western Europe.

Research questions 1, 2 and 3 will be discussed in chapters 2 through 5, while research question 4 will be treated in chapter 6 of this thesis. Chapters 2 and 3 present the palaeomagnetic, environmental magnetic and palaeoenvironmental research of the Neumark-Nord 2 archaeological site near Halle (Germany). Chapter 4 furnishes a test of the interpretation of the dataset of Neumark-Nord 2 and expands on the data collected there. This chapter is based on an interdisciplinary study of an orientated core from the village of Rutten (the Netherlands). Rutten was chosen as a location due to its vicinity to the Eemian stage “type localities” (Amersfoort, Amsterdam) and the expected presence of a complete Eemian stage pollen sequence in the sediments sampled in the core. The study uses the palaeomagnetic signal to compare the timing of the Eemian stage with the signal found in Neumark Nord 2 in order to provide better estimates on the duration of the Blake Event. Both in Neumark Nord 2 and Rutten, the palaeomagnetic Blake Event has been identified in conjunction with high-resolution and high-quality pollen data which enabled the identification of the Eemian stage, sandwiched in between Saalian and Weichselian deposits at both locations. As the Blake Event is a global chronostratigraphic marker, independent of marine or terrestrial environments, we were able to correlate the Eemian stage (*sensu stricto*) of the Neumark Nord 2 and Rutten records to the MIS record.

The final site where fieldwork was done for this thesis is the Last Interglacial archaeological site of Caours, in the Somme valley, in northern France (Antoine et al., 2006; Antoine et al., 2007) discussed in chapter 5. At this site, palaeomagnetism was used for chronostratigraphic purposes. Caours is well-dated to the Last Interglacial by means of a variety of dating methods, including U-series and electron spin resonance (Antoine et

al., 2006; Bahain et al., 2010). The identification of the Blake Event within the sequence is important as it may narrow down the uncertainty in the age range.

The palaeomagnetic behavior of the Blake Event is also briefly discussed in chapter 5 as the characteristic remanent magnetism (ChRM) directions of the Blake Event identified at Neumark Nord 2, Rutten and Caours offer possible insights into the behaviour of the earth's magnetic field during that period in north-western Europe.

A synthesis of the main conclusions of this thesis is given in chapter 6 together with some possible consequences for our understanding of hominin behaviour. This final chapter finishes with recommendations for future research.

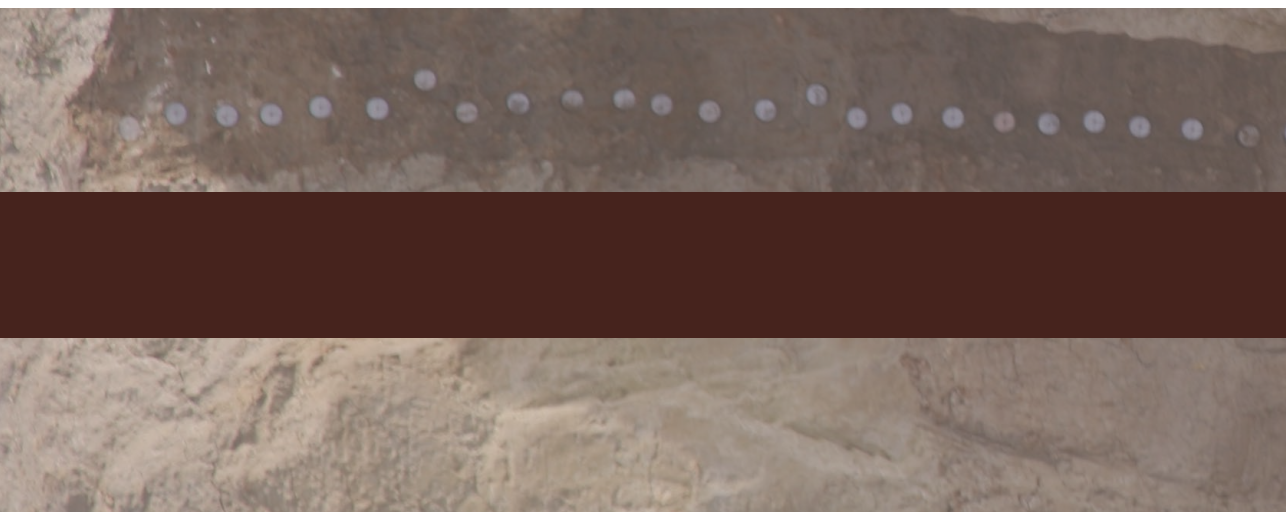
References

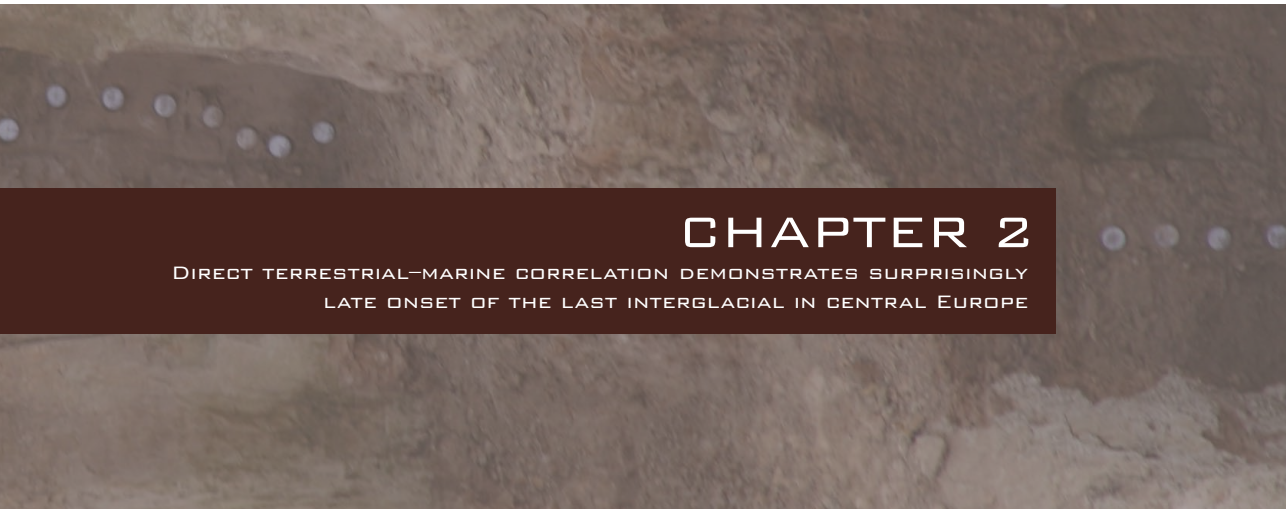
- Antoine, P., Limondin-Lozouet, N., Auguste, P., Loch, J. L., Galheb, B., Reyss, J., Escudé, E., Carbonel, P., Mercier, N., Bahain, J. J., Falguères, C., and Voinchet, P. (2006). Le tuf de Caours (Somme, France) : mise en évidence d'une séquence eemienne et d'un site paléolithique associé. *Quaternaire* 17, 281-320.
- Antoine, P., Limondin Lozouet, N., Chaussé, C., Lautridou, J. P., Pastre, J. F., Auguste, P., Bahain, J. J., Falguères, C., and Galehb, B. (2007). Pleistocene fluvial terraces from northern France (Seine, Yonne, Somme): synthesis, and new results from interglacial deposits. *Quaternary Science Reviews* 26, 2701-2723.
- Bahain, J. J., Falguères, C., Dolo, J. M., Antoine, P., Auguste, P., Limondin-Lozouet, N., Loch, J. L., Tuffreau, A., Tissoux, H., and Farkh, S. (2010). ESR/U-series dating of teeth recovered from well-stratigraphically age-controlled sequences from Northern France. *Quaternary Geochronology* 5, 371-375.
- Bosch, J. H. A., Cleveringa, P., and Meijer, T. (2000). The Eemian stage in the Netherlands: History, character and new research. *Geologie en Mijnbouw/Netherlands Journal of Geosciences* 79, 135-145.
- Cleveringa, P., Meijer, T., van Leeuwen, R. J. W., de Wolf, H., Pouwer, R., Lissenberg, T., and Burger, A. W. (2000). The Eemian stratotype locality at Amersfoort in the central Netherlands: are-evaluation of old and new data. *Netherlands Journal of Geosciences* 79, 197-216.
- Channell, J. E. T., Hodell, D. A., and Curtis, J. H. (2012). ODP Site 1063 (Bermuda Rise) revisited: oxygen isotopes, excursions and paleointensity in the Brunhes Chron. *Geochemistry Geophysics Geosystems* 13, Q02001.
- de Gans, W., Beets, D. J., and Centineo, M. C. (2000). Late Saalian and Eemian deposits in the Amsterdam glacial basin. *Netherlands Journal of Geosciences* 79, 147-160.
- Dennell, R. (2003). Dispersal and colonisation, long and short chronologies: how continuous is the Early Pleistocene record for hominids outside East Africa? *Journal of Human Evolution* 45, 421-440.
- Dennell, R., and Roebroeks, W. (2005). An Asian perspective on early human dispersal from Africa. *Nature* 438, 1099-1104.
- Fairbridge, R. W. (1972). Climatology of a glacial cycle. *Quaternary Research* 2, 283-302.
- Gamble, C. (1986). "The Palaeolithic settlement of Europe." Cambridge University Press, Cambridge.

- Gamble, C. S. (1987). Man the shoveler: Alternative models for Middle Pleistocene colonization and occupation in Northern latitudes. In "The Pleistocene old world. Regional perspectives." (O. Soffer, Ed.), pp. 81-98. Plenum Press, New York.
- Gibbard, P. L. (2003). Definition of the Middle-Upper Pleistocene boundary. *Global and Planetary Change* 36, 201-208.
- Gibbard, P. L., Cohen, K. M., and Ogg, J. G. (2008). Quaternary Period. In "The concise Geologic Time Scale." (J. G. Ogg, G. Ogg, and F. M. Gradstein, Eds.), pp. 178, Cambridge.
- Harting, P. (1874). De bodem van het Eemdal. Verslagen en Verhandelingen Koninklijke Academie van Wetenschappen, 282-290.
- Jessen, K., and Milthers, V. (1928). Stratigraphical and paleontological studies of interglacial freshwater deposits in Jutland and Northwest Germany. *Danmarks geologiske undersoegelse* 48.
- Joordens, J. C. A., Vonhof, H. B., Feibel, C. S., Lourens, L. J., van der Lubbe, H. J. L., Dupont-Nivet, G., Sier, M. J., Davies, G. R., and Kroon, D. (2011). An astronomically-tuned climate framework for hominins in the Turkana Basin. *Earth and Planetary Science Letters* 307, 1-8.
- Kukla, G. J., Bender, M. L., de Beaulieu, J.-L., Bond, G., Broecker, W. S., Cleveringa, P., Gavin, J. E., Herbert, T. D., Imbrie, J., Jouzel, J., Keigwin, L. D., Knudsen, K.-L., McManus, J. F., Merkt, J., Muhs, D. R., Müller, H., Poore, R. Z., Porter, S. C., Seret, G., Shackleton, N. J., Turner, C., Tzedakis, P. C., and Winograd, I. J. (2002). Last Interglacial Climates. *Quaternary Research* 58, 2-13.
- Laj, C., and Channell, J. E. T. (2007). Geomagnetic Excursions. In "Geomagnetism." (M. Kono, Ed.), pp. 373-416. *Treatise on Geophysics* Elsevier, Amsterdam.
- Langereis, C. G., Dekkers, M. J., Lange, G. J., Paterne, M., and Santvoort, P. J. M. (1997). Magnetostratigraphy and astronomical calibration of the last 1.1 Myr from an eastern Mediterranean piston core and dating of short events in the Brunhes. *Geophysical Journal International* 129, 75-94.
- Lourens, L. J. (2004). Revised tuning of Ocean Drilling Program Site 964 and KC01B (Mediterranean) and implications for the D180, tephra, calcareous nannofossil and geomagnetic reversal chronologies of the past 1,1 Mys. *Paleoceanography* 19, PA3010.
- Merrill, R. T., and McFadden, P. L. (1994). Geomagnetic field stability: Reversal events and excursions. *Earth and Planetary Science Letters* 121, 57-69.

- Miller, G. H., and Mangerud, J. (1985). Aminostratigraphy of European marine interglacial deposits. *Quaternary Science Reviews* 4, 215-278.
- Müller, H. (1974). Pollenanalytische Untersuchungen und Jahresschitzenzählungen an der eem-zeitlichen Kieselgur von Bispingen/Luhe. *Geologisches Jahrbuch A21*, 149-169.
- Obermaier, H. (1912). "Der Mensch der Vorzeit." AVG, Berlin.
- Potts, R. (2012). Environmental and Behavioral Evidence Pertaining to the Evolution of Early Homo. *Current Anthropology* 53, S299-S317.
- Roebroeks, W. (2001). Hominid behaviour and the earliest occupation of Europe: an Exploration. *Journal of Human Evolution* 41, 437-461.
- Roebroeks, W., Conard, N. J., and van Kolfschoten, T. (1992). Dense Forests, Cold Steppes, and the Palaeolithic Settlement of Northern Europe. *Current Anthropology* 33, 551-586.
- Roebroeks, W., and Kolfschoten, v. T. (1994). The earliest occupation of Europe: a short chronology. *Antiquity* 68, 489-503.
- Sánchez-Goñi, M. F., Eynaud, F., Turon, J. L., and Shackleton, N. J. (1999). High resolution palynological record off the Iberian margin: direct land-sea correlation for the Last Interglacial complex. *Earth and Planetary Science Letters* 171, 123-137.
- Shackleton, N. (1967). Oxygen Isotope Analyses and Pleistocene Temperatures Re-assessed. *Nature* 215, 15-17.
- Shackleton, N. J. (1987). Oxygen isotopes, ice volume and sea level. *Quaternary Science Reviews* 6, 183-190.
- Shackleton, N. J., Sánchez-Goñi, M. F., Paillet, D., and Lancelot, Y. (2003). Marine Isotope Substage 5e and the Eemian Interglacial. *Global and Planetary Change* 36, 151-155.
- Smith, J. D., and Foster, J. H. (1969). Geomagnetic Reversal in Brunhes Normal Polarity Epoch. *Science* 163, 565-567.
- Speleers, B. (2000). The relevance of the Eemian for the study of the Palaeolithic occupation of Europe. *Geologie en Mijnbouw* 79, 283-291.
- Thouveny, N., Carcaillet, J., Moreno, E., Leduc, G., and Nérini, D. (2004). Geomagnetic moment variation and paleomagnetic excursions since 400 kyr BP: a stacked record from sedimentary sequences of the Portuguese margin. *Earth and Planetary Science Letters* 219, 377-396.
- Turner, C. (2002). Problems of the Duration of the Eemian Interglacial in Europe North of the Alps. *Quaternary Research* 58, 45-48.

- Tzedakis, P. C., Frogley, M. R., and Heaton, T. H. E. (2003). Last Interglacial conditions in southern Europe: evidence from Ioannina, northwest Greece. *Global and Planetary Change* 36, 157-170.
- Van der Vlerk, I. M., and Florschütz, F. (1950). "Nederland in het IJstijdvak." De Haan Utrecht.
- van der Vlerk, I. M., and Florschütz, F. (1953). The palaeontological basis of the subdivision of the Pleistocene in the Netherlands. *Verhandeling Koninklijke Nederlandse Akademie van Wetenschappen* 1, 1-58.
- van Kolfschoten, T., and Gibbard, P. L. (2000). The Eemian - local sequences, global perspective: introduction. *Geologie en Mijnbouw/Netherlands Journal of Geosciences* 79, 129-133.
- van Leeuwen, R. J. W., Beets, D. J., Bosch, J. H. A., Burger, A. W., Cleveringa, P., van Harten, D., Waldemar Herengreen, G. F., Kruk, R. W., Langereis, C. G., Meijer, T., Pouwer, R., and de Wolf, H. (2000). Stratigraphy and integrated facies analysis of the Saalian and Eemian sediments in the Amsterdam-Terminal borehole, the Netherlands. *Netherlands Journal of Geosciences* 79, 161-196.
- Zagwijn, W. H. (1961). Vegetation, climate and radiocarbon datings in the late Pleistocene of the Netherlands: I. Eemian and Early Weichselian, *Nieuwe Serie. Mededelingen van de Geologische Stichting* 14, 15-45.





CHAPTER 2

DIRECT TERRESTRIAL-MARINE CORRELATION DEMONSTRATES SURPRISINGLY
LATE ONSET OF THE LAST INTERGLACIAL IN CENTRAL EUROPE



CHAPTER 2

DIRECT TERRESTRIAL – MARINE CORRELATION DEMONSTRATES SURPRISINGLY LATE ONSET OF THE LAST INTERGLACIAL IN CENTRAL EUROPE

Introduction

Large scale excavations of the Middle Palaeolithic site Neumark Nord 2 (NN2), Germany, carried out between 2004 and 2008, yielded a rich archaeological assemblage, containing ca. 20,000 Middle Palaeolithic flint artifacts and approximately 120,000 faunal remains, dominated by warm-temperate species. The fauna includes straight tusked elephants, rhinoceroses, bovids, equids, deer, bear, small carnivores and the pond tortoise *Emys orbicularis*. Excavations took place in an open cast lignite quarry, south of Halle (Germany), where the archaeology was contained within the infill of a small and shallow sedimentary basin, resulting from diapirism-related movements in the underlying Tertiary lignite deposits (Eissmann, 2002, Mania and Mania, 2008) (Fig. 1). In order to develop a fine-grained palaeoenvironmental and chronological framework for the unique archaeological record from the site, the basin infill was studied using a wide range of techniques. These interdisciplinary studies yielded climatic and chronological proxy records which are of great relevance to the study of the last interglacial and more importantly, enable precise terrestrial-marine correlation for the Eemian stage in central and north-western Europe.

The Neumark Nord 2 basin

The basin (51°19'28" N, 11°53'56" E) developed after the deposition of a diamicton (unit 1 in Fig. 2), a till which can be up to 10m thick in the NN2 area. The infill of the basin starts with loamy and sandy deposits that mainly consist of reworked diamicton material (unit 2 in Fig. 2), overlain by well-sorted silt loams, 6 to 8 m thick (units 3-19, Fig. 2), mostly deposited during the last interglacial. The main archaeological find horizon (within unit 8) is situated in the middle part of these silt loams (Fig. 1). The basin infill is overlain by approximately 6 m of last glacial loess.

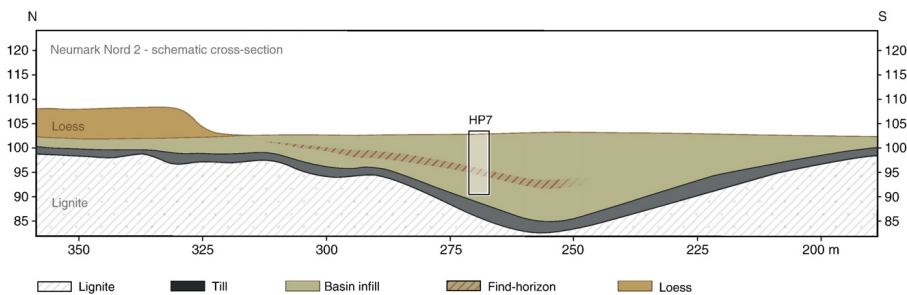


Figure 1.

Schematic north-south cross section of the Neumark-Nord 2 basin and its infill including the stratigraphic position of the archaeological find horizon. The box inset refers to the HP7 section (Fig. 2), described in detail in the Supplemental material. Vertical axis: height in meters above sea level. Horizontal axis: position of the NN2 basin in excavation grid, in meters.

The infill, its genesis, and the artifact-bearing deposits in particular were meticulously documented in a large number of sections throughout the excavation. A key section here is Hauptprofil (HP) 7 (Fig. 2), cutting through the deep part of the infill (see Fig. 1). This section was sampled for a wide range of dating techniques and palaeo - environmental studies, which include sedimentological and micromorphological studies (see Supplementary Material (SM)). Further, pollen, macrobotanical remains and molluscs (for environmental reconstruction and multiple amino acid racemisation analysis) were collected. Finally, a high-resolution set of palaeomagnetic samples was acquired. It is important to note that most samples were collected from the very same part of the HP7 section, enabling a direct comparison of the results on a 5-cm stratigraphic sampling interval over the entire sequence (see SM).

All data indicate a geologically rapid infilling of a shallow basin. Micromorphological studies (see SM) show that sedimentation was a nearly continuous process, without pronounced soil formation in periods of non-deposition. Calcareous silt loams dominate the infill; these were deposited by overland flow in a very calm sedimentary setting in placid water, with only very short (<1 decade) interruptions during which the depression fell dry. Because of the high sedimentation rate, traces of bioturbation and soil formation are virtually absent throughout the sequence, apart from some gypsum formation in the top of the sequence and occasionally occurring gley phenomena. In the upper part of the infill (the top 50 cm of the interglacial sediments), the sedimentation rate decreases.

The age of this interglacial succession is constrained by the underlying diamicton, a till of late Saalian/Drenthe age (Eissmann, 2002), and by the overlying Weichselian gravel and loessic deposits. Multiple amino acid racemisation analysis of a large series of *Bithynia tentaculata* opercula (Penkman et al., 2008) from the HP7 sequence (see SM) suggests that the deposits are contemporaneous with those at the Eemian type locality at Amersfoort (the Netherlands) (Zagwijn, 1961) and last interglacial occurrences in the United Kingdom (see also SM). Additional confirmation of the last interglacial age is provided by thermoluminescence (TL) dating of five heated flint artifacts from the archaeological level, which yielded 126 ± 6 ka as the weighted mean age estimate (see SM). Pollen studies (see SM) also demonstrate a last interglacial age for the sequence. Pollen samples were taken at sections HP7 and neighboring HP10 (cf. Figs. 1 and 2). Unit 2, the reworked diamicton, contained pollen derived from the lignite deposits only, whereas the overlying silt loam (unit 3) was deposited in an environment with sparse vegetation at most, possibly reflecting a cold period (see SM). There is a good pollen record from unit 4 onward. Pollen is well-preserved, and the data show an interglacial succession that is typical of the Eemian interglacial in northern Europe (Turner, 2000; Zagwijn, 1961). This pollen succession starts with Pollen Zone I and ends with Zone VI/VII (*sensu* Menke and Tynni, 1984) at the top of the profile.

The palaeomagnetic signal

A total of 184 palaeomagnetic samples were collected from the NN2 exposures: 159 samples were taken from HP7 and 25 from a section nearby, in excavation square 210/296-297. Drill cores of sufficient length were cut into two specimens and demagnetised using both alternating fields (AF) and thermal demagnetisation, resulting in a total of 216 demagnetised samples. A small part of the base of the HP7 section previously sampled for other methods became inaccessible for palaeomagnetic studies due to increased security restrictions within the quarry. Based on the pollen data, this 80 cm part represents a period of 300 yr at most (see also Fig. 2 and Table 1).

The samples were stepwise demagnetised progressively in AF up to 100 mT (n=122), or thermally up to 600°C (n=42). A selected sample set was first heated to 205°C followed by alternating field demagnetisation (to 100 mT, n =42) to achieve optimal resolution (for the entire palaeomagnetic procedures, see SM). Typical demagnetisation diagrams (Zijderveld, 1967) are shown in Figure S7 of the SM. In the low-temperature or field range a present-day field overprint is observed, presumably of viscous origin. The characteristic remanent magnetisation (ChRM) is resolved after demagnetisation at temperatures > 200°C or alternating fields > 15-20 mT. As expected, it shows directional scatter because of secular variation of the Earth's magnetic field. A stratigraphically coherent zone (7.70-1.70 m) in the lower part of the interglacial sequence shows the clearly deviating directions that we associate with the Blake Event (Smith and Foster, 1969). In the samples with excursions directions, the overprint is always large. This is the result of a weak field during the excursion followed by a stronger field after return to stable normal polarity conditions. On top of that, a CRM overprint from greigite (NN2 is in a fresh-water setting) is acquired in the stronger post-excursion field (see SM for further details). This interferes with a clear-cut determination of the ChRM in those samples; their directions are characterized by slightly larger mean-angular deviations. The distinction between first and second quality data points (Fig. 2) is based on visual inspection of the Zijderveld diagrams. When a stable endpoint direction is observed the quality is labeled 1 (e.g., Neu117 in Fig. S7 of the SM). When curved endpoint trajectories or the directions not trending to the origin (but with GRM acquisition excluded, see SM) are noticed, quality is obviously lower and labeled as second. The distinction between the two categories is sometimes subtle given the large overprints present.

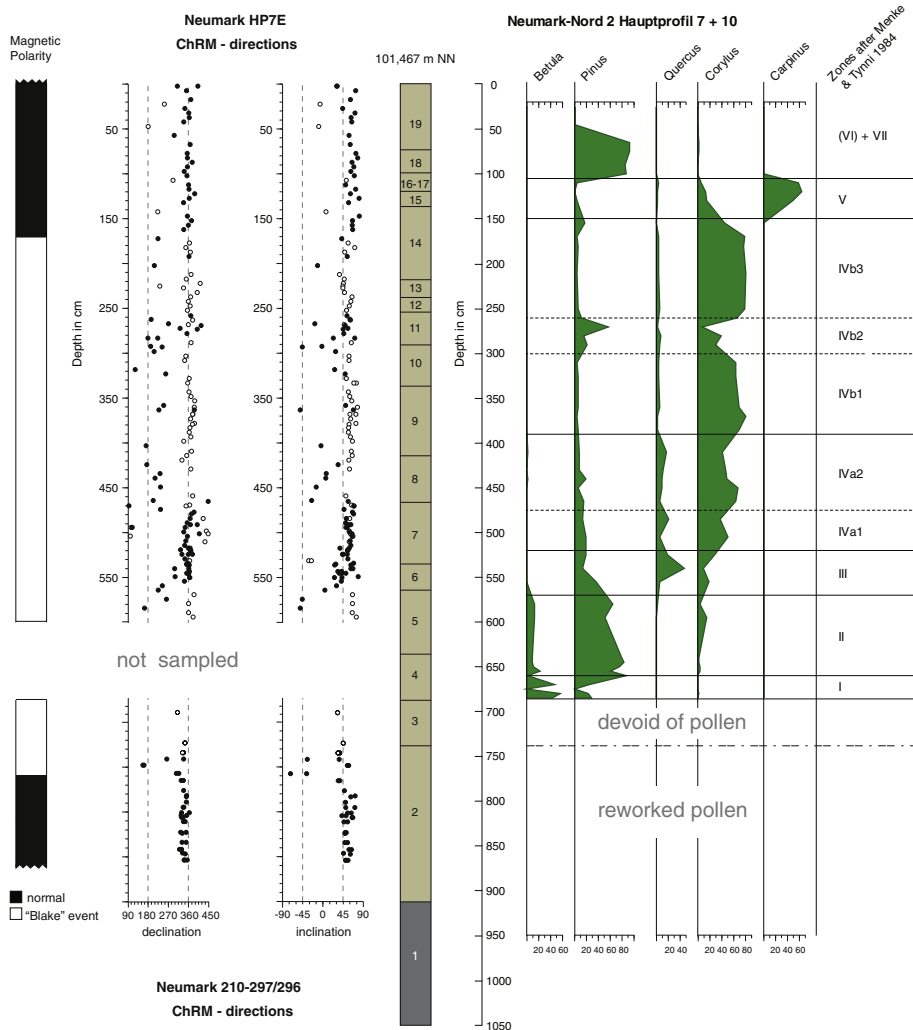


Figure 2.

Combined overview of the palaeomagnetic, stratigraphic and pollen data from HP7/10 and 210/297-296 samples. The top of the section (0 m) is at 101.467 m NN (= above sea level). The height between 570 and 455 cm in the ChRM-direction column is the normal intervening zone within the Blake Event (170-770 cm). The black dots of the ChRM directions refer to first quality data points, and the open circles are of secondary quality (see SM for details). For description of units 1 to 19 and background information on the methods see SM. The part for which no palaeomagnetic samples are available (Pollen Zone I and part of Zone II) has an estimated duration of maximally 300 yr. For duration of pollen zones and sedimentation rates see Table 1. The main archaeological find horizon is situated within unit 8.

To discriminate between regular secular variation and excursions or transitional directions, we applied the variable cut-off procedure (Vandamme, 1994) that considers directional outliers as excursions (see SM, Fig. S8). First quality excursions (i.e., the Vandamme outliers) are restricted to the stratigraphic zone 7.70-1.70 m. Below 7.70 m only first quality data points are present, yielding a firm basis for the lower boundary of the Blake Event. In the uppermost part of the sequence, above 1.70 m, all first quality data points are normal. The ChRM directions are likely to represent the field during sedimentation; i.e., the extent to which delayed acquisition of the natural remanent magnetization may have been possible is limited, given the high sedimentation rates (Table 1). Also soil formation during deposition of the NN2 sequence is virtually absent yielding a sequence that can be considered as continuous (see SM for details).

The behaviour of the magnetic field during the Blake Event (Smith and Foster, 1969) has been described by several authors (Tric et al., 1991; Reinders and Hambach, 1995; Fang et al., 1997; Laj and Channell, 2007). It is considered a 'double event' with two reversed intervals, intervened by a short normal period of about 1000 yr. The ChRMs versus stratigraphic level plot (Fig. 2) as well as the plot of directions calculated as Virtual Geomagnetic Poles (VGP) (Figs. 3a and b) show this magnetic field behaviour. It appears that the entire Blake Event is recorded at the Neumark Nord 2 site.

Table 1

Sedimentation rate in cm yr^{-1} for NN2 HP 7/10 for individual pollen zones, based on sediment thickness at NN2 (see Fig. 2) and duration of the Eemian pollen zones as counted at the Bispingen site (Muller, 1974). To calculate the time represented by the sediments containing the Blake Event below Pollen Zone I (units 3 and top of 2 in Fig. 2), we used a conservative sedimentation rate of 0.2 cm yr^{-1} .

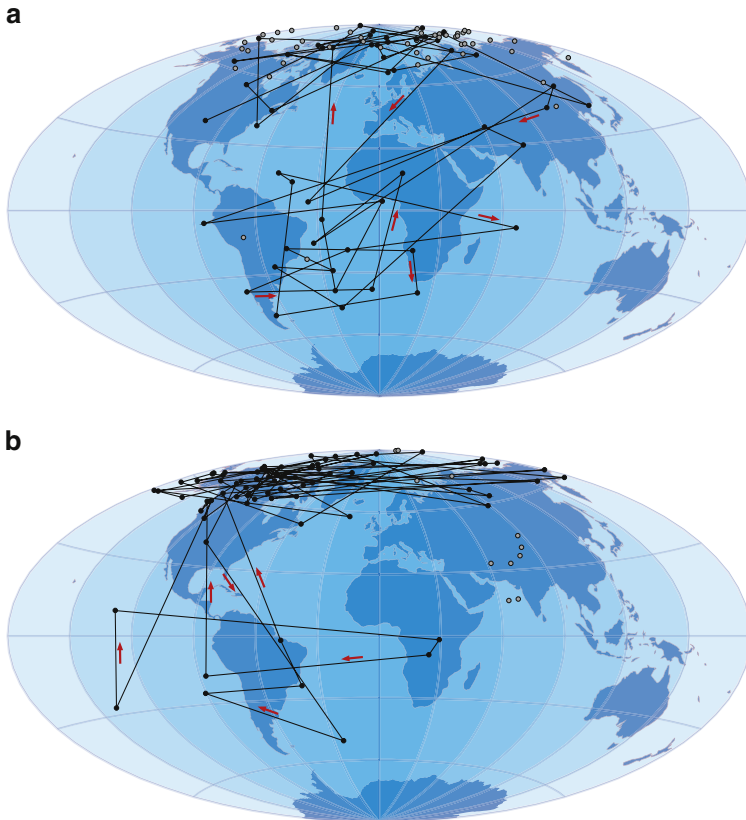
Pollen zone (Menke and Tynni, 1984)	Duration (in years) (Muller, 1974)	Sediment thickness in cm NN2 (see Fig. 2)	Sedimentation rate (cm yr^{-1}) NN2 HP7/10
	-100	30	0.33
II	-200	90	0.45
III	-450	50	0.11
IVa	-1200	130	0.11
	1000-1200	240	0.24-0.20

NN2 yields the longest well-documented record of the Blake Event in a continental setting with a high sedimentation rate (see SM for more details). Moreover it is well positioned within a high-resolution pollen sequence, which allows us to set constraints on its duration, enabling further research into the understanding of geodynamo processes that generate excursions like the Blake Event (Roberts, 2008). In the NN2 pollen sequence, the base of the Blake Event is situated in the unit 2 deposits (see SM) overlying the diamicton, more specifically at 0.87 m below the deposits of Pollen Zone I (*sensu* Menke and Tynni, 1984). The natural remanent magnetization (NRM) resumes normal polarity again within Pollen Zone IVb, in the *Corylus* phase of the interglacial. Notably, neither the beginning nor the end coincides with a vegetational or a sedimentary break in the sequence. Our record resembles that described by Tric et al. (1991), in that the lower excursion lasts for a shorter time than the upper one. Also, the recovery to post-Blake normal field directions is fairly gradual. The VGPs in Tric et al.'s record extend to almost fully reversed while those in our record are more 'intermediate', possibly related to the large overprint in the Neumark samples.

The duration of the Eemian interglacial in northern Europe is well constrained to approximately 11,000 yr by lamination counting at the Bispingen site in northern Germany (Muller, 1974), with studies from other Eemian locations yielding comparable results (Turner, 2002). At these locations, the duration of the various vegetation zones (I-IVb) has been counted for the earlier parts of the Eemian of relevance here, i.e. the pre-temperate and temperate substages (SM). Using this robust "floating" lamination chronology (Turner, 2002) we can assign sedimentation rates to the sediment units of Figure 2 (see Table 1). We conclude that the best estimate for the duration of the Blake Event is 3400 ± 350 yr. Our calculation supports the "short chronologies" in the duration estimates, which vary from 2.8 to 8.6 ka (Tric et al., 1991; Zhu et al., 1994; Fang et al., 1997; Thouveny et al., 2004).

Figure 3.

Plot of the VGP path during the Blake Event recorded in the Neumark Nord 2 basin. Panel b represents the base of the section (875 to 477 cm in Fig. 2) with a rapid (at 770 cm) first transitional phase of the record, similar to the record found by Tric et al. (1991), ending with a rebound phase, the intervening normal polarity part of the Blake Event. Panel a represents the top of the section (472 to 0 cm) with the second VGP swing and post-Blake normal NRM directions. Direction of VGP movement is indicated by the arrows. Gray dots are excluded from the VGP path.



Discussion

The NN2 record situates the Blake Event at the very end of the Saalian and in the first 3000 yr of the terrestrial Eemian of northwestern and central Europe, making it a very good marker for the much debated Middle-Upper Pleistocene boundary (Gibbard, 2003). In the terrestrial realm, using the Blake Event palaeomagnetic signal we can start large-scale comparisons of plant and animal communities within very fine time equivalent units. The NN2 data also allow us to make the first direct correlation between the terrestrial Eemian interglacial stage with Marine Isotope Stage (MIS) stratigraphy, which has been the subject of much debate in recent years (Sanchez-Goiñi et al., 1999; Shackleton et al., 2003). As in several marine cores, in cores from the Mediterranean Sea (Tucholka et al., 1987; Tric et al., 1991), the Blake Event is recorded within MIS 5e (Tucholka et al., 1987; Langereis et al., 1997; Laj and Channell, 2007) with the Blake Event beginning just above sapropel S5. For instance, in the MD84627 Blake record of Tric et al. (1991), the Blake Event starts ~400 yr after the deposition of sapropel S5 (see SM for discussion of possible delayed NRM acquisition). These data allow us to unambiguously correlate the NN2 data to the benthic $\delta^{18}\text{O}$ curve, as visualized in Figure 4, which yields the first direct correlation of a terrestrial Eemian climate sequence to the marine realm.

There are various age estimates for the S5 sapropel, with Lourens' (2004) midpoint age estimate of 124 ka generally accepted. Tucholka et al. (1987) showed a ~5 ka duration of S5 in the Tric et al.'s record, which gives the top of S5 an age of ~121.5 ka. The Blake Event started at 121.1 ± 0.5 ka under the proviso that the excursions behaviour is spatially synchronous within uncertainty (we compare an eastern Mediterranean with a central European record). In that age model the Eemian as recorded at NN2 would start at ~120.65 ka and last until ~109.65 ka.

The age of the Blake Event, and of the various Eemian vegetation zones at NN2 is dependent on the age estimate of sapropel S5; it will change along with possible future changes in the age estimate of that sapropel. The position of the terrestrial Eemian as recorded at NN2 within the MIS record is, however, fixed. Therefore, the NN2 data allow a firm correlation of a high-resolution terrestrial environmental sequence to the marine record. This will serve as a point of departure for future studies of the vegetation succession, climate change and palaeomagnetic data in a terrestrial setting, and their much debated relationships to contemporary events reflected in the deep sea record (Kukla, 2000) (Fig. 4).

The best data for correlation between the two realms thus far has come from a study

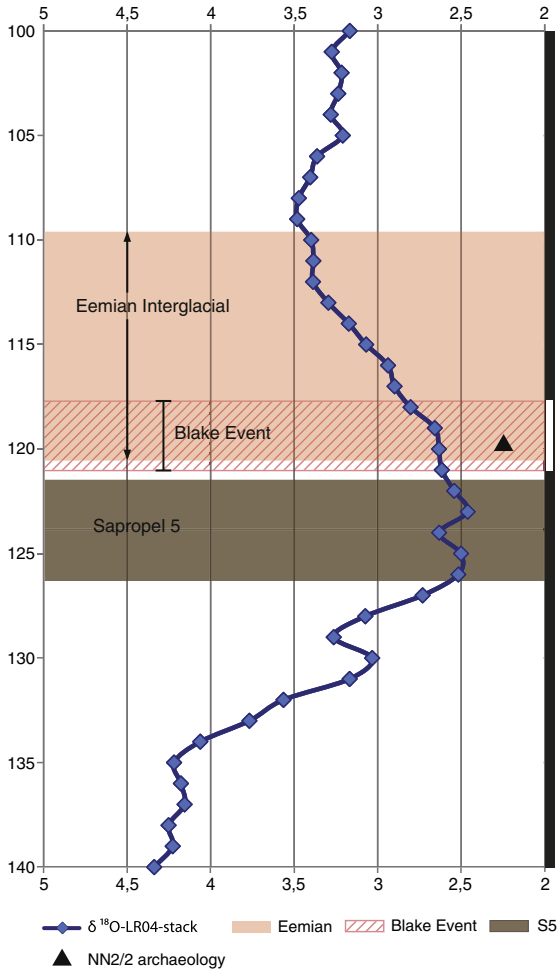


Figure 4.

Stacked $\delta^{18}\text{O}$ -LR04 record (Lisiecki and Raymo, 2005) from 140 to 100 ka, using the Lourens' (2004) time scale, with the positions of sapropel 5, the Blake Event, and the (central and northwestern European) Eemian interglacial. The summary geomagnetic polarity column is depicted farthest right. The position of the NN2/2 archaeological find-horizon is indicated as well.

of terrestrial pollen from marine sediments studied in core MD95-2042 off the coast of the Iberian Peninsula (Sánchez-Goñi et al., 1999; Shackleton et al., 2003). In contrast, the NN2 data allow us to correlate a high-resolution terrestrial record to the marine record by means of the palaeomagnetic signal of the Blake Event. Our positioning of the

Eemian interglacial as recorded at NN2 in the LR04- stack record (Lisiecki and Raymo, 2005) shows that the beginning of the Eemian interglacial was significantly later than the attainment of the MIS 5e plateau in benthic $\delta^{18}\text{O}$ (Shackleton et al., 2003). This makes for an interesting difference with the Iberian offshore record, where the beginning of the Eemian as delimited in core MD95-2042 corresponds to the lightest isotope values of MIS 5e (Shackleton et al., 2002). Our data shows that the Eemian of central and northwestern Europe starts with a return to the heavier values toward the MIS 5e/5d transition, i.e. an estimated 5000 yr later than in the south. The estimates for the end of the Eemian interglacial in both areas are remarkably similar, however (Sánchez-Goñi et al., 1999; Shackleton et al., 2002). Independent of these time scales, the beginning of the Eemian interglacial as documented at NN2 occurs not simply after the major ice sheets had melted, but considerably later, when sea levels had already begun to drop and substantial continental ice was once again accumulating (Fig. 4). These findings may have major implications for views on the relationships between events recorded in the marine record and in the terrestrial realm, and might require a revision to the current framework of understanding regarding the timing of the Eemian of central Europe relative to MIS 5e (Tzedakis et al., 2009).

References

- Eissmann, L., 2002, Quaternary geology of eastern Germany (Saxony, Saxon-Anhalt, South Brandenburg, Thüringia), type area of the Elsterian and Saalian Stages in Europe. *Quaternary Science Reviews*, 21: 1275-1346.
- Fang, X., Li, J., Van der Voo, R., Mac Niocaill, C., Dai, X., Kemp, R.A., Derbyshire, E., Cao, J., Wang, J. and Wang, G., 1997, A record of the Blake Event during the last interglacial paleosol in the western Loess Plateau of China. *Earth and Planetary Science Letters*, 146: 73-82.
- Gibbard, P.L., 2003, Definition of the Middle-Upper Pleistocene boundary. *Global and Planetary Change*, 36: 201-208.
- Kukla, G.J., 2000, PALEOCLIMATE: The Last Interglacial. *Science*, 287: 987-988.
- Laj, C. and Channell, J.E.T., 2007, Geomagnetic Excursion geomagnetism. In: Kono, M. (ed.), *Geomagnetism*. Elsevier, Amsterdam, 373-416.
- Langereis, C.G., Dekkers, M.J., Lange, G.J., Paterne, M. and Santvoort, P.J.M., 1997, Magnetostatigraphy and astronomical calibration of the last 1.1 Myr from an eastern Mediterranean piston core and dating of short events in the Brunhes. *Geophysical Journal International*, 129: 75-94.
- Lisiecki, L.E. and Raymo, M.E., 2005, A Pliocene-Pleistocene stack of 57 globally distributed benthic $\delta^{18}O$ records. *Paleoceanography*, 20: PA1003.
- Lourens, L.J., 2004, Revised tuning of Ocean Drilling Program Site 964 and KC01B (Mediterranean) and implications for the $\delta^{18}O$, tephra, calcareous nannofossil and geomagnetic reversal chronologies of the past 1,1 Mys. *Paleoceanography*, 19: PA3010.
- Mania, D. and Mania, U., 2008, La stratigraphie et le Paléolithique du complexe saalien dans la région de la Saale et de l'Elbe. *L'Anthropologie*, 112: 15-47.
- Menke, B. and Tynni, R., 1984, Das Eeminterglazial und das Weichselfrühglazial von Rederstall/Dittmarschen und ihre Bedeutung für die mitteleuropäische Jungpleistozängliederung. *Geologisches Jahrbuch*, A76: 3.
- Müller, H., 1974, Pollenanalytische Untersuchungen und Jahresschitzenzählungen an der eem-zeitlichen Kieselgur von Bispingen/Luhe. *Geologisches Jahrbuch*, A21: 149-169.

- Penkman, K.E.H., Preece, R.C., Keen, D.H. and Collins, M.J., 2008, British aggregates: an improved chronology using amino acid racemization and degradation of intra-crystalline amino acids (IcPD). English Heritage Research Department Report Series, 6.
- Reinders, J. and Hambach, U., 1995, A geomagnetic event recorded in loess deposits of the Tonchesberg (Germany): identification of the Blake magnetic polarity episode. *Geophysical Journal International*, 122: 407-418.
- Roberts, A.P., 2008, Geomagnetic excursions: Knowns and unknowns. *Geophysical Research Letters*, 35.
- Sánchez-Goñi, M.F., Eynaud, F., Turon, J.L. and Shackleton, N.J., 1999, High resolution palynological record off the Iberian margin: direct land-sea correlation for the Last Interglacial complex. *Earth and Planetary Science Letters*, 171: 123-137.
- Shackleton, N.J., Chapman, M., Sánchez-Goñi, M.F., Pailler, D. and Lancelot, Y., 2002, The Classic Marine Isotope Substage 5e. *Quaternary Research*, 58: 14-16.
- Shackleton, N.J., Sánchez-Goñi, M.F., Pailler, D. and Lancelot, Y., 2003, Marine Isotope Substage 5e and the Eemian Interglacial. *Global and Planetary Change*, 36: 151-155.
- Smith, J.D. and Foster, J.H., 1969, Geomagnetic Reversal in Brunhes Normal Polarity Epoch. *Science*, 163: 565-567.
- Thouveny, N., Carcaillet, J., Moreno, E., Leduc, G. and Nérini, D., 2004, Geomagnetic moment variation and paleomagnetic excursions since 400 kyr BP: a stacked record from sedimentary sequences of the Portuguese margin. *Earth and Planetary Science Letters*, 219: 377-396.
- Tric, E., Laj, C., Valet, J., Tucholka, P., Paterne, M. and Guichard, F., 1991, The Blake geomagnetic event: transition geometry, dynamical characteristics and geomagnetic significance. *Earth and Planetary Science Letters*, 102: 1-13.
- Tucholka, P., Fontugne, M., Guichard, F. and Paterne, M., 1987, The Blake magnetic polarity episode in cores from the Mediterranean Sea. *Earth and Planetary Science Letters*, 86: 320-326.
- Turner, C., 2000, The Eemian interglacial in the North European plain and adjacent areas. *Geologie en Mijnbouw*, 79: 217-231.
- Turner, C., 2002, Problems of the Duration of the Eemian Interglacial in Europe North of the Alps. *Quaternary Research*, 58: 45-48.

- Tzedakis, P.C., Raynaud, D., McManus, J.F., Berger, A., Brovkin, V. and Kiefer, T., 2009, Interglacial diversity. *Nature Geoscience*, 2: 751-755.
- Vandamme, D., 1994, A new method to determine paleosecular variation. *Physics of The Earth and Planetary Interiors*, 85: 131-142.
- Zagwijn, W.H., 1961, Vegetation, climate and radiocarbon datings in the late Pleistocene of the Netherlands: I. Eemian and Early Weichselian, *Nieuwe Serie. Mededelingen van de Geologische Stichting*, 14: 15.
- Zhu, R.X., Zhou, L.P., Laj, C., Mazaud, A. and Ding, Z.L., 1994, The Blake Geomagnetic Polarity Episode Recorded in Chinese Loess. *Geophysical Research Letters*, 21: 697-700.
- Zijderveld, J.D.A., 1967, Demagnetisation of rocks: analysis of results. In: Collinson, D.W., Creer, K.M. and Runcorn, S.K. (eds.), *Methods in Palaeomagnetism*. Elsevier, Amsterdam, 254-286.

SUPPLEMENTARY MATERIAL

Stratigraphical and palaeoenvironmental context of the Neumark-Nord 2 archaeological site (Saxony-Anhalt, Germany)

Introduction

The eastern part of Germany has played a key role in studies of the glaciations in Europe. There is ample evidence for two major glacier advances with many additional minor oscillations of Elsterian and Saalian age. A sequence of more than 50 horizons and complexes of glacial and periglacial facies has been identified in this geologically rich area (Eissmann, 2002). Maps of the palaeogeography of the region during the periods of the major European continental glaciations belong to the stock and trade of textbooks on the Quaternary. Quaternary deposits were and still are well exposed in the large-scale open-cast lignite mines in the area. Here we report on the results of interdisciplinary studies of the geology and archaeology of the Neumark-Nord exposures, in a lignite quarry situated approximately 10 km southwest of Halle, in the Geisel valley.

The Geisel valley area is well-known for its Eocene fossils, but intensive explorations of the Pleistocene exposures in the lignite quarries during the last three decades have uncovered large amounts of Middle and Late Pleistocene fossils, often in association with traces of hominin activities. At Neumark-Nord these have been retrieved from the infill of three shallow basins, which formed as a result of isostatic movements induced by lignite diapirism (Mania et al., 1990; Thomae, 2003). The well-known lake basin of Neumark-Nord 1 was studied in the 1980s and 1990s by a team under the direction of Dietrich Mania (Mania and Mania, 2008; Mania et al., 1990). They uncovered remarkable scatters of bones and partially articulated animal carcasses on the shores of a former lake, occasionally associated with flint artifacts. Deeper parts of the lake yielded c. 150 (more or less complete) fallow deer skeletons as well the remains of >26 straight tusked elephants.

During the fieldwork in the lignite quarry in 1996, Mania discovered a second basin, Neumark-Nord 2 (NN2), a few hundred meters to the north-east of Neumark Nord 1. In 2003 a third basin was identified, the oldest of the three (NN3) (Laurat and Brühl, 2006). The Landesamt für Denkmalpflege und Archäologie Sachsen-Anhalt started formal

excavations at NN2 in 2003. Directed by T. Laurat and E. Brühl these excavations focused on an early Weichselian find level in the upper part of the basin's infill (NN2/0). During the construction of a geological trench the interglacial find horizon discussed in this paper was discovered in the silty infill of the basin. Since 2004, the NN2/2 find levels have been under excavation, from 2006 onward in a joint project of the Landesamt für Denkmalpflege und Archäologie Sachsen-Anhalt, the Römisch-Germanisches Zentralmuseum at Mainz (Germany) and the Faculty of Archaeology of Leiden University (The Netherlands). Weather conditions permitting, an excavation crew was in the field all year round, until the end of August 2008. By then the water level in the flooding former quarry which is to be turned into a recreation resort, reached the NN2/2 find levels. In total, an area of 433 m² was excavated, yielding a rich archaeological assemblage, containing c. 20,000 Middle Palaeolithic flint artifacts and approximately 120,000 faunal remains representing a warm temperate fauna which includes straight tusked elephant, rhinoceros, bovids, equids, deer, bear, small carnivores and the pond tortoise *Emys orbicularis*.

Figure S1:

Overview of the NN 2/2 excavation, August 2008. A view from the north, on a E-W section perpendicular to the schematic section of Fig. 2. Left of the centre of the picture is an elephant tusk, in the middle of the archaeological find level NN2/2.



Description of Profile HP7 (H.J. Mucher, N. Hesse, L. Kindler & W. Roebroeks)

A key section in the geological studies of the NN2 exposures is Hauptprofil (HP) 7, one of the many sections described inside and around the excavated site. This section was sampled for a wide range of dating and palaeo-environmental techniques. All samples were collected from the very same part of the section, enabling a direct comparison of the results on a 5 cm stratigraphic sampling interval over the entire sequence, up to 600 cm below the top of the section. Stratigraphically lower samples were taken from neighbouring sections within the excavation area, excavation square section 210/296-297 for palaeomagnetic samples and for palynological sampling at HP10, 8 m from HP 7, stratigraphically partly overlapping and underlying the sampled base of HP7. The Pinus-Betula phase in this section revealed such a good overlap with the HP7 section that the results of both sections may be presented as one single pollen diagram (see Bakels, Supplementary Material (SM)).

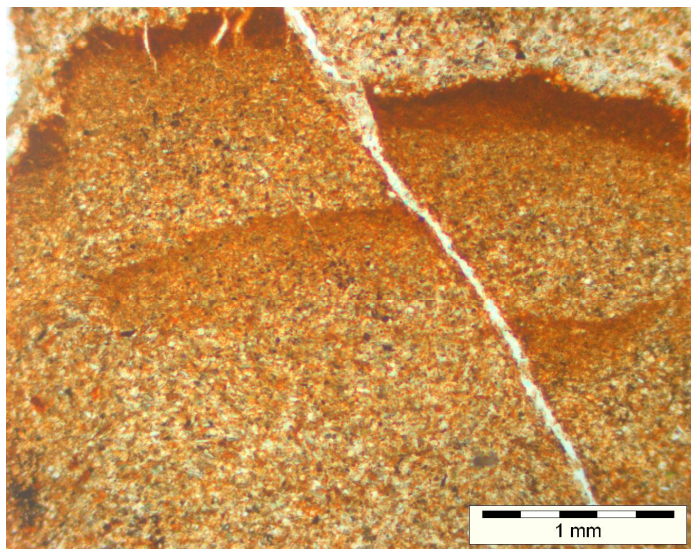
At the Neumark Nord 2 site, the basin infill is underlain by a late Saalian (Drenthian) sandy-gravelly diamicton (Unit 1 in Figure 2) and overlain by ca. 6 metres of last glacial (Weichselian) loess. The basin infill starts with sediments reworked from the diamicton (unit 2 in Fig 2), overlain by a series of mostly well-drained, moist, calcareous silt loams, which has been divided into several sublayers (units 3-19), described below, from the bottom of the sequence going towards the top of the exposed sediments at HP7, and using FAO guidelines for soil profile description (FAO, 1977). At the Neumark-Nord 2 site, data on the sediments underlying the silt loams (i.e. sedimentary units 1-2, total thickness c. 300 cm) were mainly obtained by augering. The numbering scheme adopted below refers to the layer numbers in Figure 2 of the paper.

1. Sandy loamy diamicton, with gravel and well-rounded quartz and prophy particles, dark grayish-brown in colour, up to 150 cm thick, with a more yellowish-brown top (at HP7/10 only observed through augering).
2. Series of loamy and sandy deposits with gravel particles, occasionally laminated sand layers, up to 175 cm thick (at HP7/10 only observed through augering) interpreted as reworked from the underlying diamicton.

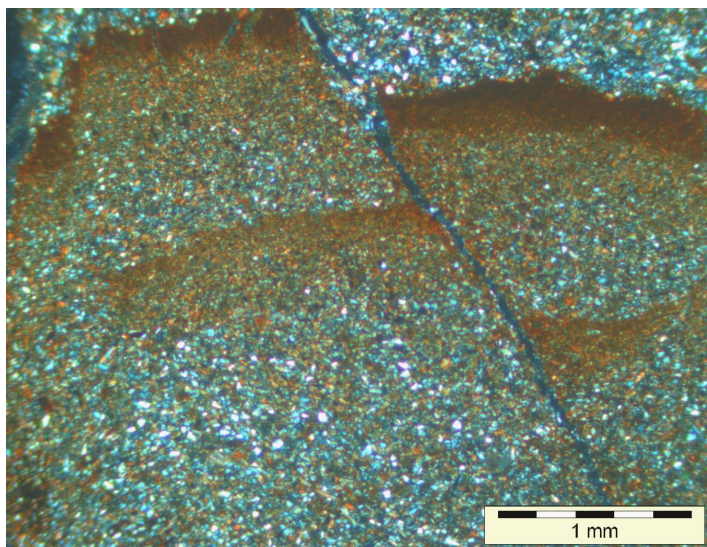
3. Light-brown to brown (7.5 YR 5/4-6/4) silt loam, calcareous, 50 cm thick, structureless, very friable, no cutans, no cementation, no pores, no stone and mineral fragments, no mineral nodules, nature with boundary below not observed.
4. Olive black (5Y 3/1) silty clay, moist, calcareous, 0-50 cm thick, structureless, abrupt and smooth boundary with horizon below.
5. Dark gray (5Y 4/1), moist, calcareous structureless silt loam, c. 70 cm thick, friable to firm, few distinct sharp brown (7.5YR 5/8) iron mottles; vertical reddish yellow (7.5 YR 6/6) infillings of cracks with silt loam and bands of silt; very few, very fine, discontinuous, in ped tubular, channels; very few very small shell fragments; abrupt and smooth boundary with horizon below. One undisturbed thin section sample: M3lo-1.
6. Pinkish gray to brown (7.5YR 6/2-5/2, moist), calcareous, structureless, silt loam, 35 cm thick, very friable; very few, fine, faint, pink (5YR 7/4) iron mottles; darker rectangular and rounded lumps of soil material with lignite, diameter resp. 4x10 and 2x2 cm; lower part contains bone fragments, flint artefacts and mollusc shells; abrupt boundary with horizon below. One undisturbed thin section sample: M3lo-2.
7. Yellowish brown (10YR 5/4), very fine laminated, sub-horizontal, moist, calcareous silt loam, 65 cm thick, very friable to friable, and pinkish gray (7.5YR 6/2) silt on top (2 cm thick); in the bottom, 10 cm thick, a very dark gray (5YR 3/1) calcareous organic band; very few fine iron mottles, reddish yellow (5YR 6/6) with distinct sharp boundaries; with very prominent laminae; one wedge infilling, 11 cm deep and 2 cm wide; abrupt and smooth boundary with horizon below. With bone fragments and flint artefacts. Three undisturbed thin section samples: M3lo-5 in top organic layer; M3lo-4 in very fine laminated silt loam; M3lo-3 in bottom organic layer (see Figures S2 and S3 for a close-up of the thin section).
8. Yellowish brown (10YR 5/4) moist, calcareous, structureless, silt loam, 50 cm thick, very friable, very few reddish yellow (5YR 6/8) medium iron mottles with distinct and sharp boundaries; abrupt and smooth boundary with horizon

Figure S2:

Laminated sediment with crust formation and a micro fault (thin section M3lo-3, PPL).

**Figure S3:**

The same part of the thin section as Figure S3 in XPL.

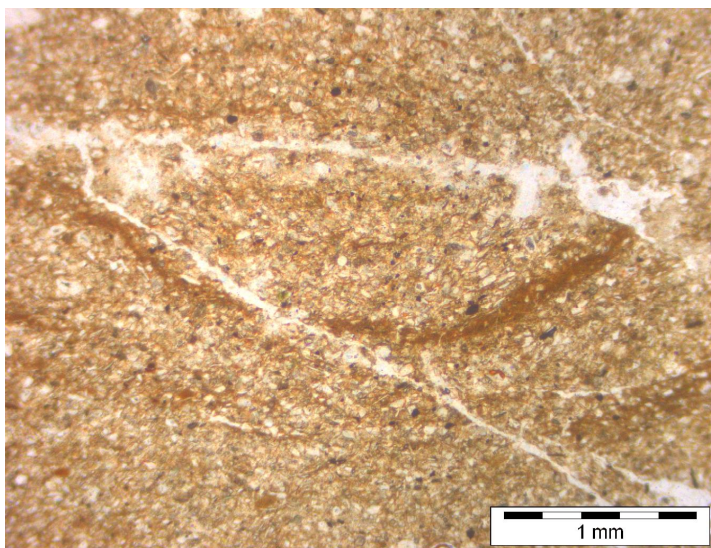


below – main find level, numerous bone fragments and flint artefacts. One undisturbed thin section sample M3lo-6.

9. Brown (10YR 5/3), calcareous, structureless, silt loam; 80 cm thick, friable to firm; very few, small to large, hard, irregular, flat, black, calcareous nodules; boundary with horizon below abrupt and smooth. Few bone fragments and flint artefacts. One undisturbed sample: M3u-1 (see Figure S4 for a close up of the thin section).
10. Yellowish brown (10YR 5/4), calcareous, medium to coarse, subangular blocky, silt loam, 50 cm thick, firm; very few gravel-sized quartz, fresh, angular and rounded; very few bones and lithics ; abrupt and smooth boundary with horizon below. One undisturbed thin section sample: M3u-2.
11. Very pale brown (10YR 7/3) calcareous, structureless, silt loam, 30 cm thick, very friable; very few, gravel-sized quartz, fresh, angular and rounded; few artefacts and bones; abrupt and smooth boundary with horizon below. One undisturbed thin section sample: M3u-3.

Figure S4:

Micro-rill with a thin clay layer at the bottom of the rill (thin section M3u-1, in PPL).



12. Pale brown (10YR 6/3) calcareous, structureless, silt loam; 20 cm thick; very friable; few, very fresh, rounded and angular, rock fragments; very few artefacts and bones ; abrupt and smooth boundary with horizon below. One undisturbed thin section sample: M3u-4.
13. Light gray to light brownish gray (2.5Y 7/2-2.5Y 6/2), calcareous, structureless, silt loam, 20 cm thick, friable; many fine prominent, sharp, reddish yellow (7.5YR 7/8) iron mottles; very few, very fine, discontinuous, oblique, inped, tubular, simple pores; very few artefacts and bones ; very few, very fine, black roots; abrupt and smooth boundary with horizon below. One undisturbed thin section sample: M3u-5 in calcium carbonate band.
14. Light gray (10YR 7/2), calcareous, structureless, silt loam, 80 cm thick, friable; very few, gravel-sized (< 0.5 cm in diameter), rounded fresh quartz; common, medium to coarse, prominent, sharp, reddish yellow (7.5YR 7/6) iron mottles; they occur also along vertical cracks; in sub-horizontal bands at 45 and 65 cm from horizon bottom, very few, large (up to 2 cm in diameter), hard, and rounded, white calcium carbonate nodules occur; in the top a gypsum layer; very few artefacts and bones ; very few pedotubules with pinkish white (7.5YR 8/4), loose infilling of silt; abrupt and smooth boundary with horizon below. One undisturbed thin section sample: M3u-6 in upper gypsum band.
15. Dark reddish gray (5YR 4/2), lower part structureless, silty clay loam, 20 cm thick, in upward direction platy silty clay loam, friable to firm; organic material increases towards the top of the horizon, the organic matter is laminated, with modern roots; common coarse prominent, sharp, brown (10YR 4/2) iron mottles; sharp and smooth boundary with horizon below. One undisturbed thin section sample: M3u-7.
16. Pinkish white (7.5YR 8/2) calcareous, structureless, silt loam, 5-10 cm thick, ("Seekreide") firm; it is covered by a 2 cm thick, laminated, dark reddish brown (5YR 3/2) organic material; abundant molluscs and fragments of it; few recent roots; abrupt and smooth boundary with horizon below. One undisturbed thin section sample M3u-8.
17. Olive brown (2.5Y 4/4) calcareous, structureless, silt loam, 10 cm thick, friable to firm; few, fine to medium, random, inped, tubular pores (root channels?);

very few bone fragments and flint artefacts and few molluscs fragments. Abrupt and smooth boundary with horizon below. One undisturbed thin section sample: M3u-9.

18. Light yellow brown (10YR 6/4) calcareous, structureless, silt loam, 30 cm thick, very friable; many medium, distinct and sharp, strong brown (7.5YR 5/8) iron mottles; few shell fragments; Clear and smooth boundary with horizon below. One undisturbed thin section sample: M3u-10.
19. Yellow (10YR 7/8), moist, calcareous, structureless, loamy sand, more than 70 cm thick (top not observed) with locally intercalated sand layers; few medium, distinct and sharp, Strong brown (7.5YR 5/8); consistence: loose to soft. Abrupt and smooth boundary with horizon below.

Micromorphological study of the thin sections: summary of results (H.J. Mùcher)

The soil formation in the silt loam sediment is very weak, consisting of incipient gleysols and cambisols (FAO-Unesco, 1988). The sedimentation by overland flow was an almost continuous process. Very weakly pronounced pedogenesis is restricted to very local occurrences of platy and blocky structures, crust formation, and in addition Ca, Fe, and Mn coatings and hypocoatings, crystals of gypsum and carbonate. The presence of these pedofeatures (Stoops, 2003) was inferred on basis of a macroscopic study of the deposits, and confirmed by micromorphological analysis of thin sections, 9 x 6 cm and 20 µm thick.

The mainly calcareous sediment was deposited by overland flow, mainly by after flow and less by rain wash (transport by splash cannot be excluded). Crusts and clay lamina suggest a very short interruption in the sedimentation process, with respectively crust formation (Figure S2: M3lo-3, plain polarized light [PPL] and Figure S3, the same object but in crossed polarized light [XPL]) and sedimentation in still waters. In addition, during these very short stable periods micro-rills were formed in the temporary soil surface Figure S4: M3u-1 in PPL).

Physical modifications after deposition are rare, examples are cracks, micro-rills followed by infillings, and wavy deformation of lamina. Indications for frost action have not been observed.

Soil formation phenomena are rare, only incipient soil formation was observed with development of platy structures in thin section M3u-4, and of blocky peds in M3u-2. Recrystallization of carbonates creating carbonate coatings, carbonate hypocoatings and carbonate nodules, and crystallization of gypsum in dry conditions occurred only in the upper part of the profile. These dry conditions were often followed by a rising groundwater table resulting in the formation of gley phenomena such as ferric and manganiferous nodules, Fe-Mn coatings and hypocoatings. The gley phenomena often cover the gypsum formation, indicating that the hydromorphic features developed after the gypsum crystallizations.

Palynology (C. C. Bakels)

During the analysis of section HP7 the pollen detected in its lowest part, 595 cm from the top of HP7, was found to represent a *Pinus-Betula* phase with a dominance of Pinus. To study the very oldest phase of the vegetation succession another excavation section at 8 m from HP7, HP10, was sampled which stratigraphically partly overlaps and underlies the sampled base of HP7. The *Pinus-Betula* phase in this section revealed such a good overlap with the HP7 section that the results of both sections may be presented as one single pollen diagram.

The sediments were treated according to standard practice with KOH, HCl, heavy liquid separation (s.g. 2.0) and acetolysis. Before treatment tablets containing a known number of *Lycopodium* spores were added, according to Stockmarr's method (Stockmarr, 1971). This procedure enables the calculation of pollen concentrations. The diagram presented here is, however, not a concentration diagram but a conventional percentage diagram, based on a pollen sum consisting of trees and herbs from non-aquatic environments. For this sum at least 300 pollen and spores were counted; only in pollen zone II and the centre of pollen zone IVb this number could not be reached because of a low pollen density. To avoid an unwieldy graph those taxa which were found not too often are presented in Table S1.

Table S1:

Pollen and spores not given in the diagram of figure S5, arranged according to their frequency in the zones and subzones. Black squares indicate presence of taxon.

Neumark-Nord 2 HP7/HP10

Zone	VII	V	IVb3	IVb2	IVb1	IVa2	IVa1	III	II	I	
Trees, shrubs, lianas											
<i>Alnus</i>	■	■	■	■	■	■	■	■	■	-	9
<i>Tilia</i>	-	■	■	■	■	■	■	■	-	-	7
<i>Salix</i>	-	-	■	-	■	■	■	■	■	■	7
Rosaceae	-	-	■	■	■	■	-	■	■	-	6
<i>Ilex</i>	-	■	-	■	-	■	-	■	-	-	4
<i>Acer</i>	-	■	-	-	■	■	-	-	-	-	3
<i>Populus</i>	-	-	■	■	■	-	-	-	-	-	3
<i>Cornus sanguinea</i>	-	-	-	-	■	■	■	-	-	-	3
<i>Humulus/Cannabis</i>	-	-	-	-	■	■	-	■	-	-	3
<i>Taxus</i>	-	■	-	-	■	-	-	-	-	-	2
<i>Hedera</i>	-	-	-	-	-	■	■	-	-	-	2
<i>Ligustrum</i>	-	-	■	-	-	-	-	-	-	-	1
<i>Rhamnus</i>	-	-	-	-	■	-	-	-	-	-	1
<i>Myrica</i>	-	-	-	-	-	■	-	-	-	-	1
<i>Frangula</i>	-	-	-	-	-	■	-	-	-	-	1
<i>Prunus</i>	-	-	-	-	-	■	-	-	-	-	1
Herbs, open space											
<i>Galium</i> type	■	■	■	■	■	■	■	■	-	■	9
<i>Filipendula</i>	■	■	■	■	■	■	■	-	-	■	8
<i>Ranunculus acris</i> type	-	■	■	■	■	■	■	■	-	■	8
Ericales	-	■	■	■	■	■	■	■	-	-	7
Apiaceae	■	-	■	■	■	■	■	■	-	-	7
Brassicaceae	-	-	■	-	-	■	■	■	■	■	6
<i>Rumex acetosa</i> type	-	■	■	-	-	■	■	■	■	-	6
<i>Caltha</i>	-	-	-	-	-	■	■	■	■	■	5
<i>Triglochin</i>	-	■	■	-	■	■	-	-	-	■	5
<i>Plantago coronopus</i>	-	-	■	■	-	■	-	■	■	-	5
<i>Trifolium</i> type	-	-	■	-	■	■	-	■	-	-	4
<i>Campanula</i>	-	-	-	-	■	■	-	■	■	-	4
<i>Thalictrum</i>	-	-	-	-	-	■	-	■	■	■	4
<i>Plantago major/media</i>	■	-	-	-	-	■	-	■	-	■	4
<i>Spergularia</i>	-	-	■	-	■	■	-	-	-	-	3
<i>Centaurea jacea</i> type	-	-	-	-	■	-	-	-	■	■	3
<i>Veronica</i>	-	-	-	-	■	■	■	-	-	-	3
<i>Equisetum</i>	■	-	■	-	-	-	-	■	-	-	3
<i>Geranium</i>	-	-	■	-	■	-	-	-	-	-	2
<i>Stachys</i> type	-	-	-	-	■	■	-	-	-	-	2
<i>Melampyrum</i>	-	-	-	-	■	-	-	■	-	-	2
<i>Scrophularia</i> type	-	■	-	-	■	-	-	-	-	-	2
<i>Polygonum bistorta</i> type	-	-	-	-	-	-	-	■	■	-	2
<i>Mentha</i> type	-	-	■	-	-	■	-	-	-	-	2
<i>Jasione montana</i> type	-	-	■	■	-	-	-	-	-	-	2
<i>Papaver rhoeas</i> type	-	-	-	■	-	■	-	-	-	-	2

The pollen and spores represent the vegetation of an interglacial and the presence of *Ilex* and *Hedera* implies that this interglacial was oceanic in character. This, together with arguments brought forward by other methods reported in this paper, concurs with the interglacial being the Eemian. The local pollen zones fit the zonation proposed by Menke and Tynni (Menke and Tynni, 1984) for Northern Germany very well and their zone numbers are used to describe the diagram further on (Turner, 2000).

The sequence starts with a phase dominated by *Betula* and herbs (zone I). Part of the *Betula* pollen in the two lowest spectra is of the *Betula nana* type. The *Betula* phase is followed by a *Pinus* phase with some *Betula* (zone II) and this again by a *Pinus-Quercus* phase (zone III). The main part of the diagram belongs to zone IV, in which firstly *Quercus* and *Ulmus*, then *Quercus* and *Corylus* and in the end *Corylus* alone dominate the pollen assemblage. Zones III and IV concord with the early-temperate phase of Turner and West (Turner and West, 1968) and the Eemian pollen zones E3 and E4 as defined in Turner (Turner, 2002). The next zone, zone V, dominated by *Carpinus*, is not present in its usual length, because of an apparent hiatus in the deposits at the very top of HP7. This hiatus is to be placed at the end of stratigraphical unit 17 (see above). The next pollen zone shows a dominance of *Pinus*.

During the zones I-IV herb pollen is present in considerable numbers. In the case of zone IV this is remarkable. Halfway zone IVb, the *Corylus* phase, the vegetation appears almost treeless. The peak in *Pinus* pollen is attributable to the absence of other trees. The NN2 basin is small, and the open aspect of the vegetation is interpreted as reflecting mostly very local conditions (Tauber, 1965; Tauber, 1967). It is probable that large mammals came here to drink, and to graze and browse along its shores. The high percentages of *Polygonum aviculare* pollen indicate the presence of much trodden areas. It is even possible that some of the herb pollen has its origin in animal dung. The presence of *Sordaria* spores in some of the samples confirms the presence of dung. During the period of *Carpinus* dominance the records lack high percentages of herbs. The vegetation must have been true woodland at that time.

Amino Acid Analysis (K.E.H. Penkman)

A new technique of amino acid analysis has been developed for geochronological purposes (Penkman, 2005; Penkman et al., 2008a; Penkman et al., 2008b; Penkman et al., 2007) combining a recent reverse-phase high-pressure liquid chromatography (RP-HPLC) method of analysis (Kaufman and Manley, 1998) with the isolation of an 'intracrystalline' fraction of amino acids by bleach treatment (Sykes et al., 1995). This combination of techniques results in the analysis of D/L values of multiple amino acids from the chemically protected protein within the biomineral, thereby enabling both smaller sample sizes and increased reliability of the analysis compared to more conventional amino acid analysis protocols. Amino acid data obtained from the intra-crystalline fraction of the calcitic *Bithynia* opercula indicate that this biomineral is a particularly robust repository for the original protein (Penkman, 2005; Penkman et al., 2008b; Penkman et al., 2009) and therefore has been targeted in this study.

Amino acid racemisation (AAR) analyses were undertaken on 42 individual *Bithynia tentaculata* opercula from Neumark-Nord 2 from HP7 (NEaar 4714-4717; 4927-4930; 5628-5650; 5687-5697). All samples were prepared using the procedures of Penkman et al. (Penkman et al., 2008a) to isolate the intra-crystalline protein by bleaching. Two subsamples were then taken from each shell; one fraction was directly demineralised and the free amino acids analysed (referred to as the 'Free' amino acids, FAA or F), and the second was treated to release the peptide-bound amino acids, thus yielding the 'total' amino acid concentration, referred to as the "Total Hydrolysable amino acid fraction (THAA or H*). Samples were analysed in duplicate by RP-HPLC. During preparative hydrolysis, both asparagine and glutamine undergo rapid irreversible deamination to aspartic acid and glutamic acid respectively (Hill, 1965). It is therefore not possible to distinguish between the acidic amino acids and their derivatives and they are reported together as Asx and Glx respectively.

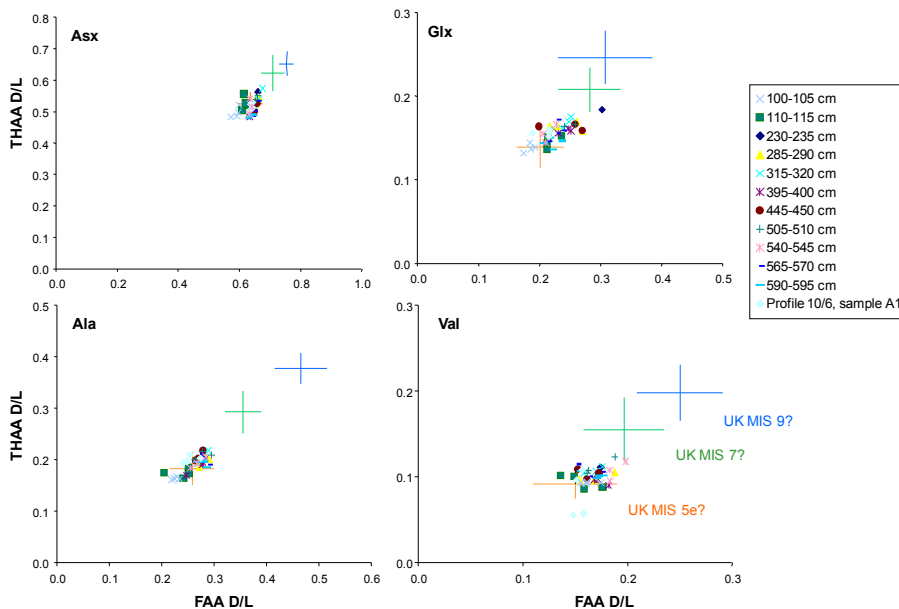
The D/L ratios of aspartic acid/asparagine, glutamic acid/glutamine, serine, alanine and valine (D/L Asx, Glx, Ser, Ala, Val) as well as the [Ser]/[Ala] value are then assessed to provide an overall estimate of protein decomposition. Serine is one of the most geochemically unstable amino acids, with one of its decomposition products being alanine (Bada et al., 1978). This enables the ratio of the concentration of serine ([Ser])

to the concentration of alanine ([Ala]) to be used as a useful indication of the extent of protein decomposition (Parfitt et al., 2005). The D/L of an amino acid will increase with increasing time, whilst the [Ser]/[Ala] value will decrease. Each amino acid racemises at different rates, and therefore is useful over different timescales. The D/L of Ser is less useful as a geochronological tool for samples of this age, but is presented here as aberrant values are useful indications of contamination.

In a closed system, the amino acid ratios of the FAA and the THAA subsamples should be highly correlated, enabling the recognition of compromised samples (Preece and Penkman, 2005). The *Bithynia tentaculata* opercula from Neumark-Nord 2 show very consistent data (Table S2; Figure S6), indicating that nearly all the samples contain closed-system protein and therefore can be reliably used for age estimation. However, three opercula showed divergent within-sample behaviour: one from a depth of 395 cm (NEaar 5642), one from a depth of 445 cm (NEaar 5643) and one from a depth of 540 cm (NEaar 4927), and data from these samples should not be used.

Figure S6:

Free vs Total D/L values of Asx, Glx, Ala and Val from bleached Bithynia tentaculata opercula from Neumark-Nord 2, compared with shells from UK sites correlated with MIS 5e, MIS 7 and MIS 9 (sample names indicate height in cm downward from the top of HP7).



The extent of protein decomposition in both the FAA and THAA increases with time, with increased levels of protein breakdown during warm stages and a slowing in the rates of degradation in cold stages. Over a small geographical area, it can be assumed that the integrated temperature histories are effectively the same. Given a similar temperature history, this then allows an aminostratigraphic framework for an area to be developed, plotting the FAA against the THAA data, with independent geochronology allowing these clusters to be correlated to marine oxygen isotope warm stages; such a framework has been developed for opercula from the United Kingdom (Penkman, 2005; Penkman et al., 2008b). The range of data for British sites has been compared to the Neumark Nord 2 dataset (Fig. S5), and it is clear that the Neumark Nord 2 samples have amino acid ratios that are similar to, but slightly higher than, those for the same species from sites correlated with the British Ipswichian (and therefore the Eemian and MIS 5e (Bowen, 1999)), including Trafalgar Square, Bobbitshole, Coston, Shropham, Crophorne New Inn, Eckington and Tattershall Castle (Penkman et al., 2008b). The integrated temperature history for more continental sites may not be identical to that experienced by the British opercula, and therefore the overall state of degradation will be different for samples of identical age. A framework for continental Europe is under development, but, importantly, the data from opercula from the Eemian type locality at Amersfoort (The Netherlands) (Zagwijn, 1961) show similar levels of protein degradation as the Neumark samples.

Table S2:

Amino acid data on opercula of Bithynia tentaculata from Neumark Nord 2. Error represent one standard deviation (s) about the mean (av) for the duplicate analyses for an individual sample. Each sample was bleached (b), with the free amino acid fraction signified by 'F' and the total hydrolysable fraction by 'H':*

NEaar no.	Sample name	Asx D/L		Glx D/L		Ser D/L		Ala D/L		Val D/L		[Ser]/[Ala]	
		av	σ	av	σ	av	σ	av	σ	av	σ	av	σ
4714bF	NN2100Bto1bF	0.596	0.002	0.186	0.001	0.862	0.002	0.219	0.007	0.156	0.006	0.665	0.017
4714bH*	NN2100Bto1bH*	0.496	0.001	0.137	0.004	0.485	0.004	0.162	0.005	0.093	0.000	0.614	0.016
4715bF	NN2100Bto2bF	0.599	0.000	0.185	0.003	0.875	0.001	0.230	0.001	0.161	0.008	0.799	0.014
4715bH*	NN2100Bto2bH*	0.521	0.002	0.144	0.002	0.572	0.004	0.167	0.004	0.094	0.002	0.649	0.004
4716bF	NN2100Bto3bF	0.573	0.000	0.174	0.000	0.875	0.000	0.234	0.001	0.161	0.007	0.782	0.003
4716bH*	NN2100Bto3bH*	0.483	0.002	0.132	0.000	0.506	0.002	0.163	0.000	0.093	0.001	0.594	0.000
4717bF	NN2100Bto4bF	0.592	0.007	0.193	0.005	0.890	0.002	0.224	0.001	0.174	0.006	0.784	0.002
4717bH*	NN2100Bto4bH*	0.485	0.002	0.139	0.001	0.529	0.000	0.163	0.004	0.093	0.000	0.576	0.004
4927bF	NN2540Bto1bF	0.770	0.002	0.971	0.008	0.191	0.270	0.877	0.000	1.033	0.021	0.010	0.002
4927bH*	NN2540Bto1bH*	0.667	0.003	0.850	0.006	0.073	0.103	0.841	0.006	0.754	0.005	0.016	0.011
4928bF	NN2540Bto2bF	0.640	0.000	0.206	0.000	0.933	0.002	0.267	0.001	0.183	0.002	0.631	0.002
4928bH*	NN2540Bto2bH*	0.515	0.003	0.155	0.000	0.576	0.000	0.193	0.002	0.108	0.001	0.524	0.003
4929bF	NN2540Bto3bF	0.633	0.001	0.210	0.008	0.924	0.005	0.255	0.002	0.183	0.009	0.661	0.004
4929bH*	NN2540Bto3bH*	0.492	0.002	0.144	0.000	0.528	0.007	0.184	0.000	0.095	0.001	0.549	0.003
4930bF	NN2540Bto4bF	0.634	0.001	0.227	0.003	0.922	0.002	0.284	0.004	0.198	0.011	0.649	0.003
4930bH*	NN2540Bto4bH*	0.540	0.001	0.166	0.001	0.610	0.002	0.205	0.002	0.118	0.002	0.514	0.000
5628bF	NN2110Bto1bF	0.610	0.025	0.212	0.008	0.938	0.016	0.242	0.002	0.158	0.002	0.871	0.001
5628bH*	NN2110Bto1bH*	0.504	0.013	0.136	0.001	0.570	0.005	0.164	0.005	0.086	0.002	0.671	0.001
5629bF	NN2110Bto2bF	0.625	0.022	0.212	0.006	0.951	0.003	0.252	0.000	0.176	0.004	0.877	0.014
5629bH*	NN2110Bto2bH*	0.522	0.008	0.144	0.000	0.575	0.011	0.174	0.001	0.088	0.001	0.669	0.014
5630bF	NN2110Bto3bF	0.615	0.017	0.214	0.003	0.909	0.010	0.205	0.023	0.136	0.002	0.726	0.029
5630bH*	NN2110Bto3bH*	0.557	0.010	0.151	0.000	0.633	0.004	0.175	0.003	0.101	0.004	0.552	0.019
5631bF	NN2110Bto4bF	0.620	0.009	0.236	0.007	0.942	0.014	0.251	0.012	0.149	0.005	0.715	0.046
5631bH*	NN2110Bto4bH*	0.526	0.005	0.152	0.000	0.574	0.018	0.185	0.007	0.101	0.001	0.603	0.020
5632bF	NN2230Bto1bF	0.661	0.015	0.303	0.066	0.951	0.017	0.282	0.000	0.174	0.000	0.606	0.000
5632bH*	NN2230Bto1bH*	0.562	0.006	0.184	0.004	0.630	0.005	0.205	0.003	0.111	0.002	0.538	0.025
5633bF	NN2285Bto1bF	0.648	0.020	0.230	0.012	0.969	0.007	0.273	0.004	0.169	0.000	0.725	0.008
5633bH*	NN2285Bto1bH*	0.534	0.005	0.164	0.002	0.589	0.002	0.193	0.002	0.096	0.001	0.582	0.006
5634bF	NN2285Bto2bF	0.656	0.018	0.270	0.034	0.986	0.001	0.271	0.007	0.169	0.002	0.687	0.004
5634bH*	NN2285Bto2bH*	0.522	0.008	0.158	0.001	0.577	0.003	0.185	0.001	0.097	0.001	0.567	0.000
5635bF	NN2285Bto3bF	0.664	0.022	0.260	0.006	0.967	0.028	0.290	0.008	0.188	0.005	0.627	0.045
5635bH*	NN2285Bto3bH*	0.546	0.008	0.169	0.003	0.594	0.010	0.201	0.001	0.106	0.002	0.526	0.017
5636bF	NN2285Bto4bF	0.655	0.003	0.217	0.020	0.924	0.008	0.281	0.006	0.154	0.002	0.730	0.013
5636bH*	NN2285Bto4bH*	0.535	0.004	0.164	0.001	0.567	0.008	0.215	0.002	0.097	0.001	0.511	0.018
5637bF	NN2315Bto1bF	0.675	0.000	0.251	0.019	0.962	0.024	0.280	0.001	0.176	0.004	0.655	0.028
5637bH*	NN2315Bto1bH*	0.573	0.010	0.176	0.000	0.649	0.014	0.215	0.004	0.112	0.000	0.504	0.012
5638bF	NN2315Bto2bF	0.662	0.003	0.248	0.015	0.964	0.011	0.269	0.004	0.170	0.003	0.652	0.015
5638bH*	NN2315Bto2bH*	0.540	0.008	0.169	0.002	0.641	0.006	0.193	0.001	0.106	0.002	0.532	0.040
5639bF	NN2315Bto3bF	0.648	0.001	0.238	0.003	0.946	0.007	0.289	0.005	0.159	0.001	0.684	0.006
5639bH*	NN2315Bto3bH*	0.521	0.000	0.161	0.000	0.564	0.001	0.218	0.005	0.104	0.002	0.593	0.001
5640bF	NN2395Bto1bF	0.643	0.002	0.248	0.026	0.929	0.013	0.279	0.003	0.168	0.008	0.819	0.021
5640bH*	NN2395Bto1bH*	0.529	0.006	0.161	0.000	0.599	0.004	0.195	0.001	0.097	0.002	0.635	0.008
5641bF	NN2395Bto2bF	0.648	0.000	0.231	0.021	0.947	0.004	0.247	0.001	0.182	0.005	0.710	0.014
5641bH*	NN2395Bto2bH*	0.497	0.010	0.155	0.002	0.565	0.006	0.170	0.001	0.090	0.005	0.579	0.025
5642bF	NN2395Bto1bF	0.635	0.000	0.251	0.020	0.753	0.013	0.277	0.002	0.172	0.009	0.708	0.014
5642bH*	NN2395Bto1bH*	0.482	0.002	0.158	0.004	0.474	0.001	0.191	0.002	0.097	0.001	0.519	0.050
5643bF	NN2445Bto1bF	0.652	0.017	0.239	0.011	0.931	0.020	0.273	0.004	0.169	0.001	0.639	0.000
5643bH*	NN2445Bto1bH*	0.578	0.001	0.199	0.000	0.847	0.021	0.248	0.025	0.160	0.001	0.730	0.037

5644bF	NN2445Bto2bF	0.657	0.023	0.258	0.007	0.987	0.006	0.271	0.005	0.173	0.006	0.667	0.002
5644bH*	NN2445Bto2bH*	0.525	0.008	0.167	0.007	0.596	0.008	0.202	0.019	0.104	0.004	0.527	0.016
5645bF	NN2445Bto3bF	0.649	0.018	0.270	0.052	0.971	0.016	0.265	0.002	0.161	0.004	0.693	0.017
5645bH*	NN2445Bto3bH*	0.500	0.004	0.159	0.006	0.555	0.006	0.198	0.021	0.098	0.006	0.492	0.053
5646bF	NN2445Bto4bF	0.639	0.005	0.199	0.010	0.922	0.015	0.279	0.001	0.153	0.015	0.720	0.002
5646bH*	NN2445Bto4bH*	0.528	0.005	0.164	0.002	0.598	0.017	0.217	0.008	0.109	0.001	0.580	0.024
5647bF	NN2505Bto1bF	0.650	0.019	0.241	0.000	0.952	0.009	0.264	0.004	0.162	0.004	0.651	0.022
5647bH*	NN2505Bto1bH*	0.531	0.005	0.164	0.005	0.592	0.006	0.201	0.016	0.104	0.003	0.510	0.007
5648bF	NN2505Bto2bF	0.660	0.021	0.259	0.018	0.936	0.006	0.278	0.003	0.188	0.001	0.624	0.001
5648bH*	NN2505Bto2bH*	0.550	0.006	0.166	0.000	0.629	0.005	0.216	0.014	0.123	0.005	0.460	0.037
5649bF	NN2505Bto3bF	0.653	0.001	0.220	0.032	0.942	0.017	0.295	0.002	0.163	0.001	0.583	0.015
5649bH*	NN2505Bto3bH*	0.534	0.007	0.160	0.004	0.592	0.008	0.209	0.015	0.108	0.004	0.476	0.011
5650bF	NN2565Bto1bF	0.659	0.005	0.230	0.004	0.960	0.005	0.273	0.001	0.107	0.065	0.612	0.018
5650bH*	NN2565Bto1bH*	0.534	0.002	0.172	0.001	0.615	0.005	0.211	0.000	0.115	0.001	0.513	0.008
5687bF	NN2565Bto2bF	0.642	0.004	0.215	0.009	0.917	0.024	0.290	0.007	0.164	0.007	0.716	0.027
5687bH*	NN2565Bto2bH*	0.486	0.002	0.146	0.001	0.526	0.001	0.191	0.010	0.101	0.006	0.617	0.006
5688bF	NN2565Bto3bF	0.648	0.007	0.229	0.005	0.906	0.023	0.280	0.013	0.176	0.008	0.625	0.008
5688bH*	NN2565Bto3bH*	0.504	0.004	0.156	0.001	0.523	0.005	0.203	0.004	0.106	0.006	0.519	0.006
5689bF	NN2565Bto4bF	0.632	0.002	0.238	0.001	0.907	0.003	0.275	0.000	0.171	0.008	0.565	0.007
5689bH*	NN2565Bto4bH*	0.517	0.001	0.159	0.001	0.565	0.010	0.206	0.007	0.101	0.004	0.471	0.012
5690bF	NN2590Bto1bF	0.635	0.009	0.218	0.023	0.875	0.027	0.281	0.013	0.173	0.001	0.773	0.005
5690bH*	NN2590Bto1bH*	0.485	0.005	0.150	0.003	0.513	0.010	0.200	0.003	0.101	0.003	0.566	0.104
5691bF	NN2590Bto2bF	0.644	0.004	0.207	0.024	0.946	0.007	0.267	0.005	0.155	0.008	0.704	0.016
5691bH*	NN2590Bto2bH*	0.489	0.002	0.144	0.008	0.515	0.019	0.195	0.001	0.107	0.003	0.565	0.008
5692bF	NN2590Bto3bF	0.643	0.006	0.237	0.017	0.940	0.050	0.282	0.001	0.177	0.012	0.652	0.000
5692bH*	NN2590Bto3bH*	0.491	0.004	0.146	0.001	0.539	0.008	0.197	0.008	0.102	0.001	0.492	0.084
5693bF	NN2590Bto4bF	0.631	0.005	0.222	0.019	0.904	0.020	0.287	0.001	0.171	0.008	0.747	0.013
5693bH*	NN2590Bto4bH*	0.480	0.002	0.136	0.005	0.532	0.005	0.186	0.003	0.098	0.007	0.651	0.008
5694bF	NN2A1Bto1bF	0.642	0.005	0.216	0.005	0.923	0.013	0.253	0.007	0.158	0.001	0.720	0.008
5694bH*	NN2A1Bto1bH*	0.511	0.004	0.156	0.002	0.566	0.005	0.210	0.001	0.057	0.072	0.555	0.015
5695bF	NN2A1Bto2bF	0.637	0.004	0.189	0.007	0.914	0.014	0.241	0.012	0.148	0.006	0.678	0.014
5695bH*	NN2A1Bto2bH*	0.522	0.002	0.155	0.000	0.596	0.004	0.193	0.007	0.056	0.072	0.607	0.002
5696bF	NN2A1Bto3bF	0.641	0.011	0.217	0.024	0.912	0.027	0.275	0.006	0.157	0.003	0.699	0.021
5696bH*	NN2A1Bto3bH*	0.530	0.004	0.160	0.001	0.579	0.013	0.203	0.004	0.108	0.013	0.531	0.009
5697bF	NN2A1Bto4bF	0.638	0.004	0.215	0.017	0.931	0.009	0.249	0.003	0.151	0.008	0.706	0.025
5697bH*	NN2A1Bto4bH*	0.507	0.002	0.152	0.003	0.567	0.010	0.197	0.012	0.096	0.002	0.584	0.009

Thermoluminescence dating (D. Richter)

Thermoluminescence (TL) dating of heated flint artefacts is a well established method for dating Middle Palaeolithic archaeological sites (Valladas et al., 1988). A past human activity can be directly dated by establishing the time elapsed since a flint artefact fell into a prehistoric fire. TL dating is based on the accumulation of electrons in excited states in the crystal lattice due to omnipresent ionizing radiation. These metastable states can be quantitatively measured by TL analysis and provide the dose the sample has received since its last zeroing (heating) in the fire when all excited states were eliminated by the prehistoric heating. Standard analysis of TL dating of heated flints is based on multiple aliquot techniques with a combined additive and regeneration (MAAR) protocol (Mercier et al., 1991; Valladas et al., 1988).

This standard approach requires sample weights of several grams, which are not available at Neumark Nord 2. Almost all flints that were macroscopically identified as having been burnt (craquelation, potlids, ect.) were in the weight range of 2-6 g and thus too small for standard TL-dating approaches. Large samples are required because for dosimetric reasons the outer two mm of samples are removed with a water-cooled diamond saw, resulting in the loss of a large amount of material of such irregularly shaped objects like flint artefacts (Richter, 2007). Therefore a single aliquot regeneration (SAR) technique had to be used, which requires in principle only a few mg of sample material after extraction (removal). This new approach employed here makes use of the almost absent sensitivity change of the TL signal of quartz in the orange-red wavelength detection band, which is also observed for many flints that basically consist of cryptocrystalline quartz. Because of these negligible sensitivity changes no test dose measurements are required (Richter and Krbetschek, 2006). The standard SAR technique can be even further reduced to the measurement of two regeneration points only (Richter and Krbetschek, 2006), which greatly reduces the time needed for measuring large palaeodoses in the laboratory. However, as a check of the assumption of negligible sensitivity change a repetition of one regeneration dose point was measured as well. The palaeodose is therefore derived from the level of the natural TL signal as defined by the intersection of this level with a straight line connecting the measurement results (TL) of two regeneration doses. If the integrated TL (as defined by the temperature range of the heating plateau) from these two regeneration dose points are close to the natural TL, any deviation of the regeneration

dose response curve from a straight line is negligible (Richter, 2009). In any case the doses for samples at Neumark Nord 2 are still well in the linear dose range of flint and therefore this issue is of no concern here and the dose response curves can be assumed as being linear in the range under investigation here. The validity of this short SAR approach was shown for different samples in the linear as well as sublinear dose range for several sites and materials (Richter and Temming, 2006).

For each sample between 12 and 24 aliquots of 4 mg were measured in order to obtain statistically more valid results. Rejection criteria for individual aliquots were defined as recycling ratios between 0.85-1.15, a palaeodose error of less than 10% and the natural TL had to be bracketed by the two regeneration dose points. An additional rejection criterion was defined as a maximum deviation of 20% of the regenerated TL from the natural TL. Failure of this criterion is a reflection of the poor knowledge of the approximate natural dose and the subsequent misjudgement of the doses to be applied by the operator. However, as these samples are certainly still well within the linear range of their TL growth curves a regeneration response beyond 20% appears to be acceptable, but there are no means to objectively determine a threshold. Subsequent analysis with a higher threshold increased the number of acceptable aliquots significantly and produced virtually identical results. The samples were measured in groups of 5-10 aliquots and knowledge of regeneration doses increased with aliquot number and led to a reduction of rejected aliquots with time. Therefore large numbers of rejected aliquots on basis of failure of this criterion are not a reflection of 'bad' behaviour of the samples but rather of the lack of experience with this new protocol. Because flints contain natural radioactive elements their, incontestably stable, contribution to the total dose rate needs to be taken into account. Samples for Neutron Activation Analysis (NAA) to determine U, Th and K were taken from crushed material of the extracted core of the samples prior to chemical treatment. This internal dose rate is established by the determination of the alpha sensitivity (b-value) for each sample separately by comparing the TL yield from calibrated alpha and beta sources on fine grained (4-11 μm) material which was zeroed for 30 min at 500°C.

The external g-dose rate was determined in situ in the excavation sections over a period of several months by five $\text{Al}_2\text{O}_3:\text{C}$ dosimeters because of the heterogeneity of the sediments containing the archaeological material and the varying thickness of the archaeological deposit. The results from these dosimeters display a variability of 10%

standard deviation from the mean and therefore such an uncertainty for the external g-dose rate was employed for the dosimeter average of $956 \mu\text{Gy a}^{-1}$, which is confirmed by moisture corrected HpGe-g-ray-spectrometry. The sediments from this deposit as well as those above and below were measured by HpGe-g-ray spectrometry in order to determine that the U- and Th-series are in secular equilibrium and therefore the assumption of stability of the external g-dose rate over time is valid. The external g-dose rate was adjusted for sample size, but no adjustments were made for water content. A cosmic dose of $90 \mu\text{Gy a}^{-1}$ was estimated according to the geographic position and sediment thickness, resulting in an effective external g-dose rate of $1046 \mu\text{Gy a}^{-1}$ for the samples.

The resulting palaeodoses display a smaller variation than the observed external g-dose rate, which is an indirect indication of the validity of the latter parameter. The age results cluster narrowly between 119 and 135 ka and belong to a normal distribution. This allows the calculation of a weighted average age of 126 ± 6 ka, which best represents the time of the last heating of these flint artefacts and testifies the time of the activity of lighting a fire by Neandertals during the Eemian at Neumark Nord 2.

Table S3:

Results of NAA and TL measurements

Sample	U	Th	K	b-value	effective internal dose rate	total dose rate	Number of accepted aliquots	average recycling ratio	palaeodose (Gy)	age (ka)
NN2-001	0.23±0.04	0.13±0.02	510±20	0.697	80±6	1117±95	23	1.13±0.02	140±6	125±12
NN2-002	0.35±0.04	0.09±0.01	290±20	0.731	81±6	1117±96	14	1.03±0.02	150±6	134±13
NN2-005	0.40±0.04	0.11±0.02	445±27	0.611	101±7	1137±95	15	1.03±0.01	153±4	135±13
NN2-009	0.50±0.05	0.12±0.02	308±22	0.805	108±8	1144±95	17	1.03±0.01	140±3	122±12
NN2-018	0.31±0.03	0.12±0.02	356±25	0.826	81±6	1118±95	17	1.06±0.03	133±7	119±12

The resulting palaeodoses display a smaller variation than the observed external g-dose rate, which is an indirect indication of the validity of the latter parameter. The age results cluster narrowly between 119 and 135 ka and belong to a normal distribution. This allows the calculation of a weighted average age of 126 ± 6 ka, which best represents the time of the last heating of these flint artefacts and testifies the time of the activity of lighting a fire by Neandertals during the Eemian at Neumark Nord 2.

PALEOMAGNETIC PROCEDURES (M.J. SIER & M.J. DEKKERS)

Sampling

Dedicated perspex sample containers with standard dimension (25 mm diameter and 22 mm height) were gently pushed into freshly prepared cut-outs in the section. After orientation with a magnetic compass and inclinometer they were taken out from the section and closed with a plastic lid and sealed for measurement in paleomagnetic laboratory 'Fort Hoofddijk' (Utrecht University, Utrecht, the Netherlands). Measurements were done within one month after retrieval of the samples to ensure that the samples were processed while still fresh. For thermal demagnetization an electrical drill powered by a portable generator was used to drill the fragile sediments on selected intervals. Orientation was done with a magnetic compass and a dedicated orientation device. Only the most sandy layers could not be drilled, cores desintegrated due to the water used to flush away the drilled sediment. All samples were processed within 14 days after collection. For the demagnetization standard-sized specimens were cut with a plastic knife from the drill cores; subsequently they were wrapped in aluminium foil to withstand the manipulating that jeopardizes the physical stability of the samples during thermal treatment.

Demagnetization

Alternating field (AF) demagnetization in 15 steps to up 100 mT was carried out with a robotized direct current superconducting quantum interference device (DC-SQUID) magnetometer manufactured by the '2G' company (Mountain View California, USA). The instrument sensitivity is 3×10^{-12} Am² and typical sample intensities were at least two orders of magnitude higher. Static three-axial AF demagnetization was done with a so-called in-line AF demagnetization coil set directly attached to the magnetometer. The instrument set-up is housed inside a magnetically shielded room (residual field < 200 nT); the robotized interface for sample manipulation was built in-house. Up to 96 samples contained in dedicated cubic holders (edge 30 mm) are loaded onto a sample plateau and the robot loads them in batches of eight onto a tray that can be slid through the

magnetometer and demagnetization coils. Samples are processed fully automatically with the so-called 'three position protocol' that compensates for the magnetic moment of the transport tray. This ensures optimal processing of weakly magnetic samples.

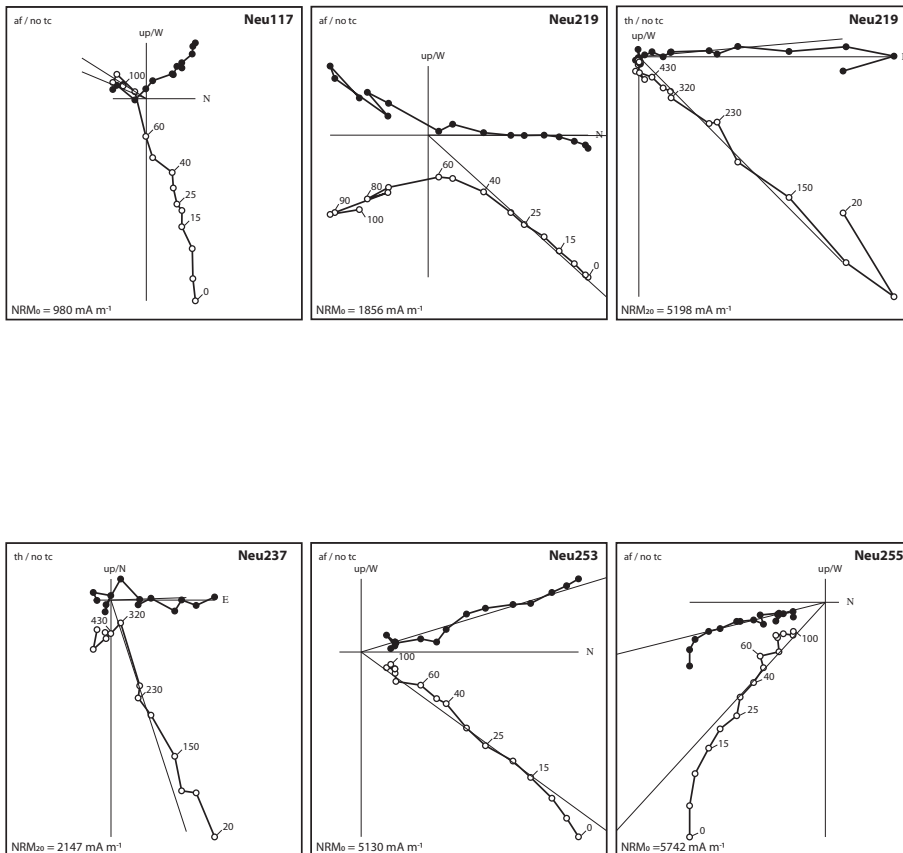
Thermal demagnetization was performed with in-house constructed thermal demagnetizers (residual field < 50 nT) and measured with another DC-SQUID magnetometer (instrument sensitivity 5×10^{-12} Am²). During thermal demagnetization the samples appeared to become highly viscous after demagnetization at temperatures > ~350°C due to neoformation of extremely fine-grained magnetite (grain size ~20 nm). To have the viscous moment decayed entirely a waiting time of 5 to 10 minutes was implemented with the sample inside the magnetometer in a very low ambient field before each instrument reading was taken. Only by processing with such a long waiting meaningful demagnetization results could be obtained. To avoid the development of disturbing viscous magnetic moments during the thermal demagnetization a sample set was thermally demagnetized up to 205°C to demagnetize the natural viscous component acquired in ~100 ka in the geomagnetic field. After this thermal treatment they were further demagnetized by AF demagnetization in the robotized magnetometer system.

Demagnetization data are plotted in orthonormal vector endpoint diagrams or Zijderveld diagrams (Zijderveld, 1967). Representative examples are shown in figure S7. Sample Neu117 is processed by AF demagnetization, it shows a large overprint and a small characteristic remanent magnetization (ChRM) with a transitional/reversed direction. The large overprint is caused by viscous overprinting but also by physical realignment of the particles in the strong geomagnetic field that prevailed directly after the Blake Event (cf. Coe and Liddicoat's (Coe and Liddicoat, 1994) explanation for features of the Mono Lake excursion record). The Blake Event is like all geomagnetic events characterized by a weak geomagnetic field intensity. Sample Neu 219 that is treated with AF demagnetization shows the development of so-called gyroremanent magnetization (GRM) (Stephenson, 1993), a characteristic property of greigite (Fe₃S₄) a magnetic mineral that may often occur in fresh-water sediments (e.g. (Hu et al., 2002; Snowball, 1997)). The greigite is formed in-situ over an undefined duration albeit that most greigite NRM is acquired shortly after deposition (i.e. within ~10 ka). The potential presence of greigite thus provides an other possibility for having large normal overprints potentially obscuring detection of the detrital ChRM component. Indeed during thermal demagnetization of

a sister specimen most NRM is demagnetized at $\sim 350^\circ\text{C}$, at the end of the temperature interval during which greigite chemically alters to a non-magnetic ferrous-ferric sulfate ($\sim 220\text{--}350^\circ\text{C}$, e.g. Dekkers et al., 2000). Also Neu 237 with its easterly declination shows this behaviour; its direction could be a composite of a transitional direction with a later normal overprint caused by prolonged greigite formation. Samples Neu 253 and Neu 255 are AF demagnetized after thermal demagnetization to 205°C and indeed the

Figure S7:

Zijderveld diagrams of some representative samples in stratigraphic coordinates (the section underwent no tilting after deposition). Neu117: AF demagnetization (af) only; first Neu219 sample: AF demagnetization only; second Neu219 and Neu237 sample: thermal demagnetization (th) only. Neu253 and Neu255: AF demagnetization after thermal demagnetization up to 205°C . See text for more details.



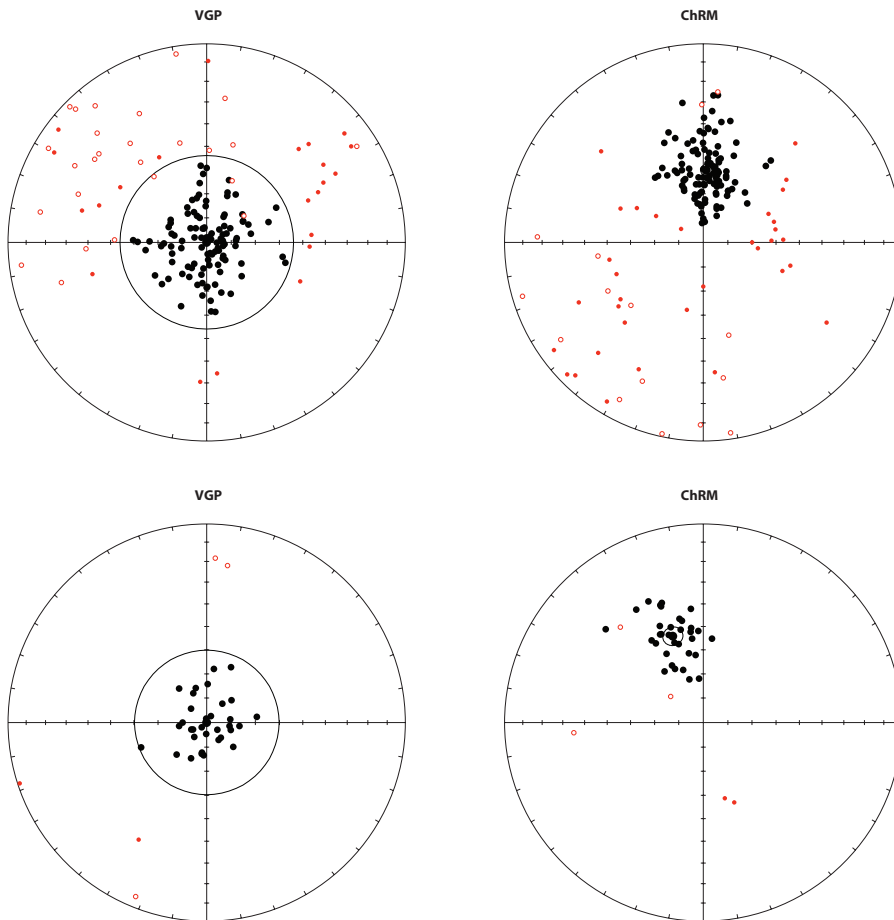
determination of the ChRM is more straightforward than with AF demagnetization only. Of course for levels devoid of greigite observed NRM directions may be representative of the (non-dipole) transitional geomagnetic field during an excursion. However, overprinting of a strong normal direction on the weak transitional ChRM may occur as well. To discriminate between directional scatter due to secular variation of the geomagnetic field and excursions, the data set was subjected to the variable cut-off procedure (Vandamme, 1994). Samples with deviating directions appeared to be stratigraphically coherent and are interpreted to derive from the Blake Event.

Delayed NRM acquisition?

The paleomagnetic age assignment of the Blake Event hinges on the quality of its recording in the sediments which is generally not straightforward. Post-depositional processes may obscure the recording and its preservation. This includes pDRM lock-in aspects that can be lithology-dependent (Hofmann and Fabian, 2007; Tauxe, 1993) post-depositional realignment in stronger post-Blake geomagnetic fields (Coe and Liddicoat, 1994), biological activity (Egli, 2004; Kruiver and Passier, 2001) and a myriad of early diagenetic processes (e.g. Calvert and Fontugne, 2001; Passier et al., 2001; Rowan and Roberts, 2006). Recording of geomagnetic events in high-latitude Arctic cores has recently been shown suspect in cases where the events are associated to horizons containing greigite that would have acquired a self-reversed NRM (Channell and Xuan, 2009). Also the loess archive on the Chinese Loess Plateau should be scrutinized before a recording of a geomagnetic excursion can be assessed as genuine: for the Blake Event Zhu et al. (Zhu et al., 1998) document a limited recording or even non-recording (or preservation) as a function of interfering pedogenesis or discontinuous loess deposition due to erosive storm events. Nonetheless there seem to exist recordings of the Blake Event that are less complicated in this sense in open ocean settings with a limited geochemical contrast in ODP Site 1062 on the Blake/Bahama Outer Ridge (Lund et al., 2006). These authors assign an age slightly older than 120 ka to the event but a record of the transition itself was not provided. The Blake Event in the Gardar Drift sediments (Channell et al., 1997) at ~119 ka has a short-lived declination swing but its inclination record appears to be subdued. On the basis of their study of a set of cores from the Kolbeinski Ridge (Iceland Sea), Nowaczyk and Frederichs (Nowaczyk and Frederichs, 1999) argue that the Blake Event is recorded

Figure S8:

Variable cut-off procedure after Vandamme (1994) for the HP7 and 210_296/297 samples. The scatter in ChRM directions caused by secular variation of the geomagnetic field are plotted in black (full symbols). Excursion directions are plotted in full red symbols (inclination positive or down) or open red symbols (inclination negative or up). Top panels HP7, lower panels excavation square section 210/296-297. VGPs (left-most panels) are centered on a vertical-up mean.



as a double event straddling 120 ka. Zhu et al. (Zhu et al., 2000) determined K/Ar ages of 123 ± 7 and 123 ± 10 ka for two lavas with intermediate palaeomagnetic directions in the Tianchi volcanic sequence (NE China) that were associated to the Blake Event.

We base our terrestrial-marine correlation primarily on the Blake Event, notably that one as described in Tric et al. (Tric et al., 1991), because that is so detailed. Regarding the issue of a possible delayed NRM acquisition two aspects needs to be discussed: 1) The Tric et al. (Tric et al., 1991) record is from an interval more or less directly above a sapropel that may have been burnt down to some degree (Higgs et al., 1994; vanSantvoort et al., 1997). Delayed NRM acquisition would imply that the Blake Event would be younger than the sediment level of its recording, thus enhancing the discrepancy between the terrestrial expression of the Eemian and MIS 5e. 2) In the Neumark record delayed NRM acquisition could have occurred during a younger phase of the terrestrial Eemian.

1. Burnt-down sapropel levels often contain traces of magnetotactic magnetite (Kruiver and F. Passier, 2001), an aspect that could not be known by Tric et al. (1991) because it was not yet discovered. Therefore detailed IRM acquisition curves to track this possibility are not available for the Tric et al. (Tric et al., 1991) record. However, there is a detailed geochemical study available (Calvert and Fontugne, 2001) for a nearby core collected during the same cruise, core MD84641. Both cores are from the northernmost outer parts of the river Nile cone. The Tric et al. (Tric et al., 1991) record derives from core MD84627, but Tucholka et al. (Tucholka, 1987) found the Blake Event also in MD84641 albeit less well expressed (the reason that Tric et al. (Tric et al., 1991) focussed on core MD84627). Geochemical proxies (all from Calvert and Fontugne (Calvert and Fontugne, 2001)) from directly above sapropel S5, notably the Si/Al and Ti/Al ratios that are not influenced by diagenetic iron mobility, do not hint at an originally much thicker sapropel. Also sulfidic sulfur (in the form of pyrite grains precipitated) did not migrate downward from S4 all the way down to S5 as a possible consequence of later re-establishment of anoxic conditions during formation of sapropel S4. Also Ba/Al levels are not enriched above S5 in that core (note below S5 they seem to be 'highish'). So, although some delayed NRM acquisition as a consequence of early diagenesis cannot be excluded, distinctly later diagenetic overprinting (with a delay of several thousands of years) is unlikely in the Tric et al. (Tric et al., 1991) record despite its close association to a sapropel.

Also it is rather difficult to surmise how to generate a double geomagnetic event with the reported relatively smooth VGP path as a result of diagenetic imprint of a weak reversed geomagnetic field onto a normal polarity NRM that represents a stronger geomagnetic field (because at that time the field is not in a transitional state).

2. The possibility of delayed NRM acquisition in the Neumark record. Also in the Neumark record delayed NRM acquisition could have occurred, particularly in darker coloured greigite-bearing strata where some delay in NRM acquisition coupled to a prolonged NRM acquisition duration is bound to have occurred. Sedimentation rates in the section are appreciable; therefore the time-span available for biologic and (very) early diagenetic processes is probably limited (most activity takes place close to the sediment-water interface). The paleomagnetic directional record does not correlate with (subtle) changes in lithology which makes diagenetic imprint of the entire Blake Event over a thickness of ~ 6 metres unlikely. Moreover, the artifact find-layer in the very same section has been dated to 126 ± 6 ka which concurs with an undelayed recording of the Blake Event in the Neumark succession.

References Supplementary Material

- Bada, J.L., Shou, M.Y., Man, E.H. and Schroeder, R.A., 1978, Decomposition of hydroxy amino acids in foraminiferal tests: Kinetics, mechanism and geochronological implications. *Earth and Planetary Science Letters*, 41: 67-76.
- Bowen, D.Q., 1999, A Revised Correlation of Quaternary Deposits in the British Isles. Geological Society of London, London
- Calvert, S.E. and Fontugne, M.R., 2001, On the late Pleistocene-Holocene sapropel record of climatic and oceanographic variability in the eastern Mediterranean. *Paleoceanography*, 16: 78-94.
- Channell, J.E.T., Hodell, D.A. and Lehman, B., 1997, Relative geomagnetic paleointensity and $[\delta]18\text{O}$ at ODP Site 983 (Gardar Drift, North Atlantic) since 350 ka. *Earth and Planetary Science Letters*, 153: 103-118.
- Channell, J.E.T. and Xuan, C., 2009, Self-reversal and apparent magnetic excursions in Arctic sediments. *Earth and Planetary Science Letters*, In Press, Corrected Proof.
- Coe, R.S. and Liddicoat, J.C., 1994, Overprinting of natural magnetic remanence in lake sediments by a subsequent high-intensity field. *Nature*, 367.
- Dekkers, M.J., Passier, H.F. and Schoonen, M.A.A., 2000, Magnetic properties of hydrothermally synthesized greigite (Fe_3S_4) High- and low-temperature characteristics. *Geophysical Journal International*, 141: 809.
- Egli, R., 2004, Characterization of individual rock magnetic components by analysis of remanence curves. 3. Bacterial magnetite and natural processes in lakes. *Physics and Chemistry of the Earth, Parts A/B/C*, 29: 869-884.
- Eissmann, L., 2002, Quaternary geology of eastern Germany (Saxony, Saxon-Anhalt, South Brandenburg, Thüringia), type area of the Elsterian and Saalian Stages in Europe. *Quaternary Science Reviews*, 21: 1275-1346.
- FAO-Unesco ed. 1988, World Soil Resources Report. Food and Agriculture Organization of the United Nations, Rome 138 p.
- FAO ed. 1977, Guidelines for soil profile description. Food and Agriculture Organization of the United Nations, Rome 66 p.
- Higgs, N.C., Thomson, J., Wilson, T.R.S. and Croudace, I.W., 1994, Modification and complete removal of eastern Mediterranean sapropels by postdepositional oxidation. *Geology*, 22: 423-426.
- Hill, R.L., 1965, Hydrolysis of proteins. *Advances in Protein Chemistry*, 20: 37-107.

- Hofmann, D.I. and Fabian, K., 2007, Rock magnetic properties and relative paleointensity stack for the last 300 ka based on a stratigraphic network from the subtropical and subantarctic South Atlantic. *Earth and Planetary Science Letters*, 260: 297-312.
- Hu, S., Stephenson, A. and Appel, E., 2002, A study of gyroremanent magnetisation (GRM) and rotational remanent magnetisation (RRM) carried by greigite from lake sediments. *Geophysical Journal International*, 151: 469.
- Kaufman, D.S. and Manley, W.F., 1998, A new procedure for determining DL amino acid ratios in fossils using Reverse Phase Liquid Chromatography. *Quaternary Science Reviews*, 17: 987-1000.
- Kruiver, P.P. and F. Passier, H., 2001, Coercivity analysis of magnetic phases in sapropel S1 related to variations in redox conditions, including an investigation of the S ratio. *Geochemistry Geophysics Geosystems*, 2: 1063.
- Laurat, T. and Brühl, E., 2006, Zum Stand der archäologischen Untersuchungen im Tagebau Neumark-Nord, Ldkr. Merseburg-Querfurt (Sachsen-Anhalt) - Vorbericht zu den Ausgrabungen 2003-2005. *Jahresschrift für Mitteldeutsche Vorgeschichte*, 90: 9-69.
- Lund, S., Stoner, J.S., Channell, J.E.T. and Acton, G., 2006, A summary of Brunhes paleomagnetic field variability recorded in Ocean Drilling Program cores. *Physics of the Earth and Planetary Interiors*, 156: 194-204.
- Mania, D., Thomae, M., Litt, T. and Weber, T., 1990, Neumark - Gröbern: Beiträge zur Jagd des mittelpaläolithischen Menschen. *Veröffentlichungen des Landesmuseum für Vorgeschichte in Halle*, 43: 1-319.
- Mania, D. and Mania, U., 2008, Stratigraphy and Paleolithic of the Saale complex in the Elbe-Saale region. *L'Anthropologie*, 112: 15-47.
- Menke, B. and Tynni, R., 1984, Das Eeminterglazial und das Weichselfrühglazial von Rederstell/Dittmarschen und ihre Bedeutung für die mitteleuropäische Jungpleistozängliederung. *Geologisches Jahrbuch*, A76: 3-120.
- Mercier, N., Valladas, H., Joron, J.-L., Reyss, J.-L., Lévêque, F. and Vandermeersch, B., 1991, Thermoluminescence dating of the late Neanderthal remains from Saint-Césaire. *Nature*, 351: 737-739.
- Nowaczyk, N.R. and Frederichs, T.W., 1999, Geomagnetic events and relative palaeointensity variations during the past 300ka as recorded in Kolbeinsey Ridge sediments, Iceland Sea: indication for a strongly variable geomagnetic field. *International Journal of Earth Sciences*, 88: 116-131.

- Parfitt, S.A., Barendregt, R.W., Breda, M., Candy, I., Collins, M.J., Coope, G.R., Durbidge, P., Field, M.H., Lee, J.R., Lister, A.M., Mutch, R., Penkman, K.E.H., Preece, R.C., Rose, J., Stringer, C.B., Symmons, R., Whittaker, J.E., Wymer, J.J. and Stuart, A.J., 2005, The earliest record of human activity in northern Europe. *Nature*, 438: 1008-1012.
- Passier, H.F., Lange, G.J.d. and Dekkers, M.J., 2001, Magnetic properties and geochemistry of the active oxidation front and the youngest sapropel in the eastern Mediterranean Sea. *Geophysical Journal International*, 145: 604-614.
- Penkman, K.E.H., 2005, Amino Acid Geochronology: A Closed System Approach to Test and Refine the UK Model. Unpublished Ph.D. Thesis, University of Newcastle, UK
- Penkman, K.E.H., Preece, R.C., Keen, D.H., Maddy, D., Schreve, D.C. and Collins, M.J., 2007, Testing the aminostratigraphy of fluvial archives: the evidence from intra-crystalline proteins within freshwater shells. *Quaternary Science Reviews*, 26: 2958-2969.
- Penkman, K.E.H., Kaufman, D.S., Maddy, D. and Collins, M.J., 2008a, Closed-system behaviour of the intra-crystalline fraction of amino acids in mollusc shells. *Quaternary Geochronology*, 3: 2-25.
- Penkman, K.E.H., Preece, R.C., Keen, D.H. and Collins, M.J., 2008b, British aggregates -An improved chronology using amino acid racemization and degradation of intra-crystalline amino acids (IcPD). English Heritage Research Department Report Series.
- Penkman, K.E.H., Preece, R.C., Keen, D.H. and Collins, M.J., 2009, Amino acid geochronology of the type Cromerian of West Runton, Norfolk, UK. *Quaternary International*, in press.
- Preece, R.C. and Penkman, K.E.H., 2005, New faunal analyses and amino acid dating of the Lower Palaeolithic site at East Farm, Barnham, Suffolk. *Proceedings of the Geologists' Association*, 116: 363-377.
- Richter, D. and Krbetschek, M., 2006, A new Thermoluminescence dating technique for heated flint. *Archaeometry*, 48: 695-705.
- Richter, D. and Temming, H., 2006, Testing heated flint palaeodose protocols using dose recovery procedures. *Radiation Measurements*, 41: 819-825.
- Richter, D., 2007, Advantages and limitations of thermoluminescence dating of heated flint from Paleolithic sites. *Geoarchaeology* 22: 671-683.
- Richter, D., 2009, Burnt flint artifacts: A new Thermoluminescence dating technique. *Preistoria Alpina*, 44: 41-55.

- Rowan, C.J. and Roberts, A.P., 2006, Magnetite dissolution, diachronous greigite formation, and secondary magnetizations from pyrite oxidation: Unravelling complex magnetizations in Neogene marine sediments from New Zealand. *Earth and Planetary Science Letters*, 241: 119-137.
- Snowball, I.F., 1997, Gyroremanent magnetization and the magnetic properties of greigite-bearing clays in southern Sweden. *Geophysical Journal International*, 129.
- Stephenson, A., 1993, Three-Axis static alternating field demagnetisation of rocks and the identification of natural remanent magnetisation, gyroremanent magnetisation, and anisotropy. *Journal of Geophysical Research*, 98: 373.
- Stockmarr, J., 1971, Tablets with spores used in absolute pollen analysis. *Pollen Spores*, 13: 615-621. Stoops, G., 2003, Guidelines for Analysis and Description of Soil and Regolith Thin section. Soil Science Society of America, Madison
- Sykes, G.A., Collins, M.J. and Walton, D.I., 1995, The significance of a geochemically isolated intracrystalline organic fraction within biominerals. *Organic Geochemistry*, 23: 1039-1065.
- Tauber, H., 1965, Differential pollen dispersal and the interpretation of pollen diagrams. *Danm. Geol. Unders.*, II R: 89.
- Tauber, H., 1967, Investigations of the mode of pollen transfer in forested areas. *Rev. Palaeobot. Palynol.*, 3: 277-286.
- Tauxe, L., 1993, Sedimentary records of relative paleointensity of the geomagnetic field - theory and practice. *Reviews of Geophysics*, 31: 319-354.
- Thomae, M., 2003, Mollisoldiapirismus - Ursache für die Erhaltung der Fundstätte Neumark-Nord (Geiseltal). In: Burdukiewicz, J.M., Fiedler, L., Heinrich, W.D., Justus, A. and Brühl, E. (eds.), *Erkenntnisjäger. Kultur und Umwelt des frühen Menschen*. Landesamt für Archäologie Sachsen-Anhalt, Halle, 601-605.
- Tric, E., Laj, C., Valet, J., Tucholka, P., Paterne, M. and Guichard, F., 1991, The Blake geomagnetic event: transition geometry, dynamical characteristics and geomagnetic significance. *Earth and Planetary Science Letters*, 102: 1-13.
- Tucholka, P., Fontugne, M., Guichard, F., Paterne, M., 1987, The Blake magnetic polarity episode in cores from the Mediterranean Sea. *Earth and Planetary Science Letters*, 86: 320-326.
- Turner, C. and West, R.G., 1968, The subdivision and zonation of interglacial periods. *Eiszeitalter und Gegenwart*, 19.

- Turner, C., 2000, The Eemian interglacial in the North European plain and adjacent areas. *Geologie en Mijnbouw - Netherlands Journal of Geosciences*, 79 (2/3): 217-231.
- Turner, C., 2002, Formal Status and Vegetational development of the Eemian Interglacial in Northwestern and Southern Europe. *Quaternary Research*, 58: 41-44.
- Valladas, H., Reyss, J.L., Joron, J.L., Valladas, G., Bar-Yosef, O. and Vandermeersch, B., 1988, Thermoluminescence dating of mousterian 'Proto-Cro-Magnon' remains from Israel and the origin of modern man. *Nature*, 331: 614-616.
- Vandamme, D., 1994, A new method to determine paleosecular variation. *Physics of the Earth and Planetary Interiors*, 85: 131.
- vanSantvoort, P.J.M., deLange, G.J., Langereis, C.G., Dekkers, M.J. and Paterne, M., 1997, Geochemical and paleomagnetic evidence for the occurrence of "missing" sapropels in eastern Mediterranean sediments. *Paleoceanography*, 12: 773-786.
- Zagwijn, W.H., 1961, Vegetation, climate and radiocarbon datings in the late Pleistocene of the Netherlands: Part I. Eemian and Early Weichselian. *Mededelingen van de Geologische Stichting. Nieuwe Serie*, 14: 15-45.
- Zhu, R., Coe, R.S., Guo, B., Anderson, R. and Zhao, X., 1998, Inconsistent palaeomagnetic recording of the Blake event in Chinese loess related to sedimentary environment. *Geophysical Journal International*, 134: 867-875.
- Zhu, R.X., Pan, Y.X. and Coe, R.S., 2000, Paleointensity studies of a lava succession from Jilin Province, northeastern China: Evidence for the Blake event. *Journal of Geophysical Research-Solid Earth*, 105: 8305-8317.
- Zijderveld, J.D.A., 1967, Demagnetisation of rocks: analysis of results. In: Collinson, D.W., Creer, K.M. and Runcorn, S.K. (eds.), *Methods in Palaeomagnetism*. Elsevier, Amsterdam, 254-286.





CHAPTER 3

MAGNETIC PROPERTY ANALYSIS AS PALAEOENVIRONMENTAL PROXY:
A CASE STUDY OF THE LAST INTERGLACIAL MIDDLE PALAEO-LITHIC SITE
AT NEUMARK-NORD 2 (GERMANY)



CHAPTER 3

MAGNETIC PROPERTY ANALYSIS AS PALAEOENVIRONMENTAL PROXY: A CASE STUDY OF THE LAST INTERGLACIAL MIDDLE PALAEOOLITHIC SITE AT NEUMARK-NORD 2 (GERMANY)

Abstract

The so-called Blake Event, an event of the geomagnetic field, was identified in the Middle Palaeolithic Neumark-Nord 2 (NN2) site in Germany by Sier et al. (2011). These authors discussed the implications for the positioning of the Eemian in the Marine isotope stage (MIS) scale in northern-central Europe. The NN2 data showed a lagtime of ~5000 years between the MIS 5e peak and the start of the Eemian in central Europe. This increased lagtime forces us to rethink the terrestrial-marine climatic relations for this part of Europe during the last interglacial. Here we analyze the magnetic properties of the sedimentary sequence at the NN2 site, and correlate these data to the pollen zonation established for the same site. This enables an assessment of the magnetic property expression of Eemian climatic and environmental changes. Our study demonstrates that the expression of the magnetic properties at NN2 is closely related to variability in open or closed environments during the Eemian in the catchment area of the NN2 basin. It indicates the presence of a wet to dry climate transition in the NN2 deposits (top pollen zone IVb3) which is typical for this period of the Eemian in Europe. Moreover, the magnetic property study supports our claim of having found a primary paleomagnetic signal of the Blake Event at NN2.

1. Introduction

The present contribution concerns an evaluation of the potential of magnetic property analysis to unravel palaeoclimatic and palaeoenvironmental information from the fine-grained deposits containing the rich Middle Palaeolithic archaeological site of Neumark-Nord 2 (NN2). We aim to illustrate the potential of this type of rock magnetic research as a quick-scan palaeoenvironmental proxy. It is possible to get a very detailed rock-magnetic record in a comparatively short period of time, compared to more labour-intensive studies such as pollen or micromorphological research. Hence, this type of data acquisition may be helpful for palaeoenvironmental interpretation when such labour-intensive studies are not possible. Also, it may allow rapid identification of zones of interest in long sequences, that can subsequently be the focus of more time-consuming other types of palaeoenvironmental analyses. The application of this type of rock-magnetic research is not yet common in palaeolithic archaeology and it should be noted that the approach differs from the more commonly applied “classic” palaeomagnetic and magnetostratigraphic analysis. In the background section below we briefly outline both approaches.

The NN2 sequence is particularly interesting as a case study for the application of rock-magnetic analysis. Previous palaeomagnetic analysis revealed a high-resolution record of the Blake Event, which could be positioned in the early part of the Eemian (Last Interglacial) pollen sequence identified from the same location (Sier et al., 2011). The NN2 data now enable a precise terrestrial-marine correlation for the Eemian stage in central Europe. They demonstrate a surprisingly large time lag between the Marine Isotope Stage (MIS) 5e ‘peak’ in the marine record and the start of the Last Interglacial in this region (Sier et al.). The Blake Event interval recorded in the NN2 section has been correlated to detailed palaeoenvironmental data retrieved from the same section. This makes the Blake Event an ideal correlation event for future studies of potential relations between palaeoenvironmental conditions and hominin behaviour, particularly when detailed palaeoenvironmental data may be lacking.

The palaeomagnetic dating and palaeoenvironmental setting of NN2 as well as the character of the relationship between the terrestrial records of the Eemian at NN2 and the last interglacial period of high sea level stand in marine records are of value to both the geological and the archaeological research communities. The Eemian represents a time slice with a typical interglacial forested environmental setting in NW Europe

(Gaudzinski, 2004), and it is also the last interglacial during which Neandertals were still present. Reconstructing the environmental conditions of this period will ultimately allow us to explore the cognitive abilities that hominins would need to survive at northern European latitudes during an interglacial. These very likely differed between interglacial forested environments and glacial open steppic conditions. This subject has triggered intense debates about Neandertals ecological adaptations and the presumed “modern” types of behaviour needed to survive in interglacial forested environments in Pleistocene mid-latitude and northern Europe (e.g. Roebroeks et al., 1992).

2. Background: paleomagnetism and magnetostratigraphy

2.1. Magnetostratigraphy

In the 1950s, palaeomagnetic data were instrumental in reviving the concept of continental drift. Together with the notion that marine magnetic anomalies should be interpreted in terms of seafloor spreading (Vine and Matthews, 1963) it has led to the formulation of plate tectonics, the current paradigm that has revolutionized Earth Sciences. For archaeologists and palaeoanthropologists, the development of the Geomagnetic Polarity Time Scale (GPTS) is of particular interest, as it provides a new way of independent dating of the archaeological and fossil record (e.g. Cande and Kent, 1992; Cande and Kent, 1995; Heirtzler et al., 1968; Lourens, 2004; Opdyke and Channell, 1996). The geomagnetic field can have two polarities: ‘normal’ as today’s field or ‘reversed’ when the magnetic poles have interchanged position. By convention the first is depicted in black and the latter in white, generating a bar code-like sequence. The GPTS is the calibrated yardstick of the normal and reversed periods or ‘chrons’, with time. By correlating the pattern of normal and reversed polarity measured for a section to the GPTS, a section can be dated. The pattern of normal and reversed periods provides the diagnostic power; a single level in a section can only be assigned normal or reversed polarity, which can be positioned in the GPTS at many places when no further information is available. In the case of short sections, other supplementary geochronological tools are needed (e.g. biostratigraphy, U-series dating, $^{40}\text{Ar}/^{39}\text{Ar}$ analysis etc.) to arrive at a well-constrained age. The GPTS is continuously being refined and extended to older geological periods (e.g. Kuiper et al., 2008). A very important refinement included so-called astronomical tuning of key sections (e.g. Hilgen, 1991; Lourens, 2004; Shackleton et al., 1990). For the last 10

Myr, of most interest to palaeoanthropology, the present GPTS has a very high resolution of 10-20 kyr (even to 5 kyr for the younger reversals) and little further improvement is anticipated for the coming 20 years or so.

Early on during the development of the GPTS, the first magnetostratigraphic correlation from a palaeoanthropological site was already published: the Olduvai Gorge locality in Tanzania (Cox et al., 1964). At present, magnetostratigraphic dating is common practice for Lower Palaeolithic or Plio-Pleistocene sites (e.g. Dirks et al., 2010; Dupont-Nivet et al., 2008; Joordens et al., 2011; Lepre and Kent, 2010; Parés and Pérez-González, 1995).

Magnetostratigraphy as a dating tool has a low resolution for Late Pleistocene palaeoanthropological and archaeological sites, since no major reversals have occurred during the last 780 kyr, the so called Brunhes chron. However, within the Brunhes chron several short reversed events or geomagnetic reversal excursions lasting a few kyr have been documented (e.g. Bonhommet and Zähringer, 1969; Smith and Foster, 1969). These events or excursions, when well-dated, add considerable diagnostic power to the magnetostratigraphic analysis tool. However, some caution is needed: while there are many records of individual isolated reversal excursions within the Brunhes chron, there are only a few reversal excursions that are considered unequivocal on a global basis, and thus can be used for correlation purposes. The following seven excursions are classified as well-documented: Mono Lake (~33 ka), Laschamp (~41 ka), Blake (~120 ka), Iceland Basin (~188 ka), Pringle Falls (~211 ka), Big Lost (~560-580 ka) and the Stage 17 Event (~670 ka) (Laj and Channell, 2007; Roberts, 2008). Of these seven excursions the Blake Event, that was also found in the NN2 sequence and extensively discussed in Sier et al. (2011), is among the least disputed. It was discovered in 1969 in marine cores taken near the Blake Outer Ridge (Smith and Foster, 1969) and, in recent years, it has served as a marker event for Marine Isotope Stage (MIS) 5e (Laj and Channell, 2007; Langereis et al., 1997; Tucholka et al., 1987). Thus, from a chronological point of view, it is closely related to the Last Interglacial (Sánchez-Goñi et al., 1999; Sánchez-Goñi et al., 2000; Shackleton et al., 2003; van Kolfschoten et al., 2003). Although its exact age, duration, and relation with MIS 5e is still under debate, the Blake Event can be used as a dated marker in geological and archaeological studies.

2.2. Magnetic properties, palaeoenvironment and palaeoclimate

Variations in magnetic properties along a geological section can be interpreted in terms of changing environment. This so-called 'environmental magnetism' (Thompson and Oldfield, 1986) is one of the youngest fields in palaeomagnetic research. The magnetic properties of the magnetic minerals contained in the sediments are used as proxy parameters for a wide range of environmental processes. Assessments of pollution, of palaeoclimate and provenance analyses can be made by measuring the temperature and field dependence of samples in various types of induced and remanent magnetizations (Dekkers, 1997; Evans and Heller, 2003). Most iron (oxy)(hydr)oxides and also some iron sulfides are magnetic and easily measurable with modern magnetometers, even when they occur in trace amounts (i.e. $\ll 1$ per mil) in the sample. Ferri- and ferromagnetic materials have a strong magnetic moment while antiferromagnetic material has a much weaker magnetic moment, that is, however, still measurable. In the NN2 sediments, the potentially present (titano)magnetite ($\text{Fe}_3\text{O}_4\text{-Fe}_2\text{TiO}_4$) and greigite (Fe_3S_4) are ferrimagnetic, while hematite ($\alpha\text{-Fe}_2\text{O}_3$), hydrohematite ($\alpha\text{-Fe}_2\text{O}_3\text{-n.H}_2\text{O}$) and goethite ($\alpha\text{-FeOOH}$) are antiferromagnetic (sometimes intimate intergrowths of hematite and goethite are referred to as limonite).

Besides the magnetic mineralogy of the material, the grain size of the magnetic material is also of importance since that is related to the magnetic domain state. Extremely small particles cannot retain a stable remanent magnetization and are called superparamagnetic (SP) because such particles when held in an applied magnetic field show a much larger response than a typical paramagnetic material would have. If the grain size is very small (but of course larger than the SP size), the particles consist of one magnetic domain and consequently are termed single domain (SD). However, if variability in grain size is larger, more magnetic domains are present ranging from a few to many (i.e. more than ~ 10), depending on particle size. The former particles are labelled pseudo-single-domain (PSD) because their magnetic behaviour resembles that of SD particles. The latter are termed multi-domain (MD). Magnetic grain size is mainly inferred from field-dependent measurements. These basic principles can be used to determine which magnetic materials are present in samples, along with their grain-size distributions. This information is subsequently interpreted in terms of environmental change.

For the present case study, two types of rock-magnetic measurements were undertaken: acquisition curves of the Isothermal Remanent Magnetization (IRM) and acquisition curves of the Anhyseretic Remanent Magnetization (ARM). An IRM is a remanent magnetization resulting from a strong magnetizing field at a constant temperature, usually room temperature. This field can occur in nature, because of lightning strikes, or can be produced in a laboratory environment by exposing the sample to a magnet (Butler, 1992). A sample acquires an ARM – only a laboratory-induced remanent magnetization – when an asymmetric Alternating Field (AF) is ramped down to zero from a certain peak level (Dekkers, 1997). In practice, a small bias field is superposed on the (symmetric) alternating field. IRM and ARM acquisition curves (for interpretation of these curves, see section Palaeomagnetic analyses and interpretation of the ARM and IRM acquisition curves) provide information on the physical properties of the magnetic components of the samples measured. These properties enable identification of environmental changes in the sampled geological sequence. Changes in the properties of the magnetic mineralogy are either the result of changes in the provenance of the sediment, or the result of changes during or shortly after sedimentation. In the interpretations presented here SP particles are not considered.

2.3 Some background information on the nn2 site and Hauptprofil 7

The Neumark Nord (NN2) site, located in the Geisel valley, was discovered in 1996 and has been excavated since 2003, and continuously between 2004 and 2008 (Sier et al., 2011). The Geisel valley basin is located west of the valley of the Saale between Mueheln and Merseburg, it has a length of 15 km and width of 5 km. The Geisel river runs through the valley in an east-west direction. Modern day mining has greatly influenced the local morphology (Mania et al., 1990) and has contributed to the discovery of many fossil localities of Eocene and Pleistocene age.

The NN2 site consists of a sedimentary basin, the development of which can be related to the ductile movement of the underlying tertiary lignite (Eissmann, 2002; Mania and Mania, 2008). The site contains abundant traces of Neandertal activity during the last interglacial (Gaudzinski-Windheuser and Kindler, 2011; Gaudzinski, 2004; Sier et al., 2011). A key section for the study of the NN2 infill is Hauptprofil (Main Section) 7 (HP7). HP7 was sampled for application of a wide range of analysis techniques including

palaeo- and rock-magnetism (this chapter), palynological analysis, micromorphology and mollusc studies (see Sier et al., 2011, Kuijper, 2013 and Bakels, 2013). This wide range of techniques, and in particular the discovery of a well preserved Eemian pollen signal within HP7, makes an assessment of the magnetic properties during the Last Interglacial possible (see Sier et al., 2011).

3. Methods

3.1. Sampling and data acquisition

Samples used for this magnetic property study were only submitted to AF demagnetization before taking the magnetic-property measurements. Thermal demagnetization would change the samples' properties making a magnetic-property interpretation irrelevant. In total 120 samples were taken at 5 cm intervals from the HP7 sediments for the determination of ARM and IRM acquisition curves. The NRM behaviour of samples taken at other profiles and the outcome of thermal demagnetization of the natural remanent magnetization (NRM) is extensively discussed in Sier et al. (2011). Often the NRM is composed of a primary or characteristic component and one or more secondary component(s). By stepwise progressive demagnetization, either with alternating field demagnetization or by thermal demagnetization, the primary NRM component is isolated, which is subsequently used for geological interpretation.

The AF samples were collected with dedicated perspex sample containers. These sample containers with standard paleomagnetic dimensions (25 mm diameter and 22 mm height) were gently pushed into freshly prepared cut-outs in the section. Measurements were done within one month after retrieval of the samples to ensure that the samples were processed while still fresh. During this period the samples remained in a cold storage (4°C). For the samples submitted to ARM and IRM measurements, first the NRM was AF demagnetized in 15 steps up to 100 mT. AF demagnetization, and ARM and IRM acquisition was done with a robotized DC-SQUID magnetometer ('direct current' superconducting quantum interference device magnetometer manufactured by the '2G' company (Mountain View, California, USA)). The instrument's sensitivity is $3 \times 10^{-12} \text{ Am}^2$ and typical sample intensities were at least two orders of magnitude higher. The instrument set-up is housed inside a magnetically shielded room (residual field < 200 nT); the robotized interface for field regulation and sample manipulation was built

in-house. Up to 96 samples contained in dedicated cubic holders (edge 30 mm) are loaded onto a sample plateau and the robot loads them in batches of eight onto a tray. This tray can be slid through the magnetometer and demagnetization coils that are used for the ARM acquisition (a bias field coil provides the asymmetry in the field which was 38 μT). In the ARM and IRM acquisition procedure, samples are processed fully automatically with the so-called 'two position protocol' that compensates for the magnetic moment of the transport tray. This ensures optimal processing of weakly magnetic samples. After the determination of the ARM acquisition curves, up to 150 mT peak AF, the samples are demagnetized at 300 mT (with the last demagnetization axis parallel to the IRM acquisition field direction) before they are loaded in different cubic holders for the determination of IRM acquisition curves with 60 steps up to a peak IRM field of 700 mT. This was done with a pulse-field coil interfaced with the robotized magnetometer set-up. ARM was measured before the IRM as the ARM is c. 2 orders of magnitude weaker. If done otherwise the IRM signal, even after AF demagnetization, interferes with the ARM acquisition.

3.2. Interpretation of the arm and irm acquisition curves

Data acquired from the ARM and IRM measurements were imported in a specially developed Excel worksheet (Kruiver et al., 2001) which can be downloaded from <http://www.geo.uu.nl/~forth> (see figure 1 and 2 for examples). The basis function fitting of the IRM acquisition curves is based on Cumulative log Gaussian analysis developed by (Robertson and France, 1994) and improved by Kruiver et al. (2001). For each sample, the IRM (or ARM) acquisition curves are visualized by plotting the logarithm of the applied field in three ways:

1. versus the acquired IRM (ARM) expressed in absolute magnetic moments or on a mass-specific basis, plotted on a linear scale (linear acquisition plot, LAP),
2. versus the acquisition curve expressed as a gradient (gradient acquisition plot, GAP)
3. versus the acquisition curve expressed on a probability scale (standardized acquisition plot, SAP) (Kruiver et al., 2001).

Each IRM (ARM) acquisition curve is considered to be the sum of one or more coercivity components, each assumed to have a cumulative log-Gaussian coercivity distribution (experimental data of Robertson and France (1994) provide support for the assumption). Each coercivity component is characterized by three free or fittable parameters: SIRM, $\log B_{1/2}$ and DP. They represent the Saturation IRM (a magnetic mineral phase will not achieve higher IRM upon exposing it to magnetic fields beyond a certain level), the log of the applied field at which the mineral phase acquires half of its SIRM, and finally the dispersion parameter, expressing the coercivity distribution (or the width of that distribution) of the corresponding magnetic mineral phase (Heslop et al., 2002; Kruiver et al., 2001). The different coercivity components can be fitted to a measured IRM or ARM acquisition curve by adjusting their SIRM (or SARM), mean coercivity ($B_{1/2}$) and dispersion (DP). It is important to realize that the basis function fitting of the IRM and ARM data points does not have a unique solution: mathematically, there are several correct solutions depending on for example the order of fitting of the components. We adopted the following procedure that has shown to yield good interpretations in the past. We first fit the dominant component in the gradient plot (GAP) with $\log B_{1/2}$ ranging from 1.4 – 1.8. Often at the low-field end there appears to be room for another component that we fit subsequently ($\log B_{1/2}$ 1.0). This extra component is an artifact (Egli, 2004; Heslop et al., 2004) and therefore does not get a physical interpretation. The artifact is a result of the log Gaussian basis function way of fitting (Kruiver et al., 2001) which can only fit distributions that are symmetric in the log-field space. Skewed-to-the-left distributions (a consequence of time-dependent magnetic behaviour and/or magnetic interaction, (cf Egli, 2004; Heslop et al., 2004) must be fitted in the Kruiver et al. (2001) package with an extra component with $\log B_{1/2}$ 1.0. The amount (SIRM or SARM value) of the skewed artifact component has to be added to the SIRM or SARM of the dominant coercivity component (with $\log B_{1/2}$ of 1.4 – 1.8) to give the intensity of this dominant component. High-coercivity IRM values (here the component with $\log B_{1/2}$ of 2.4 to 2.7) do have a physical significance and represent the high-coercivity magnetic minerals. Thus, 'skewed-to-the-right' is fitted with an extra component that is assigned physical significance. To avoid the risk of overinterpretation of the data, number of components for the fitting is kept as low as possible. Keep in mind that for fitting three components already a minimum of 9 data points is required. Therefore a minimum of 25 data points is considered realistic to meaningfully fit three (or four) components. The ARM and IRM acquisition curves in this study have 25 and 50 to 60 data points respectively.

It should be noted that the shape of the acquisition curves is dependent on the initial magnetic state (Heslop et al., 2004). In other words, the shape of the acquisition curve for the same sample will be different depending on whether or not the sample is AF demagnetized before the IRM (or ARM) acquisition curve is determined. For the Kruiver et al. (2001) method, a better fit is obtained after AF demagnetization because then the curves are more log-normal and thus less “skewed”, so that the artifact component is absent (or present in a smaller amount than otherwise would be the case). Also for comparative purposes, all IRM and ARM acquisition curves reported so far were measured starting from the static 3-axis AF demagnetized state as described earlier on: the last demagnetization axis is parallel to the axis of the IRM and ARM acquisition field as this results in a more log-normal coercivity distribution (Heslop et al., 2004).

Different magnetic minerals have ranges of standard values and can be identified by the combination of $B_{1/2}$ and DP, while the SIRM (SARM) provides information about the amount of that specific mineral in the sample (Kruiver and Passier, 2001). ARM measurements mainly give information about the properties of magnetite (because magnetite is typical of getting much higher ARM than other magnetic minerals) while IRM gives a more balanced view of different magnetic minerals. In IRM measurements, typical $B_{1/2}$ values ranges are up to 70 mT for magnetite, from 120 mT to 1.2/1.8 T for hematite, and from 1.2/1.8 T upwards for goethite (Kruiver and Passier, 2001). Greigite has similar values as magnetite but can be slightly harder: it has slightly higher coercivity values. The DP provides information on the grain-size distribution of the minerals (Kruiver et al., 2001). A low DP value ($< \sim 0.18$) means that the magnetic grains of that component are very similar. This is only possible if the grains have a magnetotactic bacterial origin (Egli, 2004; Hüsing et al., 2009; Kruiver and Passier, 2001; Vasiliev et al., 2008).

Figure 1:

IRM component analyses of samples Neu 30, Neu 47, Neu 86 and Neu 110 positioned at 150, 235, 427 and 547 cm below the top of the HP7 sequence respectively.

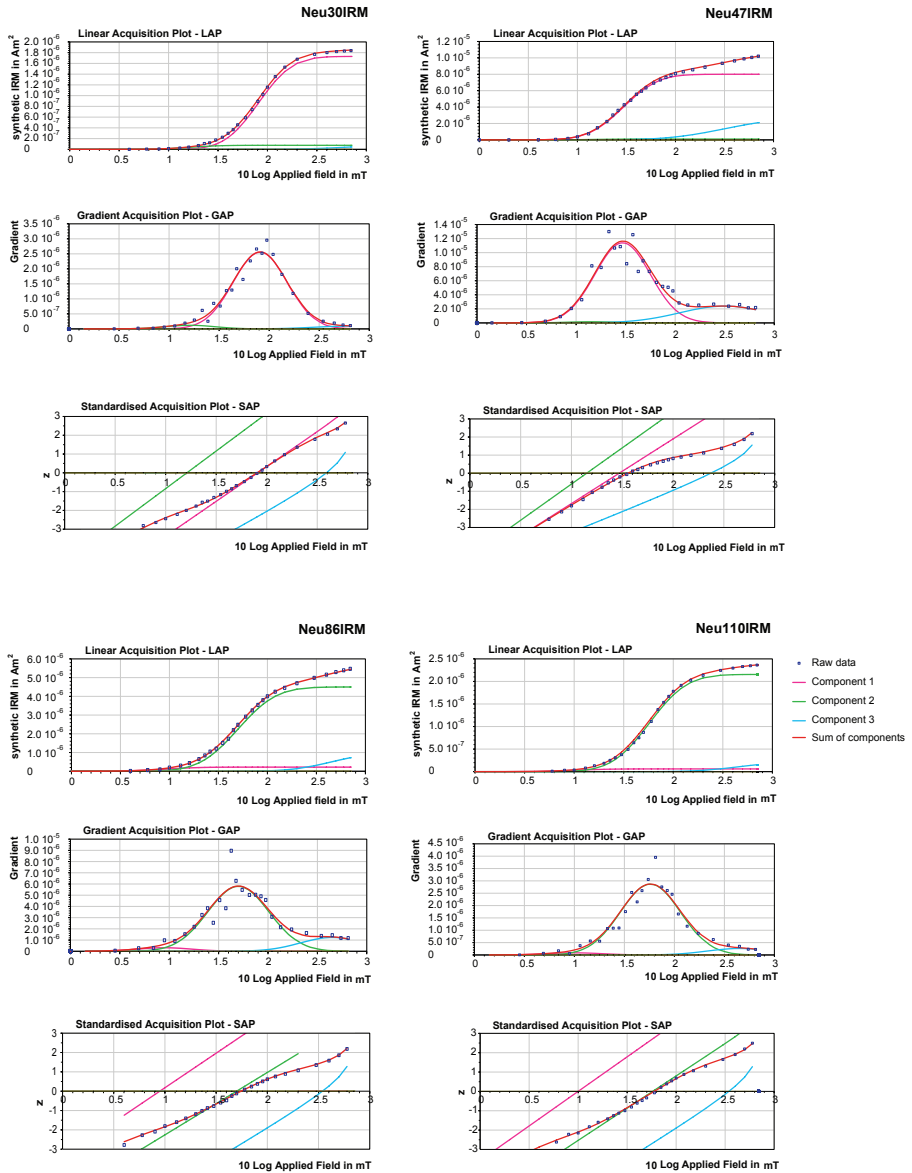


Figure 2:

ARM component analyses of samples Neu 30, Neu 47, Neu 81 and Neu 110 positioned at 150, 235, 401 and 547 cm below the top of the HP7 sequence respectively.

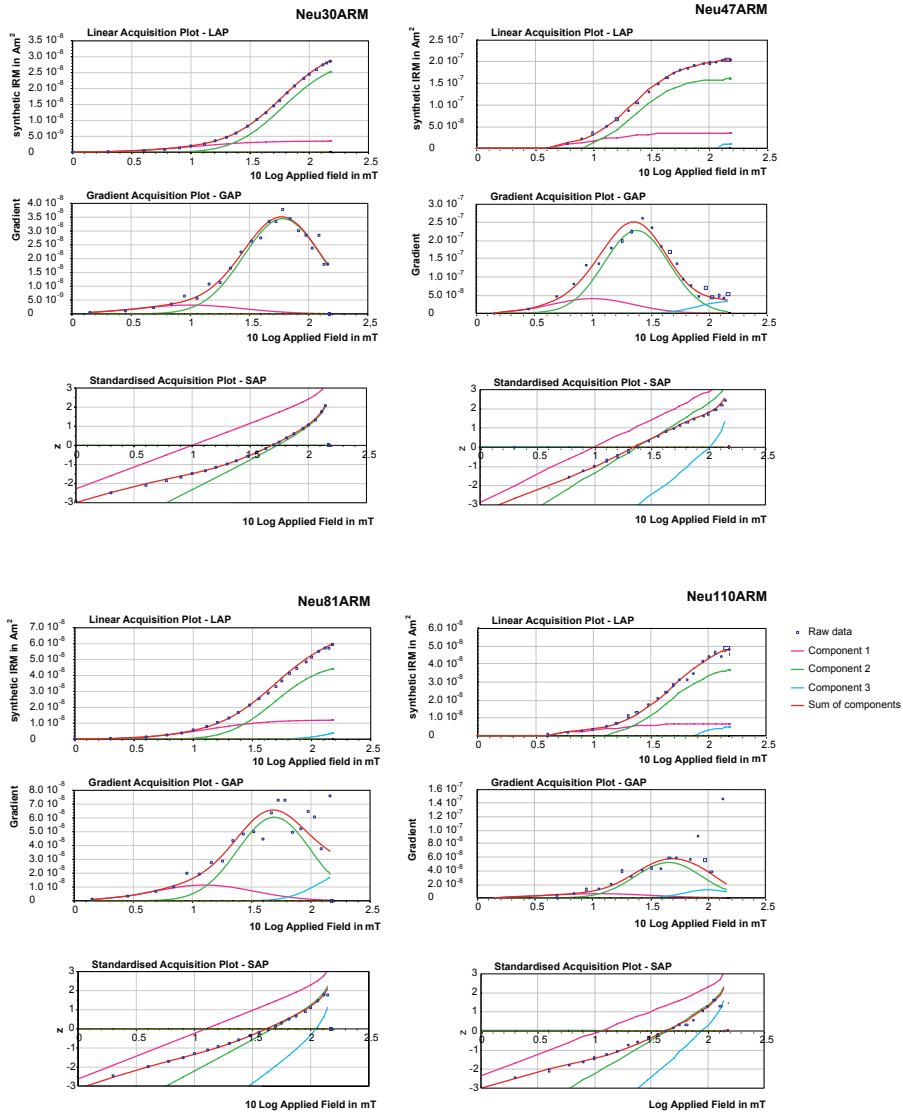
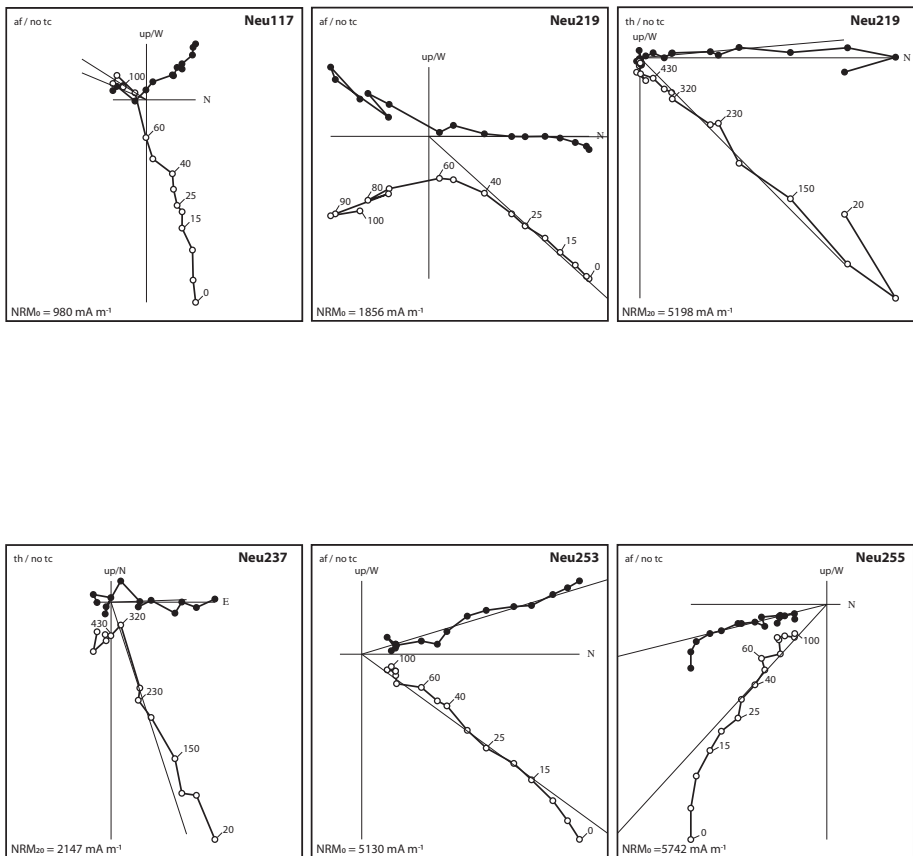


Figure 3:

Figure taken from Sier et al. (2011). Zijderveld diagrams of some representative samples in stratigraphic coordinates (the section underwent no tilting after deposition). Neu117: AF demagnetization (af) only; first Neu219 sample: AF demagnetization only; second Neu219 and Neu237 sample: thermal demagnetization (th) only. Neu253 and Neu255: AF demagnetization after thermal demagnetization up to 205°C. See text and Sier et al. (2011) for more details.



4. Results

To provide a comprehensive palaeomagnetic framework that serves as starting point for the palaeoenvironmental interpretation we briefly recapitulate the essential palaeomagnetic considerations published in Sier et al. (2011). Representative examples of the Neumark Zijdeveld diagrams are shown in figure 3. The diagrams show at low AF field range (15-20 mT), or at low temperatures (< 200 °C), a modern (< 120.000 years old) magnetic field overprint which is likely of viscous origin. The ChRM is observed after demagnetization temperatures > 200 °C and AF fields >15-20 mT. The quality of the signal varies, ChRM directions with a stable endpoint have been given a quality of 1 while ChRM directions that do not trend towards the origin were given a quality of 2. Only the samples with a quality of 1 have been incorporated in our interpretations and examples are shown in figure 3. From 7.7 meters until 1.7 meters (see figure 4) below the top of the section we see clearly deviating directions in the ChRM that indicate the presence of an excursion in the palaeomagnetic signal of the NN2 sediments.

As mentioned above, the HP7 profile has also been sampled for palynological studies. The pollen signal from NN2 clearly indicates a Eemian sequence, represented by pollenzones EI to EVII (after Menke and Tynni, 1984) (see Bakels, 2012). The base of the Blake Event is situated 87 cm below the base of the Eemian pollen zone EI (after Menke and Tynni, 1984). The top of the Blake Event (as identified on the basis of NN2 data) is situated in pollen zone IVb3 (see figure 4 of Sier et al. (2011) and figure 2). Eemian pollen zones VI and VII have been identified in the overlying sediments, in the uppermost parts of the HP7 profile.

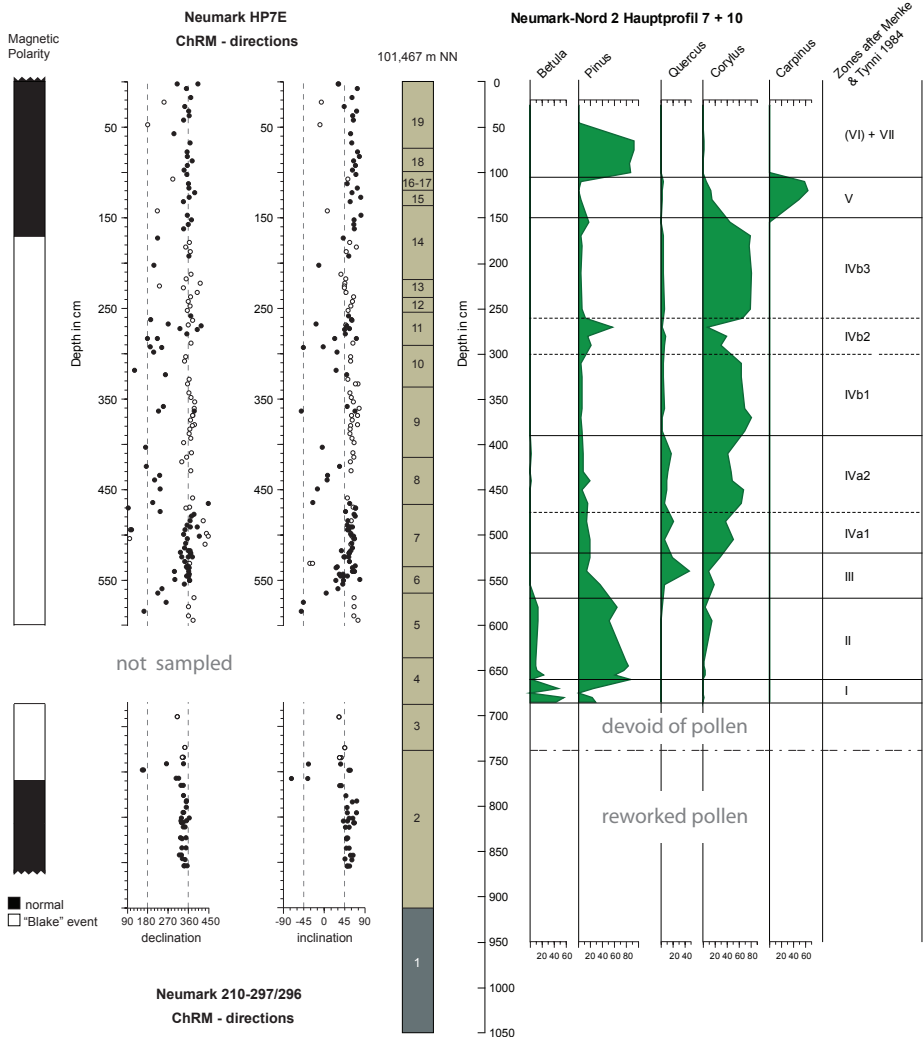
4.1 Interpretation of the irm and arm acquisition curves

Figure 1 shows four individual IRM acquisition curves, all showing distinct LAP, GAP and SAP curves, representing differences in rock-magnetic properties of the samples. Figure 2 shows four examples of ARM acquisition curves. We first treat the reading of the IRM acquisition curves in some detail before discussing the ARM acquisition more concisely. Thereafter the behaviour of IRM and ARM components as function of stratigraphy will be dealt with.

Individual IRM acquisition curves (figure 1) show two components, numbered

Figure 4:

Figure taken from Sier et al. (2011). Combined overview of the palaeomagnetic, stratigraphic and pollen data from HP7/10 and 210/297-296 samples. The top of the section (0 m) is at 101.467 m NN (=above sea level). The stratigraphic level between 570 and 455 cm in the ChRM-direction column corresponds to the normal intervening zone within the Blake Event (170-770 cm). The black dots of the ChRM directions refer to first quality data points, and the open circles are of secondary quality (see Sier et al. (2011) for details: a description of units 1 to 19 and background information on the methods see their supplementary matter section). The part for which no palaeomagnetic samples are available (Pollen Zone I and part of Zone II) has an estimated duration of maximally 300 yr. For duration of pollen zones and sedimentation rates see Table 1 Sier et al. (2011). The main archaeological find horizon is situated within unit 8.



component 2 and 3, with a third being an artifact (component 1 with the lowest coercivity) as explained in subsection 3.2. One component (component 2) is of a low coercivity, the other (component 3) of a high coercivity. The low coercivity component has a $B_{1/2}$ range of 29.5 mT to 81 mT, with most values in between 50 and 60 mT. For the high coercivity component full saturation is not reached, but the $B_{1/2}$ range is from ~ 317 mT up to ~ 1000 mT with most values in between 400 and 500 mT. As mentioned above magnetite and hematite have a distinctive range of $B_{1/2}$ values allowing interpretation of the low coercivity component as PSD magnetite and the high coercivity component as hematite. Percentage contributions of the different components vary markedly through the section. The hematite contribution can be as low as 4 per cent up to as high as 50 per cent.

Besides the lacking of component 3, the general trend of the ARM follows the one of the IRM albeit less pronounced. Component 2 has a $B_{1/2}$ range from 30 to 76 mT with the majority of the samples in between 45 and 60 mT. Component 3, when present, has $B_{1/2}$ ranges from 100 to 200 mT with the majority having values lower than 160 mT. Component 2 is interpreted as magnetite while component 3 is considered hematite. It should be realized that the ARM properties of the hematite are rather poorly characterized because

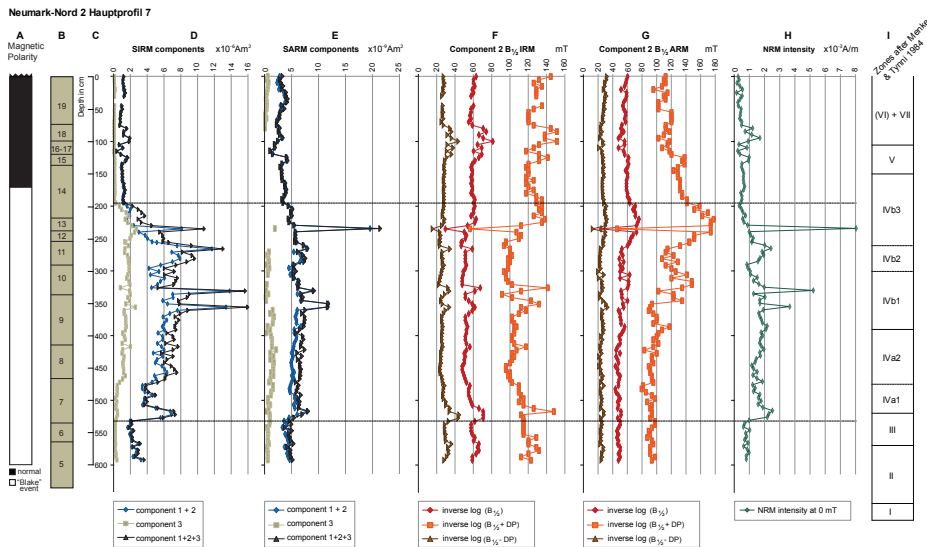


Figure 5:

Combined overview of the magnetic polarity, stratigraphic division, pollen zonation from HP7 in NN2 with the NRM intensity and IRM and ARM data plotted versus stratigraphic depth.

of the low maximum AF during the ARM acquisition (instrumentally dictated). For a large part of the section the percentage contribution is 100 per cent component 2, i.e. magnetite. In other parts the percentages vary substantially albeit that variations are smaller than in the IRM, presumably because the magnetite expression is 'enlarged' in ARM compared to IRM acquisition curves. The ARM percentage contribution of component 3 varies from 4 up to 30 per cent.

The IRM and ARM results as function of stratigraphic level are presented in figure 5, showing three distinct zones of different SIRM and SARM intensities in column 5 D and 5 E (dashed lines separate the zones). In figure 5 D the individual IRM acquisition curve data have been plotted against stratigraphic level, clearly visualising the temporal variability among the samples. In the ARM record (figure 5E) for most of the section there are 2 components, but in between 80 and 271 cm below the top component 3 is lacking (as is the case with the IRM acquisition curves, component 1 is considered an artifact).

Both hematite and magnetite show the same broad trends that divide the three zones of figure 5. The top zone (from 0 to 195 cm below the top of the section) shows little variability in intensities. From 195 cm until 532 cm below the top of the section, the zone is characterized by higher intensities and variability in SIRM and SARM values. At 195 cm the hematite values start to increase, as do the magnetite values albeit not on a one-to-one ratio. From 462 cm onwards hematite values decrease. Magnetite follows this trend in a modest manner and breaks with it 20 cm below. At 532 cm the lower zone starts, similar to the top zone albeit with higher levels of intensities than the top zone.

Superimposed on the higher magnetite values we see the following trends after the increase of SIRM up to a depth of 266 cm below the top. A zone with lower values in between 291 and 326 cm, a general decreasing trend from higher values (than the zone mentioned above) to a similar level from 336 to 472 cm. From 477 to 507 cm we find a lower level plateau of magnetite. The upper boundary of this plateau corresponds to the lower boundary of the hematite-rich level. From 512 to 532 we find higher levels and the section ends with a section with decreased values.

There are several highs and lows in figure 5 that deserve a separate mention. At sedimentary unit level 16-17 (105 and 115 cm below the top) the low coercivity component, magnetite, reach extremely low values of 0.71×10^{-6} and $0.394 \times 10^{-6} \text{ Am}^2$.

In the middle zone there are 4 peaks at sedimentary unit level 13, 11, 10 and 9 (235, 266, 331 and 356 cm below the top of the section). There are no indications of any sedimentological differences with sample below or above these samples with peak values.

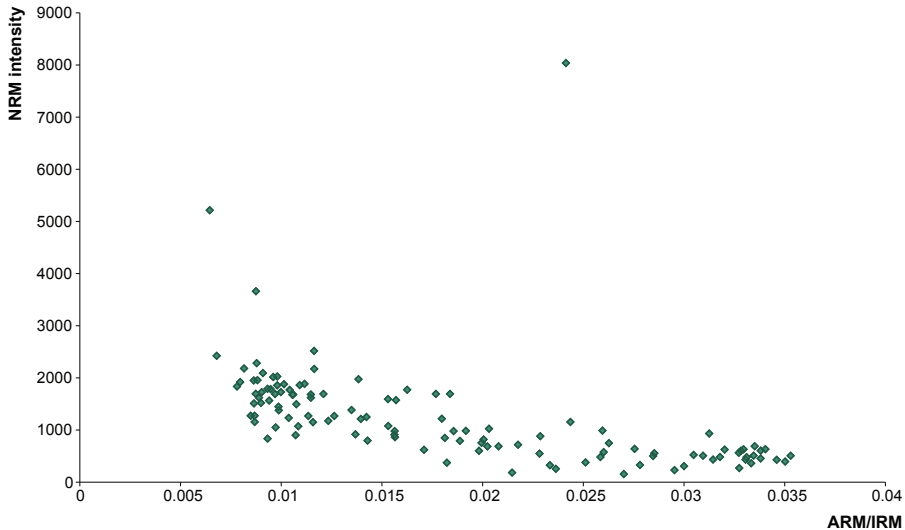


Figure 6:
NRM intensity at 0 mT and room temperature plotted against the ARM divided by the IRM.

The Zijderveld diagrams of these samples give no indication of a Gyromagnetic Remanent Magnetization (GRM) being formed. GRM causes intensities of samples to increase with increasing AF field. The presence of greigite in these zones is therefore unlikely. However, a few samples with regular values do show the presence of a GRM.

Of the low IRM values in sedimentary unit level 16-17, only the sample at 115 cm below the top has a low SARM value ($\sim 1 \times 10^{-9} \text{ Am}^2$). Four peaks were identified in the middle zone. The peak in sedimentary unit level 13 is more pronounced in the SARM (to $21.45 \times 10^{-9} \text{ Am}^2$), while sedimentary unit level 11 IRM peaks fall within the normal range. Sedimentary unit level 10 and 9 IRM peaks are slightly more pronounced in the SARM curve.

For sedimentary unit level 13 peak (at 235 cm below top of section), we find a very low values of the $B_{1/2}$ values in both ARM and IRM of this component (figure 5). For the other three samples peak values are recorded for the $B_{1/2}$ IRM values while for ARM no lows or peaks are noted. Also these samples show higher outlier SARM values. For the log $B_{1/2}$ curves we find a corresponding trend in which we find generally lower $B_{1/2}$ values from 225 to 532 cm below the top. Component 2 ARM data follows generally a more

independent trend. The three zones can be recognized:

1. a stable zone from 0 to 195 cm (units 14 to 19) with ranges from just below 100 to 140 mT;
2. a declining zone in between 195 and 376 cm (units 9 to 14) with ranges from up to 180 to 100 mT; and
3. a stable zone from 381 to 600 cm (units 5 to 9) with ranges in between 80 and 110 mT.

The NRM intensity plot versus stratigraphic level (figure 5, column H) shows similarities to graphs described above. Samples with peak values of sedimentary unit level 13, 10 and 9 clearly stick out again due to their high values, while this is less so for samples from level 11. Closer inspection reveals a general positive relation between the SIRM, SARM and the NRM intensity: higher values in one column correspond to higher values in the other two columns as well.

Figure 6 shows the NRM intensity plotted versus ARM/IRM, for both ARM and IRM only the values of component 1 and 2 were taken. Higher ARM/IRM ratios have lower NRM intensities. A higher ARM/IRM ratio indicates a smaller grain-size distribution for the magnetic components of the sample. An important observation is that the results mentioned above apparently show no correlation with the ChRM directions of NN2, i.e. low NRM intensities are distributed in both the normal and excursions directions (see figure 5). This means that rock-magnetic properties such as SIRM and SARM have no correlation with the palaeomagnetic directions which supports a primary nature of the characteristic NRM component.

5. Discussion

5.1. Blake record and age model

The Blake Event discovered at the NN2 site can be placed with great accuracy in relation to the Eemian pollen sequence found at exactly the same location and within the very same sediments. The Blake Event starts a few hundreds of years before the start of the Eemian s.s. and lasts at least 3000 years within the Eemian (figure 4). The relationship between the Eemian at NN2 and Marine Isotope Stage (MIS) 5e is extensively discussed in Sier et al. (2011). The main conclusion of that paper pertains to the implications of the positioning of the Blake Event in the NN2 Eemian pollen zones, and the apparent delay of 5000 years between the start of the Eemian in NN2 in comparison to MD95-2042 core (Sánchez-Goñi et al., 1999). In this marine core, taken at the southwestern margin of the Iberian Peninsula (37°480N; 10°100W) at a depth of 3148 m, the Eemian pollen zones (identified from pollen found in the core) were directly correlated to the MIS curve (Sánchez-Goñi et al., 1999; Shackleton et al., 2003). At Neumark, the NN2 pollen data was linked to the MIS curve by means of the Blake Event. For our correlation we used published data of several marine cores from the Mediterranean (Tric et al., 1991; Tucholka et al., 1987). In these cores both the Blake Event and the MIS 5e peak were identified, clearly showing the post MIS 5e position of the Blake Event. Furthermore the same cores contain several sapropels: black, organic rich pelagic mud layers deposited in the (eastern) Mediterranean. Formation of these sapropels is inferred to be related to climatic, monsoon-related, wet phases during precession-induced insolation maxima causing increased production and preservation of organic matter (Rohling, 1994; Rossignol-Strick, 1985; Rossignol-Strick et al., 1982). During the MIS 5e peak sapropel S5 was formed.

The cores described by Tric et al. (1991) clearly show the start of the Blake Event after the top of the S5 sapropel, enabling us to directly correlate the NN2 Eemian pollen sequence to the MIS curve. Furthermore, the duration of the S5 has been established by Tucholka et al. (1987) at ~5 kyr and the midpoint age has been dated at 124 ka (Lourens, 2004). All in all, the relative position of the Blake Event in regard to MIS 5e and to the Eemian pollen zones identified in NN2 indicates a lag time of 5 kyr for the start of the Eemian in central Europe compared to that in southern Europe (Sier et al., 2011) as published by Sánchez Goñi et al. (1999). Our estimated end of the Eemian is very similar

to the end age suggested by Sánchez Goñi et al. (1999) and Shackleton et al. (2002). Another important observation is the difference in duration of the Eemian: ~16400 years in the south (Sánchez-Goñi et al., 1999) and ~11000 years in the north of Europe (Müller, 1974). This means that, although the delay of the start of the Eemian found in at NN2 can be seen as surprising, it does fit within the data and age model published by Sánchez-Goñi et al. (1999). However it does not match with a study published on the late Saalian and early Eemian in the Amsterdam Basin, the Netherlands (Beets et al., 2006). In that study the authors argue that the Eemian starts before MIS 5e instead of after the peak, as argued here (Sánchez-Goñi et al., 1999; Shackleton et al., 2002; Shackleton et al., 2003; Sier et al., 2011). It may be an option that the oxygen isotope results of that study cannot be correlated without further ado with the global curve. The connection between the Amsterdam Basin and the truly marine realm could have been more indirect at that time than anticipated: the influence of river runoff might have been larger than considered by Beets et al. (2006). This means that the Amsterdam Basin isotope curve could have been 'disconnected' from the global isotope curve. More importantly Beets et al. (2006) assume a simultaneous start of the interglacial vegetation across Europe. This assumption has been proven to be incorrect based on the data of NN2.

The study presented in this chapter adds to the credibility of our previous paleomagnetic interpretations as it shows that the ARM and IRM data are independent from the palaeomagnetic directions described by (Sier et al., 2011). This means that the magnetic mineral formation is independent of lithology. Hence, we can rule out chemical or biological formation of the magnetic minerals at an unknown age within the NN2 sediments, which supports the validity of our claim to have identified the Blake Event. In addition, the formation of the magnetic minerals was synchronous with the water level, as subsection 5.2 will show. This excludes the possibility of a delayed acquisition of the earth's magnetic signal and again validates our claim of having found a primary in situ signal of the Blake Event.

The time interval reflected in the NN2 record is too short to allow recognition of sub-Milankovitch cycles. However the wet-dry transition found in NN2 has been identified in more Eemian sites (Brewer et al., 2008). Brewer et al. (2008) placed the transition in pollen zone V (*Carpinus*) while in NN2 the transition is slightly earlier, at the end of zone IVb3. However, data used by Brewer et al. (2008) has been obtained over a large geographic region in Europe. This means that possible lagtime effects could have been subdued because of this geographical merging.

5.2. Palaeoenvironmental interpretation

Component 2, interpreted as magnetite, is responsible for the largest part of the SIRM (figure 5). Because of its high specific remanent magnetization, small amounts of magnetite generate a large magnetic contribution and in this way, magnetite is 'overrepresented'. Generally, in between 80 and 95 percent of the signal is a magnetite signal. The magnetite amounts vary along-section. The base level of magnetite, $\sim 1.0 \cdot 10^{-6} \text{ Am}^2$, probably originates from the sediment in the vicinity of the NN2 basin which is brought in as sediment load. Higher values of the magnetite component could be the result of an increase and/or change in the catchment area during wetter periods or an increased eolian component during dry periods. These values reach a maximum of $1.6 \cdot 10^{-5} \text{ Am}^2$ but most values are in between $4.0 \cdot 10^{-6} \text{ Am}^2$ and $8.0 \cdot 10^{-6} \text{ Am}^2$. In general the main trend of the hematite amounts (component 3, figure 5) follows that of magnetite, suggesting a similar formation. Hematite has a base level around $1.0 \cdot 10^{-7} \text{ Am}^2$ and high level values between $1.0 \cdot 10^{-6} \text{ Am}^2$ and $2.0 \cdot 10^{-6} \text{ Am}^2$. Hematite has many variable compositions of which one is limonite. Limonite has been identified in the NN2 sediments (Kuiper, 2013). Limonite formation increases at the end of pollen zone IVa1 and is responsible for the increase in strength of the hematite signal.

Comparing the pollen data with the ARM/IRM magnetic signal we also see a close relation between these two data sets. The broad trends in the pollen sequence can be correlated very well to the broad trend in the rock-magnetic data. From around 2 meters and higher up in the sequence the NN2 surroundings become a closed forest and lack the near-water-edge herbs. Trampling of the water edge of water seeking mammals creates the habitat needed for these herbs. When the basin dries up or is regularly dry, animals seek other drinking wells to quench their thirst and thus the pollen signal of the NN2 surroundings changes. The zone with increased SIRM and SARM intensity corresponds with the wet zone of the basin (see figure 5, see also Bakels, 2013) and thus, with increase and/or change in size of the catchment area or a less dominant eolian contribution, which is reflected in the change of magnetic mineral contribution.

Some small correlations between the magnetic and pollen signal are worth mentioning. Unit 16-17 (figure 5) has low SIRM and SARM intensities at the 'Seekreide' level (travertine) and at the 'Algae gyttja' level (see also Bakels, 2013). From 477 to 507 cm (within unit 7) we find a lower level plateau of magnetite which corresponds with increased pondweed production (Kuiper, 2013) which indicates this zone as a wet period.

All in all, these striking correlations demonstrate the validity of the rock-magnetic approach as a tool for palaeoenvironmental research. A distinct advantage of the rock-magnetic

method is that very high resolution information can be obtained in a reasonably short time. However, this does not imply that it can replace or substitute a more classic method like palynology. Without palynological or similar data, we miss the framework for our rock-magnetic interpretation. Within the framework, rock-magnetic data does not only give support to other types of data: more than that, rock-magnetic studies do have the potential to serve as an environmental proxy independent of other methods once they can be performed within an environmental and chronological framework.

6. Conclusions

The identification of the Blake Event at the NN2 site by Sier et al. (2011) provided an refined age control for the archaeological layers. The correlation between the Blake Event and the Eemian pollen zones was interpreted as reflecting a delayed onset of the Eemian in Central Europe. The present study has added to the validity of these claims. Formation of the magnetic minerals follow changes in the water levels in the NN2 basin suggesting a in situ palaeomagnetic signal. In addition, ARM and IRM show no relation to the paleomagnetic polarity signal, excluding chemical and/or biological formation of the magnetic minerals, and validating again the primary character of the NN2 palaeomagnetic signal.

The palynological data show a cycle from open vegetation conditions to more closed vegetation conditions in the vicinity of the NN2 basin. Over the same time interval, the IRM and ARM data presented in this chapter also show a cycle from wet to dry. A probable cause for the closing of the vegetation is the drying up, at least temporarily, of the water in the basin causing a decrease in the presence of animals near the basin edge. A lack or decrease in trampling by watering animals may have resulted in a closure of the vegetation. A cycle from wet to dry has been reported in various other European Eemian sites, around the same pollen zone as suggested for the cycle in NN2. This indicates that the NN2 record may have captured a climate signal that was expressed at a continental scale. These results show the usefulness of magnetic property analyses, as they validate the magnetostratigraphic interpretations and contributes significantly to our understanding of the palaeoenvironmental development of the NN2 basin. In future studies, magnetic property analyses can be employed as a quick-scan palaeoenvironmental proxy to rapidly identify zones of interest that are worthy to be subjected to detailed labour-intensive (e.g. palynological) environmental studies.

References

- Bakels, C. C. (2013). A reconstruction of the vegetation in and around the Neumark-Nord 2 basin, based on a pollen diagram from the key section HP7 supplemented by section HP10. In "Multidisciplinary Studies of the Middle Palaeolithic Record from Neumark-Nord (Germany)." (S. Gaudzinski-Windheuser, and W. Roebroeks, Eds.). LDASA, Halle.
- Beets, D. J., Beets, C. J., and Cleveringa, P. (2006). Age and climate of the late Saalian and early Eemian in the type-area, Amsterdam basin, The Netherlands. *Quaternary Science Reviews* 25, 876-885.
- Bonhommet, N., and Zähringer, J. (1969). Paleomagnetism and potassium argon age determinations of the Laschamp geomagnetic polarity event. *Earth and Planetary Science Letters* 6, 43-46.
- Brewer, S., Guiot, J., Sánchez-Goñi, M. F., and Klotz, S. (2008). The climate in Europe during the Eemian: a multi-method approach using pollen data. *Quaternary Science Reviews* 27, 2303-2315.
- Butler, R. F. (1992). *PALEOMAGNETISM: Magnetic Domains to Geologic Terranes*. Blackwell Scientific Publications.
- Cande, S. C., and Kent, D. V. (1992). A New Geomagnetic Polarity Time Scale for the Late Cretaceous and Cenozoic. *Journal of Geophysical Research* 97, 13917-13951.
- Cande, S. C., and Kent, D. V. (1995). Revised calibration of the geomagnetic polarity timescale for the Late Cretaceous and Cenozoic. *Journal of Geophysical Research* 100, 6093-6095.
- Cox, A., Doell, R. R., and Dalrymple, G. B. (1964). Reversals of the Earth's Magnetic Field. *Science* 144, 1537-1543.
- Dekkers, M. J. (1997). Environmental magnetism. *Geologie en Mijnbouw* 76, 163-182.
- Dirks, P. H. G. M., Kibii, J. M., Kuhn, B. F., Steininger, C., Churchill, S. E., Kramers, J. D., Pickering, R., Farber, D. L., Meriaux, A., Herries, A. I. R., King, G. C. P., and Berger, L. R. (2010). Geological Setting and Age of Australopithecus sediba from Southern Africa. *Science* 328, 205-208.
- Dupont-Nivet, G., Sier, M., Campisano, C. J., Arrowsmith, R., DiMaggio, E., Reed, K., Lockwood, C. A., Franke, C., and Hüsing, S. (2008). Magnetostratigraphy of the eastern Hadar Basin (Ledi-Gerau research area, Ethiopia) and implications for hominin paleoenvironments. In "The Geology of Early Humans in the Horn of Africa." (J. Quade, and J. G. Wynn, Eds.), pp. 67-85.

- Egli, R. (2004). Characterization of individual rock magnetic components by analysis of remanence curves. 3. Bacterial magnetite and natural processes in lakes. *Physics and Chemistry of the Earth, Parts A/B/C* 29, 869-884.
- Eissmann, L. (2002). Quaternary geology of eastern Germany (Saxony, Saxon-Anhalt, South Brandenburg, Thüringia), type area of the Elsterian and Saalian Stages in Europe. *Quaternary Science Reviews* 21, 1275-1346.
- Evans, M. E., and Heller, F. (2003). "Environmental Magnetism, Principles and Applications of Enviromagnetics." Academic Press, Amsterdam.
- Gaudzinski-Windheuser, S., and Kindler, L. (2011). Research perspectives for the study of Neandertal subsistence strategies based on the analysis of archaeozoological assemblages. *Quaternary International* In Press, Corrected Proof.
- Gaudzinski, S. (2004). A matter of high resolution? The Eemian Interglacial (OIS 5e) in north-central Europe and Middle Palaeolithic subsistence. *International Journal of Osteoarchaeology* 14, 201-211.
- Heirtzler, J. R., Dickson, G. O., Herron, E. M., Pitman, W. C., III, and Le Pichon, X. (1968). Marine Magnetic Anomalies, Geomagnetic Field Reversals, and Motions of the Ocean Floor and Continents. *Journal of Geophysical Research* 73, 2119-2136.
- Heslop, D., Dekkers, M. J., Kruiver, P. P., and van Oorschot, I. H. M. (2002). Analysis of isothermal remanent magnetization acquisition curves using the expectation-maximization algorithm. *Geophysical Journal International* 148, 58-64.
- Heslop, D., McIntosh, G., and Dekkers, M. J. (2004). Using time- and temperature-dependent Preisach models to investigate the limitations of modelling isothermal remanent magnetization acquisition curves with cumulative log Gaussian functions. *Geophysical Journal International* 157, 55-63.
- Hilgen, F. J. (1991). Astronomical calibration of Gauss to Matuyama sapropels in the Mediterranean and implication for the Geomagnetic Polarity Time Scale. *Earth and Planetary Science Letters* 104, 226-244.
- Hüsing, S. K., Dekkers, M. J., Franke, C., and Krijgsman, W. (2009). The Tortonian reference section at Monte dei Corvi (Italy): evidence for early remanence acquisition in greigite-bearing sediments. *Geophysical Journal International* 179, 125-143.
- Joordens, J. C. A., Vonhof, H. B., Feibel, C. S., Lourens, L. J., van der Lubbe, H. J. L., Dupont-Nivet, G., Sier, M. J., Davies, G. R., and Kroon, D. (2011). An astronomically-tuned climate framework for hominins in the Turkana Basin. *Earth and Planetary Science Letters* 307, 1-8.

- Kruiver, P. P., Dekkers, M. J., and Heslop, D. (2001). Quantification of magnetic coercivity components by the analysis of acquisition curves of isothermal remanent magnetisation. *Earth and Planetary Science Letters* 189, 269-276.
- Kruiver, P. P., and Passier, H. F. (2001). Coercivity analysis of magnetic phases in sapropel S1 related to variations in redox conditions, including an investigation of the S ratio. *Geochemistry Geophysics Geosystems* 2, 1063.
- Kuijper, W. J. (2013). Investigation of inorganic, botanical and zoological remains of an exposure of Last Interglacial (Eemian) sediments at Neumark - Nord 2 (Germany). In "Multidisciplinary Studies of the Middle Palaeolithic Record from Neumark-Nord (Germany)." (S. Gaudzinski-Windheuser, and W. Roebroeks, Eds.). LDASA, Halle.
- Kuiper, K. F., Deino, A., Hilgen, F. J., Krijgsman, W., Renne, P. R., and Wijbrans, J. R. (2008). Synchronizing Rock Clocks of Earth History. *Science* 320, 500-504.
- Laj, C., and Channell, J. E. T. (2007). Geomagnetic Excursions. In "Geomagnetism." (M. Kono, Ed.), pp. 373-416. *Treatise on Geophysics* Elsevier, Amsterdam.
- Langereis, C. G., Dekkers, M. J., Lange, G. J., Paterne, M., and Santvoort, P. J. M. (1997). Magnetostratigraphy and astronomical calibration of the last 1.1 Myr from an eastern Mediterranean piston core and dating of short events in the Brunhes. *Geophysical Journal International* 129, 75-94.
- Lepre, C. J., and Kent, D. V. (2010). New magnetostratigraphy for the Olduvai Subchron in the Koobi Fora Formation, northwest Kenya, with implications for early Homo. *Earth and Planetary Science Letters* 290, 362-374.
- Lourens, L. J. (2004). Revised tuning of Ocean Drilling Program Site 964 and KC01B (Mediterranean) and implications for the D180, tephra, calcareous nannofossil and geomagnetic reversal chronologies of the past 1,1 Mys. *Paleoceanography* 19, PA3010.
- Mania, D., and Mania, U. (2008). La stratigraphie et le Paléolithique du complexe saalien dans la région de la Saale et de l'Elbe. *L'Anthropologie* 112, 15-47.
- Mania, D., Thomae, M., Litt, T., and Weber, T. (1990). "Neumark-Gröbern: Beiträge zur Jagd des mittelpaläolithischen Menschen."
- Menke, B., and Tynni, R. (1984). Das Eeminterglazial und das Weichselfrühglazial von Rederstall/Dittmarschen und ihre Bedeutung für die mitteleuropäische Jungpleistozängliederung. *Geologisches Jahrbuch* A76, 3-120.
- Müller, H. (1974). Pollenanalytische Untersuchungen und Jahresschitzenzählungen an der eem-zeitlichen Kieselgur von Bispingen/Luhe. *Geologisches Jahrbuch* A21, 149-169.

- Opdyke, N. D., and Channell, J. E. T. (1996). "Magnetic Stratigraphy." Academic Press, San Diego.
- Parés, J. M., and Pérez-González, A. (1995). Paleomagnetic Age for Hominid Fossils at Atapuerca Archaeological Site, Spain. *Science* 269, 830-832.
- Roberts, A. P. (2008). Geomagnetic excursions: Knowns and unknowns. *Geophysical Research Letters* 35.
- Robertson, D. J., and France, D. E. (1994). Discrimination of remanence-carrying minerals in mixtures, using isothermal remanent magnetisation acquisition curves. *Physics of The Earth and Planetary Interiors* 82, 223-234.
- Roebroeks, W., Conard, N. J., and van Kolfschoten, T. (1992). Dense Forests, Cold Steppes, and the Palaeolithic Settlement of Northern Europe. *Current Anthropology* 33, 551-586.
- Rohling, E. J. (1994). Review and new aspects concerning the formation of eastern Mediterranean sapropels. *Marine Geology* 122, 1-28.
- Rossignol-Strick, M. (1985). Mediterranean Quaternary sapropels, an immediate response of the African monsoon to variation of insolation. *Palaeogeography, Palaeoclimatology, Palaeoecology* 49, 237-263.
- Rossignol-Strick, M., Nesteroff, W., Olive, P., and Vergnaud-Grazzini, C. (1982). After the deluge: Mediterranean stagnation and sapropel formation. *Nature* 295, 105-110.
- Sánchez-Goñi, M. F., Eynaud, F., Turon, J. L., and Shackleton, N. J. (1999). High resolution palynological record off the Iberian margin: direct land-sea correlation for the Last Interglacial complex. *Earth and Planetary Science Letters* 171, 123-137.
- Sánchez-Goñi, M. F., Turon, J.-L., Eynaud, F., Shackleton, N. J., and Cayre, O. (2000). Direct land/sea correlation of the Eemian, and its comparison with the Holocene: a high-resolution palynological record off the Iberian margin *Geologie en Mijnbouw* 79, 345-354.
- Shackleton, N. J., Berger, A., and Peltier, W. R. (1990). An alternative astronomical calibration of the lower Pleistocene timescale based on ODP Site 677. *Transactions of the Royal Society of Edinburgh* 81, 251-261.
- Shackleton, N. J., Chapman, M., Sánchez-Goñi, M. F., Paillet, D., and Lancelot, Y. (2002). The Classic Marine Isotope Substage 5e. *Quaternary Research* 58, 14-16.
- Shackleton, N. J., Sánchez-Goñi, M. F., Paillet, D., and Lancelot, Y. (2003). Marine Isotope Substage 5e and the Eemian Interglacial. *Global and Planetary Change* 36, 151-155.
- Sier, M. J., Roebroeks, W., Bakels, C. C., Dekkers, M. J., Brühl, E., De Loecker, D., Gaudzinski-Windheuser, S., Hesse, N., Jagich, A., Kindler, L., Kuijper, W. J., Laurat, T., Múcher,

- H. J., Penkman, K. E. H., Richter, D., and van Hinsbergen, D. J. J. (2011). Direct terrestrial-marine correlation demonstrates surprisingly late onset of the last interglacial in central Europe. *Quaternary Research* 75, 213-218.
- Smith, J. D., and Foster, J. H. (1969). Geomagnetic Reversal in Brunhes Normal Polarity Epoch. *Science* 163, 565-567.
- Thompson, R., and Oldfield, F. (1986). "Environmental Magnetism." Allen and Unwin.
- Tric, E., Laj, C., Valet, J., Tucholka, P., Paterne, M., and Guichard, F. (1991). The Blake geomagnetic event: transition geometry, dynamical characteristics and geomagnetic significance. *Earth and Planetary Science Letters* 102, 1-13.
- Tucholka, P., Fontugne, M., Guichard, F., and Paterne, M. (1987). The Blake magnetic polarity episode in cores from the Mediterranean Sea. *Earth and Planetary Science Letters* 86, 320-326.
- van Kolfschoten, T., Gibbard, P. L., and Knudsen, K. L. (2003). The Eemian Interglacial: a Global Perspective. Introduction. *Global and Planetary Change* 36, 147-149.
- Vasiliev, I., Franke, C., Meeldijk, J. D., Dekkers, M. J., Langereis, C. G., and Krijgsman, W. (2008). Putative greigite magnetofossils from the Pliocene epoch. *Nature Geoscience* 1, 782-786.
- Vine, F. J., and Matthews, D. H. (1963). Magnetic Anomalies Over Oceanic Ridges. *Nature* 199, 947-949.



CHAPTER 4

THE BLAKE EVENT RECORDED NEAR THE EEMIAN TYPE LOCALITY:
REVISED TIMING OF THE ONSET OF THE EEMIAN IN NORTH-WESTERN EUROPE



CHAPTER 4

THE BLAKE EVENT RECORDED NEAR THE EEMIAN TYPE LOCALITY: REVISED TIMING OF THE ONSET OF THE EEMIAN IN NORTH-WESTERN EUROPE

Abstract

Multidisciplinary analysis were performed on a 25 meter orientated core taken at Rutten, close to Eemian key localities in the Netherlands. The cored sediments revealed the presence of the palaeomagnetic Blake Event in combination with an essentially complete Eemian pollen record, spanning a total thickness of around 10 meter. The position of the Blake Event in relation to the Eemian record at Rutten, supports the hypothesis of a 5000 year diachroneity in the onset of last-interglacial conditions between northern and southern Europe. Thereby confirming the observation made by Sier et al. (2011) of a 4 to 5 ka delay compared to the onset of last-interglacial conditions off southwest Iberia. It also suggests the onset of the Eemian to be delayed by up to 10 ka in north-western and central Europe, compared to the global/generic lower MIS 5e boundary. In addition, the here presented Rutten data provides evidence for a long duration of the Blake Event, with a minimum duration of 7 ka.

The use of the 'Eemian' as a synonym for Last Interglacial indifferently in northern, central and southern Europe results from a time that palynological zonation was the only means of chrono-correlation and bears in it the wrong presumption of synchronicity. Despite historical precedent and extensive data coverage and resolution, the late timing of the Eemian in the Netherlands makes it not the best region to define a global chronostratigraphical type locality for the base of Last Interglacial and Late Pleistocene.

1. Introduction

In its classic use, the “Eemian” is the pollen-defined terrestrial equivalent of the Last Interglacial in north-western Europe. Although it was first defined to describe a Lusitanian mollusk-rich stratigraphic unit near Amersfoort (the Netherlands) by Harting (1874). After pioneering work by Jessen and Milthers (1928) its boundaries are now defined by its pollen assemblage (Zagwijn, 1961). The “Eemian” terminology is also used to label the Last Interglacial pollen record in southern Europe. The terrestrial Eemian is often assumed to be the 1:1 equivalent of Marine Isotope Stage (MIS) 5e, implying a synchronous start and having the same duration. However, studies of washed-in pollen in the MD952042 core off the Iberian coast, have demonstrated a 5 to 6 ka delay of the onset of the Eemian in relation to its inferred MIS counterpart, based on paired $\delta^{18}O$ and pollen (Sánchez-Góñi et al., 1999; Shackleton et al., 2002; Shackleton et al., 2003). A recent study at the Neumark-Nord 2 (NN2) archaeological site (Germany) suggests that this delay increases with another 4 to 5 ka at higher latitudes, based on land-sea correlation via the Blake Event (Sier et al., 2011). The possibility to position these palaeomagnetic data in the NN2 Eemian pollen zones allowed to demonstrate a distinct time lag between the MIS 5e ‘peak’ in the marine record and the start of the Eemian, at least in the Neumark region (eastern Germany). If correct, such a large time lag has significant consequences for current views on the development of the Eemian in central Europe, possibly applicable to a larger area, i.e. north-western Europe. Furthermore, the positioning of the Blake Event within the NN2 Eemian pollen succession holds potential for the correlation of Last Interglacial archaeological sites on a very high resolution time scale (Sier et al., 2011). Therefore, the interpretation of the NN2 data requires rigorous testing at other Last Interglacial locations.

Here, we describe results obtained from a northerly oriented, undisturbed core in Eemian sediments from the Netherlands, providing important new evidence to constrain the position of the Blake Event with respect to the Eemian pollen zonation. The core (B15F1501) is located near Rutten in the Netherlands’ central depocenter. This depocenter hosted the Rhine estuary during the Eemian interglacial, and is part of the same ca. 70-km wide Last Interglacial shallow-marine embayment along which the other Eemian key core localities Amersfoort and Amsterdam Terminal are located (Figure 1). In the 1960’s, the Amersfoort site featured in classic work by Zagwijn (1961) who introduced a pollen zonation scheme for the Eemian that has been widely adopted across

Europe, with regional modifications. In the more recent past, the Amsterdam Terminal core has been used to define an Eemian Stage regional stratotype (Beets and Beets, 2003; Beets et al., 2006; van Leeuwen et al., 2000), and has been coined as a location to host the Global Chronostratigraphical Section and Point for the Late Pleistocene (Gibbard, 2003; Gibbard et al., 2008).

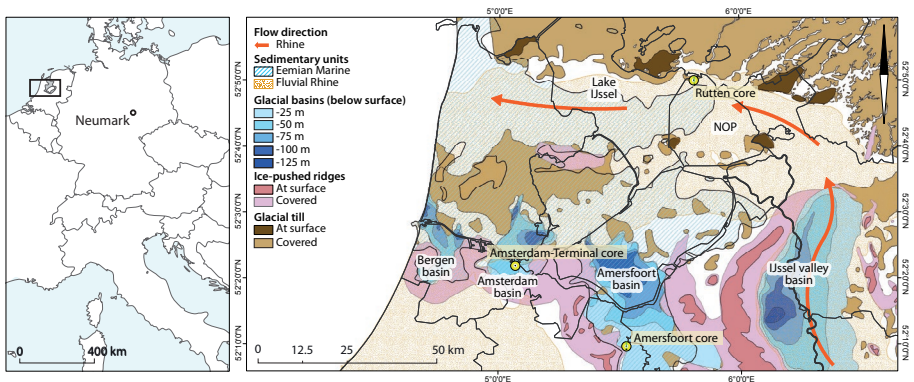


Figure 1.

Location map of the study area in the Netherlands and the German Neumark-Nord site. Detailed map of the study area shows the underlying geology and the location of the Ruten orientated core (B15F1501), Amsterdam-Terminal core and the Amersfoort core. After Busschers and Bakker (2009) and Gunnink et al. (2013).

2. Geographical and geological setting

The 25 meter long orientated (to magnetic north) core B15F1501 was taken near the village of Rutten (N 52° 49' 32.6", E 5° 41' 54.8"), the Netherlands. The coring site is located in the Noordoostpolder, with its surface at -3.62 meter below Dutch Ordnance Datum (NAP). The landscape of the northern part of the Netherlands, still echoes the advancing and retreating movements of ice sheets in its topographic features (see Supplementary Information (SI) figure 1 and figure 1).

During the Late Saalian the northern part of the Netherlands, including the Rutten site, was covered by the large ice-masses of the Drenthe substage glaciation (e.g. Van den Berg and Beets, 1987). This created the geomorphological setting of a lowland ice-marginal drainage area bounded in the north by the undulating ice-pushed topography (Texel-Gaasterland line). During and after deglaciation, the river Rhine was situated in an incised valley. (Busschers et al., 2008). During the Eemian interglacial this valley gradually drowned due to interglacial sea-level rise, and since then formed the Rhine estuary (Busschers et al., 2007). The Late Saalian to Eemian sedimentary infill of this Rhine valley is characterized by coarse-grained (glacio-)fluvial sands (up to early Eemian age, based on pollen spectra), overlain by Eemian age fine-grained deposits and organic-rich sediments which are partly estuarine and partly of fluvio-deltaic origin. At numerous locations throughout the valley most of these fine-grained deposits are eroded by extensive fluvial activity in the Last Glacial (Weichselian), thereby depositing coarse-grained sediments, as hundreds of available boreholes for the area show (TNO Geological Survey of the Netherlands (TNO-GSN); public database at www.dinoloket.nl). The Rutten site, located at the northern fringes of the palaeo Rhine valley is however exceptional in escaping this erosion and contains a unique sequence that (almost) spans the entire Eemian. For a detailed lithological description the reader is referred to the SI.

3. Methods

3.1. Coring and sampling

Core B15F1501 was taken with a Nordmeyer soil-sampler unit equipped with a sediment-catcher, which produces core segments with known orientation. The different core-segments, with a length of 1 meter and 10 centimeters in diameter, were sealed airtight with paraffin and kept in cooled storage ($<5^{\circ}\text{C}$) at the TNO-GSN core facility in Utrecht, the Netherlands.

Upon arrival the core-segments were split in two halves, photographed and described according to the TNO-GSN standard (Bosch, 2000). Palaeomagnetic samples for alternating-field (AF) demagnetization were collected with dedicated perspex sample containers. For thermal (TH) demagnetization samples, dedicated quartz-glass sample containers were used. These sample containers have standard palaeomagnetic dimensions (25 mm diameter and 22 mm height) and were gently pushed into freshly prepared core sections. A total of 252 samples were taken, 118 TH and 134 AF samples. Measurements were done within one week after retrieval of the samples and within two weeks after retrieval of the core to ensure that the samples were processed while still fresh. During this period the samples remained in cooled storage ($<5^{\circ}\text{C}$).

The remaining undisturbed half of the core was sampled for luminescence dating in a darkroom under dim orange conditions. Samples for luminescence were taken from relatively homogeneous sediment sections, about 400 grams of sediment per sub-sample was transferred into an opaque plastic bag, sealed and transported to the luminescence dating laboratory of the Netherlands Centre for Luminescence dating (formerly situated at Delft Technical University).

3.2. Palaeomagnetism and rock magnetism

Stepwise progressive thermal demagnetization of the natural remanent magnetization (NRM) was performed with an ASC thermal demagnetizer (residual field < 20 nT) at CENIEH, Burgos (Spain). Maximum demagnetization temperature was 600°C . The remaining NRM after each step was measured with a SRM 755 helium free DC-SQUID (direct current superconducting quantum interference device; 2G Enterprises (California, USA)) magnetometer (instrument sensitivity 3×10^{-12} Am², typical sample NRM intensities

were at least a couple of orders of magnitude higher) with a low-field environment at the sample loading position. Before measuring, samples were put in a shielded environment for at least a period of 30 minutes. Alternating field (AF) demagnetization was done in 16 steps up to 100 mT at the palaeomagnetic laboratory of Utrecht University (the Netherlands). AF samples were processed fully automatically with the so-called 'three position protocol' that compensates for the magnetic moment of the transport tray. To compensate for possible gyroremanent magnetization (GRM), often due to greigite (Fe_3S_4) that regularly occurs in organic-rich sediments, which can be acquired during AF demagnetization, AF samples were processed with the so-called 'per component' protocol (Dankers and Zijdeveld, 1981; Stephenson, 1993), in addition to the regular AF demagnetization. This was done for AFs ≥ 30 mT. Samples that were submitted to Anhysteretic Remanent Magnetization (ARM) and Isothermal Remanent Magnetization (IRM) measurements had first their NRM AF demagnetized. AF demagnetization (standard and per component), ARM and IRM acquisition was done with the robotized 2G DC-SQUID magnetometer. The instrument's sensitivity is 3×10^{-12} Am². The instrument set-up is housed inside a magnetically shielded room (residual field < 200 nT), the robotized interface for field regulation and sample manipulation was built in-house. Up to 96 samples contained in dedicated cubic holders (edge 30 mm) are loaded onto a sample plateau and the robot subsequently loads them in batches of eight onto a tray. Programme controlled, it slides through the magnetometer and demagnetization coils that are used for the ARM acquisition (a bias field coil provides the asymmetry in the field which was set at 38 μT). The ARM was AF demagnetized at steps of 25 and 40 mT to be able to reconstruct a relative paleointensity record. This was done by dividing the NRM intensity after AF demagnetization at 25mT by the ARM intensity after AF demagnetization at the same level conforming to general practice (e.g. Meynadier et al., 1992) Standardization took place by scaling to mean zero with a standard deviation of 1. Finally IRM acquisition curves were determined for all these samples with 60 steps up to a peak IRM field of 700 mT. This was done with a pulse-field coil, interfaced with the robotized magnetometer set-up. Data acquired from the IRM measurements was subjected to a Cumulative Log Gaussian (CLG) component analysis (Kruiver et al., 2001). Prior to the IRM acquisition the samples were AF demagnetized at 300 mT peak field with the final demagnetization axis parallel to the IRM pulse field direction to force the shape of the subsequently measured IRM acquisition curves as much as possible conform a CLG shape for most meaningful fits (cf. Egli, 2004; Heslop et al., 2004). After fitting of the data the different coercivity

components can be recognised by their saturation IRM (SIRM), remanent acquisition coercive force ($B_{1/2}$) and dispersion parameter (DP) (Kruiver et al., 2001).

The Characteristic Remanent Magnetization (ChRM) was typically determined by the steps between 280 and 340°C (6 steps), occasionally starting at 150° and continuing up to 480°C (see SI table I). ChRM's from AF demagnetized samples were all determined above 10 mT and mostly between 10 and 50 mT (see SI table). Directions of the ChRM were calculated using least-squares principle component analysis (Kirschvink, 1980) on at least 4 steps. According to common practice, line fits for TH samples were anchored towards the origin. Because then, the general trend of the ChRM component is then better appreciated. Line fits of AF samples were not anchored towards the origin because this resulted in visually poor fits with unrealistically large MAD (maximum angle of deviation) angles when compared to line fits through the same data points without forcing through the origin.

We defined three quality labels for the ChRM directions. AF demagnetization diagrams of which both 'per component' (Dankers and Zijdeveld, 1981; Stephenson, 1993) and standard AF measurements showed hardly or no indication of gyroremanent magnetization (GRM) and with an endpoint close to the origin, were labelled quality 1 (figure 2A and 2B, MAD maximum = 11.3°, 9 out of 134 AF samples). Quality 2 label was given to diagrams with a slight GRM in the standard diagrams, which could be corrected for by per component protocol and an endpoint close to the origin (MAD maximum = 14.8°, figure 2C and 2D, 76 out of 134 AF samples). ChRMs with a MAD > 15° were given a quality of 3 (2 out of 134 AF samples). All diagrams with a GRM that could not be corrected for by the per component protocol or with a too strong GRM in the standard measurement protocol were not considered in the interpretation (examples in figures 2E and 2F, 47 out of the 134 AF samples). Only quality 1 and quality 2 samples were used for the interpretation of the magnetostratigraphy (see figure 2 for examples).

TH demagnetized quality 1 samples have clear ChRM directions with endpoints close to the origin (figure 2G, 12 out of 118 TH samples). Whereas quality 2 samples have well-defined ChRM directions but endpoints were slightly off the origin (figure 2H, 49 out of 118 TH samples). Quality 3 samples are based on just four data points and/or have MADs above 15°. The ChRM directions of quality 3 TH samples were calculated but not used for the interpretation (25 out of 118 TH samples). All other samples and all great circle trajectories were rejected for magnetostratigraphic interpretational purposes (32 of 118 TH samples).

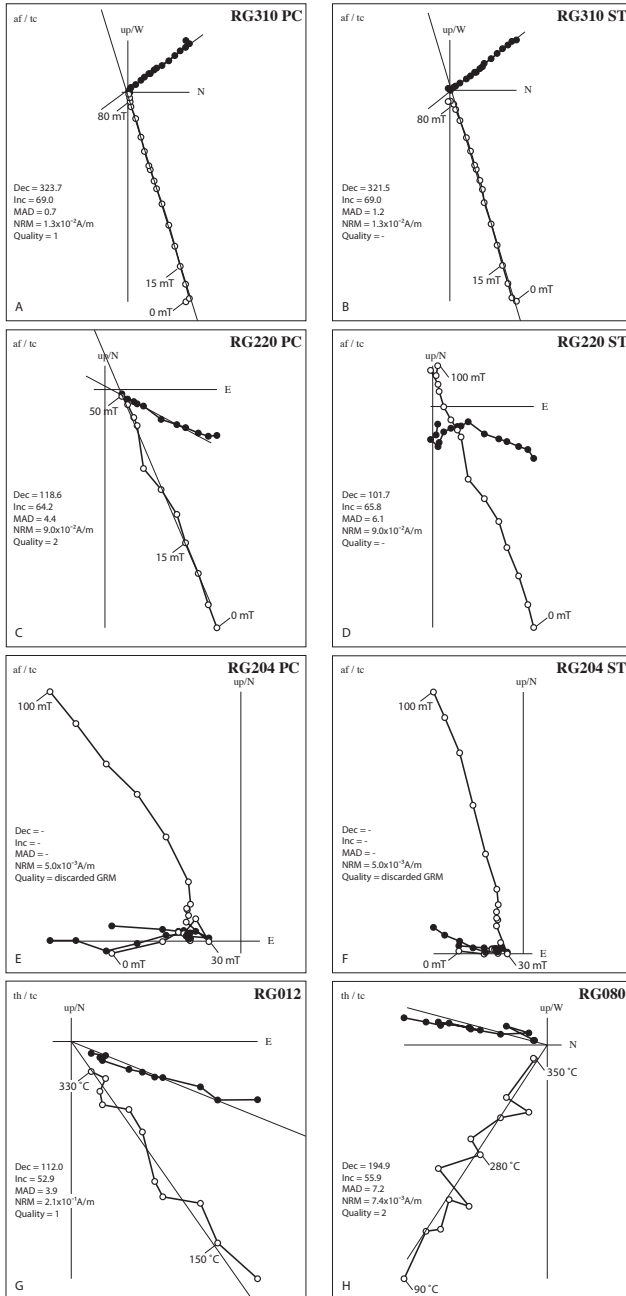


Figure 2.

Figure 2.

Representative Zijdeveld diagrams of alternating field demagnetization (AF) and thermal demagnetization (TH). Numbers next to the graphs denote alternating field step in mT or demagnetization temperature step in °C. Panels A and B show an AF quality 1 sample. Panel A shows the per component (PC) Zijdeveld diagram (for GRM correction) and panel B shows the standard (ST) demagnetization diagram of the same sample. An AF quality 2 sample is shown in panels C (PC) and D (ST). Panel E (PC) and F (ST) show an example of a discarded sample due to high GRM. Examples of quality 1 and quality 2 TH samples are given in panel G and H. Dec and Inc stand for declination and inclination in degrees. MAD is maximum angle of deviation. See main text for further explanations, for stratigraphic levels see SI table I and II.

Hysteresis loops, back-field demagnetization, and first-order reversal curves (FORCs) were measured using a MicroMag alternating gradient magnetometer (Model M2900, palaeomagnetic laboratory, Utrecht University; noise level 2×10^{-9} Am²). Hysteresis loops were measured between -1 and +1 T with a field increment of 5 mT and an averaging time of 150 ms. Back-field demagnetization curves (250 ms waiting time) started with a saturation at 1 T and were acquired with logarithmic field increments with an averaging time of 150 ms as well. Hysteresis parameters, including the saturation magnetization (Ms), the saturation remanent magnetization (Mrs) and coercivity (Bc) were determined after paramagnetic slope correction. FORC diagrams (Pike et al., 1999; Roberts et al., 2000) were obtained by measuring ~500 FORCs with maximum applied fields of 1 T, field increments of 0.5 mT. FORC diagrams were calculated using a program written by T.A.T. Mullender (paleomagnetic laboratory, Utrecht University). This software package does not consider the FORC distributions close to the vertical axis to avoid uncertain interpretation for inherently incomplete FORC grids in this region of the diagrams. A smoothing factor (SF) of 5 (Roberts et al., 2000) was used to calculate all the FORC diagrams.

3.3. Pollen analysis

For this study, pollen analysis is primarily used as a biostratigraphic correlation tool in order to pin-point the encountered sedimentary record to the pollen zonation of Zagwijn (1961) and place them in Eemian relative chronology. Pollen analysis was performed on 40 sub-samples derived from mostly clayey, gyttjaic and peaty intervals in the Rutten core. Samples were prepared following standard procedures: peptization with Na pyrophosphate (15g/l), sieving (250 and 7 µm mesh-size), HCL (30%) rinsing, acetolysis (9:1 ratio of (CH₃CO)₂O : H₂SO₄) and heavy liquid density separation (sodium-poly-

tungstate with a specific gravity 2.1 kg/dm³). Residues were mounted in glycerine on glass slides for microscopic analysis. Northwest European Pollen Assemblage Zones (PAZ) are visually determined based on relative abundances of series of indicative taxa (cf. Zagwijn, 1961; Zagwijn, 1996) and are supported by CONISS (Grimm, 1987). It should be mentioned here that *Pinus* (and partly *Picea* too) is over-represented throughout the entire diagram, caused by enrichment of fluviially transported material due to its setting (see SI figure 2 for pollen diagram).

3.4. Luminescence dating

Samples for luminescence dating were sent in duplicate. One subsample is used to determine the dose-rate using high-resolution gamma-ray spectroscopy. The sediment is dried, ground and moulded with wax, creating a puck that is measured on the gamma-spectrometer for at least 24 hours. Activity concentrations of ⁴⁰K and several nuclides of the U and Th decay chains are converted to dose rate, taking into account effects of moisture (20 ± 3 % by weight for sandy samples, 30 ± 5 % by weight for loamy samples), the contribution by cosmic rays, and a contribution from internal K and Rb in the K-feldspar grains used for analysis (internal dose rate estimated to be 0.77 ± 0.08 Gy/ka; see Kars et al., 2012). The other subsample is prepared for equivalent dose determination.

Samples are wet-sieved to obtain a fraction of 180-212 µm. These were then treated with HCl and H₂O₂ to remove carbonates and organic matter respectively. A purified extract of K-rich feldspar grains was obtained through density separation using LST fastfloat heavy liquid at 2.58 kg/dm³ and this fraction was further cleaned and etched using 10% HF, and subsequently rinsed with HCl. A Risoe TL/OSL DA 20 reader was used for luminescence measurements; this apparatus is equipped with infrared diodes for stimulation (870 nm), and a Sr/Y beta source for irradiation. A LOT/Oriel D410/30 interference filter was used to select the K-feldspar emission around 410 nm.

Measurements were made using the recently developed post-IR IRSL Single-Aliquot Regenerative (SAR) protocol (Thiel et al., 2011) in order to avoid problems with signal instability (anomalous fading). This method has yielded good results for similar deposits (Buylaert et al., 2012; Kars et al., 2012). Parameters used were a 60s preheat at 320°C, infrared bleach for 100s at 50°C, post-IR IRSL stimulation for 100s at 290°C. At the end of each SAR cycle, the signal was reset by 40s exposure to infrared at 330°C. Performance

of this protocol was tested using a dose-recovery experiment, and stability of the post-IR IRSL signal was tested using a fading experiment.

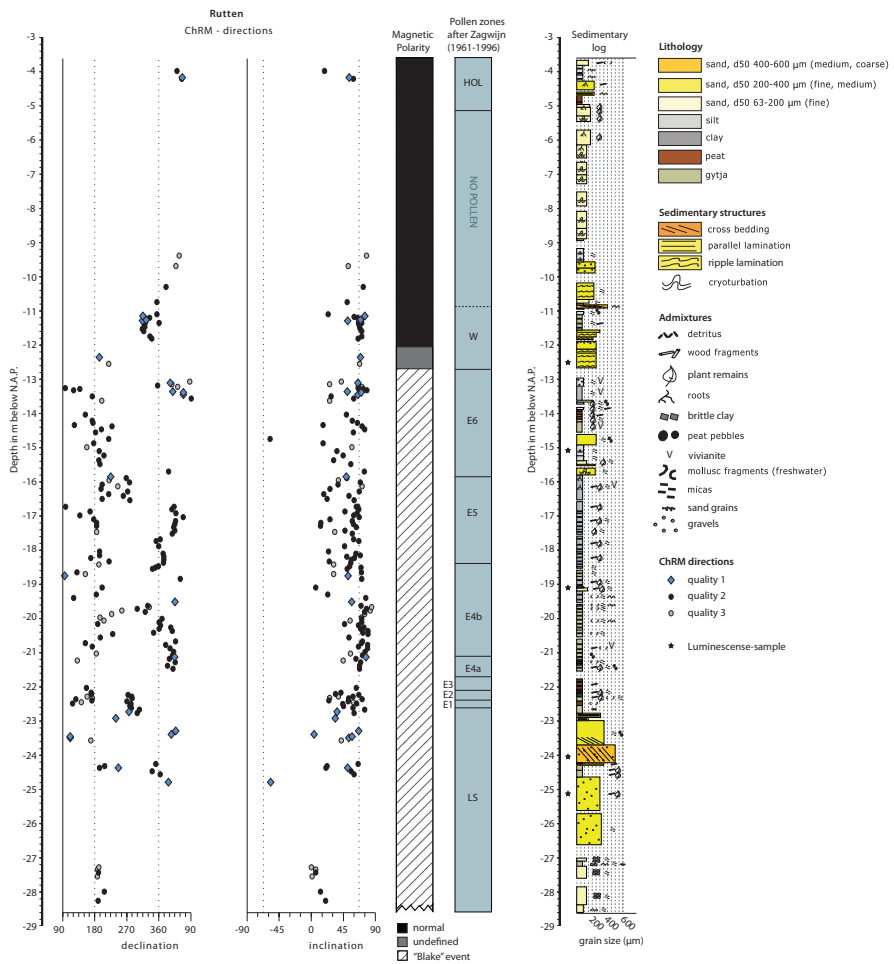


Figure 3

ChRM directions plotted against the sedimentary log and identified Pollen Assemblage Zones (PAZ) (grey circles represent quality 3 ChRM directions which are not used in the final interpretation). PAZ E1-E6 are Eemian zones (Zagwijn, 1961), HOL stands for Holocene, W for Weichselian and LS for Late Saalian. Depth is plotted in NAP (Dutch Ordnance Datum). Declination and inclination is in degrees. The hiatus is situated at the PAZ E6 to W transition.

4. Results

4.1. Palaeomagnetism

As mentioned above, the magnetic polarity is based on quality 1 and 2 ChRM directions only, of which examples are given in figure 2. All ChRM directions are provided in tables I and II in the SI. Figure 2 shows examples of Zijderveld diagrams of AF demagnetized samples of quality 1, 2 and 3 (2A to 2F). Both standard and per component diagrams are shown of each AF example. Also examples of Zijderveld diagrams of quality 1 and 2 TH samples are given (2G and 2H). From the tables and figure 3 it emerges that almost all samples have ChRM directions with a positive inclination; only two of the ChRMs have negative inclination, one with a northern declination, the other with a southern declination. TH demagnetized samples have more samples with a shallow inclination, some of them can be labeled excursions even with a normal declination (See SI table I and II). All samples that show ChRM directions with deviations of over 40° from the normal virtual geomagnetic pole of the Brunhes (Merrill and McFadden, 1994) have been labelled excursions (see SI table I and II). Plotted against their stratigraphic depth, the ChRM directions show two different zones, a zone with normal polarity from the surface (-3.62 m) down to a depth of -12.08 meters and a zone with normal and “mixed” directions from -12.08 meters down to the maximum depth of the core at -28.62 NAP (figure 3). Within core-segments from the “mixed” zone both normal and excursions directions are found, often centimeters apart. We have one quality 1 sample (-12.35 m NAP) above the Eemian deposits, in sediments containing Weichselian pollen. From this core segment we have a luminescence date of 44 ± 3 ka (Table I), indicating a hiatus with the underlying Eemian sediments (see figure 3), with luminescence dates of 105 ± 9 ka and 107 ± 6 ka (Table I). This is plausible because of the Pleniglacial erosive phase found in this region (Busschers et al., 2007). The hiatus is also established by independent geological correlations made by Peeters (unpublished material) which place the sediments of this segment (-11.92 to -12.82 m NAP) of the core in a significantly younger unit of presumably Pleniglacial age. There appears to be no correlation between the palaeomagnetic direction and the sediment lithology (figure 3; also see SI).

Table 1:

Summary of feldspar post-IR IRSL luminescence dating results.

Sample NCL	Depth NAP (m)	Water content (%)	Equivalent dose (Gy)	Dose rate (Gy/ka)	Age (ka)
NCL-6312180	-12.52	20 ± 3	77 ± 3	1.76 ± 0.09	44 ± 3
NCL-6312181	-15.12	30 ± 5	249 ± 17	2.38 ± 0.10	105 ± 9
NCL-6312182	-19.17	30 ± 5	225 ± 9	2.11 ± 0.10	107 ± 6
NCL-6312183	-24.03	20 ± 3	207 ± 12	1.31 ± 0.08	158 ± 13
NCL-6312184	-25.17	20 ± 3	654 ± 34	1.66 ± 0.09	393 ± 29

4.2. Rock Magnetism

To constrain the interpretation of the ChRM directions, rock-magnetic measurements have been carried out. The majority of the samples had the NRM decayed at temperatures below 360°C indicating a dominant contribution of iron sulphides to the NRM (see figure 4 for some examples). Rock-magnetic measurements can help distinguishing between diagenetic and biogenic iron sulphides and thus primary versus delayed NRM acquisition (e.g. Vasiliev et al., 2008). Biogenic minerals are formed in situ often at the oxic-anoxic interface in sedimentary settings (Bazylinski and Frankel, 2004) while diagenetic sulphides are either formed shortly after sedimentation by early diagenetic processes (often bacterially mediated) or later in time by remagnetization (e.g. Roberts and Weaver, 2005; Rowan and Roberts, 2006).

A wide range of four hysteresis properties was observed for the studied samples, which consist of a representative selection of quality 2 and quality 3 samples. These quality labels were selected in order to distinguish GRM affected on non GRM affected samples. No samples of quality 1 were selected because no GRM was present in these samples. Typical hysteresis loops and high-resolution FORC diagrams with single domain (SD) behavior are shown in figure 5. These hysteresis loops are relatively squared (Tauxe et al., 1996) with M_{rs}/M_s ratios of ~0.4-0.5 and B_c values of ~20-40 mT (figure 5A). High-resolution FORC measurements indicate a range of magnetic properties with variable coercivity and magnetostatic interaction distributions (figure 5B). Some FORC diagrams have a central ridge along the B_c axis with negligible vertical spread, which indicate a lack of magnetostatic interactions (Pike et al., 1999). This FORC central-ridge

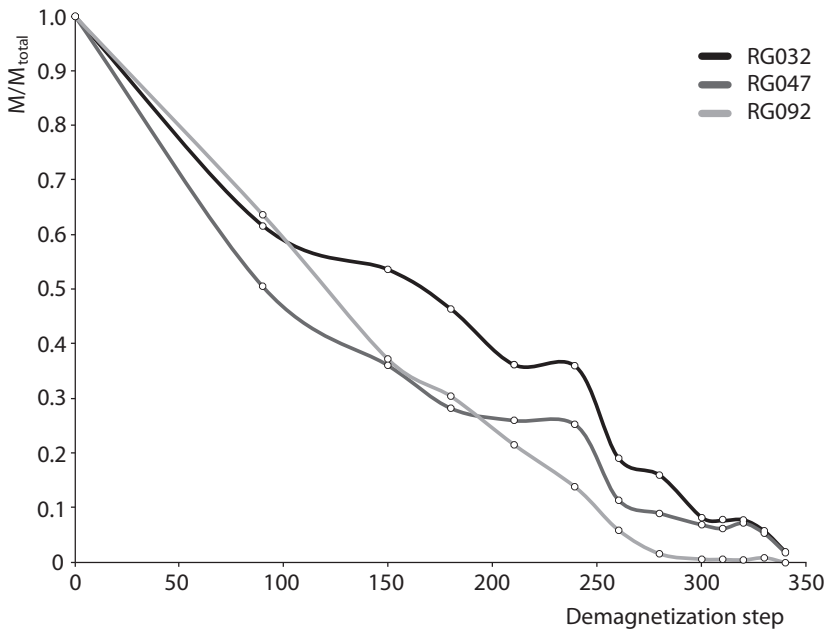


Figure 4.

Normalized decay curve of three TH demagnetized quality 1 samples. Demagnetization steps are in degrees Celsius.

signature corresponds to that of non-interacting or weakly interacting SD particles, which probably indicates presence of significant amounts of biogenic magnetic minerals produced by magnetotactic bacteria (Egli et al., 2010). The FORC diagrams also have another component consisting of concentric contours with a relatively large vertical spread, which indicate strong magnetostatic interactions (Pike et al., 1999; Roberts et al., 2000). This FORC component also has two other pronounced features. First, the centre of the concentric contours is shifted downward to negative B_i values. Second, there is a negative peak close to the B_i axis in the lower quadrant (white area in figure 5B). These signatures all indicate a strongly interacting SD magnetic particle assemblage (Newell, 2005; Pike et al., 1999; Roberts et al., 2000). This type of FORC distributions is typical of diagenetic SD greigite-bearing sediments (e.g. Roberts et al., 2011; Roberts et al., 2006; Roberts et al., 2000; Rowan and Roberts, 2006; Sagnotti et al., 2010; Vasiliev et al., 2007). Many FORC diagrams have a variable mixture of these two FORC distributions: the central ridge representing one end member and the vertically spread concentric contours the

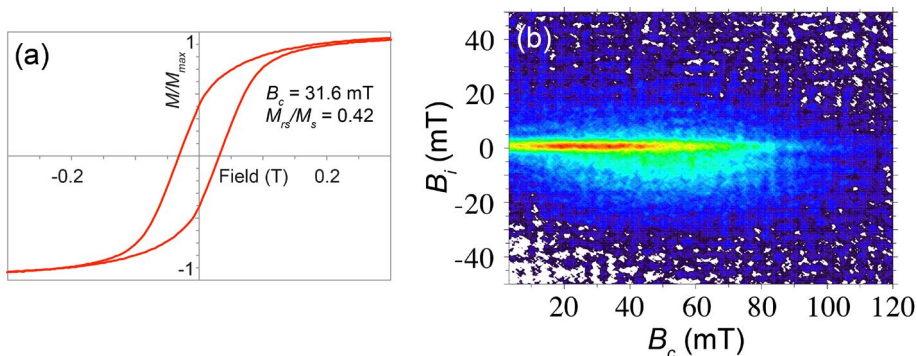


Figure 5.

Hysteresis loop (a) and high-resolution FORC diagram (b) for sample 'RG234' (clay) taken at -22.42 m NAP. The hysteresis loop is normalized to the saturation magnetization value (at 1 T) after paramagnetic slope correction. Hysteresis parameters (B_c and M_{rs}/M_s), which are determined for the entire loop to ± 1 T, are indicated. 500 FORCs were measured and a SF value of 5 was used to calculate the FORC diagram. The FORC diagram was calculated using a program written by T.A.T. Mullender at the paleomagnetic laboratory, Utrecht University. B_c in the coercivity, B_i is the interaction field.

other (figure 5B). These samples therefore contain a mixture of non-interacting and interacting SD particles. Both types of magnetic minerals are present throughout the stratigraphic column and are not restricted to a zone of magnetic polarity.

CLG IRM component analysis shows the presence of three components, a low-, a high-coercivity component and, at very low coercivities, an extra component that is required to fit the slightly skewed-to-the-left coercivity distribution. This extra component is an artifact of the fitting method and not given a physical meaning (Egli, 2004; Heslop et al., 2004). The artifact component (component 1, figure 6D, with 6A, B and C for reference to figure 3) has a mean dispersion parameter (DP) value of 0.281 (log mT) and a mean acquisition field $B_{1/2}$ of 25.23 mT. The low-coercivity component 2 has a mean DP of 0.197 (log mT) and a mean $B_{1/2}$ of 67.48 mT, with a range between 48 and 91 mT (see figure 4D and E). Component 3 has a high-coercivity with mean DP of 0.318 and $B_{1/2}$ of ~ 260 mT, with a range between 158 and 794 mT. This latter component contributes on average 6 percent to the magnetization (one clearly deviating sample has a 22 percent contribution). Component 3 most likely is hematite but was not further investigated due to its low contribution; its contribution to the NRM is marginal if present at all. Component 2 is greigite, as also shown from the hysteresis and FORC measurements. It was already suspected to be present after AF demagnetization of the NRM: a considerable portion of

the samples showed an increase of intensity after demagnetization at high AF levels. Even though samples with high GRM were not used for interpretation of ChRM directions, all samples were used for IRM analyses. No differences can be identified in the IRM intensities between the diagenetic and biogenic samples (figure 6D and SI table II).

The magnetic susceptibility (with a range of $0.19 \cdot 10^{-8} \text{ m}^3/\text{kg}$ to $446 \cdot 10^{-8} \text{ m}^3/\text{kg}$) and the NRM intensity show a clear one-to-one relationship with each other (figure 6F and G) but not with the magnetic polarity (figure 6A). Samples from the Rutten core B15F1501 show a wide range of NRM intensities from $2.76 \cdot 10^{-4} \text{ A/m}$ to over no less than $4.5 \cdot 10^{-1} \text{ A/m}$. A zone with increased intensities is observed from -18.10 to -24.56 meters (figure 6G).

Around the period of the Blake Event, Relative Palaeo-Intensity (RPI) records show a long period with low intensities from 95 to 125 ka (Channell et al., 2012; Thouveny et al., 2004). During periods of weak field intensity of the earth's magnetic field, more reversals and/or excursions are expected (e.g. Valet et al., 2005). The range of RPI at Rutten is from -1.43 to 3.36 (within excursions zone -1.42 to 2.19) with no relation to the stratigraphy (with an outlier value of 6.88 being excluded). It shows a relatively narrow range of values from a depth of -28.62 meters until a depth of -12.54 meters (SI figure 3). From the hiatus (see discussion below) at -12.54 to -11.14 meters we can see a rising trend followed by individual lower values in RPI up to the top of the core. Even though GRM occurs in the Rutten sediments above 25 mT and the RPI curve shows no distinction between GRM containing samples and samples without GRM, caution is needed when interpreting RPI in greigite bearing sediments. The Rutten RPI record is limited in time making comparison with other RPI records difficult. However, the Rutten RPI record (SI figure 3) does show fairly consistent values during the period of the Blake Event and in that sense does not contradict with the zone of low intensity as published by Thouveny and colleagues (e.g. Channell et al., 2012; Guyodo and Valet, 1996; Thouveny et al., 2004; Valet et al., 2005).

4.3. Pollen analysis

The Late Saalian base of the sequence (-28.6 m to -22.6 m NAP) is identified by scarce pollen collected from gravelly, coarse-grained fluvial sands. Retrieved pollen-material shows a herb and heathland vegetation (PAZ LS) The onset of the Eemian sequence in the Rutten core (-22.6 m to -12.7 m NAP) is characterized by peat and gyttja, indicating a wet flood basin environment (see SI for a detailed lithological description). Vegetation

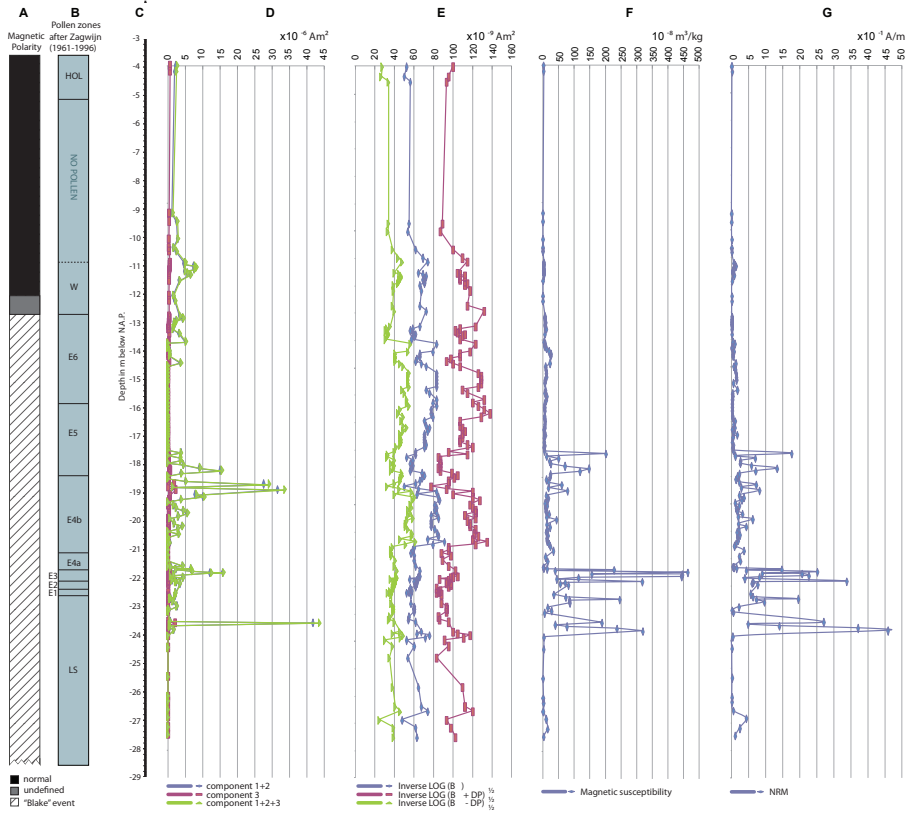


Figure 6.

Combined overview of A) magnetic polarity, B) pollen zonation, C) depth below Dutch Ordnance Datum (NAP), D) IRM data, E) component 2 of IRM data, F) magnetic susceptibility measured on a Kappabridge KLY2 and G) NRM intensity from core B15F1501 plotted versus stratigraphic depth. The Late Saalian sediments are coarsely grained and represent a short period of time (for details on the lithology see figure 3 and the SI).

succession in the early Eemian shows a rapid succession of *Betula* (PAZ E1), *Pinus* (PAZ E2) and *Tilia*, *Ulmus*, *Quercus* (PAZ E3). Maximum percentages of *Corylus* and *Quercus* mark the establishment of thermophilous trees in PAZ E4. Further, marine indicators (diatoms and dinoflagellate cysts) indicate the first transgressive marine influence within this zone. The lithology gradually changes towards organic-rich clays. Higher up in the core, the occurrence of marine indicators (also including foraminifers) continues to increase; the regional sea-level high-stand is marked in PAZ E5 (cf. Zagwijn, 1996), relatively late in the Eemian. However, *Carpinus* percentages (see SI figure 2) are lower than expected when

compared with previous studies in the records of Amersfoort and Amsterdam basins (Cleveringa et al., 2000; van Leeuwen et al., 2000). This difference is however plausibly explained by the estuarine marginal setting of the Rutten core. The Rutten locality partly turned brackish due to the marine transgression in its direct surrounding at this time. Brackish conditions will certainly not have favored the characteristic *Carpinus* expansion (PAZ E5 in Zagwijn, 1961) from the topographically high and freshwater bearing ice-pushed ridges (surrounding the glacial basins), to our research area. Finally, the end of the Eemian stage is characterized by the presence of *Picea*, *Pinus*, herbs and heathland (PAZ E6). The boundary with the Weichselian is characterized by a lithological change to moderately coarse-grained fluvial sands (-12.7 m NAP onward), and is represented by a strong decline in arboreal pollen towards a wet, herb-rich vegetation.

4.4. Luminescence dating

A dose recovery test using the adopted post-IR IRSL protocol indicated that a given dose could be accurately recovered (dose recovery ratio 1.07 ± 0.04 , $n=12$). The observed fading rate was low (1.1 ± 0.2 %/decade), no correction for fading was made as experiments on infinite-age samples have shown that the post-IR IRSL signal is not affected in nature (Kars et al., 2012; Thiel et al., 2011).

Luminescence dating results are shown in Table I, including 1-sigma errors. The obtained dose rates varied from 1.31 Gy/ka to 2.38 Gy/ka, and show a trend with the coarseness of the sediments (greatest dose rates for fine-grained sediments). Equivalent doses range from 77 to 654 Gy, with the largest result beyond the reliable range of the post-IR IRSL dose response curve, above 2 times the onset of saturation parameter D_0 (Wintle and Murray, 2006). The resulting ages range from 393 ka to 44 ka, and are in stratigraphic order. The two samples associated with Eemian pollen zones return ages of 105 ± 9 ka and 107 ± 6 ka (depths of -19.17 m and -15.12 m). For both samples the number of aliquots is 6 with respectively 3 and 2 aliquots placed outside the 2-sigma error (see SI figure 4B and 4C). The Saalian sands give ages of 393 ± 29 ka and 158 ± 13 ka (depths of -25.17 m and -24.03 m). These samples have aliquots of 6 and 5 with respectively 4 and 2 placed outside the 2-sigma error (see SI figure 4D and 4E). The Weichselian sand at a depth of -12.52 m gives an age of 44 ± 3 . This sample has 5 aliquots with only 1 placed outside the 2-sigma error (see SI figure 4A).

5. Discussion

5.1. ChRMs of Rutten core and boundaries of the Blake Event

Sedimentary context, new post-IR IRSL luminescence dates and the characteristic Eemian pollen zonation combined identify the palaeomagnetic excursions zone in core B15F1501 (figure 3) as the Blake Event. The two deepest luminescence ages (158 ± 13 ka and 393 ± 29) fall within the zone with excursions directions but are significantly older. These samples are from sediments deposited in a high turbulent setting and thus the ages presumably do not reflect the true age of deposition due to poor-bleaching effects.

The Blake Event as recorded at Rutten has a well defined upper boundary, based on the palaeomagnetic directions of high quality up to a hiatus (see below), but the lower boundary is not identified (see figure 3). However, as at NN2, the lower Blake Event boundary is recorded below the base of the Eemian deposits as we find excursions directions below Eemian PAZ E1 in sediments of Late Saalian age. Below PAZ E1 there are several AF and TH quality 1 samples, supporting a pre-Eemian onset of the Blake Event. This position of the lower boundary is similar to the record found at NN2. The lowermost AF quality 2 sample with biogenic minerals is sample RG220 with a depth of -22.48 NAP. The in situ signal biogenic signal makes the Blake Event fall within Eemian pollen zone E1 (see figure 3).

The upper boundary of the Blake Event at Rutten is positioned significantly higher in the Eemian vegetation succession than in the NN2 section, where it was placed in pollen zone EIVb3 (*sensu* Menke and Tynni, 1984) (Sier et al., 2011). In the Rutten core, the Blake event is still recorded in PAZ E6 (*sensu* zagwijn 1961, equivalent to EVI of Menke and Tynni 1984) (see figure 3).

Because the quality of both the accepted ChRM directions in the highest core segment with excursion ChRM directions and 44 ± 3 ka luminescence age, we might be dealing with a younger palaeomagnetic excursion, the Laschamp, superimposed on the Blake Event in the Rutten record. However, in contrast to the lower parts of the core (e.g. core segment containing the top of PAZ E6), this (coarser grained) segment has only one quality 1 ChRM direction, so we cannot exclude possible rotation of the core lining. In the deeper sampled core segments with excursions directions we find normal and excursions directions of high quality mixed in individual segments; this means that we can exclude independent rotation of the core lining.

Our position estimate of the Blake Event in the Rutten core assumes no, or very little, delayed acquisition in the Rutten sediments. We have good arguments for this assumption. First of all, there are similarities between the Rutten and NN2 records. Both in Rutten and NN2 we find excursions in the lower part of the Eemian (zones E1 to E4, *sensu* Zagwijn 1961 in NN2) and in the top of the Late Saalian. The NN2 palaeomagnetic record is registered by magnetite with a varying amount of hematite combined with high sedimentation rate making delayed acquisition not very likely. Also the rock-magnetic properties follow closely the local environmental changes suggesting again, an in situ signal (Sier and Dekkers, 2013). Even though the NN2 and Rutten sites are geographically reasonably close (see figure 1) the similarities of the two records is circumstantial evidence at best and alone do not proof an in situ signal of the Rutten core. Fortunately, we have evidence from the Rutten core itself that suggests an in situ palaeomagnetic signal as well. We discarded samples with strong GRM and only used AF quality 1 and 2 samples for our interpretation. Our rock-magnetic results show that the AF quality 2 samples, in which the GRM was corrected for by the per component protocol, mainly have biogenic magnetic minerals (see figure 5) which are formed at the oxic-anoxic interface in aquatic habitats (Bazylinski and Frankel, 2004) and thus represent a near-in-situ signal in these organic-rich environments. While the disregarded samples contain a higher diagenetic contribution which in general causes overprinting of the NRM by later magnetizations with an unknown age (Roberts and Weaver, 2005).

5.2. Duration of the Blake Event

With the Blake Event in Rutten still documented in pollen zone E6, we can derive a new minimum estimate of its duration. However, the position of the upper Blake Event boundary remains elusive as the top part of the last pollen-zone has probably been eroded during a regional erosive phase. The duration of the Blake Event below pollenzone E1, into the Saalian is very limited in NN2 (Sier et al., 2011), estimated to reflect approximately 200-300 years. For our estimate of the Blake Event's duration at Rutten we assume a comparable duration of this pre-Eemian part of the Blake Event. The remaining duration of the Blake Event is closely related to the duration of the Eemian in north-western and central Europe.

The duration of the Eemian has been estimated by Müller (1974) to be ca. 11.000

years. It needs however to be noted that truly counted varves only make up ~6000 years (PAZ E1 to E6) of the ~11,000 year duration (Hahne et al., 1994; Müller, 1974). The remaining ~5000 years estimate is based on extrapolation of inferred sedimentation rates in a (slightly) varying lithology (Müller, 1974). Using this ambiguous estimation of Müller (1974) for the Eemian in north-western Europe, we reach a minimum duration of ~7000 years and a maximum of ~11000 years for the Blake Event at Rutten, since the Blake Event entirely spans the pollen-defined Eemian s.s. (figure 8) A duration of ~11,000 years is conflicting with a recent well-constrained duration estimate of the Blake Event of 6.5 ± 1.3 ka from the Bahama Outer Ridge (Bourne et al., 2012). However, a duration for the Blake Event of about 7000 years would indicate an overestimation of the duration of the Eemian *sensu stricto* of at least a few thousands of years.

5.3. Comparison of the Rutten palaeomagnetic data with other Blake Event records

Only two samples in the Rutten core have a negative inclination for their ChRM directions, of which one has a northerly declination and the other a southerly declination (figure 3, and tables I and II in the SI). Most other samples with excursions directions are based on their declination and a few on very shallow inclinations (see table I and II SI). In an unoriented core these samples would have been difficult to identify as in most other regions across the globe the Blake Event is identified by its clear negative inclinations (e.g. Bourne et al., 2012; Smith and Foster, 1969). It is possible that the lack of negative inclinations is a feature of the Blake Event in north-western and central Europe. Also the ChRM directions of NN2 and Caours (Somme valley, France) were more prominent excursions in declination than in inclination (Sier et al., submitted; Sier et al., 2011).

Some clear similarities and differences can be noted when comparing the Rutten with the NN2 record. Both sites have good pollen preservation (this study, Sier et al., 2011) and both sites show a complete pollen record. The NN2 pollen record, however, is more condensed from pollen zone IVb3 (*sensu* Menke 1984), which is zone PAZ E4b in the terminology of Zagwijn (1961) onward due to a decrease in sedimentation rate (Bakels, 2012; Sier et al., 2011) as a result of a dry phase in the (small) Neumark basin and/or region (Sier and Dekkers, 2013). Both sites also have a detailed palaeomagnetic and rock-magnetic record with registration of the Blake Event. In NN2, while the lower boundary of the Blake Event is well defined on the basis of high quality palaeomagnetic

directions, the upper boundary is defined on the last undisputed high quality excursional direction only. If we exclude lower quality excursional directions, the minimum duration of the Blake Event in NN2 is around 3400 years (Sier et al., 2011).

A study of an unoriented core from Anholt, Denmark in shallow marine Saalian and Eemian sediments showed two consecutive palaeomagnetic samples with negative inclinations interpreted as the Blake Event (Abrahamsen, 1995). Two other samples with negative inclinations were not considered as the Blake Event because they were isolated samples in between normal directions. If these isolated samples were included, the duration of the Blake Event would be close to the duration we found in the Rutten core. Also the position of the Anholt-core Blake Event would be similar with respect to the Eemian and Saalian periods as found in NN2 and Rutten. A recent detailed multidisciplinary study of the Netiesos section (southern Lithuania) identified the Blake Event in combination with the Eemian pollen zonation (Baltrunas et al., 2013). In this study the authors interpret three consecutive fully reversed ChRM directions as the Blake Event. However, throughout the Eemian of the Netiesos section ChRM directions with a south declination and positive inclination are reported (see figure 8 of Baltrunas et al., 2013). According to the definition of Merrill and McFadden (1994) these ChRM directions should be interpreted as excursional. As a consequence the Blake Event of the Netiesos section would span the whole Eemian in that section, similar to our results presented in this study.

5.4. Position of the Blake Event on the MIS curve

The duration of the Eemian and the Blake Event do not affect the observed European north-south delay of the Eemian (as our correlation is based on the lower boundary) and more research is needed to support either one of these hypotheses. A drawback of this longer duration of the Blake Event is that its resolution as chronostratigraphic marker for archaeological correlations is reduced. However, identification of the Blake Event does indicate, indirectly, an Eemian *sensu stricto* age.

The Rutten core appears to offer a near-complete record of the Blake Event. The Blake Event and its position in the Mediterranean record (Tric et al., 1991; Tucholka et al., 1987) furnished the anchoring point for the correlation to the marine record in the Neumark study (Sier et al., 2011). The longer duration of the Blake Event identified in the present study warrants a reconsideration of this correlation. A main concern is that

whereas the observed Blake Event and its position in relation to the sapropel S5 and the Marine Isotope Stages (MIS) (Tucholka et al., 1987) is valid, it is possible that only part of the Blake Event was preserved in those marine settings. For example, the upper portion of the Blake Event may have been lost due to bioturbation or were difficult to identify in the sapropel sediments. The long duration of the Blake Event as inferred from the Rutten core data (and some marine records e.g Bourne et al. (2012)) strengthens the possibility that only part of the Blake Event is recognised in the marine record. If only the top part of the Blake Event has been registered in the Mediterranean deep sea floor, this would have implications for the observed delay of the Eemian between central Europe and southern Europe (see Sier et al., 2011 for details) as it could compensate for (part of) the observed delay. It has to be noted that so far the Mediterranean cores of Tucholka (1987) show no evidence for this to be the case (see also Sier et al., 2011).

A review of the Blake Event literature shows that nearly all publications yield data supporting the onset of the Blake Event after the MIS 5e peak, regardless of its subsequent event duration. In the Yemak plateau (northern Atlantic ocean), the Blake Event starts well after the onset of MIS 5 and its inferred duration is 10 kyr (Nowaczyk et al., 1994). The same applies to marine core A179-4 (Blake Outer Ridge), with an estimated duration of the Blake Event of 7 kyr (Smith and Foster, 1969; Wollin et al., 1971). The Blake Event at the Bermuda Rise has a notably short estimated duration of <1000 years and straddles the MIS 5d-5e boundary (Channell et al., 2012). Another recent study at the Blake-Bahama outer ridge comes with a substantially longer duration estimate of 6.5 ± 1.3 ka, again with the start slightly after the MIS 5e peak (Bourne et al., 2012). In a terrestrial setting the Blake Event was recognised for the first time in a speleothem in Cobre Cave, northern Spain (Osete et al., 2012). Also in this study the position is above the MIS 5e peak. Loess records in China show similar results, Blake Event-like signals are found above the S1-c (S1-3) palaeosol which has been correlated to the MIS5e peak (Fang et al., 1997; Zhu et al., 1994). A similar position was found in the lacustrine sediments of the Zoigê Basin (Eastern Tibetan Plateau) (Hu et al., 1999). In European loess the Blake Event is recorded above the Eemian palaeosol (Reinders and Hambach, 1995). However, the value of these loess records as far as the Blake Event is concerned is somehow questionable, as proper identification of palaeomagnetic “short events” is not straightforward in loessic sediments (Zhao and Roberts, 2010) and they often are not recorded (Parés et al., 2004).

The only exception on the post-MIS 5e plateau position for the Blake Event comes from the study of core MD972151 in the southern South China Sea, where the Blake Event

was identified well before the MIS 5e plateau (Lee et al., 1999; Lee, 1999). The quality of the data seems to be good but this claimed position of the Blake Event is about 11 ka at odds with all other studies (Lee et al., 1999).

Interestingly, during our review of existing literature on the Blake Event we correlated the palaeomagnetic data of core MD95-2042 (Thouveny et al., 2004) to the pollen and $\delta^{18}\text{O}$ curves of that core (Sánchez-Goñi et al., 1999). This correlation (figure 7) shows that also in that core MD95-2042 the Blake Event starts well after the MIS5e peak but also well within vegetation zones correlated to the Eemian, while both in Rutten and in NN2 the Blake Event starts in the latest Saalian. This position of the Blake Event and the Eemian within the MD95-2042 is consistent with a notable lag for the onset of the Eemian in central and north-western Europe as proposed on the basis of the NN2 data (Sier et al., 2011).

The correlation of the Rutten and NN2 data with the MIS curve is presented in figure 8 and visually summarizes large part of this study. It needs to be noted that our observations summarized in this figure are age model independent. This means that

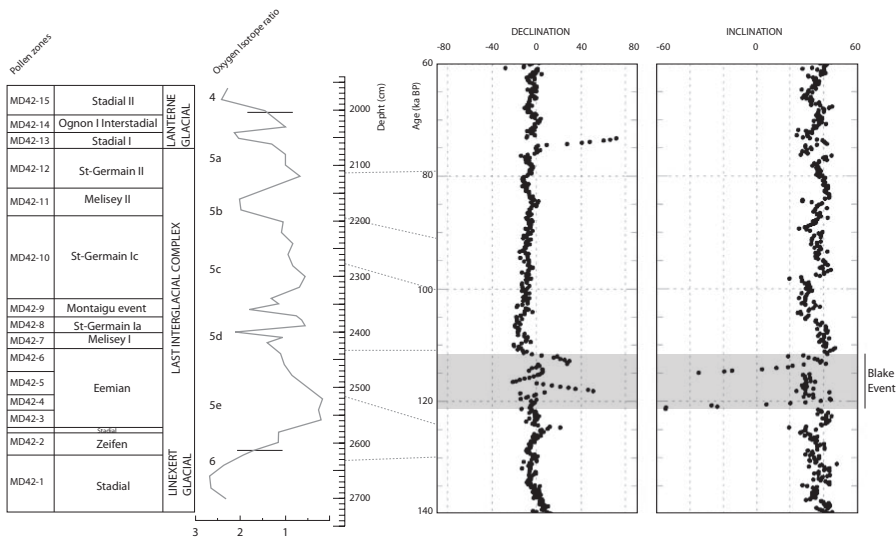


Figure 7. Figure combined and modified from Sánchez-Goñi et al. (1999) and Thouveny et al. (2004). Published data from the MD95-2042 core (south western margin off the Iberian Peninsula). Here, Eemian pollen-zones (Sánchez-Goñi et al., 1999) and the Blake Event (Thouveny et al., 2004) identified in the same core are merged in a single plot. The onset of the Eemian clearly predates the Blake Event.

changes to the ages of the MIS 5e peak or the sapropel S5 in the future do not affect our observations. For this correlation we used the recently published age and duration of sapropel 5. This sapropel S5 is now estimated at 121.4 ka to 129.5 ka (Ziegler et al., 2010). This new age and duration decreases the age of the base of the Eemian (~ 120.5 ka) with 100 years compared to our previous published estimate (Sier et al., 2011). As discussed above, the upper limit of the Eemian is rather poorly defined, which is indicated by the fading of the orange colour in the figure. In figure 8 we can also clearly see the Lower Blake Event boundary is observed after the top of sapropel S5 as documented in the Mediterranean. The same Blake Event boundary is observed below the lower boundary of the Eemian at Rutten and NN2. Combining this data in figure 8 we clearly see that the Eemian *sensu stricto* starts well after the MIS 5e peak.

The timing of the onset of the Eemian in north-western and central Europe indicates a larger than previously appreciated diachronous development of the onset of the Last Interglacial in this part of the world with its long Quaternary research tradition. The Last Interglacial is traditionally regarded as the beginning of the Late Pleistocene, and the onset of the Last Interglacial (Termination II in MIS records) functions as the Middle-Late Pleistocene boundary (Gibbard and Cohen, 2008). Some years back, the Amsterdam Terminal site has been put forward as a candidate Global Stratigraphic Section and Point for the base of the Late Pleistocene (Gibbard, 2003; Gibbard et al., 2008). The proposal in the end has not been ratified and workers are reconsidering whether an adapted proposal should be resubmitted, and then be evaluated against other candidate sites such as along the Taranto coast in the Mediterranean (e.g. Negri et al., 2013). Our new results reduce the suitability of the Eemian type area for global chronostratigraphical correlation of the onset of the last interglacial. The lower boundary of the Blake Event would be a better option due to its global registration and (assumed) global synchronous onset.

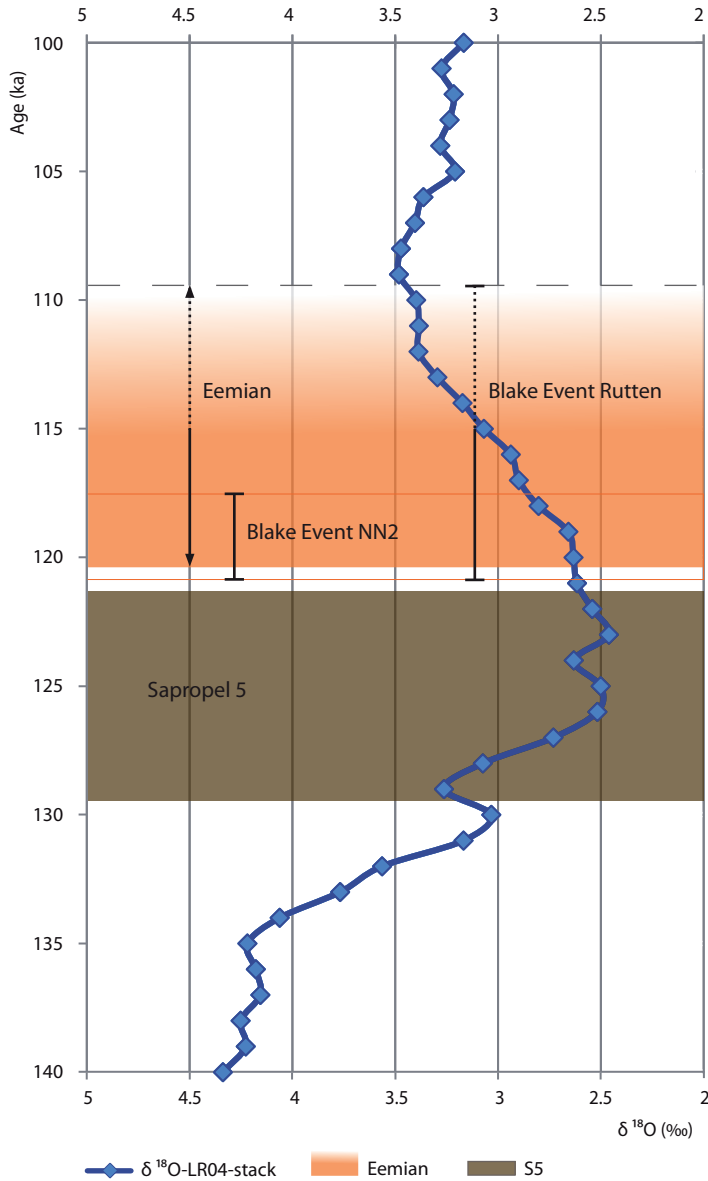


Figure 8.

Stacked $\delta^{18}\text{O}$ -LR04 record (Lisiecki and Raymo, 2005) from 140 to 100 ka (data in stack is from the MD95-2042 core (Sánchez-Goni et al., 1999)), using the Ziegler et al. (2010) time scale, with the positions of sapropel S5, the duration of the Blake Event at NN2 and Ruten sites and the (central and north-western European) Eemian interglacial. The Eemian duration as presented with the orange color, fades from the minimum counted varve duration onward, until the (maximum) duration estimate of Müller (1974).

6. Conclusions

In this study, we performed a detailed analysis of a 25 meter orientated core taken at Rutten, close to the proposed Eemian stage (regional) stratotype, in order to test previous hypotheses regarding the position of the Blake Event within the Eemian pollen sequence of NN2 and its correlation to the marine record, and to better constrain the duration of the Blake Event. Considering the new evidence presented here in combination with the Blake Event literature review, we argue that the Rutten data confirms the hypothesis of Sier et al. 2011 of a delayed north-western and central European onset of the Eemian compared to MIS 5e. The onset of the Eemian in central Europe is comparable to that in north-western Europe. While both Rutten and NN2 give a comparable (latest Saalian, pollen zone LS, immediately pre-Eemian) timing for the onset of the Blake Event, the Rutten core additionally indicates the Blake Event to stretch into the final phase of the Eemian (pollen zone E6).

Comparison to sites in southern Europe and across the rest of the world demonstrate a time lag of ca. 4 to 5 ka between the onset of the palynological Eemian in the original type area with respect to the onset of the Eemian in southern Iberia (core MD95-2042), and a possibly up to 10-ka long delay with the onset of MIS 5e. This implies a (very) late, but rapid northwest European vegetation development from essentially arctic to fully interglacial in the last part of MIS 5e.

In addition, our study supports a long duration of the Blake Event (e.g. Bourne et al., 2012), with a minimum duration of 7 ka. This minimum duration matches Müller (1974)'s warve counted duration of the Eemian *sensu stricto*. It also matches durations as estimated in palaeomagnetic studies of the event in marine and terrestrial records outside Europe. The unanticipated long duration of the Blake Event makes it a less detailed geochronological marker. As a consequence, when the Blake Event is discovered in an archaeological context, the most we could infer is that the site is of Eemian *sensu stricto* age.

Finally, the palaeomagnetic data of the Rutten core suggests a large variability in the behavior of the Earth's magnetic field. In north-western and central Europe excursions with positive inclinations seem to dominate the palaeomagnetic directions, contrary to what is found in other regions of the world, where fully reversed directions are predominantly found.

References

- Abrahamsen, N. (1995). Paleomagnetism of Quaternary sediments from Anholt, Denmark: Onset of the Blake Event and Eemk. *bulletin of the geological society of denmark* 42, 96-104.
- Bakels, C. (2012). Non-pollen palynomorphs from the Eemian pool Neumark-Nord 2: Determining water quality and the source of high pollen-percentages of herbaceous taxa. *Review of Palaeobotany and Palynology* 186, 58-61.
- Baltrunas, V., Seiriene, V., Molodkov, A., Zinkute, R., Katinas, V., Karmaza, B., Kisieliene, D., Petrosius, R., Taraskevcius, R., Piliciauskas, G., Schmolcke, U., and Heinrich, D. (2013). Depositional environment and climate changes during the late Pleistocene as recorded by the Netiesos section in southern Lithuania. *Quaternary International* 292, 136-149.
- Bazylinski, D. A., and Frankel, R. B. (2004). Magnetosome formation in prokaryotes. *Nature Reviews Microbiology* 2, 217-230.
- Beets, C. J., and Beets, D. J. (2003). A high resolution stable isotope record of the penultimate deglaciation in lake sediments below the city of Amsterdam, The Netherlands. *Quaternary Science Reviews* 22, 195-207.
- Beets, D. J., Beets, C. J., and Cleveringa, P. (2006). Age and climate of the late Saalian and early Eemian in the type-area, Amsterdam basin, The Netherlands. *Quaternary Science Reviews* 25, 876-885.
- Bosch, J. H. A. (2000). Standaard Boor Beschrijvingsmethode - versie 5.1. In "TNO-rapport: NITG 00-141-A." pp. 106.
- Bourne, M., Mac Niocaill, C., Thomas, A. L., Knudsen, M. F., and Henderson, G. M. (2012). Rapid directional changes associated with a 6.5 kyr-long Blake geomagnetic excursion at the Blake-Bahama Outer Ridge. *Earth and Planetary Science Letters* 333-334, 21-34.
- Busschers, F. S., and Bakker, M. A. J. (2009). "De Bosatlas van Ondergronds Nederlands." Noordhoff Uitgevers BV.
- Busschers, F. S., Kasse, C., van Balen, R. T., Vandenberghe, J., Cohen, K. M., Weerts, H. J. T., Wallinga, J., Johns, C., Cleveringa, P., and Bunnik, F. P. M. (2007). Late Pleistocene evolution of the Rhine-Meuse system in the southern North Sea basin: imprints of climate change, sea-level oscillation and glacio-isostasy. *Quaternary Science Reviews* 26, 3216-3248.

- Busschers, F. S., Van Balen, R. T., Cohen, K. M., Kasse, C., Weerts, H. J. T., Wallinga, J., and Bunnik, F. P. M. (2008). Response of the Rhine-Meuse fluvial system to Saalian ice-sheet dynamics. *Boreas* 37, 377-398.
- Buylaert, J.-P., Jain, M., Murray, A. S., Thomsen, K. J., Thiel, C., and Sohbati, R. (2012). A robust feldspar luminescence dating method for Middle and Late Pleistocene sediments. *Boreas* 41, 435-451.
- Cleveringa, P., Meijer, T., van Leeuwen, R. J. W., de Wolf, H., Pouwer, R., Lissenberg, T., and Burger, A. W. (2000). The Eemian stratotype locality at Amersfoort in the central Netherlands: re-evaluation of old and new data. *Netherlands Journal of Geosciences* 79, 197-216.
- Channell, J. E. T., Hodell, D. A., and Curtis, J. H. (2012). ODP Site 1063 (Bermuda Rise) revisited: oxygen isotopes, excursions and paleointensity in the Brunhes Chron. *Geochemistry Geophysics Geosystems* 13, Q02001.
- Dankers, P. H. M., and Zijderveld, J. D. A. (1981). Alternating field demagnetization of rocks, and the problem of gyromagnetic remanence. *Earth and Planetary Science Letters* 53, 89-92.
- Egli, R. (2004). Characterization of individual rock magnetic components by analysis of remanence curves. 3. Bacterial magnetite and natural processes in lakes. *Physics and Chemistry of the Earth, Parts A/B/C* 29, 869-884.
- Egli, R., Chen, A. P., Winklhofer, M., Kodama, K. P., and Horng, C.-S. (2010). Detection of noninteracting single domain particles using first-order reversal curve diagrams. *Geochemistry Geophysics Geosystems* 11, Q01Z11.
- Fang, X., Li, J., Van der Voo, R., Mac Niocaill, C., Dai, X., Kemp, R. A., Derbyshire, E., Cao, J., Wang, J., and Wang, G. (1997). A record of the Blake Event during the last interglacial paleosol in the western Loess Plateau of China. *Earth and Planetary Science Letters* 146, 73-82.
- Gibbard, P. L. (2003). Definition of the Middle-Upper Pleistocene boundary. *Global and Planetary Change* 36, 201-208.
- Gibbard, P. L., and Cohen, K. M. (2008). Global chronostratigraphical correlation table for the last 2.7 million years. *Episodes* 31, 243-247.
- Gibbard, P. L., Cohen, K. M., and Ogg, J. G. (2008). Quaternary Period. In "The concise Geologic Time Scale." (J. G. Ogg, G. Ogg, and F. M. Gradstein, Eds.), pp. 178, Cambridge.
- Grimm, E. C. (1987). CONISS: A FORTRAN 77 program for stratigraphically constrained cluster analysis by the method of incremental sum of squares. *Computer and Geosciences* 13, 13-35.

- Gunnink, J. L., Maljers, D., Gessel, S. F. v., Menkovic, A., and Hummelman, H. J. (2013). Digital Geological Model (DGM): a 3D raster model of the subsurface of the Netherlands. *Netherlands Journal of Geosciences* 92, 33-6.
- Guyodo, Y., and Valet, J.-P. (1996). Relative variations in geomagnetic intensity from sedimentary records: the past 200,000 years. *Earth and Planetary Science Letters* 143, 23-36.
- Hahne, J., Kemle, S., Merkt, J., and Meyer, K.-D. (1994). Eem-, weichsel- und saalezeitliche Ablagerungen der Bohrung "Quakenbrück GE2. *Geologisches Jahrbuch A* 134, 9-69.
- Harting, P. (1874). De bodem van het Eemdal. *Verslagen en Verhandelingen Koninklijke Academie van Wetenschappen*, 282-290.
- Heslop, D., McIntosh, G., and Dekkers, M. J. (2004). Using time- and temperature-dependent Preisach models to investigate the limitations of modelling isothermal remanent magnetization acquisition curves with cumulative log Gaussian functions. *Geophysical Journal International* 157, 55-63.
- Hu, S., Appel, E., Wang, S., Wu, J., Xue, B., Wang, Y., Qian, J., and Xiang, L. (1999). A preliminary magnetic study on lacustrine sediments from Zoigã Basin, eastern Tibetan Plateau, China: Magnetostratigraphy and environmental implications. *Physics and Chemistry of the Earth, Part A: Solid Earth and Geodesy* 24, 811-816.
- Jessen, K., and Milthers, V. (1928). Stratigraphical and paleontological studies of interglacial freshwater deposits in Jutland and Northwest Germany. *Danmarks geologiske undersøgelse* 48.
- Kars, R. H., Busschers, F. S., and Wallinga, J. (2012). Validating post IR-IRSL dating on K-feldspars through comparison with quartz OSL ages. *Quaternary Geochronology* 12, 74-86.
- Kirschvink, J. L. (1980). The least-square line and plane and the analysis of paleomagnetic data. *Geophysical Journal of the Royal Astronomical Society* 62, 699-718.
- Kruiver, P. P., Dekkers, M. J., and Heslop, D. (2001). Quantification of magnetic coercivity components by the analysis of acquisition curves of isothermal remanent magnetisation. *Earth and Planetary Science Letters* 189, 269-276.
- Lee, M. Y., Wei, K. Y., and Chen, Y. G. (1999). High resolution oxygen isotope stratigraphy for the last 150,000 years in the southern South China Sea: Core MD972151. *TAO* 10, 239-254.

- Lee, T. Q. (1999). Last 160 ka paleomagnetic directional secular variation record from core MD972151, southwestern South China Sea. *TAO* 10, 255-264.
- Lisiecki, L. E., and Raymo, M. E. (2005). A Pliocene-Pleistocene stack of 57 globally distributed benthic $\delta^{18}O$ records. *Paleoceanography* 20, PA1003.
- Menke, B., and Tynni, R. (1984). Das Eeminterglazial und das Weichselfrühglazial von Rederstall/Dittmarschen und ihre Bedeutung für die mitteleuropäische Jungpleistozängliederung. *Geologisches Jahrbuch* A76, 3-120.
- Merrill, R. T., and McFadden, P. L. (1994). Geomagnetic field stability: Reversal events and excursions. *Earth and Planetary Science Letters* 121, 57-69.
- Meynadier, L., Valet, J.-P., Weeks, R., Shackleton, N. J., and Hagee, V. L. (1992). Relative geomagnetic intensity of the field during the last 140 ka. *Earth and Planetary Science Letters* 114, 39-57.
- Müller, H. (1974). Pollenanalytische Untersuchungen und Jahresschitzenzählungen an der eem-zeitlichen Kieselgur von Bispingen/Luhe. *Geologisches Jahrbuch* A21, 149-169.
- Negri, A., Amorosi, A., Antonioli, F., Bertini, A., Mastronuzzi, G., Marabini, S., Montagna, P., Rossi, V., Scarponi, D., Taviani, M., Vigliotti, L., and Battista Vai, G. (2013). Searching for a stratotype section for the Late Pleistocene: news from the Fronte section (Taranto area). . In "Ciências da Terra Volume Speciale VII - STRATI 2013 1st International Conference on Stratigraphy." Lisboa.
- Newell, A. J. (2005). A high-precision model of first-order reversal curve (FORC) functions for single-domain ferromagnets with uniaxial anisotropy. *Geochemistry Geophysics Geosystems* 6, Q05010.
- Nowaczyk, N. R., Frederichs, T. W., Eisenhauer, A., and Gard, G. (1994). Magnetostratigraphic Data From Late Quaternary Sediments From the Yermak Plateau, Arctic Ocean: Evidence For Four Geomagnetic Polarity Events Within the Last 170 Ka of the Brunhes Chron. *Geophysical Journal International* 117, 453-471.
- Osete, M.-L., Martín-Chivelet, J., Rossi, C., Edwards, R. L., Egli, R., Muñoz-García, M. B., Wang, X., Pavón-Carrasco, F. J., and Heller, F. (2012). The Blake geomagnetic excursion recorded in a radiometrically dated speleothem. *Earth and Planetary Science Letters* 353-354, 173-181.
- Parés, J. M., Van der Voo, R., and Yan, M. (2004). After the Dust Settles: Why Is the Blake Event Imperfectly Recored in Chinese Loess? In "Timescales of the Paleomagnetic Field " (J. E. T. Channell, D. V. Kent, W. Lowrie, and J. G. Meert, Eds.).

- Pike, C. R., Roberts, A. P., and Verosub, K. L. (1999). Characterizing interactions in fine magnetic particle systems using first order reversal curves. *Journal of Applied Physics* 85, 6660-6667.
- Reinders, J., and Hambach, U. (1995). A geomagnetic event recorded in loess deposits of the Tonchesberg (Germany): identification of the Blake magnetic polarity episode. *Geophysical Journal International* 122, 407-418.
- Roberts, A. P., Chang, L., Rowan, C. J., Horng, C.-S., and Florindo, F. (2011). Magnetic properties of sedimentary greigite (Fe₃S₄): An update. *Reviews of Geophysics* 49, RG1002.
- Roberts, A. P., Liu, Q., Rowan, C. J., Chang, L., Carvallo, C., Torrent, J., and Horng, C. (2006). Characterization of hematite(a-Fe₂O₃), goethite (a-FeOOH), greigite (Fe₃S₄), and pyrrhotite (Fe₇S₈) using first-order reversal curve diagrams. *Journal of Geophysical Research* 111, B12S35.
- Roberts, A. P., Pike, C. R., and Verosub, K. L. (2000). First-order reversal curve diagrams: A new tool for characterizing the magnetic properties of natural samples. *J. Geophys. Res.* 105, 28461-28475.
- Roberts, A. P., and Weaver, R. (2005). Multiple mechanisms of remagnetization involving sedimentary greigite (Fe₃S₄). *Earth and Planetary Science Letters* 231, 263-277.
- Rowan, C. J., and Roberts, A. P. (2006). Magnetite dissolution, diachronous greigite formation, and secondary magnetizations from pyrite oxidation: Unravelling complex magnetizations in Neogene marine sediments from New Zealand. *Earth and Planetary Science Letters* 241, 119-137.
- Sagnotti, L., Cascella, A., Ciaranfi, N., Macri, P., Maiorano, P., Marino, M., and Taddeucci, J. (2010). Rock magnetism and palaeomagnetism of the Montalbano Jonico section (Italy): evidence for late diagenetic growth of greigite and implications for magnetostratigraphy. *Geophysical Journal International* 180, 1049-1066.
- Sánchez-Goñi, M. F., Eynaud, F., Turon, J. L., and Shackleton, N. J. (1999). High resolution palynological record off the Iberian margin: direct land-sea correlation for the Last Interglacial complex. *Earth and Planetary Science Letters* 171, 123-137.
- Shackleton, N. J., Chapman, M., Sánchez-Goñi, M. F., Pailler, D., and Lancelot, Y. (2002). The Classic Marine Isotope Substage 5e. *Quaternary Research* 58, 14-16.
- Shackleton, N. J., Sánchez-Goñi, M. F., Pailler, D., and Lancelot, Y. (2003). Marine Isotope Substage 5e and the Eemian Interglacial. *Global and Planetary Change* 36, 151-155.

- Sier, M. J., and Dekkers, M. J. (2013). Magnetic property analysis as palaeoenvironmental proxy: a case study of the Last Interglacial Middle Palaeolithic site at Neumark-Nord 2 (Germany). In "Multidisciplinary Studies of the Middle Palaeolithic Record from Neumark-Nord (Germany)" (S. Gaudzinski-Windheuser, and W. Roebroeks, Eds.), Saxony-Anhalt, Germany.
- Sier, M. J., Parés, J. M., Antoine, P., Locht, J. L., Dekkers, M. J., and Roebroeks, W. (submitted). The Blake Event recorded at the Eemian archaeological site of Caours, France. *Quaternary International*.
- Sier, M. J., Roebroeks, W., Bakels, C. C., Dekkers, M. J., Brühl, E., De Loecker, D., Gaudzinski-Windheuser, S., Hesse, N., Jagich, A., Kindler, L., Kuijper, W. J., Laurat, T., Mücher, H. J., Penkman, K. E. H., Richter, D., and van Hinsbergen, D. J. J. (2011). Direct terrestrial-marine correlation demonstrates surprisingly late onset of the last interglacial in central Europe. *Quaternary Research* 75, 213-218.
- Smith, J. D., and Foster, J. H. (1969). Geomagnetic Reversal in Brunhes Normal Polarity Epoch. *Science* 163, 565-567.
- Stephenson, A. (1993). Three-Axis Static Alternating Field Demagnetization of Rocks and the Identification of Natural Remanent Magnetization, Gyroremanent Magnetization, and Anisotropy. *Journal of Geophysical Research* 98, 373-381.
- Tauxe, L., Mullender, T. A. T., and Pick, T. (1996). Potbellies, wasp-waists, and superparamagnetism in magnetic hysteresis. *Journal of Geophysical Research: Solid Earth* 101, 571-583.
- Thiel, C., Buylaert, J.-P., Murray, A., Terhorst, B., Hofer, I., Tsukamoto, S., and Frechen, M. (2011). Luminescence dating of the Stratzing loess profile (Austria) - Testing the potential of an elevated temperature post-IR IRSL protocol. *Quaternary International* 234, 23-31.
- Thouveny, N., Carcaillet, J., Moreno, E., Leduc, G., and Nérini, D. (2004). Geomagnetic moment variation and paleomagnetic excursions since 400 kyr BP: a stacked record from sedimentary sequences of the Portuguese margin. *Earth and Planetary Science Letters* 219, 377-396.
- Tric, E., Laj, C., Valet, J., Tucholka, P., Paterne, M., and Guichard, F. (1991). The Blake geomagnetic event: transition geometry, dynamical characteristics and geomagnetic significance. *Earth and Planetary Science Letters* 102, 1-13.
- Tucholka, P., Fontugne, M., Guichard, F., and Paterne, M. (1987). The Blake magnetic polarity episode in cores from the Mediterranean Sea. *Earth and Planetary Science Letters* 86, 320-326.

- Valet, J.-P., Meynadier, L., and Guyodo, Y. (2005). Geomagnetic dipole strength and reversal rate over the past two million years. *Nature* 435, 802-805.
- Van den Berg, M. W., and Beets, D. J. (1987). Saalian glacial deposits and morphology in The Netherlands. . In "INQUA Symposium on the genesis and lithology of glacial deposits." (J. J. M. Van de Meer, Ed.), pp. 235-251. Balkema, Amsterdam.
- van Leeuwen, R. J. W., Beets, D. J., Bosch, J. H. A., Burger, A. W., Cleveringa, P., van Harten, D., Waldemar Hergreen, G. F., Kruk, R. W., Langereis, C. G., Meijer, T., Pouwer, R., and de Wolf, H. (2000). Stratigraphy and integrated facies analysis of the Saalian and Eemian sediments in the Amsterdam-Terminal borehole, the Netherlands. *Netherlands Journal of Geosciences* 79, 161-196.
- Vasiliev, I., Dekkers, M. J., Krijgsman, W., Franke, C., Langereis, C. G., and Mullender, T. A. T. (2007). Early diagenetic greigite as a recorder of the palaeomagnetic signal in Miocene–Pliocene sedimentary rocks of the Carpathian foredeep (Romania). *Geophysical Journal International* 171, 613-629.
- Vasiliev, I., Franke, C., Meeldijk, J. D., Dekkers, M. J., Langereis, C. G., and Krijgsman, W. (2008). Putative greigite magnetofossils from the Pliocene epoch. *Nature Geoscience* 1, 782-786.
- Wintle, A. G., and Murray, A. S. (2006). A review of quartz optically stimulated luminescence characteristics and their relevance in single-aliquot regeneration dating protocols. *Radiation Measurements* 41, 369-391.
- Wollin, G., Ericson, D. B., Ryan, W. B. F., and Foster, J. H. (1971). Magnetism of the earth and climatic changes. *Earth and Planetary Science Letters* 12, 175-183.
- Zagwijn, W. H. (1961). Vegetation, climate and radiocarbon datings in the late Pleistocene of the Netherlands: I. Eemian and Early Weichselian, *Nieuwe Serie. Mededelingen van de Geologische Stichting* 14, 15-45.
- Zagwijn, W. H. (1996). An Analysis of Eemian Climate in Western and Central Europe. *Quaternary Reviews* 15, 451-469.
- Zhao, X., and Roberts, A. P. (2010). How does Chinese loess become magnetized? *Earth and Planetary Science Letters* 292, 112-122.
- Zhu, R. X., Zhou, L. P., Laj, C., Mazaud, A., and Ding, Z. L. (1994). The Blake Geomagnetic Polarity Episode Recorded in Chinese Loess. *Geophysical Research Letters* 21, 697-700.
- Ziegler, M., Tuenter, E., and Lourens, L. J. (2010). The precession phase of the boreal summer monsoon as viewed from the eastern Mediterranean (ODP Site 968). *Quaternary Science Reviews* 29, 1481-1490.

SUPPLEMENTARY INFORMATION RUTTEN

Description of core Rutten Gemaalweg – B15F1501

The Rutten core (B15F1501) is positioned in a fluvial dominated setting throughout the entire period from the late Middle Pleistocene (after ice-sheet disintegration) to the Late Pleistocene. In particular, this pertains to the Last Interglacial, when the core was positioned at the northern fringes of the lower Rhine delta. The continuous presence of fluvial activity is reflected in the encountered sediments, both in lithology, facies and depositional style, and are visualized in the sedimentary log of figure 3 (main text) and described below.

The bottom end of the Rutten record (-28.6 m to -27 m NAP) is characterized by fine-grained (~130 μm) sands, containing brittle clay fragments, most likely deposited in a lacustrine environment at the Late Saalian. Upwards (-27 m to -22.6 m NAP), Late Saalian gravelly, coarse-grained (300-450 μm), cross-bedded fluvial sands are present. Just before the onset of the pollen-defined Eemian the depositional environment changed from channel belt to floodbasin at a depth of -22.6 m NAP, probably due to changes in river-style and/or -regime. The sediments found in this floodplain environment mainly consists of layered peats and clayey-gyttja, containing some fresh-water mollusk fragments. At a depth of -19.2 m NAP a minor shift towards more clayey, fine still layered floodplain deposit is marked by a ca. 10 cm thick fine-grained sand layer. The environment here changed to a more estuarine marginal setting related to the maximum marine transgression in the area during the Last Interglacial sea-level high-stand. Up to a depth of -15.8 m NAP this marine-influenced interval contains wood and plant fragments. Here, the deteriorating climatic conditions at the end of the Eemian are reflected in the lithological record. The thin medium-fine sand units indicate fluvial activity of smaller local (non-Rhine) rivers, while the alternation of peats, clay and incorporation of (local) heathland organic debris (SI figure 2), indicates deposition in a floodplain environment up to a depth of -12.7 m NAP. The top of this deposit is eroded by fluvial Rhine activity during presumably the Pleniglacial (Hiatus mentioned in main text), this resulted in a coarse-grained sandy unit up to -9.6 m NAP. This unit is overlain by local fluvial and eolian fine-grained sandy deposits of Late Pleniglacial – Late Glacial age, often showing cryoturbated sedimentary structures. From a depth of -5.2 m NAP up to the surface,

Holocene lagoonal and fluvio-deltaic deposits cap the sedimentary sequence, with alternating peats, and clay and fine sand deposits.

Detailed description of Core B15F1501

Description (translated from Dutch) according to TNO-NITG standards (Bosch, 2000). Top of core is at -3.62 meters below Dutch Ordnance Datum (NAP) and description goes from top to bottom.

Top	Bottom	Description
0.00	0.14	No sample
0.14	0.28	Sand, weakly silty, moderately humic, dark-brown-grey, 10YR4/2, carbonate-rich, Sand: extremely fine, Organic material: a little wood, Shells: traces of shells, traces of shell remains, ploughed soil, disturbed
0.28	0.56	Loam, weakly sandy, moderately humic, light-brown, 10YR6/3, carbonate-rich, a little mica, a few iron-rich layers, a little iron-oxide, bioturbation, many detritus-layers, a few sand-layers <i>Sub-layer: with a few sand-layers, very thin, weakly humic, light-grey, carbonate-rich, Organic material: traces of plant-remains, traces of iron-oxide</i>
0.56	0.74	Loam, weakly sandy, moderately humic, grey, 2.5Y6/1, no carbonates, a little mica, a few iron rich layers, a little iron-oxide, bioturbation, a few detritus-layers, a few peat-layers, a few sand-layers <i>Sub-layer: with a few sand-layers, very thin, weakly humic, light-grey, carbonate-rich, Organic material: traces of plant-remains, traces of iron-oxide</i>
0.74	1.00	Sand, weakly silty, moderately humic, yellow-brown, 10YR5/4, no carbonates, Sand: moderately coarse, moderately poorly-graded, moderately rounded, no multi-colored material, Organic material: traces of wood, roots, traces of loam-lenses
1.00	1.06	No sample, disturbed
1.06	1.15	Sand, weakly silty, moderately humic, yellow-brown, 10YR5/4, no carbonates, Sand: moderately coarse, moderately poorly-graded, moderately rounded, no multi-colored material, a few detritus-layers
1.15	1.35	Peat, poor-in-minerals, dark-brown, 10YR3/3, no carbonates, Organic material: Sphagnum
1.35	1.43	Peat, poor-in-minerals, dark-brown, 10YR3/3, no carbonates, Organic material: Sphagnum, traces of sand-inclusions, a little layered
1.43	1.50	Sand, weakly silty, weakly humic, brown-grey, 2.5Y5/2, no carbonates, Sand: moderately fine, rounded, no multi-colored material, Organic material: many plant-remains, a few root-remains, base sharp, at the top silty
1.50	1.75	Sand, weakly silty, weakly humic, light-grey, 2.5Y7/2, no carbonates, Sand: moderately fine, rounded, Organic material: a few plant-remains, traces of dark grains, many sand-inclusions, weakly layered <i>Sub-layer: with traces of sand-layers, very thin, light-brown</i>
1.75	1.92	Sand, weakly silty, weakly humic, light-grey, 2.5Y7/2, no carbonates, Sand: moderately fine, rounded, Organic material: a few plant-remains, traces of dark grains, a few granules, many sand-inclusions, weakly layered
1.92	2.10	No sample
2.10	2.17	No sample, disturbed
2.17	2.60	Sand, weakly silty, weakly humic, olive-grey, 5Y5/2, no carbonates, Sand: moderately fine, rounded, Organic material: a few plant-remains, a few root-remains, traces of dark grains, weakly layered
2.60	2.98	Sand, weakly silty, weakly humic, light-grey, 2.5Y7/2, no carbonates, Sand: very fine, rounded, Organic material: traces of root-remains, traces of dark grains, weakly layered <i>Sub-layer: with a few sand-layers, very thin, light-grey</i>
2.98	3.06	No sample
3.06	3.10	No sample, disturbed
3.10	3.47	Sand, weakly silty, weakly humic, light-grey, 2.5Y7/2, no carbonates, Sand: very fine, rounded, traces of dark grains, weakly layered <i>Sub-layer: with a few sand-layers, very thin, light-grey</i>
3.47	3.73	Sand, weakly silty, weakly humic, light-grey, 2.5Y7/2, no carbonates, Sand: very fine, rounded, traces of dark grains, a little granules, weakly layered <i>Sub-layer: with a few sand-layers, very thin, light-grey</i>
3.73	3.82	No sample
3.82	3.97	No sample, disturbed
3.97	4.38	Sand, weakly silty, weakly humic, light-grey, 2.5Y7/2, no carbonates, Sand: very fine, rounded, traces of dark grains, a little granules, weakly layered, burrows <i>Sub-layer: with a few sand-layers, very thin, light-grey</i>
4.38	4.54	No sample

4.54	5.03	Sand, weakly silty, weakly humic, light-grey, 2.5Y7/2, no carbonates, Sand: very fine, rounded, traces of dark grains, a little granules, weakly layered, burrows
5.03	5.34	Sand, weakly silty, weakly humic, light-grey, 2.5Y7/2, no carbonates, Sand: very fine, rounded, traces of dark grains, a little granules, traces of loam-inclusions, weakly layered, burrows
5.34	5.39	Loam, strongly sandy, strongly humic, dark-brown-grey, 2.5Y3/2, no carbonates
5.39	5.62	No sample
5.62	6.01	Loam, strongly sandy, strongly humic, dark-brown-grey, 2.5Y3/2, no carbonates, a few dark-brownish spots, traces of mica, a few sand-inclusions <i>Sub-layer: with a few sand-layers, very thin, light-grey</i>
6.01	6.18	Sand, weakly silty, weakly gravelly, light-grey, 2.5Y7/2, no carbonates, Sand: moderately coarse, moderately rounded, no multi-colored material, Gravel: traces of moderately coarse gravel, traces of Quartzite, a little layered, a few loam-layers
6.18	6.33	Sand, weakly silty, weakly gravelly, light-grey, 2.5Y7/2, no carbonates, Sand: moderately coarse, moderately rounded, no multi-colored material, Gravel: traces of moderately coarse gravel, traces of Quartzite
6.33	6.40	No sample
6.40	6.62	No sample, disturbed
6.62	7.11	Sand, weakly silty, light-brown-grey, 2.5Y6/2, no carbonates, Sand: moderately coarse, moderately rounded, no multi-colored material, weakly layered <i>Sub-layer: with a few sand-layers, very thin, weakly silty, weakly humic, light-grey, no carbonates, traces of mica, traces of dark grains</i>
7.11	7.21	Sand, weakly silty, weakly humic, light-grey, 2.5Y7/2, no carbonates, Sand: moderately fine, rounded, traces of dark grains
7.21	7.26	Loam, strongly sandy, strongly humic, dark-brown-grey, 2.5Y3/2, no carbonates, traces of mica, a little layered
7.26	7.36	Sand, weakly silty, light-brown-grey, 10YR6/2, no carbonates, Sand: very coarse, very poorly-graded, no multi-colored material, a few detritus-layers, at the base humic
7.36	7.39	Loam, strongly sandy, strongly humic, dark-olive-brown, 2.5Y3/3, no carbonates, traces of peat-fragments
7.39	7.40	No sample
7.40	7.45	No sample, disturbed
7.45	7.55	Loam, strongly sandy, strongly humic, dark-olive-brown, 2.5Y3/3, carbonate-rich, traces of mica
7.55	8.00	Gyttja, poor-in-minerals, brown-grey, 2.5Y5/2, carbonate-rich, Organic material: traces of wood, a little mica, a little calcareous gyttja, strongly layered, a few peat-layers
8.00	8.06	Sand, weakly silty, weakly humic, brown-grey, 2.5Y5/2, carbonate-poor, Sand: very coarse, no multi-colored material
8.06	8.20	Sand weakly silty, moderately humic, dark-grey-brown, 2.5Y3/2, no carbonates, Sand: moderately coarse, moderately poorly-graded, moderately rounded, no multi-colored material, a little layered, a few loam-layers, traces of peat-layers
8.20	8.27	Sand, weakly silty, weakly humic, light-brown-grey, 2.5Y6/2, no carbonates, Sand: moderately coarse, moderately poorly-graded, no multi-colored material, weakly layered
8.27	8.30	No sample
8.30	8.32	No sample, disturbed
8.32	8.55	Sand, weakly silty, moderately humic, dark-grey-brown, 2.5Y3/2, no carbonates, Sand: moderately coarse, moderately poorly-graded, moderately rounded, no multi-colored material, a few granules, weakly layered
8.55	8.67	Sand, weakly silty, strongly humic, dark-grey-brown, 10YR3/2, no carbonates, Sand: moderately coarse, Moderately poorly-graded, moderately rounded, no multi-colored material, a little layered, a few loam-layers
8.67	9.10	Sand weakly silty, weakly humic, light-brown-grey, 10YR6/2, no carbonates, Sand: moderately coarse moderately rounded, no multi-colored material, traces of mica, bioturbation, strongly layered, many loam-layers <i>Sub-layer: with many loam-layers, very thin, olive-grey</i>
9.10	9.20	No sample
9.20	9.39	No sample, disturbed
9.39	9.63	Loam, strongly sandy, weakly gravelly, weakly humic, dark-grey, 5Y4/1, carbonate-rich, Gravel: extremely much moderately coarse gravel, a little clear quartz, sturdy, traces of mica, traces of iron-oxide, traces of vivianite
9.63	10.04	Clay, weakly sandy, weakly humic, grey, 2.5Y5/1, carbonate-rich, moderately sturdy, traces of mica, a little vivianite
10.04	10.09	Sand, weakly silty, weakly humic, grey-brown, 2.5Y5/2, carbonate-rich, Sand: moderately fine, moderately rounded, no multi-colored material, traces of mica
10.09	10.16	Loam, strongly sandy, strongly humic, dark-grey-brown, 2.5Y3/2, carbonate-rich, Organic material: traces of plant-remains, a little mica, traces of peat-fragments, a few sand-inclusions
10.16	10.20	No sample
10.20	10.25	No sample, disturbed
10.25	10.31	Loam, strongly sandy, strongly humic, dark-grey-brown, 2.5Y4/2, carbonate-rich, Organic material: traces of plant-remains, a little mica, a few sand-inclusions
10.31	10.36	Peat, poor-in-minerals, dark-grey-brown, 10YR3/3, no carbonates, Organic material: a lot of wood
10.36	10.45	Peat, poor-in-minerals, dark-grey-brown, 10YR3/3, no carbonates, Organic material: a lot of wood, traces of sand-inclusions, at the base clayey
10.45	10.50	Clay, moderately silty, moderately humic, grey, 2.5Y5/1, no carbonates, Organic material: many plant-remains
10.50	10.59	Peat, poor-in-minerals, dark-grey-brown, 10YR3/3, no carbonates, Organic material: a lot of wood
10.59	10.67	Gyttja, poor-in-minerals, dark-grey, 2.5Y3/1, carbonate-rich, Organic material: many plant-remains, a little mica, no carbonates in top

10.67	10.98	Gyttja, poor-in-minerals, dark-olive-grey, 5Y3/2, carbonate-rich, Organic material: a few plant-remains, traces of vivianite
10.98	11.00	No sample
11.00	11.04	No sample, disturbed
11.04	11.34	Sand, weakly silty, moderately humic, olive-grey, 5Y4/2, carbonate-rich, Sand: moderately coarse, very poorly-graded, traces of multi-colored material, a lot of mica, traces of clay fragments, a few loam-fragments
11.34	11.66	Loam, strongly sandy, strongly humic, dark-olive-grey, 5Y3/2, carbonate-rich, moderately sturdy, a lot of mica
11.66	11.80	Loam, strongly sandy, strongly humic, olive-grey, 5Y4/2, carbonate-rich, moderately sturdy, a little mica
11.80	11.91	Sand, moderately silty, weakly humic, grey, 5Y5/1, carbonate-rich, Sand: very fine, Organic material: a few plant-remains, a lot of mica, a few clay-lenses, a few loam-lenses
11.91	11.95	Sand, weakly silty, weakly humic, grey-brown, 2.5Y5/2, carbonate-rich, Sand: moderately coarse, moderately rounded, traces of multi-colored material
11.95	12.00	No sample
12.00	12.02	No sample, disturbed
12.02	12.22	Sand, weakly silty, weakly humic, grey-brown, 2.5Y5/2, carbonate-rich, Sand: moderately coarse, Moderately rounded, traces of multi-colored material, traces of mica, a few loam-inclusions
12.22	12.95	Clay, strongly silty, weakly humic, grey, 5Y5/1, carbonate-poor, Organic material: a few plant-remains, traces of wood, moderately sturdy, traces of mica, traces of iron-oxide, a little vivianite
12.95	13.00	No sample
13.00	13.33	Clay, strongly silty, moderately humic, grey, 5Y5/1, carbonate-poor, Organic material: many plant-remains, traces of wood, moderately sturdy, traces of mica
13.33	13.80	Clay, strongly silty, strongly humic, dark-grey, 2.5Y4/1, no carbonates, Organic material: many plant-remains, a lot of wood, moderately sturdy, traces of mica, locally peaty
13.80	13.95	Clay, strongly silty, weakly humic, grey, 5Y5/1, no carbonates, Organic material: a few plant-remains, moderately sturdy, traces of mica
13.95	14.00	No sample
14.00	14.45	Clay, strongly silty, strongly humic, dark-grey, 2.5Y4/1, no carbonates, Organic material: many plant-remains, a little wood, moderately sturdy, traces of mica, locally peaty layered
14.45	14.90	Clay, strongly silty, moderately humic, grey, 5Y6/1, carbonate-rich, Organic material: many plant-remains, traces of wood, moderately sturdy, strongly layered with plant-remains <i>Sub-layer: with a few clay-layers, very thin, strongly humic, dark-grey, carbonate-rich</i>
14.90	14.94	Gyttja, poor-in-minerals, dark-grey, 5Y3/1, carbonate-rich, moderately weak, traces of mica
14.94	15.00	No sample
15.00	15.18	Gyttja, poor-in-minerals, dark-grey, 5Y3/1, carbonate-rich, a lot of yellow calcareous gyttja spots, moderately weak, a little mica
15.18	15.48	Clay, strongly silty, strongly humic, dark-grey, 2.5Y4/1, carbonate-rich, Organic material: many plant-remains, a little wood, a little mica, gyttja-like
15.48	15.51	Loam, strongly sandy, strongly humic, dark-grey, 5Y3/1, carbonate-rich, many yellow spots, moderately weak, a little mica
15.51	15.60	Sand, weakly silty, moderately humic, light-brown-grey, 2.5Y6/2, carbonate-rich, Sand: very fine, moderately poorly-graded, no multi-colored material, Organic material: many plant-remains, a little wood, a little mica
15.60	15.94	Clay, strongly silty, moderately humic, grey, 5Y5/1, carbonate-rich, a few black spots, moderately weak, Shells: traces of shells, a little mica, a little layered, traces of detritus-layers, gyttja-like
15.94	16.00	No sample
16.00	16.04	Clay, strongly silty, moderately humic, grey, 5Y5/1, carbonate-rich, a few black spots, moderately weak, Shells: traces of shells, a little mica, a little layered, traces of detritus-layers, gyttja-like
16.04	16.22	Gyttja, poor-in-minerals, olive-grey, 5Y4/2, carbonate-rich, Shells: Sh.perc.: 3, traces of shells, a lot of shell-grit, a little mica
16.22	16.74	Gyttja, poor-in-minerals, olive-grey, 5Y4/2, carbonate-rich, a few black spots, Shells: Sh.perc.: 2, traces of shells, traces of complete shells, a lot of shell-grit, a few freshwater- and terrestrial-shells, a little mica, many clay-inclusion, traces of detritus-layers
16.74	16.94	Gyttja, poor-in-minerals, olive-grey, 5Y4/2, carbonate-rich, Shells: Sh.perc.: 3, traces of shells, a lot of shell-grit, a little mica, traces of loam-inclusions, a little layered
16.94	17.00	No sample
17.00	17.59	Gyttja, poor-in-minerals, olive-grey, 5Y4/2, carbonate-rich, Organic material: traces of wood, Shells: Sh.perc.: 3, traces of shells, a lot of shell-grit, a little mica, traces of vivianite, traces of peat-fragments at the base
17.59	17.64	Peat, poor-in-minerals, dark-brown-grey, 10YR3/2, carbonate-rich, Organic material: strongly amorphic, Shells: traces of shells, a few shell remains, weakly layered, gyttja-like
17.64	17.67	Peat, poor-in-minerals, dark-brown, 10YR 2/2, carbonate-rich, Organic material: strongly amorphic, Shells: traces of shells, traces of shell-grit, sharp base
17.67	17.72	Gyttja, poor-in-minerals, olive-grey, 5Y4/2, carbonate-rich, Organic material: traces of wood, Shells: Sh.perc.: 3, traces of shells, a lot of shell-grit, a little mica
17.72	17.76	Peat, poor-in-minerals, dark-brown, 5Y 2/2, carbonate-rich, Organic material: strongly amorphic, Shells: traces of shells, traces of shell remains, gyttja-like
17.76	17.94	Gyttja, poor-in-minerals, olive-grey, 5Y4/2, carbonate-rich, Organic material: traces of plant-remains, a little mica, traces of peat-fragments, possibly calcareous gyttja
17.94	18.00	No sample
18.00	18.17	No sample, disturbed
18.17	18.52	Peat, poor-in-minerals, dark-brown, 10YR3/3, carbonate-rich, Organic material: woodpeat, a lot of wood, a lot of calcareous gyttja calcareous gyttja, strongly layered, many tiny calcareous gyttja layers
---	---	---

18.52	18.63	Calcareous gyttja, grey-brown, 10YR5/2, carbonate-rich, Organic material: a few plant-remains, traces of mica, a lot of calcareous gyttja
18.63	18.80	Gyttja, poor-in-minerals, olive-grey, 5Y4/2, carbonate-rich, Organic material: traces of plant-remains, Shells: traces of shells, traces of shell remains, traces of mica
18.80	18.94	Peat, poor-in-minerals, dark-brown, 10YR3/3, carbonate-rich, Organic material: strongly amorphous, Shells: traces of shells, traces of shell remains
18.94	19.16	Gyttja, poor-in-minerals, dark-brown, 10YR3/3, no carbonates, a few yellow spots, a little mica, a few sand-inclusions
19.16	19.29	Sand, weakly silty, weakly humic, light-brown-grey, 10YR6/2, no carbonates, Sand: very coarse, moderately poorly-graded, moderately rounded, no multi-colored material, many gyttja-layers
19.29	19.38	Sand moderately silty, weakly humic, brown, 10YR5/3, no carbonates, Sand: very fine, moderately well graded, moderately rounded, no multi-colored material, a little iron-oxide, many gyttja-layers
19.38	20.08	Sand, weakly silty, moderately humic, light-brown, 10YR6/3, no carbonates, Sand: very coarse, moderately rounded, no multi-colored material, traces of mica, a few peat-fragments, traces of peat-layers, humic at the top
20.08	20.61	Sand, weakly silty, weakly gravelly, weakly humic, grey, 2.5Y5/1, no carbonates, Sand: extremely coarse, very poorly-graded, moderately rounded, no multi-colored material, Gravel: extremely much fine gravel, a few clear quartz, traces of Quartzite, traces of white quartz, many layered wood-fragments and peat-fragments at the base <i>Sub-layer: with a few very thin sand-layers</i>
20.61	20.64	Gyttja, poor-in-minerals, brown, 10YR4/3, no carbonates, a few yellow spots, Organic material: a little wood, a little iron-oxide, a little layered
20.64	20.68	Sand, weakly silty, moderately humic, brown, 10YR5/3, no carbonates, Sand: very coarse, very poorly-graded, no multi-colored material, a little iron-oxide
20.68	20.83	Gyttja, poor-in-minerals, brown, 10YR4/3, no carbonates, a few yellow spots, Organic material: traces of plant-remains, a little iron-oxide, strongly layered <i>Sub-layer: with a few very thin sand-layers, light-brown, traces of iron-oxide</i>
20.83	21.03	Gyttja, poor-in-minerals, brown, 10YR4/3, no carbonates, a few yellow spots, Organic material: traces of plant-remains, a little iron-oxide, black and a little layered
21.03	22.00	Sand, weakly silty, weakly gravelly, light-brown-grey, 10YR6/2, no carbonates, Sand: very coarse, very poorly-graded, no multi-colored material, Gravel: traces of moderately coarse gravel, really a lot of moderately coarse gravel, traces of granules, a few clear quartz, traces of Quartzite, Organic material: traces of plant-remains, one gyttja-fragment, one gyttja-layer at the top
22.00	22.10	No sample
22.10	23.00	Sand, weakly silty, weakly gravelly, light-grey, 2.5Y7/1, no carbonates, Sand: very coarse, moderately rounded, traces of multi-colored material, Gravel: much fine gravel, traces of clear quartz, traces of Quartzite, traces of mica, a few loam-fragments
23.00	23.16	No sample
23.16	23.39	No sample, disturbed
23.39	23.47	Sand, weakly silty, light-grey, 5Y7/1, no carbonates, Sand: very fine, moderately rounded, traces of multi-colored material, a little mica, many clay-fragments in layers
23.47	23.63	Clay, strongly silty, grey, 2.5Y5/1, no carbonates, a little mica, many clay-fragments, many sand-inclusions, a lot of detritus at the base, clay consisting of fragments with sand in between <i>Sub-layer: with many sand-layers, very thin, weakly silty, light-grey, a little mica</i>
23.63	23.97	Sand, weakly silty, light-grey, 5Y7/1, no carbonates, Sand: very fine, moderately rounded, traces of multi-colored material, a little mica, a few edgy - not rounded clay-fragments
23.97	24.03	No sample
24.03	24.22	No sample, disturbed
24.22	24.75	Sand, weakly silty, light-grey, 5Y7/1, no carbonates, Sand: very fine, moderately rounded, traces of multi-colored material, a little mica, a lot edgy - not rounded clay-fragments
24.75	24.97	Sand, weakly silty, grey, 2.5Y6/1, no carbonates, Sand: extremely fine, moderately well-graded, moderately rounded, no multi-colored material, a little mica, a few detritus-layers
24.97	25.00	No sample

Table I. Paleomagnetic results of thermal demagnetization

ID#	Level	Dec. (°)	Inc. (°)	MAD	Q	Tinf (°C)	Tsup (°C)	Dir.	VGP latitude
RG001	-28.26	189.9	21.0	8.1	2	280	330	forced	-25.75
RG002	-27.99	207.6	13.6	5.8	2	280	330	forced	-25.85
RG003	-27.54	188.5	1.8	4.9	3	280	330	forced	-35.81
RG004	-27.43	190.8	7.2	3.5	2	280	330	forced	-32.84
RG005	-27.34	188.3	7.3	3.5	3	280	330	forced	-33.09
RG006	-27.28	192.4	1.2	3.7	3	280	330	forced	-35.58
RG007	-24.52	74.3	-11.4	6.0	GC	240	310	-	
RG008	-24.42	65.2	-10.9	2.2	GC	240	310	-	
RG009	-24.36	194.5	21.5	9.9	2	280	330	forced	-24.84
RG010	-24.31	208.3	23.1	8.8	2	280	330	forced	-20.75
RG011	-23.56	170.0	42.7	25.2	3	280	330	forced	-11.93
RG012	-23.49	112.0	52.9	3.9	1	150	330	forced	14.51
RG013	-23.45	111.7	57.5	5.5	1	150	330	forced	18.43
RG014	-23.38	33.2	4.8	2.8	1	150	330	forced	32.59
RG015	-23.29	45.5	66.7	4.8	1	150	330	forced	61.66
RG016	-23.26	301.7	-43.5	19.1	GC	150	330	-	
RG017	-23.19	ND							
RG018	-22.53	ND							
RG019	-22.44	143.7	59.4	10.1	3	150	330	forced	8.19
RG020	-22.39	173.3	25.4	9.0	2	280	330	forced	-23.58
RG021	-22.32	173.9	26.4	9.5	3	280	330	forced	-23.04
RG022	-22.28	159.9	38.8	12.7	3	280	340	forced	-13.26
RG023	-22.20	171.8	34.7	14.6	2	300	380	forced	-17.74
RG024	-22.16	171.1	42.4	11.8	2	300	380	forced	-12.26
RG025	-22.09	ND							
RG026	-21.96	ND							
RG027	-21.91	ND							
RG028	-21.53	ND							
RG029	-21.43	ND							
RG030	-21.32	99.6	-9.6	11.0	GC	180	310	-	
RG031	-21.23	132.2	45.2	13.0	3	280	45	forced	-0.25
RG032	-21.12	42.8	76.7	1.9	1	150	300	forced	65.48
RG033	-21.02	185.0	55.3	12.3	3	280	340	forced	-1.24

RG034	-20.92	195.3	50.2	13.4	4	280	340	forced	-5.16
RG035	-20.82	174.3	66.5	8.9	2	280	330	forced	11.92
RG036	-20.72	154.3	70.5	12.0	2	280	350	forced	19.60
RG037	-20.55	196.6	53.2	10.2	2	280	330	forced	-2.22
RG038	-20.45	230.6	79.6	14.1	2	280	350	forced	38.00
RG039	-20.36	36.7	79.9	1.8	2	210	340	forced	65.94
RG040	-20.26	32.4	74.0	8.2	2	180	340	forced	70.91
RG041	-20.16	189.0	47.2	14.7	2	280	340	forced	-8.44
RG042	-20.06	206.4	54.8	16.1	3	280	340	forced	1.09
RG043	-19.96	194.9	70.8	15.3	3	280	330	forced	18.66
RG044	-19.86	228.3	75.0	13.2	3	300	330	forced	30.82
RG045	-19.76	256.1	83.0	7.7	3	280	340	forced	47.65
RG046	-19.66	332.3	84.7	5.2	3	300	330	forced	61.76
RG047	-19.51	44.2	56.9	3.0	1	180	340	forced	55.96
RG048	-19.40	121.9	76.6	7.7	2	280	340	forced	35.58
RG049	-19.29	184.7	23.9	4.6	2	280	330	forced	-24.57
RG050	-19.19	ND							
RG051	-19.09	201.1	7.0	13.9	2	280	330	forced	-30.93
RG052	-18.99	99.4	-40.6	5.4	GC	150	300	-	
RG053	-18.89	ND							
RG054	-18.80	ND							
RG055	-18.70	155.0	31.9	15.9	3	280	330	forced	-16.63
RG056	-18.50	349.5	70.3	6.2	2	150	320	forced	83.58
RG057	-18.41	192.6	32.0	20.2	3	280	320	forced	-18.99
RG058	-18.32	220.2	25.7	11.7	2	280	320	forced	-15.21
RG059	-18.23	169.5	61.2	12.1	2	280	320	forced	5.53
RG060	-18.15	194.3	68.9	10.0	2	280	320	forced	15.84
RG061	-18.03	194.5	24.9	14.2	2	280	320	forced	-22.94
RG062	-17.92	ND							
RG063	-17.83	215.5	69.8	21.5	4	280	320	forced	20.49
RG064	-17.73	352.0	67.3	9.9	2	150	310	forced	84.32
RG065	-17.46	186.1	33.5	10.8	3	280	320	forced	-18.68
RG066	-17.37	202.0	33.5	17.3	4	300	340	forced	-16.36
RG067	-17.28	186.1	13.6	10.6	2	280	340	forced	-30.06
RG068	-17.19	185.6	14.4	13.1	2	280	340	forced	-29.68
RG069	-17.09	178.3	27.0	13.7	2	280	340	forced	-22.87

RG070	-16.98	139.2	59.8	11.3	2	280	330	forced	9.91
RG071	-16.86	167.7	47.6	10.0	2	280	330	forced	-7.78
RG072	-16.73	99.6	63.8	13.0	2	280	400	forced	29.81
RG073	-16.49	201.2	23.0	13.0	2	280	340	forced	-22.69
RG074	-16.35	219.8	18.3	13.0	2	280	340	forced	-19.16
RG075	-16.20	198.3	26.9	10.5	2	280	350	forced	-21.12
RG076	-16.07	201.5	38.3	15.9	2	280	350	forced	-13.32
RG077	-15.95	220.2	38.4	12.3	3	280	340	forced	-7.79
RG078	-15.85	224.6	49.1	8.8	1	280	420	forced	1.47
RG079	-15.70	26.6	74.9	12.2	2	320	480	forced	73.29
RG080	-15.48	194.9	55.9	7.2	2	280	350	forced	0.20
RG081	-15.37	192.1	32.1	7.4	2	280	350	forced	-18.99
RG082	-15.23	206.7	45.1	10.0	2	280	340	forced	-7.20
RG083	-15.10	193.0	36.8	7.4	2	280	380	forced	-15.81
RG084	-14.98	159.1	57.5	16.9	3	280	340	forced	2.74
RG085	-14.87	178.2	17.2	13.0	2	280	340	forced	-28.37
RG086	-14.74	220.0	-56.6	8.7	2	280	340	forced	-58.24
RG087	-14.51	ND							
RG088	-14.41	ND							
RG089	-14.33	124.5	17.5	11.9	2	280	340	forced	-12.36
RG090	-13.62	200.8	26.5	14.2	3	280	320	forced	-20.82
RG091	-13.49	173.5	28.6	14.8	2	280	330	forced	-21.70
RG092	-24.37	245.8	51.6	3.7	1	180	300	forced	12.45
RG093	-24.28	ND							
RG094	-22.92	239.2	34.3	6.7	1	180	330	forced	-2.05
RG095	-22.72	276.1	36.6	4.7	1	180	350	forced	19.73
RG096	-22.38	272.7	48.0	13.7	4	260	310	forced	24.31
RG097	-13.35	37.4	50.7	13.2	1	240	600	forced	55.59
RG098	-13.28	139.5	73.0	8.6	2	240	450	forced	26.10
RG099	-13.21	52.2	71.3	10.5	3	240	340	forced	60.16
RG100	-13.14	35.7	26.5	14.0	3	240	350	forced	41.99
RG101	-13.06	85.9	42.9	10.6	3	240	510	forced	22.02
RG102	-12.58	ND							
RG103	-12.39	ND							
RG104	-12.26	ND							
RG105	-12.21	ND							

RG106	-11.74	334.6	71.3	5.3	2	240	310	forced	74.97
RG107	-11.54	ND							
RG090	-13.62	200.8	26.5	14.2	3	280	320	forced	-20.82
RG091	-13.49	173.5	28.6	14.8	2	280	330	forced	-21.70
RG092	-24.37	245.8	51.6	3.7	1	180	300	forced	12.45
RG093	-24.28	ND							
RG094	-22.92	239.2	34.3	6.7	1	180	330	forced	-2.05
RG095	-22.72	276.1	36.6	4.7	1	180	350	forced	19.73
RG096	-22.38	272.7	48.0	13.7	4	260	310	forced	24.31
RG097	-13.35	37.4	50.7	13.2	1	240	600	forced	55.59
RG098	-13.28	139.5	73.0	8.6	2	240	450	forced	26.10
RG099	-13.21	52.2	71.3	10.5	3	240	340	forced	60.16
RG100	-13.14	35.7	26.5	14.0	3	240	350	forced	41.99
RG101	-13.06	85.9	42.9	10.6	3	240	510	forced	22.02
RG102	-12.58	ND							
RG103	-12.39	ND							
RG104	-12.26	ND							
RG105	-12.21	ND							
RG106	-11.74	334.6	71.3	5.3	2	240	310	forced	74.97
RG107	-11.54	ND							
RG108	-11.35	0.2	71.3	7.6	2	240	350	forced	86.91
RG109	-11.29	313.5	51.4	4.0	1	240	380	forced	50.85
RG110	-11.17	317.6	60.5	7.0	2	240	400	forced	59.54
RG111	-11.09	353.5	24.4	8.9	2	240	350	forced	49.63
RG112	-10.63	ND							
RG113	-10.78	ND							
RG114	-10.38	ND							
RG115	-9.68	46.7	52.5	8.7	3	240	300	forced	51.46
RG116	-9.38	56.2	77.7	17.1	3	240	350	forced	59.85
RG117	-4.20	73.4	59.3	4.8	2	240	350	forced	40.18
RG118	-4.00	ND							

Table 1:

TH palaeomagnetic results. ID#: sample identification; Level: stratigraphic level in meters below Dutch Ordnance Datum (NAP); Dec: Declination of ChRM direction; Inc: Inclination of ChRM direction; MAD: Maximum Angular Deviation; Q: quality of ChRM direction; Tinf: lowest temperature step of ChRM in °C; Tsup: highest temperature step of ChRM in °C; Dir: ChRM forced or free. ND = Non determined; GC = Great Circle.

TH steps: 20, 90 (2 hours in order to dry the sample), 150, 180, 210, 240, 260, 280, 300, 310, 320, 330, 340, 350, 380, 400, 420, 450, 480, 510, 540, 580, 600°C

Table II. Paleomagnetic results of AF demagnetization

ID#	Level	Dec. (°)	Inc . (°)	MAD	Q	Afinf (mT)	Afsup (mT)	Dir.	VGP latitude
RG201	-28.4	ND	GRM	-	-	-	-	-	
RG202	-28.12	ND	GRM	-	-	-	-	-	
RG203	-27.76	ND	GRM	-	-	-	-	-	
RG204	-27.48	ND	GRM	-	-	-	-	-	
RG205	-27.17	ND	GRM	-	-	-	-	-	
RG206	-26.99	ND	GRM	-	-	-	-	-	
RG207	-26.28	ND	GRM	-	-	-	-	-	
RG208	-25.21	ND	GRM	-	-	-	-	-	
RG209	-24.78	25.0	-55.8	8.7	1	30	80	free	-1.77
RG210	-24.56	3.3	60.3	3.5	2				78.21
RG211	-24.47	340.7	56.4	2.1	2	30	60	free	69.20
RG212	-24.39	ND	GRM	-	-	-	-	-	
RG213	-24.25	351.1	66.2	6.4	2	15	45	free	82.96
RG214	-23.89	ND	GRM	-	-	-	-	-	
RG215	-23.7	ND	GRM	-	-	-	-	-	
RG216	-23.52	ND	GRM	-	-	-	-	-	
RG217	-23.41	ND	GRM	-	-	-	-	-	
RG218	-23.33	ND	GRM	-	-	-	-	-	
RG219	-23.22	ND	GRM	-	-	-	-	-	
RG220	-22.48	118.6	64.2	4.4	2	15	50	free	21.82
RG221	-22.36	127.9	71.9	7.0	2	15	50	free	27.63
RG222	-22.25	ND	GRM	-	-	-	-	-	
RG223	-22.02	157.8	63.4	6.6	2	20	50	free	9.61
RG224	-21.85	ND	GRM	-	-	-	-	-	
RG225	-21.64	ND	GRM	-	-	-	-	-	
RG226	-21.47	38.6	68.2	3.4	2	20	50	free	66.52
RG227	-21.38	23.4	68.1	2.7	2	15	50	free	75.57
RG228	-21.27	44.9	69.6	1.5	2	10	50	free	63.48
RG229	-21.17	28.5	63.2	0.7	2	10	50	free	69.71
RG230	-21.07	37.9	72.3	1.7	2	10	50	free	68.15
RG231	-20.97	40.5	75.6	0.9	2	10	50	free	66.73
RG232	-20.87	50.5	79.2	1.7	2	15	50	free	61.81
RG233	-20.77	18.7	79.4	2.4	2	10	50	free	71.23
RG234	-20.67	46.0	72.3	3.8	2	10	50	free	63.82
RG235	-20.5	ND	GRM	-	-	-	-	-	
RG236	-20.41	344.6	72.8	3.8	2	10	50	free	79.77

RG237	-20.3	359.8	69.6	1.7	2	10	60	free	89.45
RG238	-20.2	4.3	66.7	2.0	2	10	50	free	85.53
RG239	-20.1	0.5	71.3	1.7	2	10	50	free	86.90
RG240	-20	8.1	71.4	3.1	2	10	50	free	84.29
RG241	-19.9	ND	GRM	-	-	-	-	-	
RG242	-19.8	321.5	75.3	5.6	2	10	50	free	67.71
RG243	-19.71	299.0	77.7	7.2	2	10	50	free	57.93
RG244	-19.62	328.3	70.3	9.8	2	10	50	free	71.28
RG245	-19.45	ND	GRM	-	-	-	-	-	
RG246	-19.34	ND	GRM	-	-	-	-	-	
RG247	-19.24	ND	GRM	-	-	-	-	-	
RG248	-19.14	ND	GRM	-	-	-	-	-	
RG249	-19.04	ND	GRM	-	-	-	-	-	
RG250	-18.94	ND	GRM	-	-	-	-	-	
RG251	-18.84	58.8	71.4	2.8	2	10	50	free	56.69
RG252	-18.74	96.3	52.0	6.5	1	15	50	free	21.94
RG253	-18.64	131.2	70.5	2.2	2	15	50	free	24.84
RG254	-18.54	341.5	51.1	3.2	2	10	45	free	65.07
RG255	-18.46	358.2	54.5	1.7	2	15	50	free	72.17
RG256	-18.37	12.6	56.1	1.6	2	10	40	free	71.58
RG257	-18.27	13.0	56.4	1.3	2	10	40	free	71.73
RG258	-18.19	12.8	50.1	1.6	2	10	45	free	66.16
RG259	-18.1	10.8	63.0	1.4	2	10	35	free	79.03
RG260	-17.99	ND	GRM	-	-	-	-	-	
RG261	-17.88	358.9	47.3	5.4	2	15	45	free	65.62
RG262	-17.79	ND	GRM	-	-	-	-	-	
RG263	-17.68	2.8	59.8	1.7	2	10	50	free	77.70
RG264	-17.51	37.0	57.8	0.9	2	10	50	free	60.86
RG265	-17.42	43.4	47.6	1.6	2	10	50	free	50.16
RG266	-17.32	41.0	63.6	0.7	2	10	50	free	62.47
RG267	-17.23	43.6	59.3	4.8	2	10	50	free	57.99
RG268	-17.14	46.1	57.9	1.8	2	10	50	free	55.52
RG269	-17.03	67.3	67.8	0.8	2	10	50	free	49.88
RG270	-16.92	46.8	64.8	0.8	2	10	70	free	59.74
RG271	-16.8	36.0	67.2	1.6	2	10	70	free	67.59
RG272	-16.73	41.8	65.7	1.6	2	10	70	free	63.28
RG273	-16.54	278.5	60.3	4.9	2	15	70	free	36.32
RG274	-16.41	260.2	53.4	3.6	2	15	70	free	21.08
RG275	-16.28	273.0	67.6	6.6	2	10	70	free	39.41

RG276	-16.13	245.2	71.8	15.3	3	15	50	free	31.76
RG277	-16.01	277.6	69.0	1.5	2	10	60	free	42.89
RG278	-15.89	268.2	50.2	5.3	2	15	50	free	23.18
RG279	-15.78	ND	GRM	-	-	-	-	-	
RG280	-15.53	ND	GRM	-	-	-	-	-	
RG281	-15.42	ND	GRM	-	-	-	-	-	
RG282	-15.31	ND	GRM	-	-	-	-	-	
RG283	-15.17	ND	GRM	-	-	-	-	-	
RG284	-15.04	ND	GRM	-	-	-	-	-	
RG285	-14.92	ND	GRM	-	-	-	-	-	
RG286	-14.81	ND	GRM	-	-	-	-	-	
RG287	-14.55	183.0	59.3	4.4	2	10	50	free	2.95
RG288	-14.46	1298.9	75.1	2.0	2	10	60	free	28.84
RG289	-14.37	228.8	71.9	1.7	2	15	50	free	26.68
RG300	-13.18	355.8	66.7	8.4	2	15	35	free	85.57
RG301	-13.1	30.3	65.5	10.0	1	10	45	free	70.11
RG302	-12.54	219.5	68.1	24.9	3	20	45	free	19.19
RG303	-12.35	193.7	69.3	6.1	1	10	50	free	16.35
RG304	-11.8	339.2	66.1	9.0	2	20	45	free	76.16
RG305	-11.59	317.1	71.0	1.2	2	10	70	free	65.13
RG306	-11.52	313.0	69.2	1.5	2	15	70	free	62.10
RG307	-11.46	319.9	68.3	1.1	2	10	60	free	65.68
RG308	-11.39	318.0	67.3	2.1	2	20	70	free	64.06
RG309	-11.33	322.6	66.7	1.2	2	10	60	free	66.49
RG310	-11.26	323.7	69.0	0.7	1	15	80	free	68.21
RG311	-11.2	333.6	64.9	0.7	2	10	60	free	72.09
RG312	-11.14	313.8	75.2	1.6	1	20	60	free	64.14
RG313	-24.32	ND	GRM	-	-	-	-	-	
RG314	-23.82	ND	GRM	-	-	-	-	-	
RG315	-23.43	ND	GRM	-	-	-	-	-	
RG316	-22.88	ND	GRM	-	-	-	-	-	
RG317	-22.83	ND	GRM	-	-	-	-	-	
RG318	-22.79	ND	GRM	-	-	-	-	-	
RG319	-22.76	299.4	60.4	2.6	2	10	40	free	48.51
RG320	-22.66	304.9	75.3	2.2	2	20	50	free	60.01
RG321	-22.61	282.8	58.9	2.8	2	10	45	free	37.70
RG322	-22.56	278.6	46.0	3.6	2	10	45	free	26.52
RG323	-22.49	281.6	44.7	3.5	2	10	45	free	27.53
RG324	-22.42	271.0	52.2	2.6	2	10	50	free	26.14

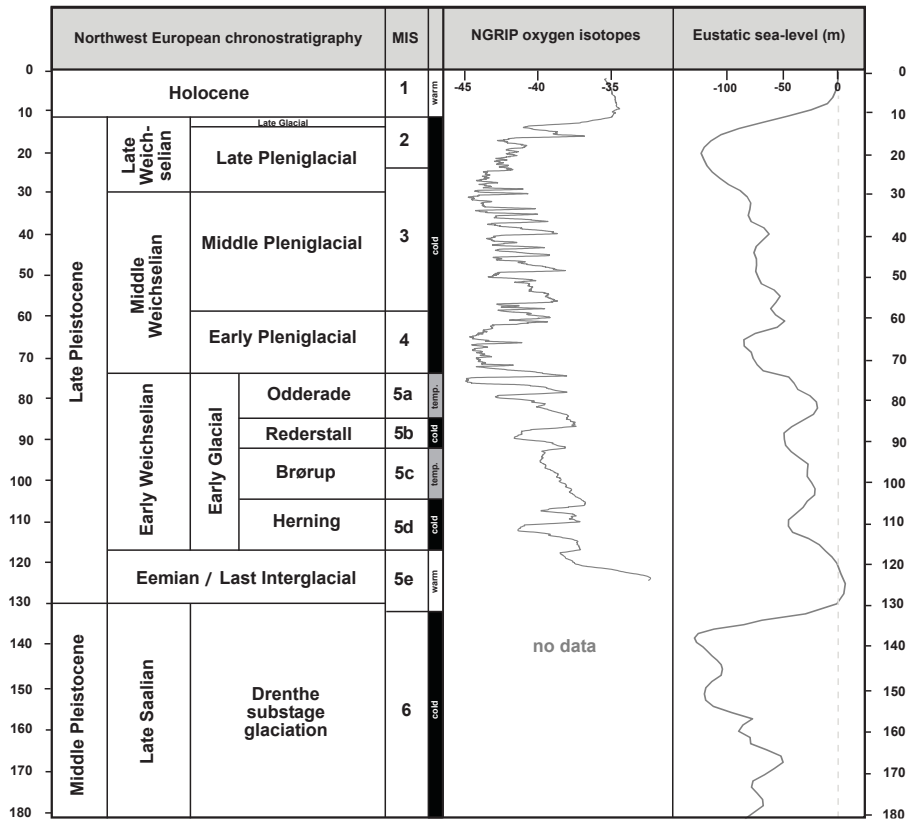
RG325	-22.33	285.2	53.0	4.3	2	10	50	free	34.93
RG326	-22.28	283.7	58.9	1.6	2	10	50	free	38.22
RG327	-22.23	273.6	67.1	2.3	2	10	50	free	39.28
RG328	-10.74	354.2	50.9	12.4	2	25	50	free	68.37
RG329	-10.6	ND	GRM	-	-	-	-	-	
RG330	-10.29	19.1	73.2	9.5	2	20	45	free	77.75
RG331	-9.64	ND	Noise	-	-	-	-	-	
RG332	-9.34	ND	Noise	-	-	-	-	-	
RG333	-4.17	73.7	53.2	8.4	1	25	70	free	35.71
RG334	-3.97	49.4	19.4	13.0	2	40	60	free	31.70

Table II:

AF palaeomagnetic results. ID#: sample identification; Level: stratigraphic level in meters below Dutch Ordnance Datum (NAP); Dec: Declination of ChRM direction; Inc: Inclination of ChRM direction; MAD: Maximum Angular Deviation; Q: quality of ChRM direction; AFin: lowest AF step of ChRM in mT; AFsup: highest AF step of ChRM in mT; Dir: ChRM forced or free.

ND = Non determined; GRM = GyroRemanent Magnetization.

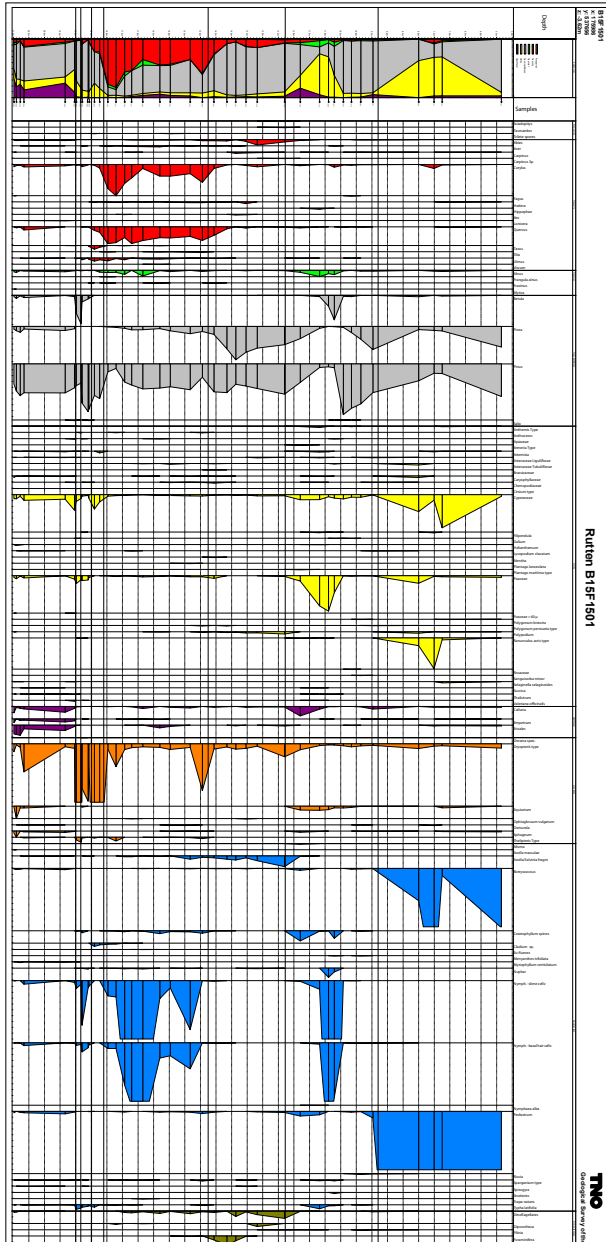
AF Steps: 0, 5, 10, 15, 20, 25, 30, 35, 40, 45, 50, 60, 70, 80, 90 and 100 mT.



SI Figure 1:

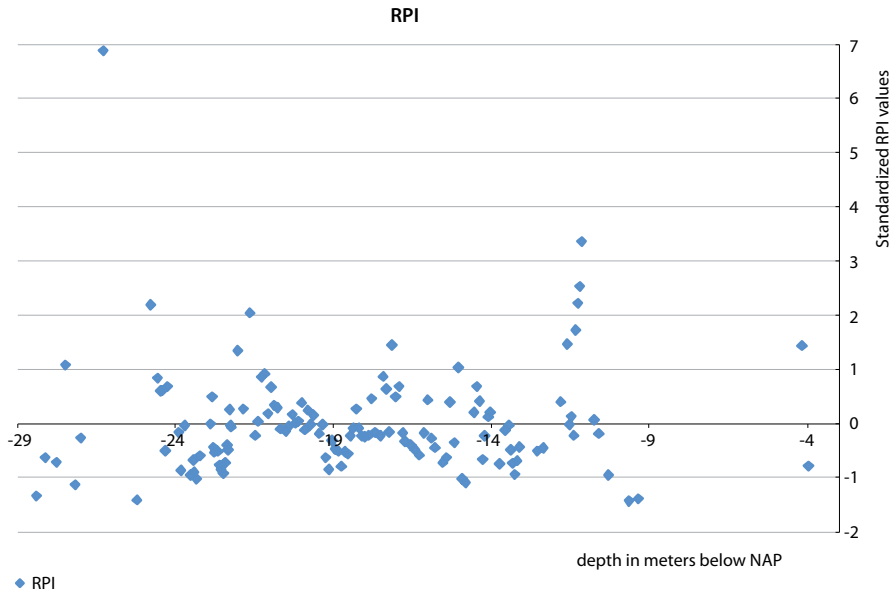
Chronostratigraphic overview of the last 180.000 years after Busschers et al. (2007).

Compilation of northwest European Late Pleistocene climatic history, (mondial) eustatic sea-level position and glaciation history. Chronostratigraphic framework following Vandenberghe (1985) and Van Huissteden and Kasse (2001). The Marine Isotope Record after Bassinot et al. (1994). NGRIP Oxygen Isotope Data were taken from NGRIP (2004). Weichselian Pleniglacial mean annual temperature following Vandenberghe et al. (2004) (note that this curve should be read in 14C years). The coleopteran and palaeobotanical based temperature reconstruction derived from the French La Grande Pile crater lake record (Guiot et al., 1989). Eustatic sea-level record derived from North Atlantic and Equatorial Pacific benthic Oxygen Isotope Data (Waelbroeck et al., 2002). Glacial history of Scandinavia based on Mangerud (2004). Error envelopes in all records were taken from their original sources.



SI Figure 2:

Pollen diagram of Rutten B15F1501 core. Eemian PAZ according to Zagwijn (1961). Hiatus (mentioned in main text) is situated between PAZ E6 and PAZ W



SI Figure 3:

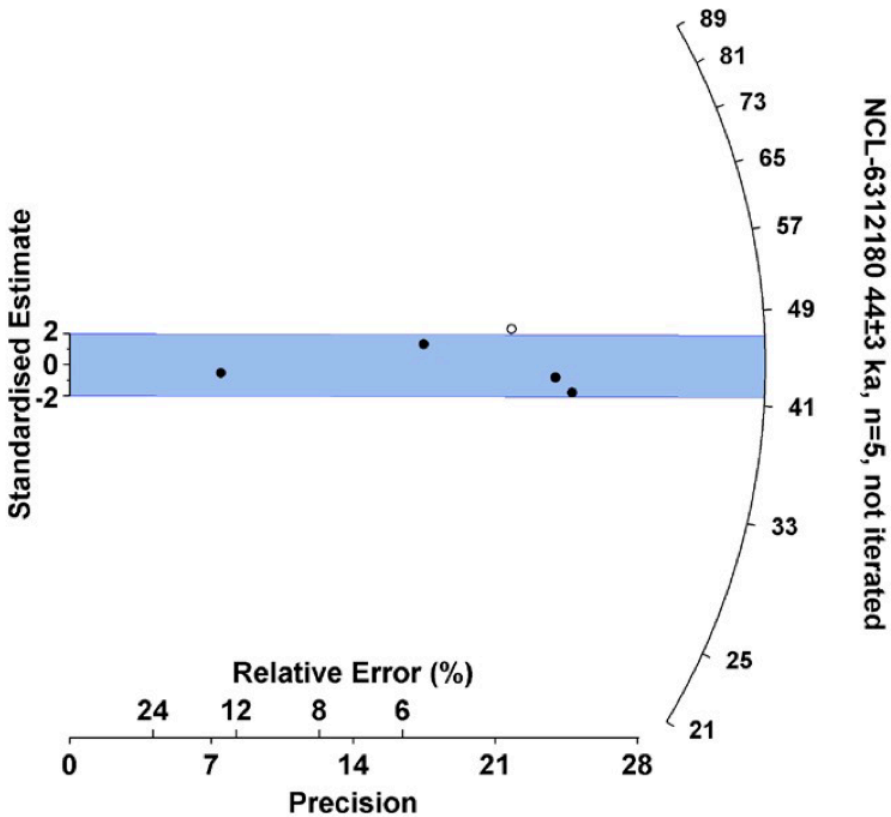
Relative Palaeointensity (RPI) curve of the Rutten AF samples obtained by dividing the natural remanent magnetization (NRM) intensity after AF demagnetization at 25 mT by the anhysteretic remanent magnetization (ARM) also AF demagnetized at 25 mT. Values are standardized, and plotted against depth in meters.

During the inferred Blake excursions interval mostly vary approximately one standard deviation around the mean (-28.62 m to -12.54 m NAP). At c. -11 m intensities become higher but drop again at c. -9 m. Although this lithology is not ideal for RPI given the potentially prolonged NRM acquisition duration related to early diagenetic processes the relatively uniform values could correspond to the low RPI segment between ~130 and ~100 ka.

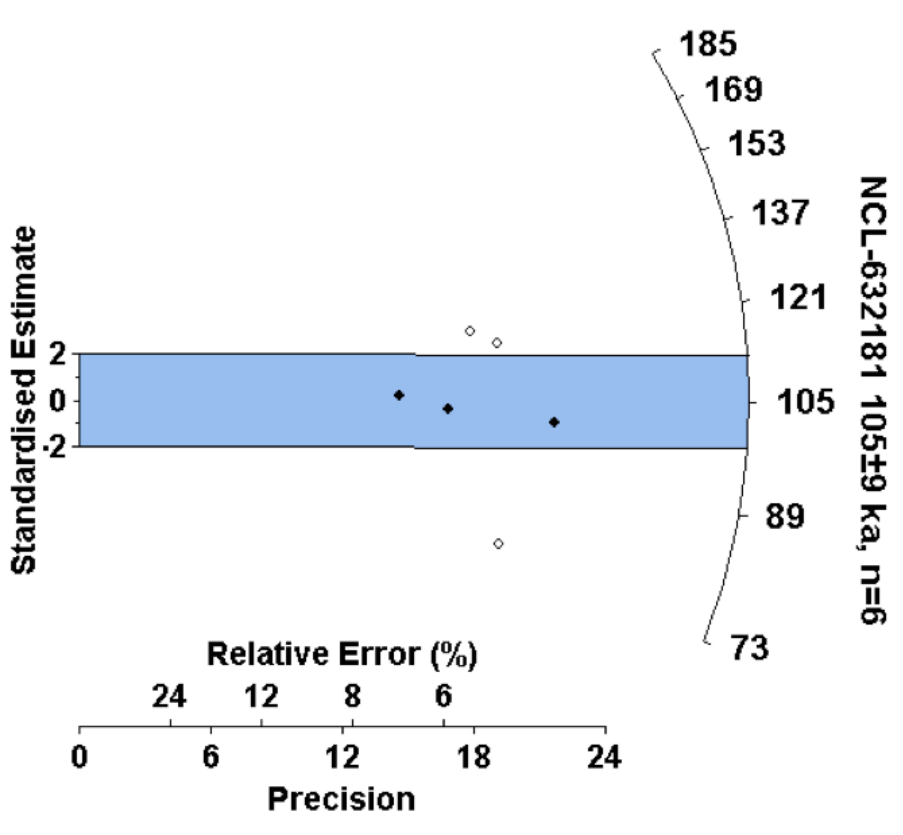
SI Figure 4-8:

Radial plots for the dated Ruten samples (Wallinga and Versendaal, 2012). Each sample is indicated by an open or closed dot. Open dots are not included in age estimate. The curved y-curve indicates the age estimate, whereas the x-axis reflects the precision of the individual estimates. Figures taken from Wallinga and Versendaal (2012)

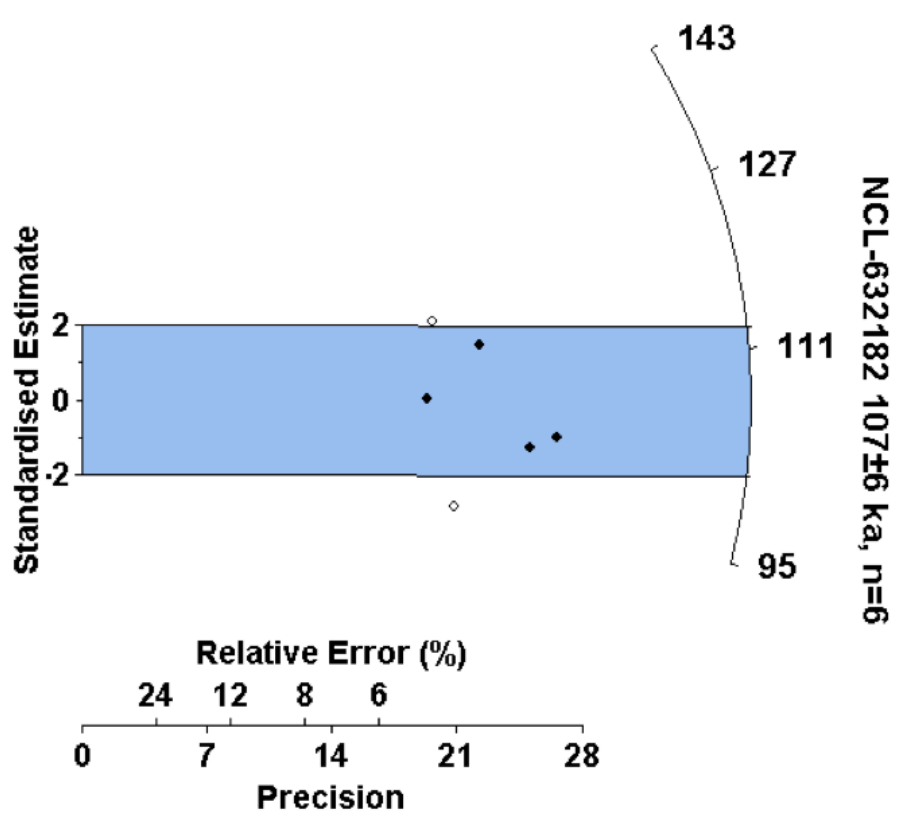
SI Figure 4



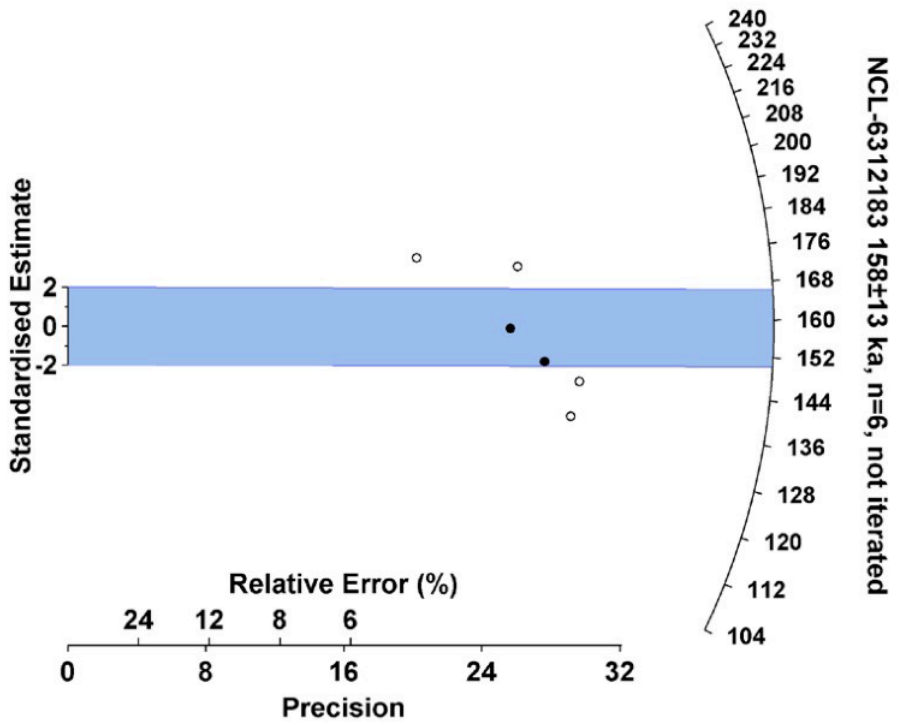
SI Figure 5



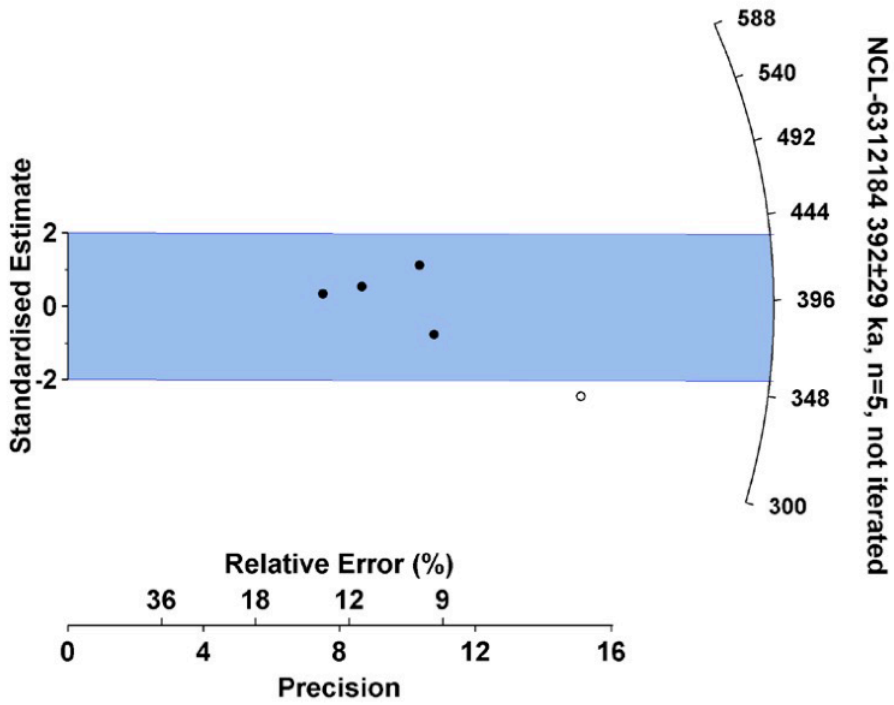
SI Figure 6



SI Figure 7



SI Figure 8



References

- Bassinot, F. C., Labeyrie, L. D., Vincent, E., Quidelleur, X., Shackleton, N. J., and Lancelot, Y. (1994). The astronomical theory of climate and the age of the Brunhes-Matuyama magnetic reversal. *Earth and Planetary Science Letters* 126, 91-108.
- Bosch, J. H. A. (2000). Standaard Boor Beschrijvingsmethode - versie 5.1. In "TNO-rapport: NITG 00-141-A." pp. 106.
- Busschers, F. S., Kasse, C., van Balen, R. T., Vandenberghe, J., Cohen, K. M., Weerts, H. J. T., Wallinga, J., Johns, C., Cleveringa, P., and Bunnik, F. P. M. (2007). Late Pleistocene evolution of the Rhine-Meuse system in the southern North Sea basin: imprints of climate change, sea-level oscillation and glacio-isostasy. *Quaternary Science Reviews* 26, 3216-3248.
- Guiot, J., Pons, A., de Beaulieu, J. L., and Reille, M. (1989). A 140,000-year continental climate reconstruction from two European pollen records. *Nature* 338, 309-313.
- Mangerud, J., Ehlers, J., and Gibbard, P. L. (2004). Ice sheet limits in Norway and on the Norwegian continental shelf. In "Developments in Quaternary Sciences." pp. 271-294. Elsevier.
- NGICP. (2004). High-resolution record of Northern Hemisphere climate extending into the last interglacial period. *Nature* 431, 147-151.
- van Huissteden, J., and Kasse, C. (2001). Detection of rapid climate change in Last Glacial fluvial successions in The Netherlands. *Global and Planetary Change* 28, 319-339.
- Vandenberghe, J. (1985). Paleoenvironment and stratigraphy during the last glacial in the Belgian-Dutch border region. *Quaternary Research* 24, 23-38.
- Vandenberghe, J., Lowe, J., Coope, R., Litt, T., and Zöller, L. (2004). Climatic and environmental variability in the Mid-Latitude Europe sector during the last interglacial-glacial cycle. In "Past Climate Variability through Europe and Africa." pp. 393-416. *Developments in Paleoenvironmental Research*. Springer Netherlands.
- Waelbroeck, C., Labeyrie, L., Michel, E., Duplessy, J. C., McManus, J. F., Lambeck, K., Balbon, E., and Labracherie, M. (2002). Sea-level and deep water temperature changes derived from benthic foraminifera isotopic records. *Quaternary Science Reviews* 21, 295-305.
- Wallinga, J., and Versendaal, A. (2012). NCL-6312 Luminescence Dating Report, Rutten Gemaalweg 2 (B15F1501).
- Zagwijn, W. H. (1961). Vegetation, climate and radiocarbon datings in the late Pleistocene of the Netherlands: I. Eemian and Early Weichselian, *Nieuwe Serie. Mededelingen van de Geologische Stichting* 14, 15-45.



CHAPTER 5

THE BLAKE EVENT RECORDED AT THE EEMIAN ARCHAEOLOGICAL SITE
OF CADURS, FRANCE



CHAPTER 5

THE BLAKE EVENT RECORDED AT THE EEMIAN ARCHAEOLOGICAL SITE OF CAOURS, FRANCE

Abstract

A palaeomagnetic study of the Last Interglacial calcareous tufa sequence at the archaeological site of Caours (northern France) identified a geomagnetic excursion that we interpret as the Blake Event. Palaeontological studies (molluscs, mammals) and geochemical proxy studies at the site of Caours allowed to reconstruct full interglacial conditions that were present during the deposition of the tufa sequence. The tufa sequence and associated Palaeolithic levels have been dated to the Eemian interglacial by a set of TIMS U/Th measurements on calcitic concretions (average : 123 ± 3 ka). By previous correlations of the Blake Event with the Eemian *sensu stricto* (as defined by Zagwijn (1961) in the Netherlands) pollenzones at Neumark Nord 2 (Germany) and Rutten (the Netherlands) it has been shown that the continental Eemian starts after the Marine Isotope Stage (MIS) 5e peak. The identification of the Blake Event at Caours implies a post MIS 5e peak age (Sier et al., in prep; Sier et al., 2011) for all four levels of the Palaeolithic occupations. Given the time lag between the MIS 5e peak and the beginning of the Eemian identified in previous studies (Sier et al., in prep; Sier et al., 2011), this strongly suggests that during the main occupations of Caours a significant barrier was in place between north-western France and Great Britain, in the form of the English Channel. It is possible that the chronological position of the Last Interglacial environments in north-western Europe in relation to sea-level change is a key factor behind the apparent absence of Last Interglacial Palaeolithic sites in Great Britain.

1. Introduction

The character of occupation of interglacial Europe by hominins has been a topic of a long debate. Extensive research has been devoted to finding the limits of European hominin occupation, both in time (e.g. Carbonell et al., 2008; Roebroeks and Van Kolfschoten, 1995) and in geographic space (e.g. Parfitt et al., 2010; Roebroeks et al., 1992). The geographic and environmental limits to the spatial distribution of specific hominins are of major interest since they provide important information about hominin social and/or technological abilities to adapt to a specific ecosystem, or to find new ways of exploiting or competing for resources (e.g. Dennell, 2003; Potts, 2012; Roebroeks, 2001). Thus, improving the chronological and environmental framework of the pattern of hominin presence in a given region can provide us with data to infer changes in their behaviour as well as to assess the emergence of corridors or barriers that may have influenced their dispersals (e.g. Dennell and Roebroeks, 2005; Joordens et al., 2011; Roebroeks and Kolfschoten, 1994; Speleers, 2000). In this context, and due to its climate during the Palaeolithic, north-western Europe has been considered a marginal area for hominin occupation, stretching to the limits the biological and cultural adaptations of its inhabitants (Roebroeks et al., 2011). This is also important during the last interglacial, in which *Homo neanderthalensis* dominated Europe. This warm and temperate period was first described as the Eemian by Harting (1874). During his investigations of the subsurface near Amsterdam and Amersfoort (the Netherlands), he identified sands and clays containing abundant diatom and mollusk fossils. Among the fossil mollusks, there were Mediterranean and Lusitanian species which he could not correlate to any known stratigraphic unit. For this reason, Harting defined a new unit, the Eemian. Currently, the Eemian is defined by its terrestrial pollen zonation (Zagwijn, 1961). Due to the long research history in Europe and a relatively good preservation compared to previous interglacials, the Eemian has become a key period for study of the technological and social adaptations of *Homo neanderthalensis*.

In the early days of Palaeolithic research, interglacial Europe was seen as an ideal environment for hominins (Mortillet, 1883; Obermaier, 1912). Temperate interglacial climates were interpreted as periods in which survival and subsistence was relatively easy. Hominins could do without the protection of cliff overhangs and caves and thus move into regions that lacked these natural shelters (Mortillet, 1883), such as northern Europe. During the mid 1980's, this view shifted to the opposite side of the spectrum. Inspired

by the work of Kelly (1983), who stated that most of the primary biomass in forested environments consists of plant leaves and stems which are difficult to access for hominins, Gamble postulated (1986; 1987) that interglacial northern Europe was actually a hostile environment for hominins. In his view, *Homo neanderthalensis*, who was occupying more southern parts of Europe during the last interglacial, lacked the set of specialized skills and/ or social structure which would have been necessary for successful exploitation of the resources in the forested northern regions (Gamble, 1986). The apparent lack of archaeological sites during this period in northern Europe gave support to Gamble's view. However, Roebroeks and colleagues (1992) refuted Gamble's hypothesis by presenting evidence that *Homo neanderthalensis* was present in Europe in interglacial periods. Their extensive review of a number of northern European sites not only indicated the presence of *Homo neanderthalensis* in pre-Eemian interglacial periods but also indicated occupation in mixed-oak forest (fully interglacial) environments of the Last Interglacial.

Still, many questions remain to be answered regarding the character of Neandertal occupation of northern Europe and the adaptations and abilities required for long-term occupation of this region. Although there is plenty of evidence suggesting that Neandertals were able to colonize middle latitudes up to 55° N, it has been suggested that their presence in northern environments was discontinuous and strongly influenced by climatic fluctuations (Hublin and Roebroeks, 2009). Environmental degradation may have obliged *Homo neanderthalensis* to search for southern refuges for survival, although local extinctions due to the hard climatic conditions cannot be excluded either (e.g. Hublin and Roebroeks, 2009; Roebroeks et al., 2011).

One region of Europe, which seems to have remained unoccupied during the last interglacial is Great Britain, where unambiguous traces of Last Interglacial Middle Palaeolithic sites are absent. However, the archaeological record is a strongly biased one, and various workers have stressed the role of preservation processes in this apparent absence (Roebroeks et al., 1992; Roebroeks and Speleers, 2002). Explaining the absence of Neandertals in Great Britain could give valuable insights about migration speeds, migration barriers or preferred habitats of *Homo neanderthalensis*. Ashton (2002) proposed two hypotheses to explain the lack of human occupation in Great Britain during the last interglacial. The first one, termed "insularity of Britain", explains the absence of Neandertals as the result of fast sea level rise during the last interglacial; the newly formed English Channel between Great Britain and France would have acted as a barrier for the Neandertal expansion. In the second model, focussing on "climatic extremes and the

occupation of northwest Europe”, the absence is explained as the result of the preference of Neandertals for mammoth-steppe-like environments in the eastern regions of Europe. This preference would explain the presence of Last Interglacial archaeological sites for instance in Germany, as well as their absence in the more Atlantic parts of northern Europe, which lacked a mammoth-steppe type of environment during the Eemian.

Related with both models, studies about the hominin occupation of north-west France have become key for understanding the character of Neandertal occupation in northern Europe in general, and in Great Britain in particular. Despite a long research history, no unambiguous traces of occupation during the Eemian were discovered in north-west France (Roebroeks and Speleers, 2002) until recently (Antoine et al., 2006; Loch et al., 2009). Research in the 1940’s and 1950’s at exposures at Caours (01°52’59” /50°07’53”, Figure 1), situated on a tributary of the Somme river near the town of Abbeville (northern France), however had yielded some tantalizing evidence in the form of Levallois flakes and an interglacial fauna (Bourdier, 1974; Breuil, 1952; Breuil and Barral, 1955), as pointed out by Roebroeks and Speleers in their 2002 review paper.

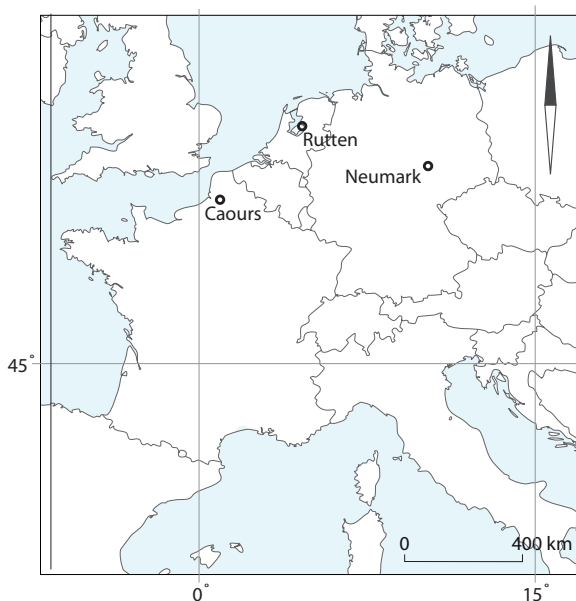


Figure 1. Location map with the sites of Caours (France), Rutten (The Netherlands) and Neumark (Germany).

Recent multidisciplinary studies have now enabled the unambiguous identification of Caours as Eemian in age and containing large numbers of in situ Palaeolithic flint artefacts and faunal remains (Antoine et al., 2006). The site is situated on a terrace 6 meters above the current valley floor and on basis of its position in the terrace system, the Caours fluvial sequence has been correlated to Marine Isotope stage (MIS) 6/5 (Antoine et al., 2006; Dabkowski et al., 2011). The sediments are dominated by calcareous tufa and contain abundant fossil remains (large mammals, micro-mammals, molluscs, leaf imprints). The fossils represent a temperate fauna indicating an Eemian age for the site (Antoine et al., 2006; Breuil and Barral, 1955). This age assessment is supported by ten U/Th (TIMS) ages of the tufa of ~ 120 ka (123 ± 3 ka) (Antoine et al., 2006), thermoluminescence ages of heated flints of 127.2 ± 10.4 ka and 119.6 ± 9.3 ka (Locht et al., 2009), and finally, electron spin resonance (ESR) age determinations of a deer molar of 124 ± 15 ka (Bahain et al., 2010). The ongoing work at Caours unambiguously confirms the Last Interglacial presence of *Homo neanderthalensis* in this region of Europe; hence, the site plays a major role in our understanding of human occupation and migration to this region of Europe during the last interglacial.

While the ages are reasonably well-constrained, having a tighter age control on the four layers with Neandertal artefacts in Caours would help with its interpretation and facilitate comparison to other sites in north-western Europe of similar age. Also the site is located just south of the English Channel and could potentially yield information regarding the accessibility of Great-Britain in the Last Interglacial, giving support to one of the hypotheses for the absence of human occupation in Great Britain mentioned above (Asthon and Lewis, 2002).

This paper reports the result of a study which attempted to constrain the period of Neandertal presence at Caours by the identification of the palaeomagnetic Blake Event which is tightly correlated to the Eemian, as we will explain below. The Blake Event was discovered in 1969 in a core from the Bermuda rise in the Atlantic Ocean (Smith and Foster, 1969). It is a period with transitional to reversed directions of the earth's magnetic field (e.g. Laj and Channell, 2007; Langereis et al., 1997; Merrill and McFadden, 1994). Estimates of its duration are notably variable, ranging from less than 1000 to over 10,000 years (e.g. Channell et al., 2012; Nowaczyk et al., 1994). The Blake Event has also been correlated to the Eemian pollen zonation of north-western and central Europe (Sier et al., in prep; Sier et al., 2011). At the onset of this Caours study, the Blake Event was correlated with the early part of the Eemian (e.g. Sier et al., 2011). However, a recent study of an oriented

undisturbed core, taken at the Rutten site, in the region of the Eemian type locality in the Netherlands, provides evidence that the Blake Event may have lasted throughout the entire Eemian *sensu stricto* (Sier et al., in prep). Even with this new evidence, the identification of the Blake Event at Caours would firmly place the archaeology yielding sediments in the Eemian *sensu stricto*. In the Neumark Nord and Rutten studies, the Blake Event was used to correlate the terrestrial Eemian record to the Marine Isotope Stage (MIS) record. Based on our correlation, we estimated that the Eemian lasted from ~120.5 ka to 109.5 ka (Sier et al., in prep; Sier et al., 2011). More importantly, in the context of the present paper, the correlation of the Eemian with the MIS record situates the Eemian in north-western and central Europe well after the MIS 5e peak. This would mean that already during the first phases of the Eemian *sensu stricto*, high sea levels in the English Channel would have been in place constituting a strong physical barrier for hominin movements from France into Great Britain.

A second focus of the study presented here is the behaviour of the magnetic field during the period of the Blake event. The Blake Event is recognized in sediments at Neumark Nord 2 (NN2) (Germany) (Sier et al., 2011) and at Rutten (the Netherlands) (Sier et al., in prep) mainly by excursions of declinations, while in most cases the inclination remained normal. This is in contrast to the Blake Event as recognized in other northern hemisphere regions (e.g. Bourne et al., 2012; Smith and Foster, 1969; Tucholka et al., 1987) where mainly negative inclinations were identified. Confirmation of Rutten and NN2 type of palaeomagnetic directions for the Blake Event at Caours could help to give important insights on the behaviour of the palaeomagnetic field during the Blake Event.

To summarize, the main goal of this study is to identify the palaeomagnetic Blake Event in the Caours sediments. This identification could confirm the Eemian *sensu stricto* age of the site and would allow a more precise positioning of the hominin occupation at Caours on the global (MIS) sea-level curve. This research would potentially provide new data on the character of the occupation of north-western Europe by Neandertals and would allow the discussion of more specific scenarios such as the absence of humans during the last interglacial in Great Britain.

2. Methods and sampling

Palaeomagnetic samples were taken during the 2009 and 2010 excavations of the Caours site at sector 1 and 2. The geological units (See supplementary information (SI) for description of the units) consist of a basal periglacial fluvial gravel (flint and chalk: ~ 3m), overlain by calcareous silts (~ 0.6m) and then by carbonate tufas (~3.5m). The tufas have a range from fine grained laminated to massive porous tufa. The type of tufa had its direct reflection on its sample potential, with the fine grained units yielding a significant higher amount of samples. In total 78 samples were taken, 46 samples for Alternating Field (AF) demagnetization, and 32 samples for Thermal (TH) demagnetization of the natural remanent magnetization (NRM). In addition, five hand samples of various dimensions were taken in order to identify the main magnetic carriers within the sediment. All studied geological units were sampled with dedicated sample containers for both AF and TH demagnetization. AF samples taken were collected with perspex containers, while for TH samples custom-made quartz glass containers were used. Both sample container types have standard palaeomagnetic dimensions (25 mm diameter and 22 mm height) and were gently pushed into freshly prepared sections. One oriented hand sample was of sufficiently large size to be sub-sampled, in the laboratory, with a 36 cm long u-channel. A u-channel is a plastic container with a square 2 by 2 cm cross-section and clip-on lid (Weeks et al., 1993). The u-channel was measured intact with a measurement interval of 2 cm. Measurements of the samples were done within a couple weeks after retrieval of the samples to minimize possible alteration. During this period the samples remained in a cold storage (<5°C).

AF demagnetization was done with a robotized 2G DC-SQUID magnetometer with in-line AF demagnetization at the palaeomagnetic laboratory "Fort Hoofddijk" (Utrecht, The Netherlands). The instrument's sensitivity is 3×10^{-12} Am²; typical sample magnetic moments were at least two orders of magnitude higher. The instrument set-up is housed inside a magnetically shielded room (residual field < 200 nT); the robotized interface for field regulation and sample manipulation was built in-house. Up to 96 samples contained inside dedicated cubic holders (edge 30 mm) are loaded onto a sample plateau and the robot loads them in batches of eight onto a tray that slides through the magnetometer and AF demagnetization coils. Samples are processed fully automatically with the so-called 'three position protocol' that compensates for the magnetic moment of the transport tray. This ensures optimal processing of weakly magnetic samples. Maximum demagnetization field was 100 mT.

Thermal demagnetization of the NRM was performed with an ASC thermal demagnetizer (residual field < 20 nT) at CENIEH, Burgos (Spain). Maximum demagnetization temperature was 630°C. The remaining NRM was measured after each step with a SRM 755 4K DC-SQUID magnetometer (with built-in AF demagnetizer, instrument sensitivity 3×10^{-12} Am², typical sample NRM magnetic moments were at least a couple of orders of magnitude higher) with a low-field (< 5 nT) environment at the sample loading position. The u-channel was demagnetized and measured with the same equipment up to a maximum AF peak field of 100 mT.

Demagnetization results were analyzed by visual inspection of orthogonal demagnetization diagrams (Zijderveld, 1967) using the “Fort Hoofddijk” “paldir” software. Directions of the Characteristic Remanent Magnetisation (ChRM) were calculated using least-squares principle component analysis (Kirschvink, 1980) on at least 4 steps. Four different quality labels were assigned to the ChRM directions, with only quality 1 and quality 2 ChRM directions being used for interpretation. ChRM directions from samples of quality 1 are those with vector end points close to the origin (quality 1, see figure 2A, 2B and 2C). Diagrams with the endpoint slightly offset from the origin or the last step does not reach the origin or have ChRM directions that are forced to the origin are given quality 2 (figure 2D). Noisy diagrams with MAD below 15° or diagrams which show indications of a not completely resolved NRM component during high demagnetization levels (which cannot be calculated with 4 steps but do from a great-circle) are given quality 3 (figure 2E). Directions of samples with the minimum of 4 steps that however disintegrated in an early stage during measuring, were completely demagnetized in an early stage (below 20/30 mT or 360°C or have an maximum angular deviation (MAD) > 15° have been given quality label 4. All other diagrams were rejected (37 out of 96, see table I of the supplementary information).

For rock-magnetic purposes hand samples were measured to better understand their magnetic properties in support of the interpretation of the ChRM directions. A selection of samples were pulsed in three perpendicular axes according to Lowrie (1990). Maximum field was 1 T, intermediate field 0.4 T and the low field 0.12 T. Thermal demagnetization was performed up to a max temperature of 600 degrees °C in 16 steps.

Figure 2.

Representative Zijderveld diagrams of alternating field demagnetization (AF) and thermal demagnetization (TH) from discrete samples (C21, C35, C50, C39, C70, C10= and from a u-channel (CHS6.1 level 0.10). Quality 1 samples are in panels A, B and C, quality 2 in panel D, quality 3 in panel E, quality 4 in panel F. Finally examples of quality 1 u-channel are shown in panels G and H. Panel G is un-rotated and panel H rotated according to sampled direction.

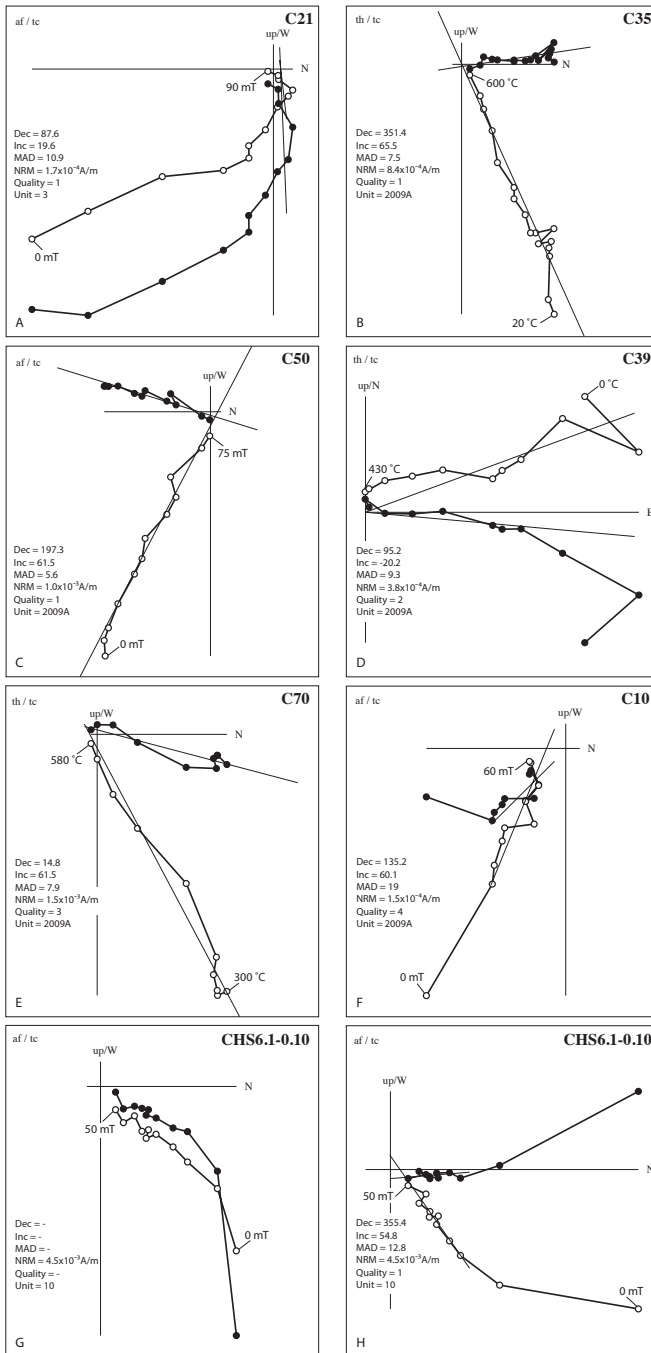


Figure 2.

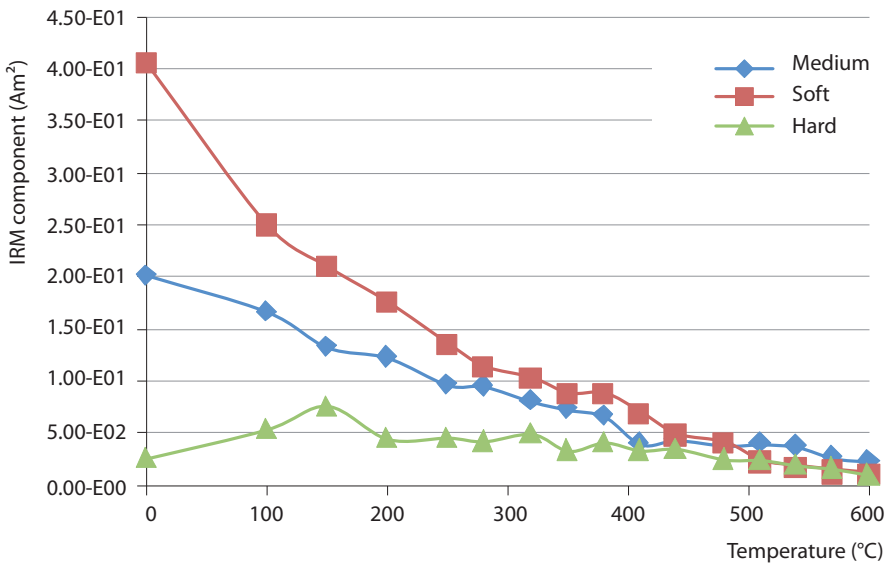
3. Results

Intensities of the NRM range from $1.7 \cdot 10^{-5}$ A/m to $1.0 \cdot 10^{-2}$ A/m (see SI table I). Thermal demagnetization of 3 axial Isothermal Remanent Magnetisation (IRM) acquisition curves (figure 3 and SI figure 1 a-d) show that the magnetic mineralogy in the Caours sediments is dominated by a “medium” and “soft” coercivity, indicative of fine-grained magnetite as the maximum unblocking temperature is slightly higher than 500 °C. No goethite is traced and very little high coercivity minerals like hematite is detected. It is important to note that our rock-magnetic studies have not found any indication of magnetic sulphides.

The ChRM directions for the samples treated with AF demagnetization were typically determined between 15 and 60 mT peak AF with occasionally a maximum of 80 mT. No indications of gyroremanent magnetisation (GRM) were observed during AF demagnetization. ChRM directions from the thermal demagnetization are not based on a typical set of temperatures; minimum temperatures vary from 230°C to 300°C. Upper temperatures show a broad range: from as low as 360°C to as high as 600°C. Notably

Figure 3.

Thermal demagnetization of 3 axial Isothermal Remanent Magnetisation (IRM) acquisition curves. Sample was taken from geological unit 5.



varying upper temperatures can even occur within a single geological unit; it indicates that different magnetic minerals carry the ChRM directions. There is a strong relation between the NRM intensity and the quality of the Zijdeveld diagrams: intensities above 10^{-4} A/m give significantly better results than samples with lower NRM intensities (SI table 1). However, the polarity of the ChRM directions is not related to the NRM intensity.

No fully reversed ChRM directions are identified, but of the 59 samples (including the 18 u-channel measurements, SI table 1) that were given a quality label (between 1 and 4), 23 have virtual geomagnetic poles (VGP's) that deviate more than 40° of the expected VGP position (SI table 1) and can be labelled "excursionals" (Merrill and McFadden, 1994). Excursionals directions are present throughout the sampled units (figure 2 and SI table 1). A few Zijdeveld diagrams show a clear overprint between components. An example of a clear excursional direction due to an overprint, from 0 to 35 mT, on an excursional ChRM is given in figure 2A. In other samples it is not that clear-cut. An example is sample C70 (figure 2E) where the ChRM direction in the Zijdeveld diagram passes the origin and could develop into an excursional orientation. This, however, cannot be determined with certainty because consecutive steps do not show a linear trend. The last steps are situated on a great circle indicative of a hidden component.

4. Discussion and Conclusions

As mentioned above, the quality of the Zijdeveld diagrams and the intensity of the NRM show a positive correlation. There is no clear relation between the direction of the ChRM and the quality of the Zijdeveld diagrams. The geological units (see figure 4 and figure 5) sampled, except unit 7, yielded Zijdeveld diagrams of quality 2 or higher. All geological units above unit 7 have high quality samples with VGPs of over 40° deviation of the expected VGP position (SI table 1) which are considered as excursionals (e.g. Merrill and McFadden, 1994). Unit 6a, 6b (coarse fluvial gavels, see SI) have not been sampled and unit 8 was sampled unsuccessfully, whereas units 9 and 10 give both directions of normal polarity in samples of high quality and excursionals in some of the lower quality samples. Insert Figure 4 and 5 around here As only high quality ChRM directions are included in the interpretation these units are interpreted to have normal palaeomagnetic polarity. Based on the position of the Caours terrace in the Somme valley terrace sequence, given the presence of warm-temperate animals, and in view of the numerical age estimates

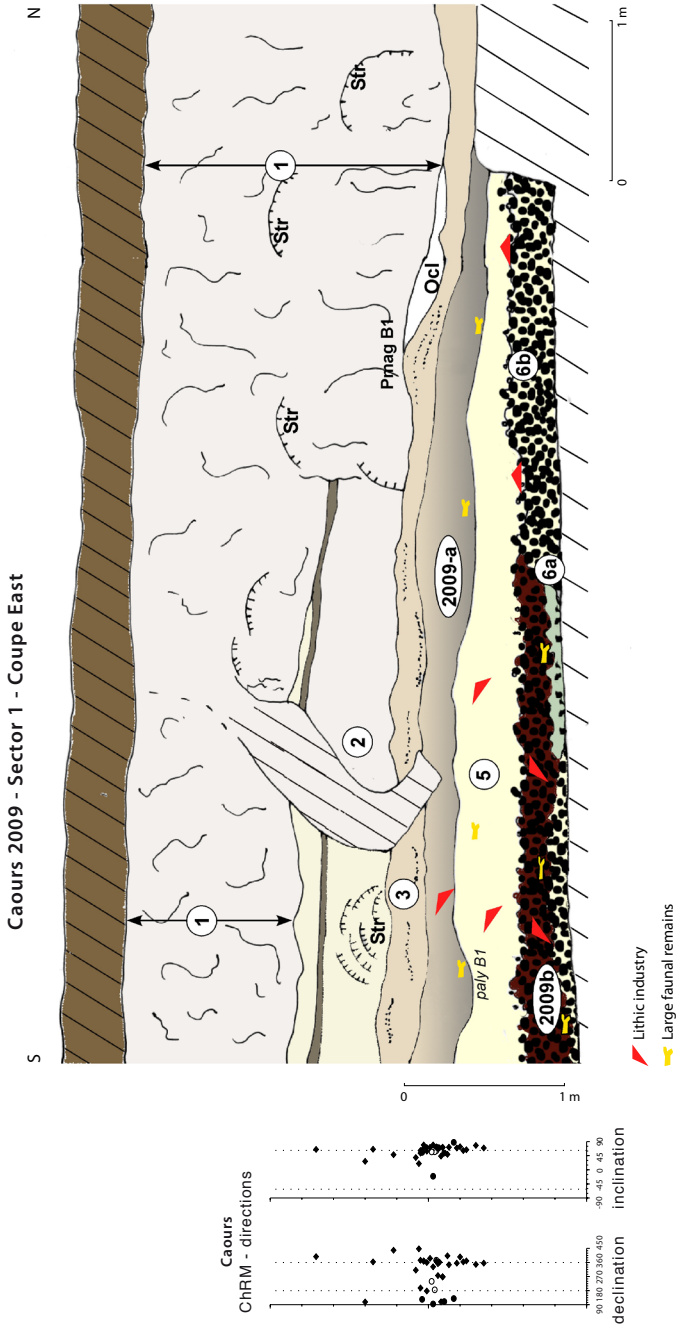


Figure 4.

Figure 4.

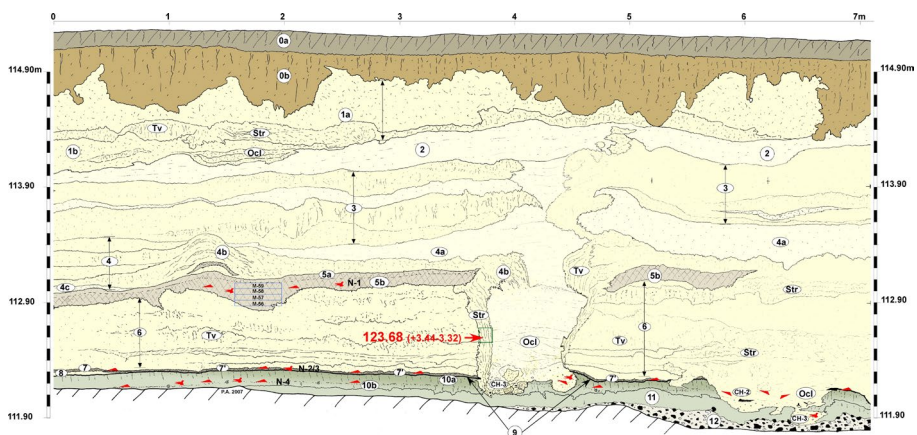
ChRM directions of sector 1 plotted next to the samples from the East profile of sector 1. Numbers represent different stratigraphic units, for details see SI. Ocl is oncolith, Str is stromatolith.

(Antoine et al., 2006; Bahain et al., 2010) which suggest a last interglacial age for the sediments, we interpret these excursions as the Blake Event. The Blake Event is known to consist of two reversed parts interrupted by a brief period of normal polarity and also known for its elusiveness (Parés et al., 2004). The zones of normal polarity have been described for several locations from various parts of the globe (e.g. Fang et al., 1997; Thouveny et al., 2004). In one publication of the Jiuzhoutai section (Lanzhou, western Loess Plateau, China) even three zones with excursions or reversed directions were identified (Zhu et al., 1994). In addition, recent studies have given support for a long duration of the Blake Event. These studies suggest a duration of at least 6000 years and even up to possibly 11.000 years (Bourne et al., 2012; Sier et al., in prep) and in strong correlation with the Eemian *sensu stricto* (Sier and Dekkers, 2013; Sier et al., in prep; Sier et al., 2011).

The lower boundary of the Blake Event at Caours is possible situated between unit 7 and 9 (note: at Caours units are labelled from top to bottom), as the higher quality ChRM directions all have a normal direction. However, ChRM directions of lower quality (SI table I) show excursions, but these are due to the low quality excluded

Figure 5.

South profile of sector 2. Taken in 2007 but similar to the 2010 profile. Ocl is oncolith, Str is stromatolith, Tv is travertine.



from interpretation (see methods and sampling). The lower boundary of the Blake would identify these Caours sediments as late Saalian in age if we correlate with the NN2 and Rutten sites. At NN2 the lower boundary of the Blake Event was identified in late Saalian age sediment (Sier et al., 2011). At the site of Rutten this boundary could not be identified with certainty, though a late Saalian age is very probable based on the stratigraphical position of the sediments (Sier et al., in prep).

The numerical ages of the concerned units at Caours (Antoine et al., 2006) fall well with the estimated age and duration of the Blake Event (Sier et al., in prep; Sier et al., 2011). Fossils found at the lower units of the Caours sequence, between units 10 and 11 (archaeological level 4), also suggest fully temperate conditions (Antoine et al., 2006; Locht et al., 2009). More importantly, the study of the malacological succession at Caours shows that unit 10, and the contemporaneous Palaeolithic level N4, is fully interglacial (Limondin-Lozouet, 2011). Considering this evidence we interpret that the lower part of the Caours section is most likely of Blake Event age, at least up to the unconformity that separates unit 10 and the lower unit 11. This unit 11 contains evidence of a cold climate malacological assemblage (Limondin-Lozouet, 2011).

At NN2 and Rutten, the Blake Event has been identified in conjunction with an Eemian pollen record, together in the same sections and core, respectively. From this we can infer that the Caours sediments not only record the Blake Event age but can be considered of Eemian *sensu stricto* age as defined at its type locality (Zagwijn, 1961). This is well in-line with numerical and biostratigraphic ages derived in the previous studies (Antoine et al., 2006; Antoine et al., 2007; Bahain et al., 2010; Breuil and Barral, 1955; Limondin-Lozouet, 2011).

Another aspect worth mentioning is the lack of fully reversed directions at Caours, similar to the Rutten site (Sier et al., in prep) and the NN2 locality (Sier et al., 2011). All together the data of Caours, NN2 and Rutten seem to suggest that these excursions, rather than truly reversed ones, characterize the Blake Event in north-western and central Europe. This issue, although is beyond the scope of the present work, gives important insights for modellers of the behaviour of the Earth's geomagnetic field during excursions or events, but it also complicates the identification of the Blake Event in unorientated cores (e.g. IODP cores, where declination can only be analysed on a relative basis within individual core segments).

Finally, as mentioned above, the Blake Event has been directly linked to the Eemian

pollen sequence which in turn has been correlated to the MIS record via the same event, positioning the Eemian *sensu stricto* and the Blake Event after the MIS 5e peak (Sier et al., in prep; Sier et al., 2011). Placing the archaeological occupation layers of Caours within the Eemian *sensu stricto* is an important fact since it tells us when Caours was occupied but also that the occupation was well after the “window of opportunity” (as Ashton 2002 calls it) for range expansion into Great-Britain, i.e., before the last interglacial sea level maximum. This means that the “dry path towards Great Britain” was already submerged by high sea level for some time when Neandertals discarded their first stone artefacts at Caours (unit 10). The presence of a physical barrier in the form of the sea water in the English Channel may have been the main obstacle to a Last Interglacial occupation of England by Neandertals.

References

- Antoine, P., Limondin-Lozouet, N., Auguste, P., Loch, J. L., Galheb, B., Reyss, J., Escudé, E., Carbonel, P., Mercier, N., Bahain, J. J., Falguères, C., and Voinchet, P. (2006). Le tuf de Caours (Somme, France) : mise en évidence d'une séquence eemienne et d'un site paléolithique associé. *Quaternaire* 17, 281-320.
- Antoine, P., Limondin Lozouet, N., Chaussé, C., Lautridou, J. P., Pastre, J. F., Auguste, P., Bahain, J. J., Falguères, C., and Galehb, B. (2007). Pleistocene fluvial terraces from northern France (Seine, Yonne, Somme): synthesis, and new results from interglacial deposits. *Quaternary Science Reviews* 26, 2701-2723.
- Ashton, N. (2002). Absence of human in Britain during the last interglacial (oxygen isotope stage 5e). In "Publications du CERP" (A. Tuffreau, and W. Roebroeks, Eds.), Lille.
- Asthon, N., and Lewis, S. G. (2002). Deserted Britain: declining populations in the British Late Middle Pleistocene. *Antiquity* 76, 388-396.
- Bahain, J. J., Falguères, C., Dolo, J. M., Antoine, P., Auguste, P., Limondin-Lozouet, N., Loch, J. L., Tuffreau, A., Tissoux, H., and Farkh, S. (2010). ESR/U-series dating of teeth recovered from well-stratigraphically age-controlled sequences from Northern France. *Quaternary Geochronology* 5, 371-375.
- Bourdier, F. (1974). La « marne blanche » d' Abbeville, gisement type de l'Abbevillien. *Quaternaire* 11, 161-163.
- Bourne, M., Mac Niocaill, C., Thomas, A. L., Knudsen, M. F., and Henderson, G. M. (2012). Rapid directional changes associated with a 6.5 kyr-long Blake geomagnetic excursion at the Blake-Bahama Outer Ridge. *Earth and Planetary Science Letters* 333-334, 21-34.
- Breuil, H. (1952). Glanes conchyliologiques en France (Nord et Sud-Ouest) déterminés par A.S. Kennard. In "Congrès Préhistorique de France. Compte rendu de la XIIIe Session, 1950." pp. 191 -240., Paris.
- Breuil, H., and Barral, L. (1955). Bois de Cervidés et autres os travaillés sommairement au Paléolithique ancien vieux monde et au Moustérien des grottes de Grimaldi et de l'observatoire de Monaco. *Bulletin du Musée d'anthropologie préhistorique de Monaco* 2, 1-32.
- Carbonell, E., Bermudez de Castro, J. M., Pares, J. M., Perez-Gonzalez, A., Cuenca-Bescos, G., Olle, A., Mosquera, M., Huguet, R., van der Made, J., Rosas, A., Sala, R., Vallverdu, J., Garcia, N., Granger, D. E., Martinon-Torres, M., Rodriguez, X. P., Stock, G. M., Verges,

- J. M., Allue, E., Burjachs, F., Caceres, I., Canals, A., Benito, A., Diez, C., Lozano, M., Mateos, A., Navazo, M., Rodriguez, J., Rosell, J., and Arsuaga, J. L. (2008). The first hominin of Europe. *Nature* 452, 465-469.
- Channell, J. E. T., Hodell, D. A., and Curtis, J. H. (2012). ODP Site 1063 (Bermuda Rise) revisited: oxygen isotopes, excursions and paleointensity in the Brunhes Chron. *Geochemistry Geophysics Geosystems* 13, Q02001.
- Dabkowski, J., Limondin-Lozouet, N., Antoine, P., Marca-Bell, A., and Andrews, J. (2011). Recording interglacial climatic changes from stable isotopes of pleistocene tufa calcite in northern France: Examples from Caours (Mis 5e; Somme) and La Celle-sur-Seine (Mis 11; Seine-et-Marne). *Quaternaire* 22, 275-283.
- Dennell, R. (2003). Dispersal and colonisation, long and short chronologies: how continuous is the Early Pleistocene record for hominids outside East Africa? *Journal of Human Evolution* 45, 421-440.
- Dennell, R., and Roebroeks, W. (2005). An Asian perspective on early human dispersal from Africa. *Nature* 438, 1099-1104.
- Fang, X., Li, J., Van der Voo, R., Mac Niocaill, C., Dai, X., Kemp, R. A., Derbyshire, E., Cao, J., Wang, J., and Wang, G. (1997). A record of the Blake Event during the last interglacial paleosol in the western Loess Plateau of China. *Earth and Planetary Science Letters* 146, 73-82.
- Gamble, C. (1986). "The Palaeolithic settlement of Europe." Cambridge University Press, Cambridge.
- Gamble, C. S. (1987). Man the shoveler: Alternative models for Middle Pleistocene colonization and occupation in Northern latitudes. In "The Pleistocene old world. Regional perspectives." (O. Soffer, Ed.), pp. 81-98. Plenum Press, New York.
- Harting, P. (1874). De bodem van het Eemdal. Verslagen en Verhandelingen Koninklijke Academie van Wetenschappen, 282-290.
- Hublin, J. J., and Roebroeks, W. (2009). Ebb and flow or regional extinctions? On the character of Neandertal occupation of northern environments. *Comptes Rendus Palevol* 8, 503-509.
- Joordens, J. C. A., Vonhof, H. B., Feibel, C. S., Lourens, L. J., van der Lubbe, H. J. L., Dupont-Nivet, G., Sier, M. J., Davies, G. R., and Kroon, D. (2011). An astronomically-tuned climate framework for hominins in the Turkana Basin. *Earth and Planetary Science Letters* 307, 1-8.
- Kelly, R. L. (1983). Hunter-Gatherer Mobility Strategies. *Journal of Anthropological Research* 39, 277-306.

- Kirschvink, J. L. (1980). The least-square line and plane and the analysis of paleomagnetic data. *Geophysical Journal of the Royal Astronomical Society* 62, 699-718.
- Laj, C., and Channell, J. E. T. (2007). Geomagnetic Excursions. In "Geomagnetism." (M. Kono, Ed.), pp. 373-416. *Treatise on Geophysics* Elsevier, Amsterdam.
- Langereis, C. G., Dekkers, M. J., Lange, G. J., Paterne, M., and Santvoort, P. J. M. (1997). Magnetostratigraphy and astronomical calibration of the last 1.1 Myr from an eastern Mediterranean piston core and dating of short events in the Brunhes. *Geophysical Journal International* 129, 75-94.
- Limondin-Lozouet, N. (2011). Successions malacologiques à la charnière Glaciaire/Interglaciaire: du modèle Tardiglaciaire/Holocène aux transitions du Pléistocène. *Quaternaire* 22, 211-220.
- Locht, J. L., Antoine, P., Auguste, P., and Limondin Lozouet, N. (2009). Rapport de fouille programmée. Caours 2009 (Somme). Amiens. In "SRA Picardie." pp. 40.
- Lowrie, W. (1990). Identification of ferromagnetic minerals in a rock by coercivity and unblocking temperature properties. *Geophysical Research Letters* 17, 159-162.
- Merrill, R. T., and McFadden, P. L. (1994). Geomagnetic field stability: Reversal events and excursions. *Earth and Planetary Science Letters* 121, 57-69.
- Mortillet, G. d. (1883). "Le Préhistorique, antiquité de l'homme." C. Reinwald, Paris.
- Nowaczyk, N. R., Frederichs, T. W., Eisenhauer, A., and Gard, G. (1994). Magnetostratigraphic Data From Late Quaternary Sediments From the Yermak Plateau, Arctic Ocean: Evidence For Four Geomagnetic Polarity Events Within the Last 170 Ka of the Brunhes Chron. *Geophysical Journal International* 117, 453-471.
- Obermaier, H. (1912). "Der Mensch der Vorzeit." AVG, Berlin.
- Parés, J. M., Van der Voo, R., and Yan, M. (2004). After the Dust Settles: Why Is the Blake Event Imperfectly Recored in Chinese Loess? In "Timescales of the Paleomagnetic Field " (J. E. T. Channell, D. V. Kent, W. Lowrie, and J. G. Meert, Eds.).
- Parfitt, S. A., Ashton, N. M., Lewis, S. G., Abel, R. L., Coope, G. R., Field, M. H., Gale, R., Hoare, P. G., Larkin, N. R., Lewis, M. D., Karloukovski, V., Maher, B. A., Peglar, S. M., Preece, R. C., Whittaker, J. E., and Stringer, C. B. (2010). Early Pleistocene human occupation at the edge of the boreal zone in northwest Europe. *Nature* 466, 229-233.
- Potts, R. (2012). Environmental and Behavioral Evidence Pertaining to the Evolution of Early Homo. *Current Anthropology* 53, S299-S317.
- Roebroeks, W. (2001). Hominid behaviour and the earliest occupation of Europe: an Exploration. *Journal of Human Evolution* 41, 437-461.

- Roebroeks, W., Conard, N. J., and van Kolfschoten, T. (1992). Dense Forests, Cold Steppes, and the Palaeolithic Settlement of Northern Europe. *Current Anthropology* 33, 551-586.
- Roebroeks, W., Hublin, J. J., and MacDonald, K. (2011). Continuities and Discontinuities in Neandertal Presence: A Closer look at Northwestern Europe. In "Developments in Quaternary Science." (N. M. Ashton, S. G. Lewis, and C. B. Stringer, Eds.). Elsevier, Amsterdam.
- Roebroeks, W., and Kolfschoten, v. T. (1994). The earliest occupation of Europe: a short chronology. *Antiquity* 68, 489-503.
- Roebroeks, W., and Speleers, B. (2002). Last interglacial (Eemian) occupation of the North European plain and adjacent areas. In "Publications du CERP." (A. Tuffreau, and W. Roebroeks, Eds.), pp. 9. Université des sciences et technologies de Lille, Villeneuve-d'Ascq, France.
- Roebroeks, W., and Van Kolfschoten, T. (1995). The Earliest Occupation of Europe. University of Leiden, Leiden.
- Sier, M. J., and Dekkers, M. J. (2013). Magnetic property analysis as palaeoenvironmental proxy: a case study of the Last Interglacial Middle Palaeolithic site at Neumark-Nord 2 (Germany). In "Multidisciplinary Studies of the Middle Palaeolithic Record from Neumark-Nord (Germany)" (S. Gaudzinski-Windheuser, and W. Roebroeks, Eds.), Saxony-Anhalt, Germany.
- Sier, M. J., Peeters, J., Dekkers, M. J., Chang, L., Busschers, F. S., Wallinga, J., Parés, J. M., and Roebroeks, W. (in prep). The Blake Event recorded near the Eemian Type locality, revised timing of the onset of the Eemian in north western Europe.
- Sier, M. J., Roebroeks, W., Bakels, C. C., Dekkers, M. J., Brühl, E., De Loecker, D., Gaudzinski-Windheuser, S., Hesse, N., Jagich, A., Kindler, L., Kuijper, W. J., Laurat, T., Mûcher, H. J., Penkman, K. E. H., Richter, D., and van Hinsbergen, D. J. J. (2011). Direct terrestrial-marine correlation demonstrates surprisingly late onset of the last interglacial in central Europe. *Quaternary Research* 75, 213-218.
- Smith, J. D., and Foster, J. H. (1969). Geomagnetic Reversal in Brunhes Normal Polarity Epoch. *Science* 163, 565-567.
- Speleers, B. (2000). The relevance of the Eemian for the study of the Palaeolithic occupation of Europe. *Geologie en Mijnbouw* 79, 283-291.

- Thouveny, N., Carcaillet, J., Moreno, E., Leduc, G., and Nérini, D. (2004). Geomagnetic moment variation and paleomagnetic excursions since 400 kyr BP: a stacked record from sedimentary sequences of the Portuguese margin. *Earth and Planetary Science Letters* 219, 377-396.
- Tucholka, P., Fontugne, M., Guichard, F., and Paterne, M. (1987). The Blake magnetic polarity episode in cores from the Mediterranean Sea. *Earth and Planetary Science Letters* 86, 320-326.
- Weeks, R., Laj, C., Endignoux, L., Fuller, M., Roberts, A., Manganne, R., Blanchard, E., and Goree, W. (1993). Improvements in long-core measurement techniques: applications in palaeomagnetism and palaeoceanography. *Geophysical Journal International* 114, 651-662.
- Zagwijn, W. H. (1961). Vegetation, climate and radiocarbon datings in the late Pleistocene of the Netherlands: I. Eemian and Early Weichselian, *Nieuwe Serie. Mededelingen van de Geologische Stichting* 14, 15-45.
- Zhu, R. X., Zhou, L. P., Laj, C., Mazaud, A., and Ding, Z. L. (1994). The Blake Geomagnetic Polarity Episode Recorded in Chinese Loess. *Geophysical Research Letters* 21, 697-700.
- Zijderveld, J. D. A. (1967). Demagnetisation of rocks: analysis of results. In "Methods in Palaeomagnetism." (D. W. Collinson, K. M. Creer, and S. K. Runcorn, Eds.), pp. 254-286. Elsevier, Amsterdam.

SUPPLEMENTARY INFORMATION

Geological Descriptions

Sector 1 2009 / 2010

Description of the units

- 1 - Massive porous tufa, highly indurated, with very big concretions, local occurrence of stromatolith layers and subvertical tubular stromatoliths (columns \varnothing : 2-5cm), secondary carbonate coatings in the porosity (mycelium).
 - 2 - White to light beige granular to sandy tufa facies, weakly stratified, including little oncoliths and incrustated twig fragments. This unit shows numerous in situ incrustated unrolled twigs and mosses. Locally it shows some porous laminated and undulated stromatolith layers ("floor"). A thin grey tufa layer with some scattered large mammal remains has been observed at the top.
 - 3 - Horizontal lens of fine grained laminated tufa (silty to medium sandy light grey to beige grey) with thin dark grey layers including numerous mollusc shells and humified vegetal debris. The upper part of this unit shows a coarser facies with thicker laminations (3a), alternating with layers of granular tufa.
 - 4 - Porous granular tufa with low cohesion, made from rolled and incrustated twig fragments and oncoliths (average \varnothing : 5mm, locally 2-3 cm to the base of profile West), marked fluvial structure (tilted stratification and discordances). The basal boundary of this unit is very sharp indicating relatively strong erosion processes as supported by the occurrence of downcutting features down to the upper part of the gravels (unit 6)
- 2009-a - Finely laminated grey to beige silty tufa (\pm 10cm). In the lower part: more homogeneous and darker facies including lenses of granular tufa a few centimetres large. A reworked archaeological layer (a) is included in the base of this unit.
- 5 - Fine grained beige tufa with sandy to silty texture, weak coherency and poor stratification. Close to the boundary with unit 6, this unit is richer in scattered little flint gravels reworked from the top of the gravel (reworked archaeological layer b).
- 2009-b - Heterogeneous rounded flint gravels (\sim 1 to \sim 10 cm) with brown to brown red clayey-silty organic matrix (organic carbon: 1.4%). This layer includes numerous reworked lithic artefacts and large mammal remains.

- 6a - Heterogeneous coarse fluvial gravels (flint and chalk) with calcareous sandy matrix. The upper part of these gravels (~ upper 5 cm) shows a finer matrix composed by calcareous light grey to greenish silts showing the same facies as described in sector 2 (Unit 10).
- 6b - Heterogeneous coarse fluvial gravels composed by rounded flint and chalk blocks (coarse alluvial gravels of the terrace)

The in situ archaeological layer, excavated in 2009-2010, is localised at the top of the coarse gravels of unit 6a, on which the larger artefacts and large mammal bones have been found. Some reworked flint artefacts and fragments of large mammal remains have nevertheless been observed at the base of unit 5 (a few cm) and in the fine grained tufa matrix that penetrates between the blocks at the top of the gravels.

Sector 2 2010

Description of the units

Caours Sector 2 : units 5 to 11 / archaeological layers 1 to 4

- 5 - Massive porous tufa, highly indurated, with very big concretions, local occurrence of stromatolith layers and subvertical tubular stromatoliths (columns \varnothing : 2-5cm), secondary carbonate coatings in the porosity (mycelium).
- 7 - White to light beige granular to sandy tufa facies, weakly stratified, including little oncoliths and incrustated twig fragments. This unit shows numerous in situ incrustated unrolled twigs and mosses. Locally it shows some porous laminated and undulated stromatolith layers ("floor"). A thin grey tufa layer with some scattered large mammal remains has been observed at the top.
- 8 - Horizontal lens of fine grained laminated tufa (silty to medium sandy light grey to beige grey) with thin dark grey layers including numerous mollusc shells and humified vegetal debris. The upper part of this unit shows a coarser facies with thicker laminations (3a), alternating with layers of granular tufa.
- 9 - Porous granular tufa with low cohesion, made from rolled and incrustated twig fragments and oncoliths (average \varnothing : 5mm, locally 2-3 cm to the base of profile West), marked fluvial structure (tilted stratification and discordances). The basal boundary of this unit is very sharp indicating relatively strong erosion processes as supported by the occurrence of downcutting features down to the upper part of the gravels (unit 6)
- 10 - Finely laminated grey to beige silty tufa (\pm 10cm). In the lower part: more homogeneous and darker facies including lenses of granular tufa a few centimetres large. A reworked archaeological layer (a) is included in the base of this unit.
- 10/11 - Fine grained beige tufa with sandy to silty texture, weak coherency and poor stratification. Close to the boundary with unit 6, this unit is richer in scattered little flint gravels reworked from the top of the gravel (reworked archaeological layer b).
- 11 - Heterogeneous rounded flint gravels (\sim 1 to \sim 10 cm) with brown to brown red clayey-silty organic matrix (organic carbon: 1.4%). This layer includes numerous reworked lithic artefacts and large mammal remains.

Table I:

Thermal (TH) and alternating field (AF) palaeomagnetic results. ID#: sample identification; Sample Type (AF or TH); Level: stratigraphic level in meters; sublevel in case of u-channel measurements; sector: excavation sector (1 or 2); unit: geological unit; NRM natural remanent magnetization; Dec: Declination of characteristic remanent magnetization (ChRM) direction; Inc: Inclination of ChRM direction; MAD: Maximum Angular Deviation; Q: quality of ChRM direction, with 1 the highest quality and 4 the lowest; AF/Tinf: lowest AF level or temperature step of ChRM in mT/°C; Tsup: highest AF level or temperature step of ChRM in mT/°C; Dir: ChRM forced or free; VGP: latitude of the virtual geomagnetic poles. - = Non determined.

Table I:

ID#	Level	Sublevel	Sector	Unit	NRM	Dec.	Inc.	MAD	Q	AF/T_inf (mT/°C)	AF/T_sup (mT/°C)	Dir.	VGP
C01	AF	11,475	1	5	82	135,4383	50,9191	5,068226	4	0	20	free	0,76
C02	AF	11,6	1	5	42	-	-	-	-	-	-	-	-
C03	AF	11,645	1	5	1309	355,7295	69,49532	3,787332	1	20	80	free	85,93
C04	AF	11,7	1	5	852	348,3316	77,84927	1,25818	1	20	70	free	72,39
C05	AF	11,755	1	5	4519	10,15761	64,27957	1,358973	1	20	60	free	82,11
C06	AF	11,775	1	2009A	5877	4,375075	61,64964	1,702286	1	20	60	free	82,11
C07	AF	11,795	1	2009A	2386	35,55967	73,94691	0,9697142	1	20	60	free	67,71
C08	AF	11,815	1	2009A	1053	356,3341	69,73158	2,355098	1	15	50	free	85,89
C09	AF	11,835	1	2009A	191	129,8695	87,85837	11,09703	2	15	60	free	47,27
C10	AF	11,86	1	2009A	148	135,1635	60,128	19,03379	4	15	50	free	9,26
C11	AF	11,88	1	2009A	101	42,27478	49,12875	9,265203	1	15	50	free	52,63
C12	AF	11,9	1	2009A	112	110,824	53,65593	10,72291	2	15	70	forced	14,05
C13	AF	11,915	1	2009A	89	109,0835	43,92373	10,06761	1	15	50	free	8,28
C14	AF	11,94	1	2009A	687	352,9843	68,24062	4,728421	1	15	50	free	85,38
C15	AF	11,95	1	2009A	1077	11,01876	73,12807	2,056628	1	15	80	free	79,27
C16	AF	11,975	1	2009A	264	240,124	57,60479	11,71148	3	15	50	free	12,95

C17	AF	11,99		1	2009A	709	26,81013	71,68762	2,886008	1	15	70	free	72,89
C18	AF	12,01		1	2009A	666	359,7549	71,10347	1,759465	1	15	80	free	84,51
C19	AF	12,025		1	3	305	9,947073	79,35636	1,560843	1	40	70	free	70,14
C19/2	AF	12,025		1	3	433	8,435709	69,31351	3,576263	1	15	80	free	84,05
C20	AF	12,04		1	3	101	125,114	55,95523	10,01412	2	15	50	free	9,21
C21	AF	12,06		1	3	171	87,59654	19,55246	10,93568	1	40	80	free	9,24
C22	AF	12,08		1	3	81	311,4322	38,92595	10,95501	1	15	40	free	42,90
C23	AF	12,11		1	3	83	-	-	-	-	-	-	-	-
C24	AF	12,13		1	3	130	307,5316	61,19757	17,20543	4	25	70	free	53,64
C25	AF	12,215		1	3	91	78,74007	48,37146	13,06034	1	15	70	free	29,04
C26	AF	12,4		1	2	179	108,2321	26,71798	7,528283	1	15	50	free	-0,42
C27	AF	12,71		1	2	113	37,82857	65,16662	13,56956	1	15	40	free	65,12
C28	TH	11,74		1	5	2350	-	-	-	-	-	-	-	-
C29	TH	11,78		1	2009A	3551	-	-	-	-	-	-	-	-
C30	TH	11,815		1	2009A	70	-	-	-	-	-	-	-	-
C31	TH	11,85		1	2009A	17	-	-	-	-	-	-	-	-
C32	TH	11,89		1	2009A	30	-	-	-	-	-	-	-	-
C33	TH	11,93		1	2009A	355	2,098184	70,11536	9,528232	1	230	490	free	85,80
C34	TH	11,965		1	2009A	429	332,9986	79,30524	12,95322	1	230	560	free	66,89
C35	TH	12		1	2009A	589	351,4187	65,54382	7,532476	1	230	600	free	83,87

C36	TH	12,04	1	3	63	-	-	-	-	-	-	-	-	-	-	-	-	-
C37	TH	12,11	1	3	37	-	-	-	-	-	-	-	-	-	-	-	-	-
C38	TH	12,71	1	2	93	-	-	-	-	-	-	-	-	-	-	-	-	-
C39	TH	11,97	1	2009A	375	95,15664	20,16062	9,360264	2	230	360	free	11,26					
C40	TH	11,95	1	2009A	no sig	-	-	-	-	-	-	-	-					
C41	TH	11,92	1	2009A	no sig	-	-	-	-	-	-	-	-					
C42	TH	12,09	1	3	52	-	-	-	-	-	-	-	-					
C43	TH	12,05	1	2009A	4469	14,2	53,6	4,5	1	230	580	free	70,94					
C44	TH	12,005	1	2009A	191	-	-	-	-	-	-	-	-					
C45	TH	11,965	1	2009A	134	-	-	-	-	-	-	-	-					
C46	TH	11,94	1	2009A	80	-	-	-	-	-	-	-	-					
C47	TH	11,9	1	2009A	50	-	-	-	-	-	-	-	-					
C48	TH	11,87	1	2009A		345,9	72,2	8,9	1	230	520	free	79,03					
C49	AF	12,09	1	3	48	-	-	-	-	-	-	-	-					
C50	AF	12,05	1	2009A	1017	197,3	61,5	5,7	1	20	75	free	3,98					
C51	AF	12,005	1	2009A	183	178,3	59,3	11,7	1	20	75	free	0,23					
C52	AF	11,955	1	2009A	114	186,5	57,8	13,5	3	20	65	forced	-1,25					
C53	AF	11,915	1	2009A	80	-	-	-	-	-	-	-	-					
C54	AF	11,9	1	2009A	54	-	-	-	-	-	-	-	-					
C55	AF	11,87	1	2009A	8319	115,0	70,5	2,8	1	20	60	free	28,01					

C76	AF	11.995		1	2009A	70	-	-	-	-	-	-	-	-	-	-	-	-	-
C77	AF	11,94		1	2009A	1133	277,0	71,5	7,7	1	20	55	free	42,94					
C78	AF	11,91		1	2009A	708	268,8	71,5	7,4	1	20	55	free	39,07					
CHS6.1_0.04	AF	1,78	-0,04	2	9	3531	331,5	48,2	10,6	2	15	45	free	60,04					
CHS6.1_0.06	AF		-0,06	2	10	4529	338,3	56,9	10,2	1	15	45	free	70,01					
CHS6.1_0.08	AF		-0,08	2	10	4605	346,8	62,9	16,5	4	15	50	free	79,36					
CHS6.1_0.10	AF		-0,10	2	10	4507	355,4	54,8	12,8	1	15	50	free	74,84					
CHS6.1_0.12	AF		-0,12	2	10	3582	355,3	54,3	12,8	1	15	50	free	74,33					
CHS6.1_0.14	AF		-0,14	2	10	2768	349,6	58,8	17,0	4	15	50	free	77,13					
CHS6.1_0.16	AF		-0,16	2	10	2396	345,0	55,4	18,3	4	15	50	free	72,14					
CHS6.1_0.18	AF		-0,18	2	10	2181	350,6	51,2	20,4	4	15	50	free	70,47					
CHS6.1_0.20	AF		-0,20	2	10	2070	338,6	66,6	7,2	4	15	30	forced	76,15					
CHS6.1_0.22	AF		-0,22	2	10	2047	52,0	23,8	25,4	4	15	30	free	33,42					
CHS6.1_0.24	AF		-0,24	2	10	2315	66,5	52,6	18,1	4	15	50	free	39,34					
CHS6.1_0.26	AF		-0,26	2	10	2529	67,6	46,9	17,6	4	15	50	free	35,25					
CHS6.1_0.28	AF		-0,28	2	10	2558	56,6	54,5	16,0	4	15	50	free	46,84					
CHS6.1_0.30	AF		-0,30	2	10	2612	30,1	49,4	14,2	2	15	50	free	59,98					
CHS6.1_0.32	AF		-0,32	2	10	2450	37,6	51,6	12,7	3	15	40	free	57,05					
CHS6.1_0.34	AF		-0,34	2	10	2340	14,5	46,7	21,4	4	25	50	free	65,24					
CHS6.1_0.36	AF		-0,36	2	10	2560	35,0	64,5	14,6	2	20	60	free	66,61					

Demagnetization steps of AF and TH palaeomagnetic samples and u-channel

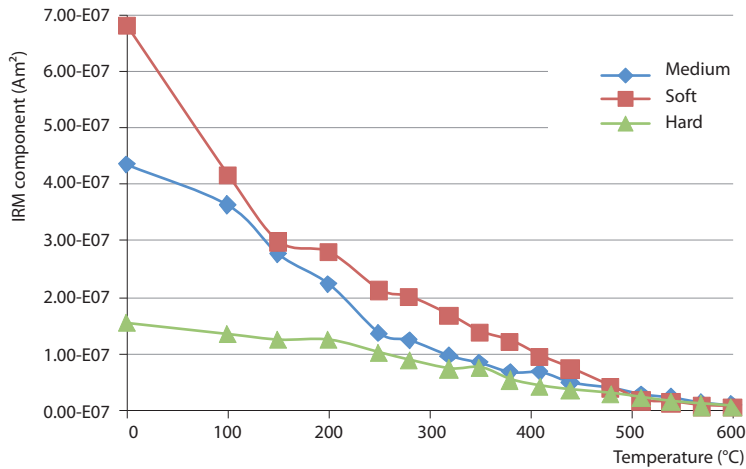
Steps 2009 AF: 0, 5, 10, 15, 20, 25, 30, 40, 50, 60, 70, 80, 90, 100 mT

Steps 2010 AF: 0, 10, 15, 20, 30, 40, 45, 50, 55, 60, 65, 70, 75, 80, 85, 90, 95, 100 mT

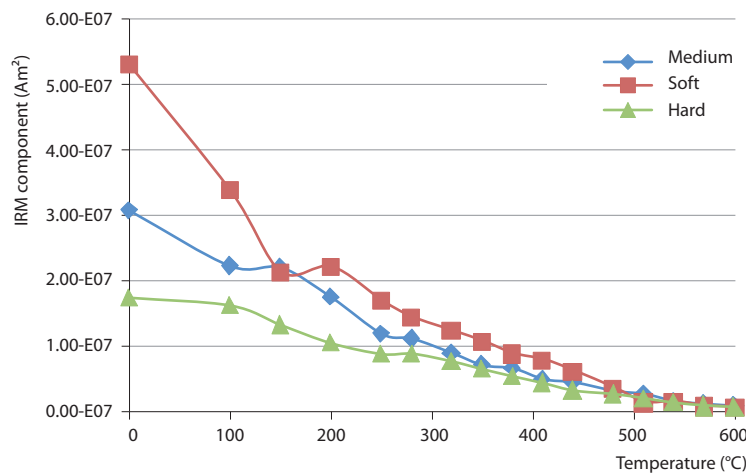
Steps 2009 and 2010 TH: 20, 90, 150, 200, 230, 260, 300, 330, 360, 400, 430, 460, 490, 520, 540, 560, 580, 600, 620, 630°C

Steps u-channel: 0, 5, 10, 15, 20, 20, 25, 30, 30, 40, 45, 50, 55, 60, 65, 70, 80, 90, 100 mT

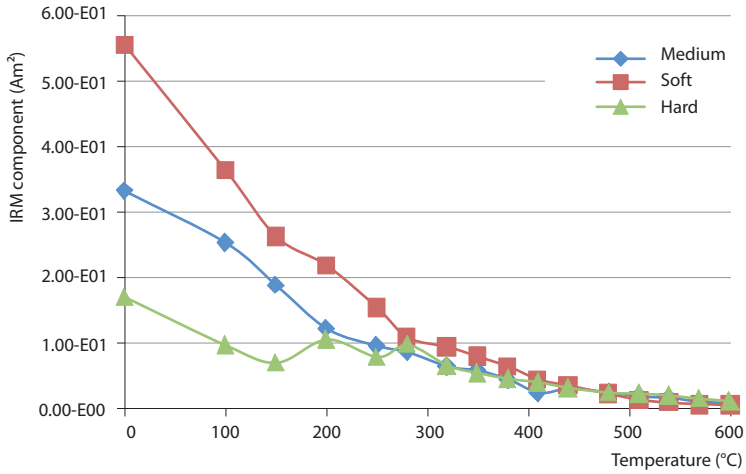
SI Figure 1 a



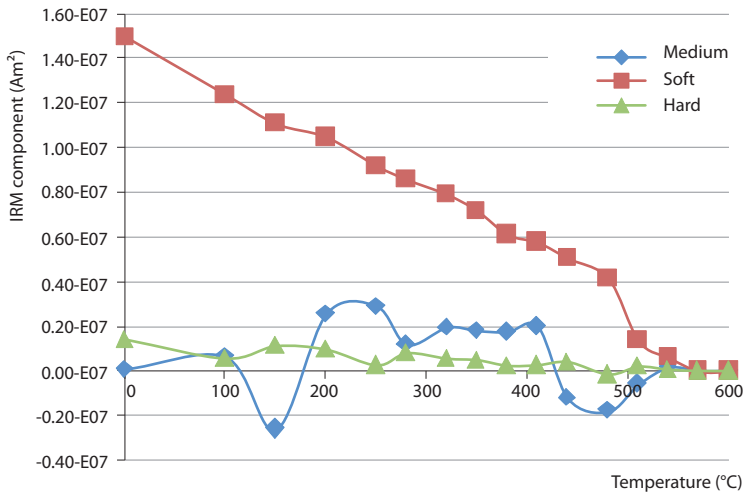
SI Figure 1 b



SI Figure 1 c



SI Figure 1 d



Thermal demagnetization of 3 axial Isothermal Remanent Magnetisation (IRM) acquisition curves. Samples were taken from geological unit 10 (a, b), unit 6 (c) and unit 3 (d)



CHAPTER 6

CONCLUSIONS



CHAPTER 6

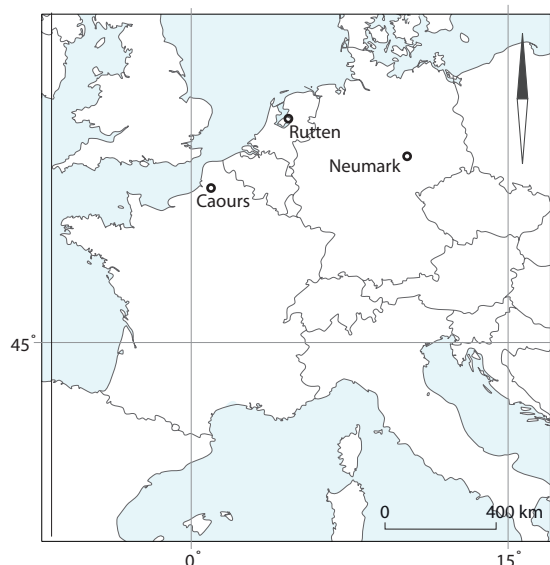
CONCLUSIONS

The main goal of this thesis-research was to provide a better geochronological control of the Last Interglacial, or more specifically the Eemian, in north-western Europe and to add to the palaeoenvironmental dataset of this period (see Introduction). During the Late Pleistocene, north-western Europe, the region where the Eemian was defined, was under the strong influence of glaciations which, in turn, had a profound effect on the presence and absence of hominins in this area. This thesis-research aimed to contribute to the long running debate on Neandertal (and other pre-modern hominins) environmental tolerances, focused on the issue of their occupation of Last Interglacial environments in Europe (e.g. Gamble, 1986; Gamble, 1987; Roebroeks et al., 1992; Roebroeks and Speleers, 2002). For this, detailed palaeomagnetic and environmental studies were carried out at the “interglacial” sites of Neumark Nord 2 (Germany), Rutten, (the Netherlands) and Caours (France). Neumark-Nord 2 and Caours (figure 1) were selected because of the presence of Neandertal archaeology in association with sediments thought to have been deposited during the Last Interglacial, a key period in the study of Neandertal adaptations, as explained in the introduction to this thesis (e.g. Gamble, 1986; Gamble, 1987; Roebroeks et al., 1992).

During the Last Interglacial, we can find a global stratigraphic marker, the Blake Event, the focus of this study (see Chapter 1). This palaeomagnetic event is recorded in both marine and terrestrial sediments (e.g. Baltrunas et al., 2013; Bourne et al., 2012; Osete et al., 2012; Smith and Foster, 1969; Thouveny et al., 2004) and has been found in settings which allows direct correlation with the MIS curve (Bourne et al., 2012; Channell et al., 2012; Tucholka et al., 1987). Our palaeomagnetic studies at Neumark Nord 2, Rutten and Caours have provided a strong indication for the presence of a palaeomagnetic event. This data, in combination with new or published direct and indirect dating methods for

Figure 1.

Location map with the sites of Caours (France), Rutten (The Netherlands) and Neumark (Germany).



the sites at stake has led us to conclude that the palaeomagnetic event identified at the three sites was indeed the Blake Event (See chapters 2, 4 and 5). Through the combination of a wide range of methods, including palaeomagnetism and palynology it was possible to establish better age control and palaeoenvironmental constraints for these sites.

In addition, this study has provided new data of relevance for our understanding of the relationships between developments recorded in the terrestrial and the marine records. Finally, our results have contributed to a better knowledge of possible time lags in the development of the Eemian vegetation in southern versus northern parts of Europe (see below).

For all the studied sites the inferred Eemian *sensu stricto* age was confirmed (see chapters 2 and 4). At Rutten and at Neumark Nord 2 the Eemian age was confirmed via the identification of the typical pollen sequence for this period (Bakels, 2012; Sier et al., in prep; Sier et al., 2011; Strahl et al., 2010), while at Caours the Eemian was identified indirectly (see below and chapter 5). At Neumark Nord 2, pollen studies identified the virtually complete Eemian vegetation succession, (Bakels, 2012; Sier et al., 2011; Strahl et al., 2010).

In relation to our research questions, the main conclusions of this thesis are (see also figure 2):

1. At all three sites a zone with excursionsal palaeomagnetic directions has been identified. In combination with the dating evidence obtained at the sites, these zones have been identified as the Blake Event (see chapters 2, 4 and 5).
2. The Blake Event was directly correlated to the pollenzones of the Eemian *sensu stricto* in north-western Europe at Rutten and in central Europe at Neumark Nord 2 (Chapter 2 and 4).

This correlation was possible because we identified both the Eemian pollenzones and the palaeomagnetic excursion within the Rutten core and within the Neumark Nord 2 section. This enabled a direction correlation between the palynological and palaeomagnetic data.

3. In north-western and central Europe, the lower boundary of the Blake Event is positioned below the first Eemian pollenzone.

In both Rutten and Neumark Nord 2 excursionsal directions of the Blake Event are found below the lower boundary of the Eemian (see chapter 2 and 4). This leads to the simple observation, crucial for our correlation, that the lower boundary of the Blake Event is older (estimated at a few hundreds of years at NN2) than the lower boundary of the Eemian in central and north-western Europe.

4. The upper boundary of the Blake Event is situated within pollenzone EVI (*sensu* Menke and Tynni, 1984), and might extend into the early Weichselian. Future study of an undisturbed EVI pollenzone and early Weichselian might clarify the true location of the Blake Event upper boundary.

At Neumark Nord 2 the upper boundary of the Blake Event was positioned within pollenzone EIV (*sensu* Menke and Tynni, 1984) on the basis of the quality of the ChRM directions. However, at Rutten the excursionsal directions are found up to the hiatus that caps of the Eemian sediments (see chapter 4). This implies that the minimum duration of the Blake Event is similar in length as the Eemian up to

pollenzone EVI, or even the duration of the complete Eemian and possibly into the Weichselian.

5. The Blake Event has a minimum duration similar to the duration of the Eemian up to pollen zone EVI in north-western and central Europe. For this region a minimum duration for the Eemian of ~6000 years (Hahne et al., 1994; Müller, 1974) has been confirmed, with its total duration estimated at ~11000 years (Müller, 1974).

The generally accepted duration estimate of the Eemian in north-western and central Europe is the one of Müller (1974). This estimate was partly based on varve counting and on extrapolation by using an estimated sedimentation rate. Since the study of Müller (1974), more varve counting has been done on different pollenzones by Hahne and colleagues (1994). We used the counted varves of around 6000 as the minimum duration of the Eemian and the estimation of Müller (1974) as an arbitrary upper limit for the duration.

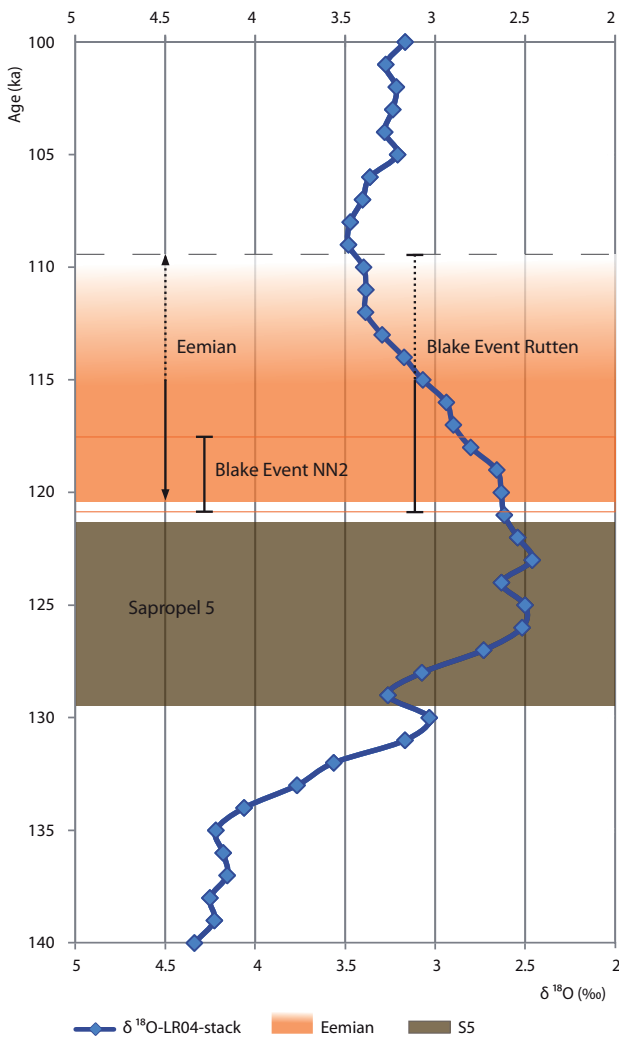
6. The ChRM directions of the Blake Event at all three sites are dominated by south and down ChRM directions. This means that the orientation of a compass during the Blake Event would have been pointing towards the south but that the dip of that same compass was dipping down. This direction of dipping is normally associated with a northward pointing compass in the northern hemisphere.

The ChRM directions of the Blake Event at all three sites are dominated by south and down ChRM directions which are indicative of a non fully dipole field. This finding contrasts with the results obtained in other regions where fully reversed directions have been identified (e.g. Bourne et al., 2012; Smith and Foster, 1969), and becomes an important observation for future studies of the directions of the earth's magnetic field during the Eemian. This might also explain why the Blake Event was not observed in some non orientated cores (e.g. van Leeuwen et al., 2000), as its identification is more dependent on inclination of the ChRM direction.

7. The Eemian in north-western and central Europe is now directly correlated to the MIS record via the Blake Event (see figure 2), and is entirely situated after the MIS 5e peak of the marine record (Sier et al. 2011).

Figure 2.

Stacked $\delta^{18}\text{O}$ -LR04 record (Lisiecki and Raymo, 2005) from 140 to 100 ka, using the Ziegler et. al. (2010) time scale, with the positions of sapropel 5, the duration of the Blake Event at Neumark Nord 2 and Rutten and the (central and north-western European) Eemian interglacial. The Eemian duration in orange is fading from the minimum duration of counted varves to the estimate of Müller (1974).



The Blake Event was identified in all the studied sites by palaeomagnetic analysis of their sediments in combination with a wide variety of dating methods. All these methods, ranging from pollen analysis, bio-stratigraphy and different types of luminescence, all indicated a Last Interglacial age range. Due to the global registration of the Blake Event in both marine and terrestrial sediments, it was possible to make a correlation between the terrestrial and marine interglacial record. Via the Blake Event we were able to position the north-western and central European Eemian within the MIS record. Prior to the study presented here, only the Eemian record of Iberia had been correlated to the marine record in off shore deposits in southern Europe (Sánchez-Goñi et al., 1999).

8. The onset of the Eemian in north-western and central Europe is delayed by 4 to 5 ka compared to the onset of the Eemian in southern Europe.

Our first correlation between the MIS record and the Eemian was done on the basis of new data from Neumark Nord 2 and work published by many others (for details see chapter 2). We identified a large time-lag between our correlation and the Iberian correlation made by Sánchez-Goñi and colleagues (1999). In their study, Sánchez-Goñi et al. (1999) situated the beginning of the Eemian at 5000 to 6000 years after the onset of MIS 5e (Sánchez-Goñi et al., 1999; Shackleton et al., 2002; Shackleton et al., 2003). Our study of the Neumark Nord 2 dataset, in combination with a review of published data, suggests that the onset of the Eemian in north-western and central Europe, dates to around 5000 years after the onset of the Eemian in southern Europe (Sier et al., 2011). This hypothesis has been tested at the site of Rutten, situated in the region of the type locality of the Eemian. Both the Neumark data and the Rutten evidence, as presented in this thesis, indicate a significant time lag, of about 10.000 years, between the beginning of MIS 5e and the beginning of the Eemian. We came to this conclusion by matching the Eemian pollen signal of the Neumark Nord 2 site with the MIS curve via the Blake Event. Many identified Blake Event records have been matched to the global MIS curves (e.g. Channell et al., 2012; Tric et al., 1991) with nearly all situating the Blake Event on the declining side of the MIS 5e to MIS 5d curve. However, in the Mediterranean record published by Tric and colleagues (1991), the Blake Event, well-positioned on the MIS curve, was identified just above the sapropel S5 (Tric et al., 1991). This

sapropel has been well dated from 121.4 to 129.5 ka (Ziegler et al., 2010). Using the sapropel ages we were able to estimate the lower boundary of the Blake Event at around 121 ± 0.5 ka (Sier et al., in prep; Sier et al., 2011). The main results of the Rutten and Neumark Nord 2 studies presented in this thesis are visualized in figure 2.

It is important to note that the position of the onset of Eemian after the MIS 5e peak is age-model independent. The beginning of the Blake Event has been recorded above the sapropel S5 and the onset of the Eemian is situated in Neumark Nord 2 above the onset of the Blake Event.

9. Provided that stratigraphy can constrain the position of deposits between late Saalian and Weichselian, the Blake Event can serve as coarse scale chronostratigraphic ($\sim 10,000$ years) and palaeoenvironmental marker for the Eemian *sensu stricto*.
10. Using the Neumark Nord 2 and Rutten data, we have obtained an indirect confirmation of the inferred Eemian *sensu stricto* age of the Caours site (France) through the recording of the Blake Event (Chapter 5).

At the archaeological site of Caours we were not able to contribute to the dataset of marine terrestrial correlation of the Eemian, as no well-preserved pollen assemblages have been identified there. However, our study did contribute to a better age control of the archaeological levels. The site of Caours was already identified as Last Interglacial of age (e.g. Antoine et al., 2006; Bahain et al., 2010). Through our identification of the Blake Event, we were able to restrict the age of Caours to the Eemian *sensu stricto*, due to the establishment of the close relationship of the Eemian as defined by Zagwijn (1961) and the Blake Event at Rutten and Neumark Nord 2 (Sier et al., in prep; Sier et al., 2011).

11. Our data suggests that at the studied sites delayed acquisition of the palaeomagnetic signal did not occur.

For our correlation to be valid, it is not only important to have high quality data regarding the position of the Blake Event with respect to the deep sea record, but we firstly needed to exclude the possibility of delayed acquisition of the palaeomagnetic signal. Delayed acquisition in the Mediterranean record used in our studies would signify an even larger time gap, as this would increase the gap between the MIS 5e peak and the Blake Event (SI Sier et. al., 2011). Furthermore, the position of the Blake Event in the MIS record is well established, as discussed in chapter 4 of this thesis. Delayed acquisition at both Rutten and the Neumark Nord 2 site could have serious consequences for our main conclusions, as visualized in figure 2. The delayed acquisition could, in theory, be responsible for the observed north-south lag-time of the Eemian. Our study indicated that for both the Rutten as for the Neumark Nord 2 delayed acquisition of the Blake Event can be excluded (for details see chapters 2, 3 and 4). As seen in chapter 3, the rock-magnetic study of the Neumark Nord 2 sediments is very comparable to the local pollen signal, which constitutes a good indication for an in situ palaeomagnetic signal.

12. Fully interglacial human occupation in central Europe (Roebroeks et al., 1992) is confirmed by the position of the Neumark Nord 2 main find horizon within the Eemian pollen zonation.

The main find horizon of the Neumark Nord 2 site is situated in pollen zone IVa2 (sensu Menke and Tynni, 1984) indicating a fully interglacial environment. This position in the Eemian pollen zonation re-affirms the presence of Neandertals in fully interglacial central Europe as already indicated by Roebroeks and colleagues (1992). However, a study by Bakels (2012) indicated that the surrounding of the Neumark Nord 2 basin was relatively open (see also SI Sier et.al., 2011 and chapter 3). It is true that due to taphonomic reasons, site preservation is higher in lacustrine or fluvial settings but it cannot be excluded that Neandertals avoided the “dense forest” parts of interglacial environments. This means that more than 20 years after the Gamble and Roebroeks (Gamble, 1986; Gamble, 1987; Roebroeks et al., 1992) Eemian occupation of northern Europe debate (see introduction of this thesis) the character of Neandertal presence in northern Europe in an interglacial context is still not completely understood.

13. At the time of Neandertal Last interglacial presence at Caours, and also at Neumark Nord 2, access to England was blocked by high sea-levels in the English Channel. This can be concluded by the position of the Caours occupation on the global MIS curve.

Another interesting conclusion resulting from this thesis is related to the timing of the occupation of the site of Caours in regard to former sea levels. As discussed in chapter 1 and chapter 4, a puzzling issue in the debate on Neandertal occupation of northern Europe during the Eemian is the absence of Neandertal sites of last interglacial age in Great Britain. In this study, we were able to correlate the Eemian to the global MIS curve and situated both Neumark Nord 2 and Caours well after the MIS 5e global high sea level stand. This implies that during these occupations, easy access to the British Isles was blocked by the fully developed English Channel. We cannot reject the hypothesis that Great Britain lacked the preferred habitat of Neandertals, as suggested by Ashton (2002) as one of the two possible hypotheses to explain the absence of Neandertal occupation in Great Britain during that period. However, the timing of occupation at Caours (as well as at Neumark Nord 2) as known so far, suggests that high sea levels played an important role, making the missed “window of opportunity” for the crossing into Great-Britain a more likely explanation for their absence (Ashton, 2002).

Implications outside the scope of this thesis and directions for future research

The hypotheses developed in this thesis research regarding position and timing of the Eemian have consequences for various models of palaeoclimate reconstructions (e.g. Sánchez Goñi et al., 2012) and isostatic modelling of the earth crust after deglaciation of northern Europe (e.g. Lambeck et al., 2006; Sánchez Goñi et al., 2012). These models assume a much smaller lag-time between the Eemian interglacial in southern and northern Europe than the one suggested here. It could be interesting to make a systematic assessment of the consequences of the lag-time proposed in this thesis for these models.

Another aspect worth investigating is the development of the Eemian lag-time in a larger geographical context. For example, how does the lag develop over a north to south transect? Do we have a linear development of the lag, which would suggest a steady pace migration of the Eemian vegetation from south to north? Or can we observe a fast migration of the Eemian to one or more spatial thresholds that first need to be overcome before further migration of the vegetation can occur? If thresholds indeed exist, are these climatic, geographic or of other type? Needless to say, one or the other outcome would have different implications for our thinking about past vegetation and climate change and hence, on the climatic models now in use to predict future changes.

As mentioned in the introduction of this thesis, the Amsterdam borehole section has been proposed as the type section for the Middle to Late Pleistocene boundary (Gibbard, 2003; Gibbard et al., 2008). The conclusions of this research underlines that this boundary is a diachronous one; hence, it would be better to use the lower boundary of the Blake Event as the boundary of the Middle to Late Pleistocene: this boundary corresponds (more or less) with the lower boundary of the Eemian in the Netherlands and when properly identified, it is not diachronous and it is retraceable in both marine and terrestrial sequences.

Finally, once a proper framework of the development of the Eemian in the whole of Europe has been established, we can start to systematically evaluate the patterns of Neandertal presence and absence in this area, which will contribute to our understanding of hominin behavior on a large European scale.

References

- Antoine, P., Limondin-Lozouet, N., Auguste, P., Loch, J. L., Galheb, B., Reyss, J., Escudé, E., Carbonel, P., Mercier, N., Bahain, J. J., Falguères, C., and Voinchet, P. (2006). Le tuf de Caours (Somme, France) : mise en évidence d'une séquence eemienne et d'un site paléolithique associé. *Quaternaire* 17, 281-320.
- Ashton, N. (2002). Absence of human in Britain during the last interglacial (oxygen isotope stage 5e). In "Publications du CERP" (A. Tuffreau, and W. Roebroeks, Eds.), pp. 93-103. Université des sciences et technologies de Lille, Villeneuve-d'Ascq, France.
- Bahain, J. J., Falguères, C., Dolo, J. M., Antoine, P., Auguste, P., Limondin-Lozouet, N., Loch, J. L., Tuffreau, A., Tissoux, H., and Farkh, S. (2010). ESR/U-series dating of teeth recovered from well-stratigraphically age-controlled sequences from Northern France. *Quaternary Geochronology* 5, 371-375.
- Bakels, C. (2012). Non-pollen palynomorphs from the Eemian pool Neumark-Nord 2: Determining water quality and the source of high pollen-percentages of herbaceous taxa. *Review of Palaeobotany and Palynology* 186, 58-61.
- Baltrunas, V., Seiriene, V., Molodkov, A., Zinkute, R., Katinas, V., Karmaza, B., Kisieliene, D., Petrosius, R., Taraskevicius, R., Piliciauskas, G., Schmolcke, U., and Heinrich, D. (2013). Depositional environment and climate changes during the late Pleistocene as recorded by the Netiesos section in southern Lithuania. *Quaternary International* 292, 136-149.
- Bourne, M., Mac Niocaill, C., Thomas, A. L., Knudsen, M. F., and Henderson, G. M. (2012). Rapid directional changes associated with a 6.5 kyr-long Blake geomagnetic excursion at the Blake-Bahama Outer Ridge. *Earth and Planetary Science Letters* 333-334, 21-34.
- Channell, J. E. T., Hodell, D. A., and Curtis, J. H. (2012). ODP Site 1063 (Bermuda Rise) revisited: oxygen isotopes, excursions and paleointensity in the Brunhes Chron. *Geochemistry Geophysics Geosystems* 13, Q02001.
- Gamble, C. (1986). "The Palaeolithic settlement of Europe." Cambridge University Press, Cambridge.
- Gamble, C. S. (1987). Man the shoveler: Alternative models for Middle Pleistocene colonization and occupation in Northern latitudes. In "The Pleistocene old world. Regional perspectives." (O. Soffer, Ed.), pp. 81-98. Plenum Press, New York.

- Gibbard, P. L. (2003). Definition of the Middle-Upper Pleistocene boundary. *Global and Planetary Change* 36, 201-208.
- Gibbard, P. L., Cohen, K. M., and Ogg, J. G. (2008). Quaternary Period. In "The concise Geologic Time Scale." (J. G. Ogg, G. Ogg, and F. M. Gradstein, Eds.), pp. 178, Cambridge.
- Hahne, J., Kemle, S., Merkt, J., and Meyer, K.-D. (1994). Eem-, weichsel- und saalezeitliche Ablagerungen der Bohrung "Quakenbrück GE2. *Geologisches Jahrbuch A* 134, 9-69.
- Lambeck, K., Purcell, A., Funder, S., Kjaer, K., Larsen, E., and Möller, P. (2006). Constraints on the Late Saalian to early Middle Weichselian ice sheet of Eurasia from field data and rebound modelling. *Boreas* 35, 539-575.
- Lisiecki, L. E., and Raymo, M. E. (2005). A Pliocene-Pleistocene stack of 57 globally distributed benthic $\delta^{18}O$ records. *Paleoceanography* 20, PA1003.
- Menke, B., and Tynni, R. (1984). Das Eeminterglazial und das Weichselfrühglazial von Rederstall/Dittmarschen und ihre Bedeutung für die mitteleuropäische Jungpleistozängliederung. *Geologisches Jahrbuch A* 76, 3-120.
- Müller, H. (1974). Pollenanalytische Untersuchungen und Jahresschitzenzählungen an der eem-zeitlichen Kieselgur von Bispingen/Luhe. *Geologisches Jahrbuch A* 21, 149-169.
- Osete, M.-L., Martín-Chivelet, J., Rossi, C., Edwards, R. L., Egli, R., Muñoz-García, M. B., Wang, X., Pavón-Carrasco, F. J., and Heller, F. (2012). The Blake geomagnetic excursion recorded in a radiometrically dated speleothem. *Earth and Planetary Science Letters* 353-354, 173-181.
- Roebroeks, W., Conard, N. J., and van Kolfschoten, T. (1992). Dense Forests, Cold Steppes, and the Palaeolithic Settlement of Northern Europe. *Current Anthropology* 33, 551-586.
- Roebroeks, W., and Speleers, B. (2002). Last interglacial (Eemian) occupation of the North European plain and adjacent areas. In "Publications du CERP" (A. Tuffreau, and W. Roebroeks, Eds.), pp. 31-39. Université des sciences et technologies de Lille, Villeneuve-d'Ascq, France.
- Sánchez-Goñi, M. F., Eynaud, F., Turon, J. L., and Shackleton, N. J. (1999). High resolution palynological record off the Iberian margin: direct land-sea correlation for the Last Interglacial complex. *Earth and Planetary Science Letters* 171, 123-137.
- Sánchez Goñi, M. F., Bakker, P., Desprat, S., Carlson, A. E., Van Meerbeeck, C. J., Peyron, O., Naughton, F., Fletcher, W. J., Eynaud, F., Rossignol, L., and Renssen, H. (2012). European climate optimum and enhanced Greenland melt during the Last Interglacial. *Geology* 40, 627-630.

- Shackleton, N. J., Chapman, M., Sánchez-Goñi, M. F., Pailler, D., and Lancelot, Y. (2002). The Classic Marine Isotope Substage 5e. *Quaternary Research* 58, 14-16.
- Shackleton, N. J., Sánchez-Goñi, M. F., Pailler, D., and Lancelot, Y. (2003). Marine Isotope Substage 5e and the Eemian Interglacial. *Global and Planetary Change* 36, 151-155.
- Sier, M. J., Peeters, J., Dekkers, M. J., Chang, L., Busschers, F. S., Wallinga, J., Parés, J. M., and Roebroeks, W. (in prep). The Blake Event recorded near the Eemian Type locality, revised timing of the onset of the Eemian in north western Europe.
- Sier, M. J., Roebroeks, W., Bakels, C. C., Dekkers, M. J., Brühl, E., De Loecker, D., Gaudzinski-Windheuser, S., Hesse, N., Jagich, A., Kindler, L., Kuijper, W. J., Laurat, T., Mücher, H. J., Penkman, K. E. H., Richter, D., and van Hinsbergen, D. J. J. (2011). Direct terrestrial-marine correlation demonstrates surprisingly late onset of the last interglacial in central Europe. *Quaternary Research* 75, 213-218.
- Smith, J. D., and Foster, J. H. (1969). Geomagnetic Reversal in Brunhes Normal Polarity Epoch. *Science* 163, 565-567.
- Strahl, J., Krbetschek, M. R., Luckert, J., Machalet, B., Meng, S., Oches, E. A., Rappsilber, I., Wansa, S., and Zöller, L. (2010). Geologie, Paläontologie und Geochronologie des Eem-Beckens Neumark-Nord 2 und Vergleich mit dem Becken Neumark-Nord 1 (Geiseltal, Sachsen-Anhalt). *Quaternary Science Journal* 59, 120-167.
- Thouveny, N., Carcaillet, J., Moreno, E., Leduc, G., and Nérini, D. (2004). Geomagnetic moment variation and paleomagnetic excursions since 400 kyr BP: a stacked record from sedimentary sequences of the Portuguese margin. *Earth and Planetary Science Letters* 219, 377-396.
- Tric, E., Laj, C., Valet, J., Tucholka, P., Paterne, M., and Guichard, F. (1991). The Blake geomagnetic event: transition geometry, dynamical characteristics and geomagnetic significance. *Earth and Planetary Science Letters* 102, 1-13.
- Tucholka, P., Fontugne, M., Guichard, F., and Paterne, M. (1987). The Blake magnetic polarity episode in cores from the Mediterranean Sea. *Earth and Planetary Science Letters* 86, 320-326.
- van Leeuwen, R. J. W., Beets, D. J., Bosch, J. H. A., Burger, A. W., Cleveringa, P., van Harten, D., Waldemar Herngreen, G. F., Kruk, R. W., Langereis, C. G., Meijer, T., Pouwer, R., and de Wolf, H. (2000). Stratigraphy and integrated facies analysis of the Saalian and Eemian sediments in the Amsterdam-Terminal borehole, the Netherlands. *Netherlands Journal of Geosciences* 79, 161-196.

- Zagwijn, W. H. (1961). Vegetation, climate and radiocarbon datings in the late Pleistocene of the Netherlands: I. Eemian and Early Weichselian, *Nieuwe Serie. Mededelingen van de Geologische Stichting* 14, 15-45.
- Ziegler, M., Tuenter, E., and Lourens, L. J. (2010). The precession phase of the boreal summer monsoon as viewed from the eastern Mediterranean (ODP Site 968). *Quaternary Science Reviews* 29, 1481-1490.

Summary

One of the key periods to understand the Neandertal ecological niche and tolerances in Europe is the Eemian. This interglacial stage is the last and best documented interglacial stage in which Neandertals were present in Europe. This study aims to contribute to the debate on Neandertal environmental tolerances of this period in Europe by improving our knowledge of the timing of Neandertal occupation.

In order to further specify the timing and character of this occupation, detailed palaeomagnetic and environmental studies were carried out at the interglacial sites of Neumark Nord 2 (Germany), Rutten (The Netherlands), and Caours (France). For the Last Interglacial, a global stratigraphic marker has been documented, the so-called Blake Event. This palaeomagnetic event is recorded in both marine and terrestrial sediments and has been found in settings which allow direct correlation with the Marine Isotope Stage record.

Our palaeomagnetic studies at Neumark Nord 2, Rutten and Caours have provided a strong indication for the presence of a palaeomagnetic event which we have identified as the Blake. We were able to correlate this Blake Event to the pollenzones of the Eemian *sensu stricto* at Rutten and at Neumark Nord 2. The observed position of the Blake Event in relation to the Eemian in north western and central Europe supports a time lag of 5000 years between the onset of the Eemian in the south and the northern-central parts of Europe. This result has consequences for views of the chronological and geographical limits of the Neanderthal range. As an example, our correlation indicates that both Neumark Nord 2 and Caours were occupied well after the MIS 5e global high sea level stand. This implies that during these occupations, easy access to the British Isles was blocked by the fully developed English Channel, possibly explaining the absence of hominins in what is now Great Britain at that period.

Samenvatting

Voor een beter begrip van de ecologische niche en de tolerantiegrenzen van de Neanderthaler in Europa is het Eemien cruciaal. Deze interglaciaal is de laatste en best gedocumenteerde interglaciale periode waarin Neanderthalers nog in Europa aanwezig waren. Het voorliggende onderzoek heeft tot doel een bijdrage te leveren aan de discussie over de ecologische tolerantiegrenzen van Neanderthalers gedurende deze periode. De studie richt zich specifiek op het nader bepalen van de periode gedurende welke de Neanderthalers hier aanwezig waren.

Om de duur en het karakter van de Neanderthaler-bewoning nader te kunnen bepalen zijn gedetailleerde paleomagnetische en milieustudies uitgevoerd op de interglaciale archeologische vindplaatsen Neumark Nord 2 (Duitsland), Rutten (Nederland) en Caours (Frankrijk). Voor het laatste interglaciaal bestaat een internationale stratigrafische marker, bekend onder de naam 'Blake Event'. Deze paleomagnetische excursie is gedocumenteerd in zowel mariene als landafzettingen en kan in sommige gevallen direct worden gekoppeld aan de Marine Isotope Stage Record.

Het paleomagnetisch onderzoek in Neumark Nord 2, Rutten en Caours heeft duidelijke aanwijzingen opgeleverd voor de aanwezigheid van een paleomagnetische excursie, die overeen bleek te komen met het 'Blake Event'. Deze 'Blake Event' kon worden gecorreleerd met de pollenzones van het Eemien sensu stricto van Rutten en van Neumark Nord 2. Deze correlatie wijst uit dat het Eemien in het noordwesten en het midden van Europa 5000 jaar later begon dan in het zuiden van Europa. Dit heeft consequenties voor het inzicht in de chronologische en geografische grenzen van de verspreiding van Neanderthalers. De gevonden correlatie toont onder andere aan dat zowel Neumark Nord 2 als Caours pas ruim na de wereldwijde MIS 5e hoge zeespiegelstand bewoond werden. Dit impliceert dat de Britse eilanden tijdens deze fase van bewoning niet zonder meer bereikbaar waren, aangezien het Kanaal al volledig ontwikkeld was. Mogelijk verklaart dit de afwezigheid van Neanderthalers in het Eemien in het huidige Groot-Brittannië.

Acknowledgements

Scientific life starts with a PhD title is an often heard expression. Even though I do not agree with this statement, it is true that with this title you are able to apply for grants which in turn, if granted, are the lifeblood of your scientific life. My scientific life started late and it took me a while to realise that I wanted to pursue a scientific career. In retrospect this is strange because from an early age I was very much interested in science, especially geology and archaeology. I remember clearly asking my parents at an age of 4 what existed before us, humans, and being fascinated with the fossils I found during our summer holidays. If I was not looking for fossils I loved to visit the local archaeological excavations and when my sisters and mom had enough I went to visit the archaeological museums alone with my dad, while the “girls” spent the day at the beach. Some years later it turned out that one of my sisters, Maaïke, did enjoy all the visits to the archaeological sites as she decided to study archaeology in Leiden. She in turn saved me from going to study Economy in Rotterdam (the one subject that I disliked intensely in high school) by suggesting that geology in Utrecht might be a better choice for me. It was thanks to you Maaïke!

Most of you know that I did not start working in geology after finishing my studies in Utrecht. Instead I joined the ING bank in Amsterdam, a place where I enjoyed working. During my ING days I spent my overtime hours with Douwe van Hinsbergen in Greece, helping him sample the whole Greek country for his PhD. In total we spent 11 weeks together in the field spread over two years. It was a great time! And definitely, it also rekindled my interest in science. Thank you, Douwe.

Some years later I knew it was time for a change in my career but I could not see clear where I wanted to go. I hired a job-coach and we sat down to talk about my interests, dreams and ambitions. After a few hours the job-coach told me: I have never been able to advise anybody within the first session until today. You should do a PhD in geology or study archaeology or history. Do not mention this to anyone yet as they will try to talk you out of it. We will meet in three months and talk about it some more when you had time to think about it. My first reaction was WHAT??? I just spent a lot of money and this is the advice I get... That evening I called my parents to tell them about the meeting. After a while they said: when we hear you talking about it, it seems clear you are going to study archaeology... Parents know you better than anyone. Thank you, mom and dad. And thank you also for the love and support you have given me over the years, for providing me the

room to be myself and achieve my dreams. For being an example of loyalty and devotion, and for giving me my great three sisters Marieke, Maaïke and Maartje, accomplices and guardian angels.

Three months later, when I met my job-coach again I was already a part-time student in Archaeology (thank you ING) and had already passed my first exams. Thank you, job-coach.

From there on, it did not take long for me to realise that I wanted to pursue a scientific career in Palaeolithic archaeology. Fortunately, Wil Roebroeks was awarded the Spinoza premium (thank you NWO) and I was awarded one of the Spinoza funded PhD positions (Thank you, Wil) co-promoted by 2 world renowned scientists, one a rock-magnetist, and the other one a palaeo-magnetist, Mark Dekkers and Josep Parés. I believe that I have been very lucky with my promoters; not only they are experts in their field but they are also easy going and good advisors, albeit all three in their own personal way. The way you do your science is an inspiration for me. Wil, many thanks for the opportunity you gave me over these years to pursue my vocation. It is a pleasure to be part of the Human Origins Group and I hope to be part of it for many years to come. You have been always generous with me and you were the first one to definitely bet on the scientist I had inside. And something else! Before I started my PhD, unknowingly, Wil had a big influence on my life. Due to his contacts, Leiden students had the opportunity to go to Dmanisi, in Georgia. I was one of them, supposedly to do some palaeomag work. This did not happen but I did meet my wife! Endless thanks for this, Wil! Josep, your trust and your support have been crucial for me to be able to combine my personal and professional life. Also your Spanish and US background has given me new perspectives on the scientific world. Mark, you have been called the walking encyclopaedia in the past. This is true but for me you are mostly the man of detail, both in structure of the text as in structure of the research. I learned and learn a lot from you but most importantly, you know how to pick a good wine. Many thanks to the three of you I could not have done it without you.

Many other people deserve an acknowledgement; so many, that I decided to group them and avoid unintentional forgets.

To my friends, neighbours and the Amsterdam Crusaders! To Miolnir, a great group who gave me at least 15 weeks extra field experience, my jaarclub (including Astrid). To the people from the Fort with Cor Langereis at its head, who leads by example both in science as in life enjoyment. Tom you are missed! To all the staff from the faculty of Archaeology with its Human Origins group at its core. To the teams and support staff of Dikika, West

Turkana and Atapuerca research projects. To the Neumark, Caours and Rutten colleagues with special mention of Jan Peeters. To Claudia from the CENIEH paleomag lab. To the Kennis brothers for letting me use one of their beautiful drawings. To Woef and the old boys. To Joanne Porck for all her help with the illustrations over the last few years. To José María Bermúdez de Castro for all his support in the last few years and being a great person in all senses. I also appreciated that you and Eudald Carbonell cleared the TD1 section for me with sledgehammers. Finally, some people have made my life in Burgos warmer and funnier. Laura, Angel, Pili and Elena are part of that Spanish world.

For different reasons there are a few people I want to give a separate mention: Jose, Corrie, Kim and Adam.

The SNMAP for funding part of my Dikika research. This research is not published yet and in the end is not part of this thesis, but your financial contribution was an important stepping stone for the research that I will be doing the next few years. Many thanks! With this respect I want to give a special mention to Guillaume. I published my first paper with you and many more are on its way. Thank you for giving me that opportunity!

Also I would like to thank my family in the Netherlands and Spain and those family members who are not longer with us. Especially Apa en Aaldert would have loved my research. Oma Sier would have been so proud, maybe of me, but mostly because she has a great-grandchild named after her.

To my wife María I want to give the biggest thanks. She followed the path of the PhD before me and knows how it's done. We make a good team together. We have two great kids and she makes and continues to make me better a person and scientist. LOML!

Finally I want to thank my kids Mark and María. It is pure joy to have you around and to see you grow and learn. You are a guarantee of something good in my life, ever and forever. No words can come close to describe what the two of you mean for your father and mother. Life has gained a whole new meaning with your arrival. Love you!

Curriculum Vitae

Mark Jan Sier was born on the 27th of august 1972 in Amstelveen, the Netherlands. After graduating in Geology in the faculty of Earth Sciences at Utrecht University he pursued a career at ING bank in Amsterdam. In this period he spent his holidays helping Douwe van Hinsbergen with palaeomagnetic fieldwork in Greece, rekindling his interest for science. Some years later this resulted in, first part-time later full-time, studying Archaeology in the faculty of Archaeology of Leiden University (MA 2008). Coffee visits to the “Fort Hoofddijk” palaeomagnetic laboratory in Utrecht led to Mark being asked to join the African stratigraphic projects in hominin-bearing sites of Guillaume Dupont-Nivet. Subsequently, Mark started a palaeomagnetic stratigraphy project in the Neandertal Neumark Nord archaeological site, together with Mark Dekkers. This site forms an important part of the PhD research presented here which started in 2009 at the Human Origins Group led by Wil Roebroeks of the Faculty of Archaeology, Leiden. For this thesis also collaboration was started with Josep Parés of the CENIEH, Spain. Mark’s thesis allowed him to combine his interests in Geology and Archaeology. Other interests are skiing, american football, ice skating and reading.

Mark is married to the beautiful and brilliant scientist Maria Martín Torres, who has an excellent sense of humor and shares (or exceeds) Mark’s taste for beer. Together, they have two kids, Mark and Maria.

THIS STUDY CONTRIBUTES TO THE LONG RUNNING DEBATE ON NEANDERTAL ENVIRONMENTAL TOLERANCES, FOCUSED ON THE ISSUE OF THE LAST INTERGLACIAL (OR EEMIAN) OCCUPATION OF EUROPE. IN ORDER TO FURTHER SPECIFY THE TIMING AND CHARACTER OF THIS OCCUPATION, DETAILED PALAEOMAGNETIC AND ENVIRONMENTAL STUDIES WERE CARRIED OUT AT THE INTERGLACIAL SITES OF NEUMARK NORD 2 (GERMANY), RUTTEN (THE NETHERLANDS), AND CADURS (FRANCE). FOR THE LAST INTERGLACIAL, A GLOBAL STRATIGRAPHIC MARKER HAS BEEN DOCUMENTED, THE SO-CALLED BLAKE EVENT. THIS PALAEOMAGNETIC EVENT IS RECORDED IN BOTH MARINE AND TERRESTRIAL SEDIMENTS AND HAS BEEN FOUND IN SETTINGS WHICH ALLOW DIRECT CORRELATION WITH THE MARINE ISOTOPE STAGE RECORD.

OUR PALAEOMAGNETIC STUDIES AT NEUMARK NORD 2, RUTTEN AND CADURS HAVE PROVIDED A STRONG INDICATION FOR THE PRESENCE OF A PALAEOMAGNETIC EVENT WHICH WE HAVE IDENTIFIED AS THE BLAKE. WE WERE ABLE TO CORRELATE THIS BLAKE EVENT TO THE POLLENZONES OF THE EEMIAN *SENSU STRICTO* AT RUTTEN AND AT NEUMARK NORD 2. THE OBSERVED POSITION OF THE BLAKE EVENT IN RELATION TO THE EEMIAN IN NORTH WESTERN AND CENTRAL EUROPE SUPPORTS A TIME LAG OF 5000 YEARS BETWEEN THE ONSET OF THE EEMIAN IN THE SOUTH AND THE NORTHERN-CENTRAL PARTS OF EUROPE. THIS RESULT HAS CONSEQUENCES FOR VIEWS OF THE CHRONOLOGICAL AND GEOGRAPHICAL LIMITS OF THE NEANDERTHAL RANGE. AS AN EXAMPLE, OUR CORRELATION INDICATES THAT BOTH NEUMARK NORD 2 AND CADURS WERE OCCUPIED WELL AFTER THE MIS 5E GLOBAL HIGH SEA LEVEL STAND. THIS IMPLIES THAT DURING THESE OCCUPATIONS, EASY ACCESS TO THE BRITISH ISLES WAS BLOCKED BY THE FULLY DEVELOPED ENGLISH CHANNEL, POSSIBLY EXPLAINING THE ABSENCE OF HOMININS IN WHAT IS NOW GREAT BRITAIN AT THAT PERIOD.